Structural and functional studies of HomA and HomB, outer membrane proteins of *Helicobacter pylori*

Ph.D. Thesis

By

ANUBHAV TAMRAKAR

DEPARTMENT OF BIOSCIENCES AND BIOMEDICAL ENGINEERING

INDIAN INSTITUTE OF TECHNOLOGY INDORE

March 2022

Structural and functional studies of HomA and HomB, outer membrane proteins of *H. pylori*

A THESIS

Submitted in partial fulfillment of the

requirements for the award of the degree

of

DOCTOR OF PHILOSOPHY

By

ANUBHAV TAMRAKAR

Roll No. 1501271007

DEPARTMENT OF BIOSCIENCES AND BIOMEDICAL ENGINEERING

INDIAN INSTITUTE OF TECHNOLOGY INDORE

March 2022

INDIAN INSTITUTE OF TECHNOLOGY INDORE

CANDIDATE'S DECLARATION

I hereby certify that the work which is being presented in the thesis entitled **"Structural and functional studies of HomA and HomB, outer membrane proteins of *Helicobacter pylori*"** in the partial fulfillment of the requirements for the award of the degree of **DOCTOR OF PHILOSOPHY** and submitted in the **DEPARTMENT OF BIOSCIENCES AND BIOMEDICAL ENGINEER, Indian Institute of Technology Indore**, is an authentic record of my own work carried out during the time period from July 2016 to December 2021 under the supervision of Dr. Prashant Kodgire, Professor, BSBE, IIT Indore.

The matter presented in this thesis has not been submitted by me for the award of any other degree of this or any other institute.

10.08.22

signature of the student with date

(ANUBHAV TAMRAKAR)

This is to certify that the above statement made by the candidate is correct to the best of my knowledge.

P.V. Kodgire 10/08/22

Signature of Thesis Supervisor with date

(DR. PRASHANT KODGIRE)

ANUBHAV TAMRAKAR has successfully given his Ph.D. Oral Examination held on 10/08/22

P.V. Kodgire 10/08/22

Signature of Thesis Supervisor with date

(DR PRASHANT KODGIRE)

ACKNOWLEDGEMENTS

This work is a collective effort of many people, some of them are co-authors and some of them did not get their name printed on paper but do get printed on my neuronal plasticity. I'd like to extend my sincere gratitude to everyone that has been followed thermodynamics law in making this work done.

To begin with, I'd like to thank **Professor Prashant Kodgire** for giving me an opportunity to work in a well-equipped research laboratory. However, his lab is constructed with four walls and one roof but there were no boundaries for imagination, ideas, thoughts. I had not thought to work on core molecular immunology, rather to work on infection and immunology research areas. I am thankful to him for giving me countless chances of exploration in all research areas. Professor Prashant is made of a part keen observer, multidimensional, long-slightness, hope and curiosity, probably the best recipe for a great teacher. He offered me many useful suggestions related to research work and presentation by which I tried to grow as a researcher. Besides, I have faced several uncomfortable situations as a part of life, his support and suggestions during this journey helped me recover fast. I have used many of his statements to catch many moments. One of them is '*Life is between B (Birth) and D (Death) and in between is C (choice) so you are the men of your choice*'. finally, I am thankful to him for supervising me patiently and helping me in developing an independent researcher aptitude. I look forward to continuing our ongoing projects, which I hope will yield results that we can both be proud of.

Further, I would like to thank my PSPC members Professor Avinash Sonavane and Dr. Amrendra Kumar Singh for their valuable suggestions and continuous support. I am grateful to all faculty members of BSBE for their direct or indirect contributions to my research work. In particular, I express my gratitude to Dr. Debasis Nayak for the scientific discussions.

I would like to extend my thank the Sophisticated Instrumentation Centre (SIC), IIT Indore for confocal experiments. In particular, I would like to extend my thanks to Dr. Ravindra (SIC IIT Indore) for confocal microscopy, Mr. Gaurav Singh Mr. Murphy Bhaskar Ganveer (Deputy Lab Manager, BSBE, IIT Indore), and Mr. Arif Patel for dealing with various issues related with instruments. I would also like to thank the academic staff of IIT Indore, the library staff of IIT Indore and all other technical and non-technical staff for their constant help and support.

I'd also like to express my gratitude and thanks to Molecular immunology group

Ankit Jaiswal has joined PhD with me in the same lab. We have given interviews on the same day and stayed in same hostel same room. He also briefed me about Professor Prashant's lab. We have become so inseparable that from morning to evening all the time we talk, discuss, eat, roam together. He helped me in each of my experiments and troubleshoot them. He always stood with me whenever I felt hopeless, broken. Words cannot measure his contributions. I could not imagine this journey without him.

Dr. Amit Kumar Singh, is the first student of our lab and one of the very generous senior fellows I could have. He helped me with each little thing and always been available for discussion.

Rahul Chaudhary, a kind helping hand and colleague, I am thankful for making my 2021 birthday special and lifting me on your shoulder.

Surbhi Jaiswal, Brijeshwar Singh, Kanika and Kritika Malik, are wonderful newcomers and bright-minded colleagues. Unfortunately, we had very little time together, thankful for making my 2021 birthday special. Your tearful eyes and love have been imprinted on my cardiac muscles. Thank you Surbhi for all your love and support.

I personally want to extend my thanks to Ms. Nirali, Dr. Rinki, Mr. Sajjan, Pramod, Khandu, Kapil, Subhas (Chubhas), Anurag, Dr.

Venkat, Uma, Krishna, Vedant, Praveen. All my friends, seniors and colleagues from BSBE and other departments. Please don't mind if you don't find your name here, nobody is going to read this thesis except my lab group members. You all have a soft corner in my cardiac chamber (left side). Special thanks to Mr. Rajarshi Roy for being with me and for all the delicious food.

My special thanks to all the collaborators Dr. Debasis Nayak, IIT Indore, Dr. Amit Kumar, IIT Indore, Dr. Ravindra Makde RRCAT Indore, Dr. Ashish Ganguly IMTECH Chandigarh, Dr. Ashish Kumar Mukopadhyay, NICED, Kolkata, Prof. Solnick, University of California, Davis.

I thank the University Grant Commission, Govt. of India, for the PhD fellowship and the Department of Science and Technology, Department of Biotechnology, the Indian Council of Medical Research (ICMR) for all the research funding to our laboratory.

My family have always supported me during the journey, their contribution cannot be measured.

- **Anubhav Tamrakar**

DEDICATION

This thesis is dedicated to *Taxpayers, citizens and the Government of India*.

SYNOPSIS

Introduction

We are surrounded by incredible kinds of living microorganisms that are invisible to our naked eyes and present almost everywhere. Several of these microbes live with us and within us, and are vital for our survival, as they protect the skin from the external parasites, aid in the synthesis of vitamins, digestion of food and nutrient absorption, as well as train the immune system to fight against infectious agents. Nevertheless, some of these microbes can cause infections in humans. These pathogenic microbes can enter our body through the ingested food, cuts and wounds, insect bites, etc. and infect the host for their survival and reproduction. In response to the infections caused by these pathogens, our immune system gets activated to fight against them. After entering the body, pathogenic bacteria interact with the host cells and induce the production of several inflammatory molecules, sometimes this inflammation gets unbalanced or uncontrolled, leading to inflammation storms and causing severe sepsis and septic shocks[1].

Outer membrane proteins (OMPs) are distinctive features of Gram-negative bacteria. Apart from their structural role, they play a crucial role in host-pathogen interaction, virulence, and pathogenesis of bacteria. Upon interaction with the host immune cells, OMPs stimulate the production of proinflammatory molecules that may result in an uncontrolled inflammation, leading to severe sepsis or septic shock, which is a major cause of many deaths worldwide. A distinct group of OMPs is composed of antiparallel β-barrels connected via long loops. Several studies suggested that these surface-exposed loops interact with the host cell and participate in virulence. OMPs of Gram-negative infectious bacteria demonstrate significant conservation in the sequences, and share structural similarities within and among different species, making them useful diagnostic targets and effective vaccine candidates (**Fig. 1**).

Background of work and Objectives

Outer membrane proteins (OMPs) of *H. pylori* play a crucial role in the host-pathogen interaction, virulence, and pathogenesis. Upon interaction with the host immune cells, OMPs stimulate the production of pro-inflammatory molecules that may result in an uncontrolled inflammation leading to the transformation of a normal cell to a cancerous cell.

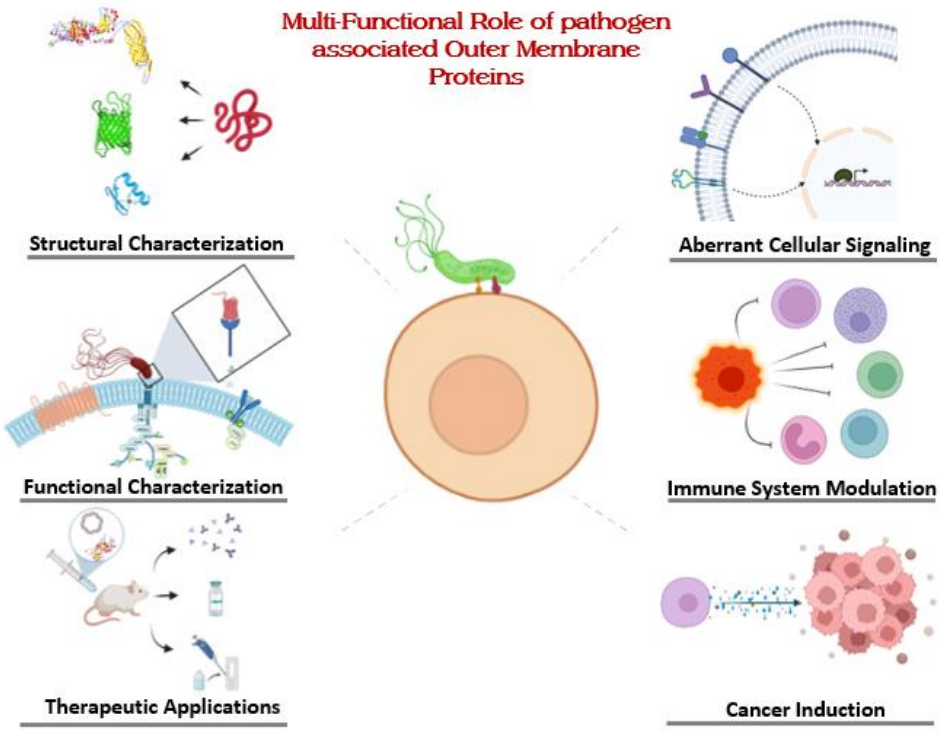

Figure 1. Multifunctional role of Outer membrane proteins (OMPs). Right panel from top to bottom, schematic representation of Host-pathogen interaction leading to host aberrant signaling, immune cells and communication system modulation, and cell signaling induction leading to cancer cell transformation. Left panel from top to bottom, identification, and structural and functional characterization of virulence factor (here OMPs) thereby using them as therapeutic targets such as monoclonal antibody therapy, vaccine, and inhibitors development.

Hom (Helicobacter outer membrane) family of OMPs in *H. pylori* consists of four members (HomA, B, C and D). *homB* gene is 90% similar to another OMP of the *H. pylori*, which is the *jhp*0649 ORF *homA*, with differences between the 300 bp middle region of

these ORFs[2]. HomB outer membrane protein is associated with many stomach diseases and is a novel co-marker for peptic ulcer disease (PUD)[3,4] and is the most studied and evaluated for its prevalence in various peptic diseases. Oleastro *et al*. investigated pathogenesis and immunological response caused by HomB protein in clinical patients and 190 *H. pylori* strain isolated from patients with peptic ulcer disease (PUD) or gastritis were evaluated for the clinical importance of *homB*. HomB protein contributes to the colonization and persistence of *H. pylori*, and the presence of *homB* genes affects the number of bacteria adhering to the host cells. Additionally, HomB is also associated with the secretion of the proinflammatory cytokine interleukin-8 (IL-8)[5]. Additionally, HomB protein also assists in hyper biofilm formation and antibiotic resistance thereby likely to enhance bacterial survival by evading host immune responses and antibiotic treatments[6,7].

With the agreement of these studies, HomA and HomB can be considered as virulence markers of aggressive *H. pylori* virulent strains. However, the structural and functional characteristics and details of HomA and HomB have not been reported yet. Thus, it is not clear how these proteins contribute to ulcer or gastric cancer, and the exact molecular mechanism is not explored.

The present investigation study consists of the following main objectives:

1. To study the structural aspect of potential virulence factors, HomA and HomB outer membrane proteins of *H. pylori*. Methods involve bioinformatic tools, biophysical characterization to reveal important physical states, secondary structure content and 3D models of proteins. This information is likely to help in better understanding the role of HomA and HomB in *H. pylori* pathogenesis.
2. To investigate the molecular mechanism of HomA and HomB associated immune system modulation and consequences of the interaction between *H. pylori* and immune cells specifically B-cells. Here, we explored the possible molecular mechanism of

reduced antibody diversity in patients with *H. pylori*-associated gastric diseases.

3. To explore the potential of HomA and HomB to be utilized as prognosis and vaccine candidates. Here, we characterize the immunoinformatics properties, such as potential antigenic and immunogenic epitopes present on to the globular domain of HomA and HomB, which are likely to activate host immune response. This information further can be utilized for therapeutic applications.

Biophysical characterization of the homodimers of HomA and HomB, outer membrane proteins of *Helicobacter pylori*

OMPs play a crucial role in several important physiological functions like ionic regulation, cell adhesion, host-pathogen interaction as well as pathogenesis, and structural information of these OMPs is vital for understanding their function and regulation. The present study provides several structural insights for OMPs of the Hom (*Helicobacter* outer membrane) family members of *H. pylori*, HomA and HomB. HomB is reported to be expressed at the *H. pylori* outer membrane and participates in bacterial adherence and inflammation.

Interestingly, *in-silico* studies demonstrated that HomA and HomB possess characteristics of β-barrel OMP, such as a signal peptide at the N-terminal and β-barrel signal at the C-terminal. HomA and HomB both have mixed secondary structure content, nevertheless, β-sheets are predominantly present in both proteins. Additionally, HomA and HomB localize in the outer membrane with 8 transmembrane antiparallel N+C-terminal β-strands connected by the large surface-exposed globular domain. Furthermore, the secondary structure was confirmed with ATR-FTIR, amid I spectra for HomA and HomB both contain mixed α helices and β-sheets spectra. CD spectra showed HomA and HomB both favors β-barrel structure and the addition of lipids and detergents to the denatured HomA and

HomB rearranged proteins favoring antiparallel β-sheets. Interestingly, HomA and HomB were stable at a pH range from 3 to 11 which is likely to assist in low pH environment adaptation. Additionally, both proteins start unfolding at 2M of urea, the addition of denatured HomA and HomB to lipids, and detergents refold which was observed in the tryptophan fluorescence spectra.

We performed size exclusion chromatography for HomA and HomB and observed peaks that correspond to dimer and monomer. Moreover, incubation of HomA and HomB with detergents shows oligomerization/aggregation of proteins, however, incubation with lipids shows peaks corresponding to dimer and monomer. Furthermore, the solution structure analysis of HomA and HomB using small-angle X-ray scattering (SAXS) experiments confirmed that both HomA and HomB form homodimers. Thus, the unique predicted 3D model of HomA and HomB provide crucial structural insights (**Fig. 2**) thereby our studies will help in a better understanding of *H. pylori* pathogenesis and host-pathogen interactions via OMPs.

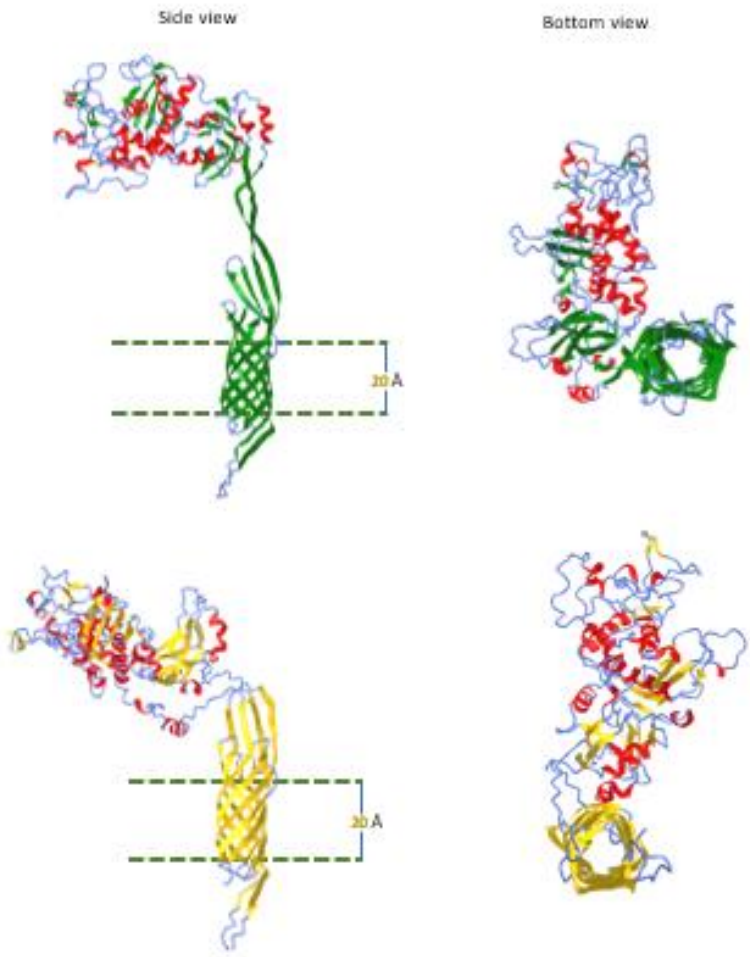

Figure 2. Alphafold 2 3D structure prediction of HomA and HomB.. 3D structure predictions of HomA and HomB (without signal peptide) using Alphafold2, side and bottom view for HomA from left to right β-sheets (green), α-helices (red) and coils (blue); side and bottom view for HomB from left to right β-sheets (yellow), α-helices (red) and coils (blue).

HomA and HomB, outer membrane proteins of *Helicobacter pylori* down-regulate Activation-induced cytidine deaminase (AID) and Ig switch germline transcription and thereby affect class switch recombination (CSR) of Ig genes in human B-cells

OMPs play a significant role in bacterial pathogenesis. The significance of HomA and HomB has been associated with gastric malignancies, both HomA and HomB are reported to help in the adherence to host cells. Here in this report, we have analysed the potential role of the HomA and HomB in B-cell's functions. HomA

and HomB treated cells shows repression of AID at mRNA and protein level, which is a crucial player in generating antibody diversity. To reveal the possible cause of AID suppression, we investigated the expression levels of known AID transcription regulators. NFκB, cMYC, PAX5, SMAD3 and STAT6 acts as transcriptional activators of AID, whereas cMYB and E2F1 act as transcriptional repressors of AID. Although the activators of AID were largely unchanged in the HomA and HomB stimulated cells, interestingly, we observed significant upregulation in the expression of an AID repressor, cMYB, which could be responsible for the reduced AID levels in these cells. Since, AID is one of the important factors of CSR, suppression of AID and commutatively reduced expression of Ig switch germline, likely affects the CSR process. Thus, we analysed the levels of mature CSR immunoglobin products of IgM, IgA and IgG.

Interestingly, we observed reduced IgA:IgM and IgG:IgM expression in HomA and HomB treated cells as compared to the unstimulated control cells. We also checked expression levels of the other two important CSR factors, BATF and HOXC4, and observed that the expression of both was not affected in HomA and HomB treated cells. A subset of B-cells namely B_{reg} cells take part in B-T cells communication and usually these cells show T-cell inhibitory consequences *via* secreting IL10, IL35, TGFβ and PDL1. We observed upregulated levels of PDL1, IL10 and IL35 in HomA and HomB treated cells. These observations suggest an important role of HomA and HomB in polarising B-cells to B_{reg} cells. T-cells inhibition by B_{reg} cells could be the important mechanism used by pathogens to evade the host immune system or disruption of B-Tcells communication. Our report suggests the unique molecular mechanism (**Fig. 3**) of the dual-functional role of HomA and HomB, OMPs of *H. pylori*, in suppressing antibody diversity and expressing the T-cells inhibitory markers. This dual role of OMPs can help bacteria in survival and likely assist in escaping the host immune system.

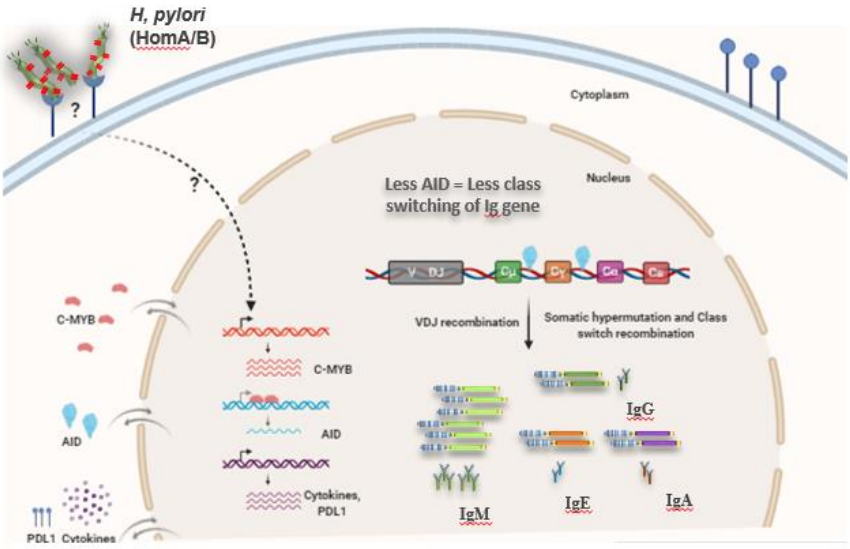

Figure 3. Molecular mechanism of B-cell response with HomA and HomB. Stimulation of HomA and HomB triggers up-regulation of cMYB, one of the silencers of AID which further binds to the AID regulatory region and suppresses AID expression in B-cells. In addition, HomA and HomB also suppress IgG and IgA germline transcription which together with suppressed AID leads to less CSR. Interestingly HomA and HomB also upregulates T-cell inhibition marker PDL1 and cytokines IL10 and IL35.

Immunoinformatic characterization of globular domains of HomA and HomB, for potential sub-unit vaccine candidate against *Helicobacter pylori*

Gastric cancer is the second most common cause of cancer-associated deaths[8]. Chronic gastritis is the major cause of human gastric cancer caused by the Gram-negative bacterium *Helicobacter pylori*. The long-term persistence of *H. pylori* can stimulate a severe immune response that can damage the mucosal lining. Chronic inflammation due to *H. pylori* infection makes it a potentiate agent of acute and chronic gastritis, peptic ulcer disease (PUD), and two forms of cancers, namely, mucosa-associated lymphoid tissue (MALT) lymphoma and gastric adenocarcinoma[9-12].

In addition, HomB has been found to be associated with drug resistance and hyper biofilm formation and can be considered as virulence markers. We have reported that HomA and HomB consist of small β-barrel with a surface-exposed globular domain. In this study, we have explored and characterized the immunological properties of HomA and HomB.

The surface-exposed globular part of HomA and HomB was used for the prediction of the B-cell and T-cell epitopes, which indicates the possible accessibility by the immune system. Continuous linear B-cell epitopes were predicted using BCPred, and FBCpred tools. The epitope length varies from 9-16 amino acids (aa) for all three predictions. We predicted conformational B-cell epitopes which happen to be discontinuous epitopes, generated through close positioning of aa present onto the folded 3D structure of proteins. Ellipro server predicted a total of 10 epitopes with a maximum score of 0.91 and a minimum of 0.52. The minimum threshold was taken as 0.6. We have also checked different epitopes characteristics such as antigenicity, flexibility, surface accessibility, hydrophilicity, and beta-turn. Further, we have docked globular domains of HomA and HomB

with TLR4 structure to assess the possibility of TLR4 based immune system activation by antigen-presenting cells.

The study revealed the B-cell and T-cell epitopes of globular domains of HomA and HomB. Interestingly, these globular domains also bind with TLR4 on B-cells which indicated initiation of immune cell activation process (**Fig. 4**). These observations provide promising utilization of HomA and HomB as vaccine subunits, developing them as therapeutics and for other clinical applications.

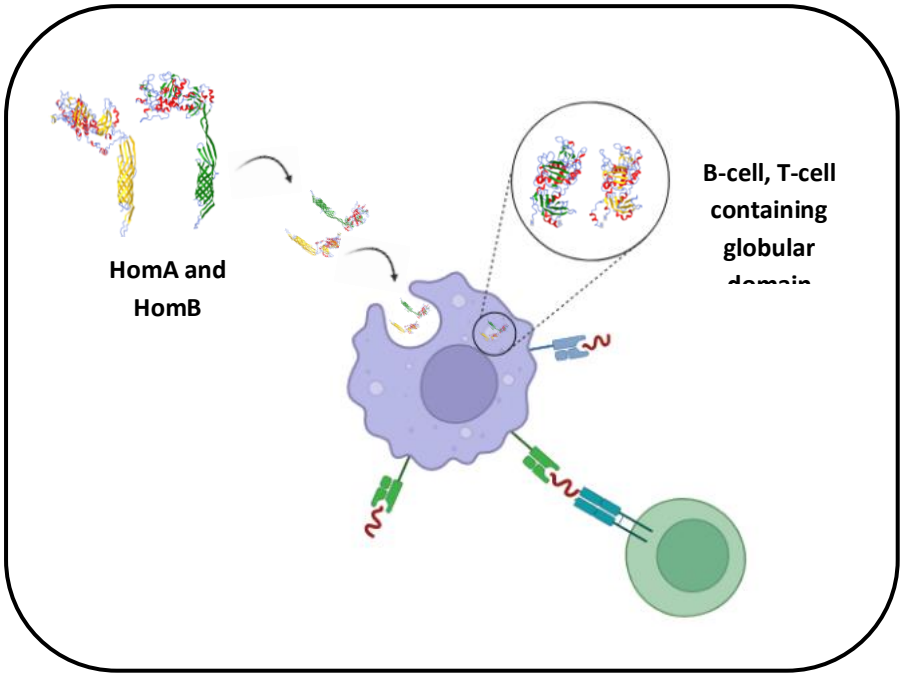

Figure 4. Potential predicted B-cell and T-cell epitopes on HomA and HomB. A graphical representation of the B-cell and T-cell predicted linear and conformational epitopes present onto the surface exposed globular domains of HomA and HomB which subsequently processed and presented onto the cell surface by antigen processing cells (APCs) to other immune cells.

Scope of the thesis

The thesis is composed of 6 chapters. Chapter 1 of the thesis contains a review of the relevant literature which brings up the objectives of the present investigation. In Chapter 2, experimental methodologies and materials are described. The observations and outcomes of the studies reveal structural properties of HomA and HomB, the molecular mechanism of suppression of antibody diversity, immune system escape and potential immunoinformatics properties of HomA and HomB are presented in Chapter 3, 4 and 5, respectively. Chapter 6 concludes the present study and outcomes, with a summary and scope for future work, which will provide insights into the multifunctional role of HomA and HomB with the great potential for development and utilization for therapeutic applications.

The present study provides a better understanding of the outer membrane protein's contribution to the pathogenesis of *H. pylori*. Our results revealed that HomA and HomB are made up of unique topology which is likely to play a crucial role in bacterial adaptation and survival in adverse conditions. In addition to that HomA and HomB also suppresses AID and Ig germline transcription in B-cells, leading to compromised antibody diversity and overexpression of T-cell inhibition markers which is likely to assist *H. pylori* in escaping cellular immunity of the host, thus prolonged survival, and a chance to causing chronic infection. Furthermore, this study also provides insights about immunoinformatic properties of HomA and HomB where these proteins can be utilized as potential prognosis and vaccine candidates for *H. pylori*-associated gastric diseases and MALT lymphoma.

References

1. Tamrakar A, Singh A, Choudhary M, Kodgire P. Fighting with Gram-negative enemy: Can outer membrane proteins aid in the rescue. Chem. Biol. Lett. 2017 Jan 10;4(1):9-19.
2. Hussein, N.R. A study of *Helicobacter pylori* outer-membrane proteins (*hom*) A and B in Iraq and Turkey. *J. Infect. Public Health* 2011, *4*, 135–139.
3. Kang, J.; Jones, K.R.; Jang, S.; Olsen, C.H.; Yoo, Y.J.; Merrell, D.S.; Cha, J.H. The geographic origin of *Helicobacter pylori* influences the association of the *hom*B gene with gastric cancer. *J. Clin. Microbiol*. 2012, *50*, 1082–1085.
4. Alm RA, Bina J, Andrews BM, Doig P, Hancock RE. Comparative genomics of Helicobacter pylori: analysis of the outer membrane protein families. *Infect. Immun.*, 2000 Jul 1;68(7):4155-68.
5. Oleastro M, Cordeiro R, Ferrand J, Nunes B, Lehours P, Carvalho-Oliveira I, Mendes AI, Penque D, Monteiro L, Mégraud F, Ménard A. Evaluation of the clinical significance of *homB* a novel candidate marker of *Helicobacter pylori* strains associated with peptic ulcer disease. *J. Infect. Dis.*, 2008 Nov 1;198(9):1379-87.
6. Servetas SL, Doster RS, Kim A, Windham IH, Cha JH, Gaddy JA, Merrell DS. ArsRS-dependent regulation of homB contributes to Helicobacter pylori biofilm formation. Frontiers in microbiology. 2018 Aug 2;9:1497.
7. Haddadi MH, Negahdari B, Asadolahi R, Bazargani A. Helicobacter pylori antibiotic resistance and correlation with cagA motifs and homB gene. Postgraduate medicine. 2020 Aug 17;132(6):512-20.
8. Neugut, A. I., M. Hayek, and G. Howe. 1996. Epidemiology of gastric cancer. *Semin. Oncol.* 23:281–291.
9. Matysiak-Budnik, T., and F. Megraud. 1997. Epidemiology of *Helicobacter pylori* infection with special reference to professional risk. *J. Physiol. Pharmacol.*48(Suppl. 4):3–17.

10. Blaser MJ. Helicobacter pylori and gastric diseases. *Bmj*. 1998 May 16;316(7143):1507-10.Ernst, P. B., and B. D. Gold. 2000. The disease spectrum of *Helicobacter pylori*: the immunopathogenesis of gastroduodenal ulcer and gastric cancer. *Annu. Rev. Microbiol.* 54:615–640.

11. Parsonnet J, Friedman GD, Vandersteen DP, Chang Y, Vogelman JH, Orentreich N, Sibley RK. Helicobacter pylori infection and the risk of gastric carcinoma. *N. Engl. J. Med.* 1991 Oct 17;325(16):1127-31.

LIST OF PUBLICATIONS

(A) Publications from PhD thesis work:

1. **Tamrakar A**, Singh AK, Chaudhary M, and Kodgire P*. Fighting with Gram-negative Enemy: Can Outer Membrane Proteins Aid in the Rescue? *Chem. Biol. Lett.*, 2017, 4(1): 9-19. (Impact factor: 4.1)
2. **Tamrakar A**, Singh R, Kumar A, Makde R D, Ashish and Kodgire P*. Biophysical characterization of the homodimers of HomA and HomB, outer membrane proteins of *Helicobacter pylori*. (In press). *Scientific Reports*. 2021 (Impact factor: 5.1)
3. **Tamrakar A**, Kodgire P*. HomA and HomB, outer membrane proteins from *Helicobacter pylori* down regulates Activation-induced cytidine deaminase (AID) and affects class switch recombination (CSR) of Ig genes in human B-cells. *Molecular Immunology*. 2021 (Impact factor: 4.4)
4. **Tamrakar A**, Kodgire P*. Immunoinformatic characterization of globular domains of HomA and HomB, for potential sub-unit vaccine candidate against *Helicobacter pylori***.** (Manuscript in preparation)

(B) Other publications during PhD:

1. Jaiswal A, Singh AK, **Tamrakar A**, and Kodgire P*, Unfolding the role of splicing factors and RNA debranching in AID mediated antibody diversification, *Int. Rev. Immunol.*, 2020, 14:1-18. (Impact factor 4.5)
2. Singh AK, **Tamrakar A**, Jaiswal A, Kanayama N and Kodgire P*, SRSF1-3, a splicing and somatic hypermutation regulator, controls transcription of IgV genes via chromatin regulators SATB2, UBN1 and histone variant H3.3, *Mol. Immunol.*, 2020, 119:69-82. (Impact factor 4.4)
3. Singh AK, **Tamrakar A**, Jaiswal A, Kanayama N, Agarwal A, Tripathi P and Kodgire P*, Splicing regulator SRSF1-3 that controls somatic hypermutation of IgV genes interacts with

Topoisomerase 1 and AID, *Mol. Immunol.*, 2019, 116:63-72. (Impact factor: 4.4)

4. Choudhary M, **Tamrakar A**, Singh AK, Jain M, Jaiswal A and Kodgire P*, AID Biology: A Pathological and Clinical Perspective, *Int. Rev. Immunol.*, 2018, 37(1):37-56. (Impact factor: 4.5)

TABLE OF CONTENTS

LIST OF FIGURES

Chapter 4: HomA and HomB, outer membrane proteins of *Helicobacter pylori* down-regulate Activation-induced cytidine deaminase (AID) and Ig switch germline transcription and thereby affect class switch recombination (CSR) of If genes in human B-cells

LIST OF TABLES

NOMENCLATURE

Hom	*helicobacter* outer membrane
AID	activation-induced cytidine deaminase
CSR	class-switch recombination
SHM	somatic hypermutation
TLR	Toll-like Receptor
Th1	T-helper Cell 1
TNFα	Tumor Necrosis Factor alpha
DAPI	4′,6-diamidino-2-phenylindole
EBV	epstein-Barr virus
BSA	bovine serum albumin
cDNA	complementary DNA
ChIP	chromatin immunoprecipitation
IFN-γ	interferon-γ
ILs	interleukins
MYC	myc avian myelocytomatosis oncogene
NF-κ B	nuclear factor-κ B
PKA	protein kinase A
RAG	recombination-activating gene
TGF-β	transforming growth factor
VJ	variable and joining region
AP1	Activator Protein 1
APC	Antigen Presenting Cells
Co-IP	Co-Immunoprecipitation
DMSO	Dimethyl Sulfoxide
GAPDH	Glyceraldehyde-3-Phosphate Dehydrogenase
LPS	Lipopolysaccharide
PAMP	Pathogen Associated Molecular Pattern
PDB	Protein Data Bank
q-RTPCR	Quantitative Real-Time PCR
ROS	Reactive Oxygen Species

ACRONYMS

mAB	monoclonal antibody
ml	milli litre
μL	micro litre
$^{\circ}C$	degree centrigrade
mM	milli molar
cmc	critical micelle concentration
μM	micro molar

Chapter 1

Chapter 1
Introduction and literature review

1.1 Gram-negative bacteria

We are surrounded by incredible kinds of living microorganisms that are invisible to our naked eyes and present almost everywhere. These microorganisms are classified based on different parameters, such as their habitats, environmental conditions, mode of nutrition and morphology. Several of these microbes live with us and within us, and are vital for our survival, as they protect the skin from the external parasites, aid in the synthesis of vitamins, digestion of food and nutrient absorption, as well as train the immune system to fight against infectious agents. Nevertheless, some of these microbes can cause infections in humans. These pathogenic microbes can enter our body through the ingested food, cuts and wounds, insect bites, etc. and infect the host for their survival and reproduction. In response to the infections caused by these pathogens, our immune system gets activated to fight against them. After entering into the body, pathogenic bacteria interact with the host cells and induce the production of several inflammatory molecules, sometimes this inflammation gets irregular or uncontrolled, leading to inflammation storms and causing severe sepsis and septic shocks.

Gram-negative bacteria have a unique outer membrane structure, which is absent in Gram-positive bacteria. The outer membrane of Gram-negative bacteria has three distinct layers: the inner cell membrane, which is in contact with the cytoplasm of bacteria, a peptidoglycan stratum that is sandwiched in between, and an outer membrane which is the outermost layer of bacteria that deals with outer biotic and abiotic factors (**Fig. 1.1**). Lipopolysaccharide, a glycolipid moiety, is attached to the outer surface of the outer membrane of Gram-negative bacteria, which also interacts with the outside environment. The outer membrane also has some embedded

proteins which transport molecules across the membrane, some of them perform enzymatic activities, whereas some lipoproteins present in the inner leaflet of the outer membrane anchor in the peptidoglycan stratum. Conversely, Gram-positive bacteria possess two layers of membrane, thick peptidoglycan as an outermost layer and an inner cell membrane, whereas it completely lacks the outer lipid bilayer membrane that is present in Gram-negative bacteria.

1.2 Structural insights of Outer membrane proteins (OMPs)

The OMPs are categorized into three groups; first: nonspecific proteins which transport small inorganic molecules, and they generally have 8 to 16 β-strands, second: substrate-specific proteins which have 18 to 22 β-strands, and third: porins. OMPs are involved in several cellular functions, such as maintenance of cell structure, transport of nutrients, efflux of bactericidal agents as well as adhesion to the host cell. Typically, most of the bacterial proteins including the inner membrane proteins contain α-helices and are composed of hydrophobic amino acids. On the other hand, OMPs have completely different structures. They are composed of unique antiparallel amphipathic β-strands. In these β-strands, hydrophobic amino acid residues are exposed to the surface lipid environment to meet the hydrogen bonding requirement of the membrane with the outer environment and to perform several important biological tasks. In contrast, the hydrophilic residues are present in the interior of protein which forms an aqueous pore in porins (Koebnik *et al* 2003). Interestingly, the β-barrel shows heat modifiable property when treated with 2% SDS. In fact, native and heat-denatured forms of protein show differential migration in the gel (Dekkar *et al* 1995, Nakamura *et al* 1976). It seems that the β-barrel structure of protein present in the outer membrane, and not in the inner membrane, is due to the biogenesis and translocation machinery of these proteins. These barrel-shaped proteins are classified on two parameters: the number of strands present in the β-sheet (n) and sheer number(s), which is a measure of stagger of strands in the β-sheet. These parameters specify major geometrical features of the β-barrel proteins.

In *E. coli*, a few of the OMPs are expressed at a high level, e.g. OmpA and general porins. Conversely, some of the porins are expressed in specific conditions such as stress, nutrients depletion, e.g. PhoE and LamB, TonB-dependent receptor (e.g. FhuA and FepA) proteins involved in the biogenesis of flagella and pili, (Macnab *et al* 1999, Soto *et al* 1999) in addition to enzymes, such as OmpT protease (Magel *et al* 1994) and Phospholipase-A (Demot *et al* 1994). Interestingly, some of the OMPs are used as the receptor for adhesion by bacteriophages and bacteriocins. In fact, the iron-siderophore transporter FhuA was first recognized as a protein that is necessary for infection by phage T1 and, named TonA (Tone protein A). Likewise, maltoporin was initially identified as a receptor for phage λ. 1 Bacterial OMPs have been studied in great detail for many years with the help of X-ray crystallography, (Macnab *et al* 1999) and a few important OMPs from Gram-negative infectious bacteria and their crucial structural features are described in this report.

OmpA, one of the major OMPs of *E. coli,* is expressed at a very high level. It is important for the virulence and integrity of the bacterial cell surface. It has two domains an N-terminal domain of 170 amino acid residues, which serves as a membrane anchor (**Fig. 1.3A**) and a C-terminal domain of 155 amino acid residues, which is located in the periplasmic space and has been proposed to interact specifically with peptidoglycan layer (Soto *et al*, 1999, Mangel *et al* 1994). Studies with recombinant OmpA from *Klebsiella pneumoniae* showed that kbOmpA interacts via cell surface receptors of the macrophages as well as the dendritic cells, and thereby activates these cells. (Dakker *et al* 2000) kbOmpA is involved in cellular recognition by the scavenger receptors, such as SRC-1 and LOX-1, as well as TLR2, leading to cellular activation of innate immunity (Schulz *et al* 2002). Another important OMP in Gram-negative bacteria is OmpX. Schulz laboratory proposed a three-dimensional structure of OmpX as a small β-barrel membrane protein (Poolman *et al* 1996) (**Fig. 1.3B**). OmpX protein family is highly conserved and plays an important role in virulence by

neutralizing the host defence mechanisms (Demot *et al* 1994). OmpX homologue proteins are reported in different microbes, such as, Ail from *Yersinia enterocolitica* promotes adhesion as well as entry into eukaryotic cultured cells, whereas, *Salmonella typhimurium* produces two related proteins, PagC and Rck, which have an important role in their survival within the macrophages. Outer membrane Phospholipase-A (OMPLA) is an enzyme present in Gram-negative bacteria and likely responsible for membrane disruption during host cell invasion and thus plays the role of a virulence factor in some bacteria and fungi. Phospholipase-A is involved in the colicin release and virulence of *Campylobacter* and *Helicobacter* strains. It is the only outer membrane enzyme whose three-dimensional structure has been solved. Its structure is composed of 12 transmembrane βstrands, and the barrel interior is polar with a hydrogen-bonding network, which provides a rigid structure (**Fig. 1.3C**). The two polypeptide termini and the surface-exposed loops L1, L4 and L6 obstruct the barrel from outside, thus excluding a pore function as it was proved by black lipid bilayer experiments (Demot *et al* 1994, Koebnik *et al* 1995). Calcium ions act as an activator for Phospholipase-A. As it binds with calcium ions, Phospholipase-A acquires a dimeric form being catalytically active, however, normally it exists in a monomeric form in the outer membrane (Jeannin *et al* 2000). The monomeric protein has three polar amino acid residues (Tyr-92, Gln-94 and Ser-96) at its membrane-exposed surface, and these residues allow them to partition into the hydrophobic membrane environment. Upon dimerization, this network is modified to involve another hydrogen bond between the side-chains of Gln94 of both monomer units. This strict conservation of residue suggests that it plays an important role in the functional dimerization of OMPLA (Koebnik *et al* 1995).

Some bacterial OMPs are called porins, as they act as pores and molecular filters, which form channels with various degrees of selectivity (Schulz *et al* 2002). Porins have a super secondary protein structure that forms β-barrels and is composed of typically 14, 16 or 18

anti-parallel β-sheets. Typically, most of these porins have 16 or 18 strands and the general motif of their structural architecture is the closure of the barrel by the pairing of the first and last β-strand in an antiparallel way. These are connected by eight or nine long loops, facing towards the extracellular side, and seven or eight small turns embedded in the periplasmic space (**Fig. 1.3**). In all porins, the β-barrel center is formed by an inserted long loop L3 that is not exposed to the cell surface but folds back into the barrel and forms a pore-like structure that contributes to the permeability of the membrane. This loop contains a PEFGG amino acid sequence motif which is highly conserved among the enterobacterial porins (Jeanteur *et al* 1991). As expected, the substitution of the two glycine residues in the PEFGG sequence results in altered channel characteristics (Gelder *et al* 1997). Porins, which have 16 strands are called general or non-specific porins and allow the diffusion of hydrophilic inorganic molecules without any specificity, whereas, the 18 strands porins are substrate-specific porins and have particular substrate specificity, such as sugar specific porins (ScrY and LamB). Some of the porins, such as OmpG or CymA, have 14-strand monomeric and quaternary structures. Usually, porins are passive diffusion channels with a pore diameter ranging from 15 Å for the general porins to 6 Å for the highly selective porins (Galdiero *et al* 2012). There are some OMPs having higher molecular weight, containing a 22 stranded β-barrel, which are active iron transporters, e.g. FhuA (**Fig. 1.3G**) and FepA (TonB apparatus) (**Fig. 1.3H**). These porins play a unique role in overcoming the problem of lack of ATP or other energy carrier sources for transport of any solute against a concentration gradient in the periplasm.

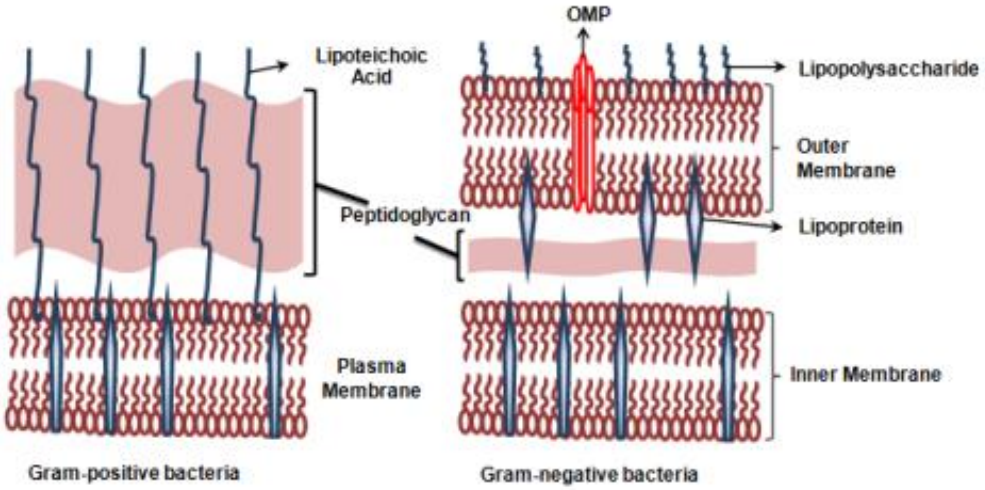

Figure 1.1 Schematic representation of Gram-negative and Gram-positive cell membrane. Gram-positive bacteria have a thick peptidoglycan layer embedded with lipoteichoic acid, whereas Gram-negative bacteria have an additional lipid bilayer as an outer membrane embedded with outer membrane protein (OMP) and a thin peptidoglycan layer in the middle.

Molecular analysis of several OMPs reveals that they have high sequence similarities and conserved patterns. Conserved sequences are present mainly in the β-strand structure. For example, five enterobacterial OmpA have 74% identity within the β-sheets and 54% amino acid identity within the periplasmic turns as well as surface-exposed loops (Braun *et al* 1984). In the same way, four Phospholipase-A proteins show 71% identity in the turn residues and 76% identity in the loop residues, whereas 83% of their β-strand residues are strictly conserved (Brok *et al* 1994). A similar trend is also observed with four enterobacterial FhuA proteins, which have both 52% amino acid identity within the periplasmic turns and 32% identity within the surface-exposed loops and 56% identity within the β-sheet (Killmann *et al* 1998). Structural analysis of β-barrels of various OMPs shows that the interior residues are more conserved than the surface exposed residues (OmpA: 77% versus 70%; OMPLA: 85% versus 82%; FhuA: 61% versus 51%; OmpX homologues: 33% versus 14%). The OmpX, a family of virulence-related membrane proteins, shows that the membrane-spanning part of the proteins is better conserved than the extracellular loops. OmpX shows 86% sequence identity with OmpK17 from *K. pneumoniae* and 84% identity with OmpX from *E. cloacae*. The sequence identities with Ail from *Y. enterocolitica*, PagC and Rck from *S. typhimurium* are 45%, 39% and 38%, respectively. Following an earlier model of OmpA, it is suggested that *E. cloacae* OmpX consists of a similar eight-stranded β-barrel with short periplasmic and longer extracellular loops (Vogel *et al* 1986, Stoorvogel *et al* 1991). Here the percentage sequence identities with OmpK17, OmpX (*E. cloacae*), Ail, Rck and PagC are 100%, 100%, 71%, 69% and 67%, respectively. Interestingly, the OmpX protein family has a specific conserved signature sequence Gly-X-Asn-X-Lys-Tyr-Arg-Tyr-Glu, which is located in strand β-2 within the barrel. Other OMPs families, e.g. Omp21 from *Comamonas acidovorans*, the Opa proteins from Neisseriaceae and PorF from *Pseudomonas aeruginosa* also have 8 stranded antiparallel β-barrels (Baldermann *et al* 1998) and are structurally related to OmpX and

OmpA. All OMPs of bacteria have a common C-terminal consensus sequence X-Z-X-Z-X-Z-XTyr-X-Phe (where X is any amino acid and Z is a nonpolar residue) (Vogel *et al* 1986). In *E. coli* porin OmpF is closely homologous to the porins PhoE (Cowan *et al* 1992) and OmpC (Basle *et al* 2006). These three porins help cells to adjust in different environmental conditions; additionally, PhoE allows an efficient uptake of phosphate. OmpC from *E. coli* shows homology with OmpK36 from *Klebsiella pneumoniae*, whereas Omp32 from *Comomonas acidovorance* have homology with porin from *Paracoccus denitrificans*, and share homologous general features (Dutzler *et al* 1999). It seems the core residues of the β-barrel in most of the OMPs are stringently conserved during evolution.

1.3 Functional insights of Outer membrane proteins (OMPs)

Several proteins are present in the outer membrane of Gram-negative bacteria and contribute about 50% of the outer membrane mass. Proteins of the outer membrane assume a β-barrel secondary structure that mediates transport of molecules across the membrane, which also serves as a filter. Additionally, these β-barrel structures are involved in the host-pathogen interactions. A few integral proteins, such as outer membrane protein A (OmpA), are expressed at a high level in *E. coli*, whereas another class of OMPs, such as LamB and PhoE, are temporally regulated and expressed in the specific environmental conditions. Interestingly, some of them also perform enzymatic activities e.g. Phospholipase-A (Koebnik *et al* 2000).

The molecular mechanism of interaction between the OMPs and immune cells is not well understood. It is proposed that OMPs may be activating the host cells similar to that of the LPS, but not via an identical mechanism (Galdiero *et al* 2003). The intracellular pathway of any receptor-ligand interaction is a complex and sequential network of biochemical events,

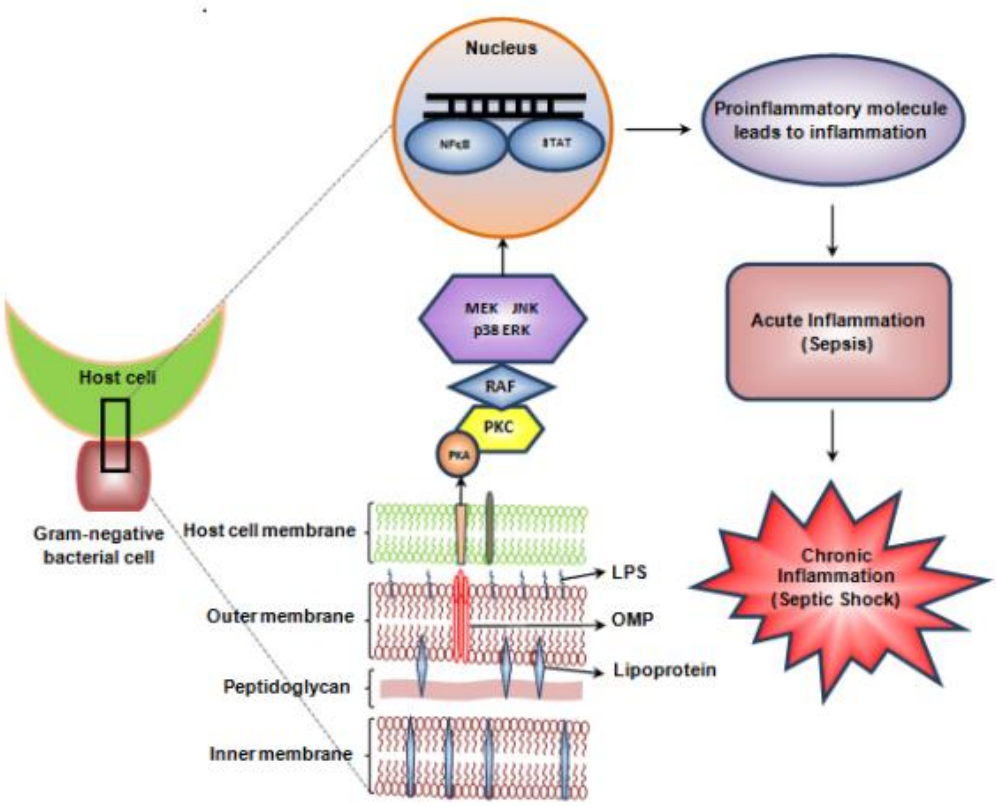

Figure 1.2. Signal transduction pathway induced by OMPs. OMPs interact via host transmembrane receptors and stimulate protein kinase A (PKA), protein kinase C (PKC) thus activating downstream effectors, such as, RAF, MEK, p38, ERK, JNK, which induces nuclear localization of NFκB and thus stimulates the production of inflammatory molecules. Uncontrolled inflammation leads to sepsis which ultimately can result in organ failure.

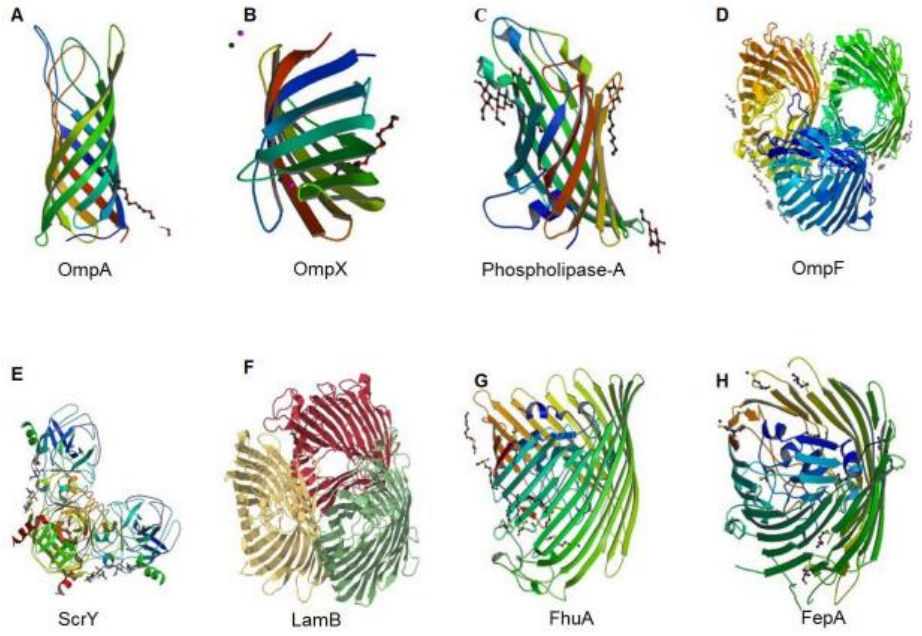

Figure 1.3. The graphical representation of OMPs by X-ray crystal structure shows β-sheet connected via amino acid loops and forms β-barrel structure. (A) OmpA (PDB code: 1BXW) and (B) OmpX (PDB code: 1QJ8) are small β-barrel proteins; (C) Phospholipase-A (PDB code: 1QD5) acts as an enzyme; (D) OmpF (PDB code: 2OMF) is general non-specific porin which forms trimer β-barrel structure; (E) ScrY (PDB code: 1AO5), (F) LamB (PDB code: 1MAL), (G) FhuA (PDB code: 1BY3) and (H) FepA (PDB code: 1FEP) are trimer βbarrel structure substrate-specific large porins.

leading to the expression of the target genes. Upon adhesion of bacteria to the host cell, several cytoplasmic signal transduction pathways are triggered, in which the mitogen-activated protein kinase (MAPK) pathway is especially activated (Evans *et al* 1998, Rosenshine *et al* 1992). Binding of the extracellular signals, such as OMPs, triggers pathways such as MAPK, serine-threonine kinases, c-Jun N-terminal kinases (JNK) and extracellular signal-regulated kinases (ERK), (Davis *et al* 2000) which subsequently activate several transcription factors, such as, activating protein-1 (AP-1) and nuclear factor kappa B (NFκB) (Karin *et al* 1997). NFκB is a dimeric transcription factor that turns on the expression of inflammatory and immunity-related genes. Typically, NFκB is present in the cytoplasm in a resting state, combined with IκB, an inhibitor of NFκB. Extracellular signals, such as OMPs, activate the MAPK pathways, consequently, IκB is phosphorylated and eventually degraded through ubiquitination. Subsequently, NFκB forms a dimer that translocates into the nucleus, binds to target genes and thereby turns on the expression of genes, which are mainly involved in the inflammatory and immunological responses (Galdiero *et al* 2002) (**Fig 1.2**). It is reported that OmpA from *Shigella flexineri* induces the release of pro-inflammatory cytokines through activation of NFkB via toll-like receptor-2 (TLR-2). Moreover, OmpA also plays a critical role in the development of Th1 cells by induction of IFN-γ in CD4+ T cells through IL-12 production in the macrophages (Pore *et al* 2012). It has been reported that TLR1, TLR2, TLR6, and MD2 receptors are involved in the recognition of a broad range of OMPs (Massari *et al* 2002, 2006, Rau *et al* 2003 Banerjee *et al* 2008). Similarly, Galdiero *et al*, reported that Hib from *Haemophilus influenzae* and PorB from *Neisseria* are recognized by TLR-2 (Galdiero *et al* 2004). As the surface-exposed loops of the OmpA play a fundamental role in the pathogenesis of meningitis, this feature of OMP may help to design therapeutic strategies against the disease (Mittal *et al* 2011). The loop 1 and 2 of OmpA play an important role in the survival of *E. coli* in the dendritic cells and the

Table 1. List of outer membrane proteins of Gram-negative bacteria involved in infections.

Gram-negative bacteria	Diseases	Outer membrane protein(s)
Bordetella	Pertussis	P70
Borrelia burgdoferi	Lyme disease	OspA, OspB, OspC (lipoprotein)
Brucella	Brucellosis	Omp10, Omp16, Omp19 (lipoprotein)
Francisella	Tularemia	FopA
Haemophilus	Pneumonia, bacteremia, meningitis, epiglottitis, septic arthritis, cellulitis, otitis media, purulent pericarditis, and other less common infections such as endocarditis and osteomyelitis	OmpP6, Hib
Helicobactor pyroli	Gastritis[#]	AlpA, AlpB, BabA, SabA, HopZ
Klebsiella	Pneumonia, bloodstream infections[#]	OmpK36
Leptospira	Leptospirosis (No widely useful vaccine available)	Lip32, Lip36, Lip41, Lip48, OmpL37
Neisseria gonorrhoeae, meningitides	Sexually transmitted disease Gonorrhea[#]	OpcA, OpcB, OpcD, Opa Protein rA and B, protein п, protein ш
Pseudomonas	Pneumonia, urinary tractinfections (UTIs), and bacteremia[#]	OprL, OprC, OprE, OprF, OprG, OprH, PorF
Rickettsia	Spotted and typhus fever[#]	rOmpB, rOmpA
Salmonella	Salmonellosis, typhoid fever, food poisoning, gastroenteritis, enteric fever	OmpA sal, PagC, Rck
Shigella	Shigellosis, diarrhea	OmpA
Triponema pallidum	Syphilis, bejel, pinta, and yaws[#]	TP0136
Vibrio	Cholera	OmpU
Yersinia	Yersiniosis	YopD, YopB, YopM, YopT, Ail

#No vaccine available.

loop 1 and 3 are essential for survival in the macrophages. Additionally, the loop 2 is involved in many of the host cell interactions and thus can be an effective target for immunization. Some common Gram-negative infectious bacteria and their OMPs have been listed in **Table 1**, which have been studied for their role in pathogenesis and host-pathogen interactions. Porins, interaction with the host immune system induces inflammation similar to the OMP-induced inflammation. Recognition of pathogenic bacteria by the host TLRs is the first step in the activation of the inflammatory responses of the innate immune system (Akira *et al* 2006, West *et al* 2006).

Porins are considered as pathogen-associated molecular patterns (PAMP) due to their ability to trigger signals via TLR molecules and other pattern recognition receptors. Similar to OMPs, porins are demonstrated to induce signal transmission, stimulate nuclear factors, thereby activating gene expression and finally leading to the release of cytokines (Massari *et al* 2003). It is reported that porins from *Salmonella enterica* serovar typhimurium induce the production of TNF-α, TGF, IL-6, and IL-1 by the macrophages, and IFN-γ and IL-4 by the lymphocyte cells. Furthermore, *Salmonella enterica* serovar typhimurium porin is reported to enhance the synthesis and release of IL-6 in U937 cells, in which NF-κB regulate the transcriptional activity of the IL-6 gene (Finamore *et al* 2009). Moreover, porin from *S. enterica* serovar typhimurium also induces transduction in mouse macrophages that leads to increased inositol triphosphate and intracellular Ca++ mobilization as well as Protein Kinase C (PKC) translocation to the membrane (Gupta *et al* 1999). In fact, it is reported that *S. enterica* serovar typhimurium porin induces tyrosine phosphorylation of ERK-1, PKA and PKC in U937 cells. Likewise, *Neisseria* porin stimulates tyrosine phosphorylation and affects the expression of B-7 co-stimulatory molecules (Massari *et al* 2003). Similarly, Hib, a porin from *Haemophilus influenza* induces an inflammatory response. It is reported that inoculation of Hib into the fourth ventricle of the brain induces expression of IL-1α, TNF-α and

MIP-2 mRNA at the inoculation site (Galdiero *et al* 2001). In short, OMPs are present in all the Gram-negative infectious bacteria and are involved in the stimulation of the host immune system. Moreover, these studies OMPs open wide opportunities for a better understanding of the pathogenesis and development of combating strategies (**Fig. 1.4**).

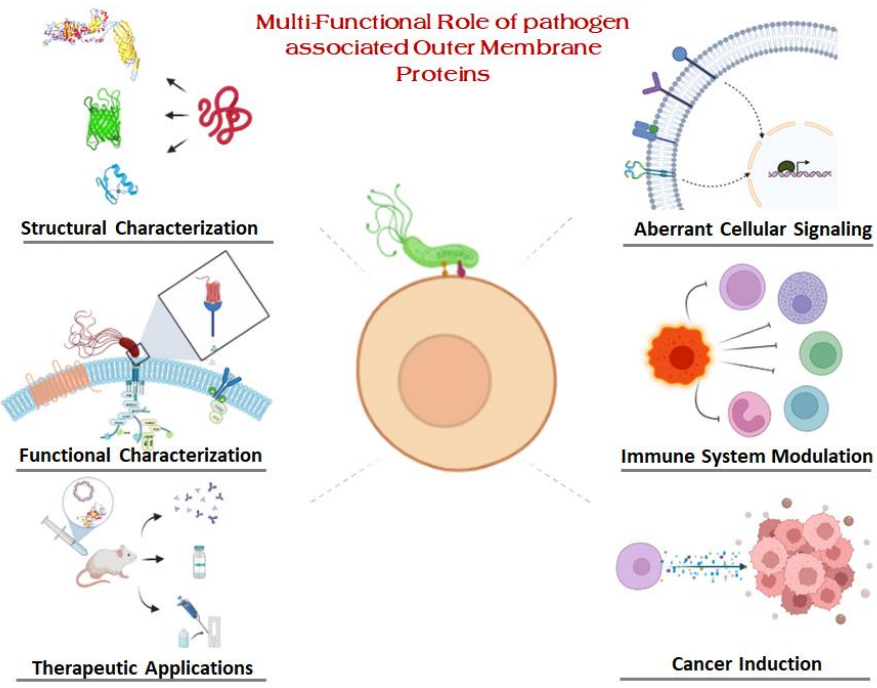

Figure 1.4 Multifunctional role of Outer membrane proteins (OMPs). Right panel from top to bottom, schematic representation of Host-pathogen interaction leading to host aberrant signaling, immune cells and communication system modulation, and cell signaling induction leading to cancer cell transformation. Left panel from top to bottom, identification, and structural and functional characterization of virulence factor (here OMPs) thereby using them as therapeutic targets such as monoclonal antibody therapy, vaccine, and inhibitors development.

1.4 Host Immune system

We are protected by the immune system from the pathogens such as bacteria, viruses, fungi and parasites, present outside the environment and continuously get in touch with us intentionally and unintentionally. The immune system is a system of collection of cells and array or biological process of cell-cell communication. The immune system simply can be categorised into two lines of defence, innate and adaptive immunity. Innate immunity works as a quick first line of defence for attacking pathogens which is generally non-specific (antigen-independent) in nature. Since the innate immune system is non-specific hence do not form memories thus reencounter of the same pathogen will not be remembered in future. Whereas the adaptive immune system is antigen-dependent and creates memories therefore it takes lag time in building immunity as the pathogens attack, but subsequent exposure to the same pathogen is rapidly neutralized due to developed immune memories. Both the immune system, innate and adaptive, are not exclusive but rather works as complementary to each other via communicating through cells and cytokines. Defects in either of them lead to impairment of effective immune system further leading to host vulnerability to pathogens (Turvey *et al* 2010, Bonilla *et al* 2010, Murphy *et al* 2007).

1.4.1Innate immunity

Majorly innate immunity comprises of the four types of defensive barriers namely, anatomic which includes skin and mucosa, physiological barriers mediated by temperature, pH and chemical mediators, inflammatory barriers include cytokines and chemokines which recruits the different cells and lastly endocytic and phagocytic barriers which involves variety of the cell to neutralize or kill the pathogens. In general, innate immunity to pathogens depends on pattern recognition receptors (PRRs) which allow innate immune cells to detect and respond to pathogens which commonly share structural patterns which are characterized as pathogen-associated molecular

patterns (PAMPs) such as lipopolysaccharides (LPS) present of bacteria surface and double-stranded ribonucleic acid (RNA) produced during viral infection. Cytokine production during and at the site of infection is the key hallmark of innate immunity which further recruits immune cells. Some of the important cytokines to bacterial infections are tumour necrosis factor (TNF), interleukin 1 (IL-1) and interleukin 6 (IL-6). Many times dysregulation of cytokines also leads to immunopathological conditions and is often associated with cytokine storm, sepsis, and autoimmune disease. Various cells participate in the innate immunity in response to pathogens such as NK cells (natural killer), macrophages and neutrophils, dendritic cells, mast cells, basophils, and eosinophils. Phagocytotic cells (neutrophils and macrophages) engulf microbes and kill them via many bactericidal, granules and enzymatic pathways (Turvey *et al* 2010).

1.4.2 Adaptive immunity

The adaptive immune system's primary function is to identify non-self antigens present on the pathogens. The innate immune system is critical in the development of follow-on adaptive immunity when innate immunity becomes ineffective. Adaptive immunity recognises antigens and targets pathogens and pathogens infected cells via generating immunologic effector pathways generating an immunologic memory for the subsequent infection and eliminating pathogens quickly. The adaptive immune system includes T-cells which directly attack pathogens or infected cells when activated by antigen-presenting cells (APCs), known as cellular immune response and B-cells which are part of humoral immunity and produces antibody (Bonilla *et al* 2010).

1.4.2.1 B-cells

B-cells originates and mature from hematopoietic stem cells in the bone marrow. B-cell can recognise antigen own self via unique antibody expressed on their surface. When B-cells are activated by a foreign antigen, undergo proliferation, and differentiate into antibody-

secreting plasma cells and memory B-cells. Upon antigen activation B-cells produces a wide variety of antibody from limited sets of immunoglobulin genes, this phenomenon is known as antibody diversity which is an exceptional feature of B-cells. Interestingly, this process begins even before encountering the antigens via the process of VDJ recombination. V(D)J recombination increases antibody repository by rearrangements of the variable (V), diversity (D) and joining (J) gene segments mediated by RAG recombinase (Oettinger *et al* 1990). In addition to that somatic hypermutation (SHM) and class switch recombination (CSR) further diversify antibodies upon antigen stimulation. SHM and CSR both are crucial processes in generating B-cell immune response, especially antibody production and diversification. Failing either of them leads to paralysing humoral immunity and antibody-mediated immune system as well. A key mutator enzyme known as activation-induced cytidine deaminase (AID) is essential for SHM and CSR both processes.

AID acts by induction of point mutation to the immunoglobulin gene. SHM is confined to the variable region of light and heavy chain of immunoglobulin gene, whereas CSR is related to the switching of the constant region of mature antibody transcript which is also initiated by inducing point mutations via AID to switch region present at the constant region of immunoglobulin gene, which further leads to double-strand breaks and switching from one constant region to another. SHM process takes place in the dark zone of the germinal centre, further SHM generated antibody moves to the light zone where the clonal selection of high-affinity antibody and CSR process occurs. AID induces point mutation via deaminating the cytosine to form uracil which leads to mis-match further repaired by cellular repair pathways and have various fates in B-cells (Chaudhary *et al* 2018). Similar to this, in CSR, AID induces point mutation at the constant region of the immunoglobulin gene. Each of the constant regions possesses its own individual promoter and switch region locus. Switching from IgM, a less or non-specific antibody which is produced

upon the first activation of B-cells to IgG, IgA and IgE high-affinity antibody produced during second exposure of antigen results from AID induced point mutations which lead to double-strand breaks and subsequently repaired by MMR, BER pathways.

Physiologically, AID activity is limited to Ig genes but its off-target activity on non-Ig genes, including some oncogenes, results in deregulated expression of these genes which is the leading cause of B-cell lymphomas. AID being the mutator enzyme, its expression and activity are precisely regulated at the transcriptional, post-transcriptional, translational and post-translational levels. At mRNA levels, AID is regulated by microRNAs, for example, miR-155 and miR-181b binds to the 3' UTR of AID and represses its translation. Thus, SHM and CSR are reduced by the expression of miR155 (Kolhaas *et al* 2009, Thai *et al* 2007). As expected miR-155 acts as a tumor suppressor, as the activated B-cell deficient in miR155 showed a higher level of translocation compared to wild type. In mice, AICDA genomic locus is enriched in binding sites for numerous transcription factors, such as NF-kB, STAT6, C/EBP, Smad3=4, HoxC4, c-MYB, E2F, Pax5 and E protein, which positively and negatively regulate the expression of AID upon B-cell activation (Tran *et al* 2010, Dedeoglu *et al* 2004, Gonda *et al* 2003).

B-cells generally functions as the positive counterpart of the immune system via performing T-cell activation through antigen presentation, antibody production and regulation of inflammation (Meffre *et al* 2019, Lebien *et al* 2008, Lumen *et al* 2020). Besides, a subset of B-cells also negatively modulates the immune system. Several studies have revealed that immunoregulatory functions are performed by a distinct subset of B-cells known as regulatory B-cells (B_{reg} cells). The term was first coined by Mizoguchi and his colleagues in 2002. B_{reg} cells have been reported to suppress T-cells and prompted T cells to differentiate in suppressor T-cell (Kim *et al* 2019, Kroniotis *et al* 2016, Kalampokis *et al* 2017, Giacomini *et al* 2018, Katz *et al* 1974, Neta *et al* 1974, Shimamura *et al* 1982, 1984). B_{reg} cells carry

unique characteristics of producing cytokines such as IL10, IL35 and transforming growth factor (TGF-B). IL10 has been recognised as a negative regulator and it inhibits CD4+ T cell proliferation and CD8+ T cell responses in chronic hepatitis B virus (HBV) infection (Akdis *et al* 2016, Khoder *et al* 2014, Cerqueira *et al* 2019, Wu *et al* 2020, Das *et al* 2012). IL10 has been reported in gastric cancer patients where it dampens the T-cell activation (Li *et al* 2015). Moreover, IL10, IL35 and TGF-B producing B_{reg} cells interfere with T-cells activation and macrophages, dendritic cells, and NK cells antigen presentation thereby acting as a negative modulating subset of B-cells (Butz *et al* 2012).

1.4.2.2 T-cells

T-cell originates from hematopoietic stem cells in the bone marrow and after migration, attains maturation in the thymus. T-cells are equipped with a special type of antigen-binding receptors on their membrane, known as T-cell receptors (TCRs). T-cells are dependent on APCs (B-cells, dendritic cells, epithelial cells and macrophages) for the reorganization of antigens and for their functions. APCs expresses a set of surface receptor proteins known as major histocompatibility complex (MHC). These MHC receptors present intracellular and extracellular antigenic peptides which are processed by APCs. MHC are categorised as class I, Human leukocyte antigen (HLA) which are present on all nucleated cells and class II HLA DP, DQ, and DR which are found on macrophages, B-cells, and dendritic cells. Class I MHC displays intracellular peptides which are present to T-cytotoxic (T-CD8) cells while class II MHC molecule displays extracellular peptides to T-helper cells (T-CD4) (Bonilla *et al* 2010, Murphy *et al* 2007).

T-cell's response began upon antigenic peptide recognition by TCRs which binds to appropriate MHC complexes. The complex of antigenic peptide MHC-TCR activates T-cell to secrete cytokines which further stimulates T-cells to differentiate into cytotoxic CD8 T-

cells and helper CD4 T-cells. T helper cells do not have cytotoxic and phagocytic activity while they activate and direct other cells to maximise immune response whereas cytotoxic CD8 T-cells are directly involved in killing pathogens and pathogen-infected cells. Once activated by the MHC class I-TCR complex, these T CD8 cells migrate to the site of infection and phagocytose the pathogen-infected cells. Similar to B_{reg} cells, a subset of T helper cells also known as regulatory T-cells (T_{reg}) plays important role in developing appropriate non-self immune responses. T_{reg} cells regulate and suppress the aberrant immune response to self-antigens thereby prohibiting the development of autoimmune disease. Moreover, T_{reg} cells play a crucial role in maintaining immune tolerance to certain kinds of antigens which commonly found in food (Bonilla *et al* 2010, Murphy *et al* 2007).

1.5 *H. pylori* infection in gastric diseases

H. pylori is a spiral-shaped, flagellated, motile Gram-negative bacterium. Two scientists Barry Marshall and Robin Warren discovered Helicobacter pylori and isolated it from gastric mucosa of patients with chronic gastritis (Marshall *et al* 1984). *H. pylori* has been classified as a class I carcinogen by the World Health Organization (WHO). *H. pylori* is one of the most common human stomach infectious factors with a prevalence of up to 70% in developing countries. It often remains asymptomatic and has been found to be associated with gastric malignancies such as chronic gastritis, peptic ulcer, gastric cancer. In all the infection cases approximately 10% develop ulcer disease, 1-3% gastric cancer and 0.1% progresses mucosa-associated lymphoid tissue (MALT) (Noto *et al* 2007).

Chronic inflammation is the key player in the *H. pylori* infection leading to gastric diseases. Persistent inflammation of gastric mucosa triggers the expression of a wide array of transcription factors that mediate the aberrant cellular signalling. Adherence of *H. pylori* to epithelial cells initiates the inflammatory responses which further expand to circulating immune cells which recruits to the site of

infection. *H. pylori* infections have been reposted with many pro-inflammatory cytokines, transcription factors and interleukins such as IL-1, IL-6, IL-8, TNF-a, NF-κB (Lamb *et al* 2013).

There are a variety of virulence factors produced by *H. pylori* that leads to cellular transformation. Cytotoxin-associated gene A (CagA) and its pathogenicity island (CagA PAI), VacA (vacuolating cytotoxin A), outer membrane proteins such as BabA, SabA are the most studied pathogenic factors. CagA protein is encoded by CagA PAI genomic locus which is approximately 40 kb long consisting of a Cag type IV secretion system (T4SS) (Muller *et al* 2012). The T4SS develops a syringe-like pilus protrusion which is used to deliver CagA into the host cells (Nhieu et al 2009). Upon injection of CagA, a vast verity of downstream host cell signalling pathways are modulated such as nuclear factor jB (NF-jB) pathway and b-catenin pathway, the Ras/mitogen-activated protein kinase (MEK)/extracellular signal-regulated kinase (ERK) pathway (Xu *et al* 2012, Muller *et al* 2012). CagA binds to the inner surface of the membrane and gets its glutamate-proline-isoleucine-tyrosine-alanine (EPIYA) motif by Src family kinases. Studies have shown non-phosphorylated CagA could activate hepatocyte growth factor c-Met and Grb2 an adaptor protein and induce phosphorylation of phospholipase C gamma (PLCY) (Mimuro *et al* 2002, Kamiya *et al* 2007, Wroblewski *et al* 2010). In addition to that non-phosphorylated CagA also inhibits the PARP1 and MARK protein kinase C signalling leading to disruption of cell-cell junctions (Turkoz *et al* 2012).

EPIYA motif of C-terminal domain of CagA is phosphorylated by Src and Abl kinase present in the eukaryotic cells, and the N-terminal of unphosphorylated CagA interact with the multiple intracellular factors such as it disrupts the association between the apoptosis-stimulating protein of p53-2 (ASPP2) and p53 to stimulate the proteasomal degradation of p53 (Buti *et al* 2011), and it inactivates the RUNX3 a gastric tumor suppressor Runt-related transcription factor3 (Tsang *et al* 2010). The N-terminal of CagA also binds the

ectodomain of a5b1 integrin and thus is responsible for the translocation of CagA into the host cells (Nhieu *et al* 2009). Moreover, together C and N terminal of CagA protein facilitates the pathogenesis of *H. pylori*.

In addition to CagA, vacuolating cytotoxin is also secreted by *H. pylori* via a type V autotransporter secretion system. It is a 88 kDa protein made up of the p33 (N-terminal 33 kDa) and p55 (C-terminal 55 kDa) subunits. The p33 forms an inner channel for chloride transport while the p55 unit help in the binding of the toxin to the target cell (Boquet *et al* 2012). The VacA toxin binds and is internalized to the host cell and creates severe vacuolation consisting of large vesicles. Additionally, VacA also interferes with mitochondria transmembrane potential and cause the release of cytochrome C and activation of pro-apoptotic factor Bcl-2 associated X protein (Bax), thus leading to apoptosis (Rassow *et al* 2012). Further, VacA is also involved in the polarization of tight junction between epithelial cells and disrupt T-cell activation, together with these leads to inflammation and promotes the progression of gastric carcinogenesis (Palframan *et al* 2011, Raju *et al* 2012).

1.6 *H. pylori* infection and host immune system

1.6.1 Innate immune response to *H. pylori*

Bacterial antigenic molecules are recognized by TLRs which are expressed by a wide variety of cells throughout the gastrointestinal tract. TLRs are the important players of the innate immune system, TLR4 especially contribute to the recognition of bacterial PAMPs. APCs such as dendritic cells, monocytes and epithelial cells expresses TLR4 and upon bacterial contact these cells secret pro-inflammatory cytokines such as TNF-α (tumour necrosis factor-α), IL (interleukin)-1β and IL-8. *H. pylori* infection is associated with increased expression of IL10, IL8, TNF-α and TLR2, TLR4, TLR5 TLR9 (Lagunes *et al* 2013, Pimentel *et al* 2013). In addition, *H. pylori* uses TLR4 receptor to adhere to gastric epithelial cells and promotes IL8 secretion via

upregulation of NFκB transcription factor. However, other studies suggest that IL8 secretion and recognition of *H. pylori* is TLR4 independent (Backhed *et al* 2003, Suzuki *et al* 2001). TLR2 is also expressed onto the gastric epithelial cells, and it can recognise *H. pylori* and can induce inflammation signalling pathways. Mostly, TLR2 recognise lipoproteins, lipoteichoic acid, and peptidoglycan, besides it can also sense other *H. pylori* antigens and can induce immunomodulatory responses. HSP60, an *H. pylori* antigen which is recognised by TLR2 and inflammatory cytokine production from monocytes and gastric epithelial (Takenaka *et al* 2004, Zhao *et al* 2007).

1.6.2 Adaptive immune response to *H. pylori*

Failure of the innate immune system leads to activation of the adaptive immune system to eliminate the pathogen. During the *H. pylori* infection, a versatile group of immune responses are generated which are both protective and damaging in nature to the host. Aberrant innate and adaptive immune responses lead to persistent inflammation and damage the host mechanism which further makes the host vulnerable to other infections. Persistent *H. pylori* infection is associated with a mucosal infiltration of different cells like poly-morphonuclear leukocytes (PMN), plasma cells, T-cells, macrophages (Ihan *et al* 2012, Aviles *et al* 2012). In addition to it, the epithelial cell also secrets cytokines which further modulates the function of the epithelial cell during persistent *H. pylori* infection. In the condition of chronic gastritis, an increased CD4/CD8 T-cell ratio has been reported. However, immune repose via Th1 is predominantly found to be associated with the release of several pro-inflammatory cytokines such as s IL-12, IL-18 and TNF-α (Chatterjee *et al* 2012, Tummala *et al* 2004).

In course of *H. pylori* infection, B-cells induces strong specific local antibody response. Patients infected with *H. pylori* showed strong antibodies against whole bacteria and increased levels of plasma cells

in gastric mucosa which predominantly secret IgA (Nessa *et al* 2001, Mattsson *et al* 1998). However, some patients with increased IgG production also reposted with an increased level of phagocytosis of *H. pylori* via activation of complement pathway (Tosi *et al* 1990, Berstad *et al* 2001). In humoral immune response to *H. pylori*, especially IgA antibody found against VacA and urease of *H. pylori*. Neutralization of both VacA and urease inhibits adherence of *H. pylori* to epithelial cells of the gastric mucosa (Portal *et al* 2006).

1.6.3 Evasion of the immune system by *H. pylori*

For the persistence of infection and prolonged survival, *H. pylori* try to evade the host immune system by altering different mechanism including apoptosis of macrophages and changing intracellular pathways via injecting toxins such as CagA and VacA. VacA, a potent immunomodulatory factor has been reported to dampen the integrin-linked kinase (ILK) and endothelial nitric oxygen synthase (eNOS) and production of reactive oxygen species (ROS) which in turn help *H. pylori* escape host immunoreaction and persist gastric infection (Yuan at al 2009). In addition to that VacA not only interfere with antigen presentation mediated by MHCII complex and IL2 signalling pathway in T-cells but also act as immunosuppressive by directly acting on T-cells (Boncristiano *et al* 2003, Molinari *et al* 1998, Gebert *et al* 2003). γ-glutamyl transpeptidase (GGT) is another secreted protein of *H. pylori* has been reported to be interfering with T-cell responses and T-cell proliferation. Additionally, it also mediates extracellular cleavage of glutathione which further leads to the production of ROS and aberrantly induce cell cycle arrest in lymphocytes via modulating Ras signalling pathways (Schmees *et al* 2007). However, Cag PAI promotes T-cell apoptosis with the induction of Fas ligand signalling in T-cells (Wang *et al* 2001).

T_{reg} cells are negative regulators of immune response which in turn results in increased pathogen load (here *H. pylori* bacteria) and facilitate chronic infection. In *H. pylori*-infected patients, an increased

amount of T_{reg} has been reported in the gastric tissue as compared with healthy controls (Lundgren *et al* 2003, Cheng *et al* 2012). A subset of T-cells known as Th17 cells plays a crucial role in the clearance of *H. pylori*. Induction of T_{reg} cells keep a sub-optimal level of Th17 cell, this mechanism depends on optimal induction of T_{reg} cells by *H. pylori* which requires cytokines, TGF-β and IL-10 and this strategy was independent of VacA and CagA (Kao *et al* 2010).

1.7 Outer membrane proteins of *H. pylori* infection

H. pylori strains show a lower abundance of OMPs compared to other Gram-negative bacteria species. Only 4% of the *H. pylori* genome encodes a large set of OMPs (~64 OMPs) which indicated the evolutionary development of paralogous gene families which is possibly due to acquiring the adaptation to the gastric environment. The OMPs family broadly can be divided into five families namely, The largest family is family 1, Hop (for *H. pylori* OMP, 21 members) and family 2 and 3 Hor (for Hop related, 12 members) proteins, Hof (for Helicobacter OMP, 8 members) and Hom (for Helicobacter outer membrane, 4 members) proteins. Hop family proteins share identical sequences at their amino and carboxyl termini and include porins which generally form unique β-barrel topology to perform porin like functions (Doig *et al* 1995, Exner *et al* 1995), and several known or predicted *H. pylori* adhesins which act as a binding partner to the gastric epithelial cells (Ilver *et al* 1998, Mahdevi *et al* 2002). In addition, another OMP from the third family Hom, HomB, was shown to be involved in *H. pylori* adherence and IL8 production (Oleastro *et al* 2008). For becoming the successful pathogen *H. pylori* have evolved over time with altering the gene expression of OMPs via gene conversion and gene duplication and allelic variation for the adaptation to the host environment.

1.8 HomA and HomB in *H. pylori* infection

The Hom family is the smallest family of OMPs of *H. pylori* which is constituted of four members HomA, B, C and D. Out of four members

HomB is the most studied protein (~75 KDa) expressed in the *H. pylori* outer membrane (Oleastro *et al* 2008). homB has closely related to its other family member, homA and shares 90% sequence identity, especially at the 5' and 3' ends with the differences between the middle region of the open reading frames due to allelic diversity (Alm *et al* 2000, Oleastro *et al* 2009). HomA/B have been reported to show allelic variations which likely occur via the accumulation of single nucleotide polymorphisms, suggesting that homA/homB allelic variants are independent of the geographical origin of the strain. In *in-silico* approach revealed that the homologous recombination between the middle regions results in allelic variation (Oleastro *et al* 2010). homA/homB reported being present at multiple well-conserved genome loci (Oleastro *et al* 2008, 2006) with a geographical specificity, suggesting an involvement of these genes in host gastric environment adaptation. HomB is reported for its antigenicity in humans and in addition to that the protein is also associated with IL-8 secretion *in vitro* and contributes to bacterial adherence. These functions of HomB are associated with the number of *homB* gene copies present in a strain. Both the gene *homA*, *homB* is associated with the presence of cagA, contributing to more virulence *H. pylori* strains (Jung *et al* 2009, Abadi *et al* 2011). Moreover, homB is considered as a virulence marker of more virulent *H. pylori* strains, which leads to the severity of disease and persistent infection contributes to more severe clinical outcomes. However, the exact involvement of HomB and HomA gastric cancer outcomes is not completely known. Despite HomB's role in adherence, structural and functional insights remain to be determined and will be a major challenge for future research for developing therapeutic strategies against *H. pylori*.

1.9 Background of work and Objectives

Outer membrane proteins (OMPs) of *H. pylori* play a crucial role in the host-pathogen interaction, virulence, and pathogenesis. Upon interaction with the host immune cells, OMPs stimulate the production

of pro-inflammatory molecules that may result in an uncontrolled inflammation leading to the transformation of a normal cell to a cancerous cell.

Hom (Helicobacter outer membrane) family of OMPs in *H. pylori* consists of four members (HomA, B, C and D). *homB* gene is 90% similar to another OMP of the *H. pylori*, which is the *jhp*0649 ORF *homA,* with differences between the 300 bp middle region of these ORFs (Alm *et al* 2000). HomB outer membrane protein is associated with many stomach diseases and is a novel co-marker for peptic ulcer disease (PUD) (Oleastro *et al* 2008) and is the most studied and evaluated for its prevalence in various peptic diseases. Oleastro *et al*. investigated pathogenesis and immunological response caused by HomB protein in clinical patients and 190 *H. pylori* strain isolated from patients with peptic ulcer disease (PUD) or gastritis were evaluated for the clinical importance of *homB*. HomB protein contributes to the colonization and persistence of *H. pylori*, and the presence of *homB* genes affects the number of bacteria adhering to the host cells. Additionally, HomB is also associated with the secretion of the proinflammatory cytokine interleukin-8 (IL-8) (Oleastro *et al* 2008). Moreover, HomB protein also assists in hyper biofilm formation and antibiotic resistance thereby likely to enhance bacterial survival by evading host immune responses and antibiotic treatments.

With the agreement of these studies, HomA and HomB can be considered as virulence markers of aggressive *H. pylori* virulent strains. However, the structural and functional characteristics and details of HomA and HomB have not been reported yet. Thus, it is not clear how these proteins contribute to ulcer or gastric cancer, and the exact molecular mechanism is not explored.

The present investigation study consists of the following main objectives:

1. To study the structural aspect of potential virulence factors, HomA and HomB outer membrane proteins of *H. pylori*. Methods involve bioinformatic tools, biophysical characterization to reveal important physical states, secondary

structure content and 3D models of proteins. This information is likely to help in better understanding the role of HomA and HomB in *H. pylori* pathogenesis.

2. To investigate the molecular mechanism of HomA and HomB associated immune system modulation and consequences of the interaction between *H. pylori* and immune cells specifically B-cells. Here, we explored the possible molecular mechanism of reduced antibody diversity in patients with *H. pylori*-associated gastric diseases.
3. To explore the potential of HomA and HomB to be utilized as prognosis and vaccine candidates. Here, we characterize the immunoinformatics properties, such as potential antigenic and immunogenic epitopes present on to the globular domain of HomA and HomB, which are likely to activate host immune response. This information further can be utilized for therapeutic applications.

Chapter 2

Chapter 2

Materials, methods, and Instrumentation

2.1 Materials

2.1.1 Primers and enzymes

All oligos used in this study were procured from Sigma Aldrich Pvt. Ltd. (Appendix B). All restriction enzymes used in this study were purchased from New England Biolabs and Fermentas (Thermo Fisher).

2.1.2 Genomic DNA. Cloning vectors and competent cells

The bacterial cloning vectors used are pBSSK+ vector (Stratagene) and expression vector pET43 (Novagen). Bacterial competent cells used were *E. coli* DH5α., *E. coli* Rosetta (DE3).

2.1.3 Chemicals

The chemical agent used in this study are as follows: Trizma base, Glycine ($C_2H_5NO_2$), Ethylene diamine tetra acetic acid (EDTA), Potassium hydrogen phosphate (K_2HPO_4), Potassium dihydrogen phosphate (KH_2PO_4), Sodium hydrogen phosphate (Na_2HPO_4), Sodium dihydrogen phosphate (NaH_2PO_4), Ethidium bromide (EtBr), Potassium chloride (KCl), Sodium chloride (NaCl), Magnessium chloride ($MgCl_2$), Calcium chloride ($CaCl_2$), Sodium hydroxide (NaOH), Sodium thiosulphate (Na_2S2O_3), Sodium hydrogen carbonate ($NaHCO_3$), Silver nitrate ($AgNO_3$), Sodium carbonate (Na_2CO_3), Dimethyl formamide (C_3H_7NO), Sodium dodecyl sulphate or Sodium lauryl sulphate (SDS), Commassie brilliant blue G-250, β-mercaptoethanol ($HOCH_2CH_2SH$), Agarose, Luria-Bertani agar (LB-agar), Luria-Bertani broth (LB-broth), Ampicillin, Kanamycin, Acrylamide (C_3H_5NO), N, N′-Methylene bisacrylamide (MBAA), Triethylenetetramine or Tetramethylethylene diamine (TEMED), Ammonium per sulphate ($(NH_4)_2S_2O_8$), Polysorbate 20 or Tween 20 ($C_{58}H_{114}O_{26}$), non-fat dry skimmed milk powder, Glycerol ($C_3H_8O_3$),

bromophenol blue or 3′,3″,5′,5″-tetrabromophenolsulfonphthalein ($C_{19}H_{10}Br_4O_5S$), Bovine serum albumin (BSA), 4',6-Diamidino-2-Phenylindole, Dihydrochloride ($C_{16}H_{15}N_5$), Paraformaldehyde ($OH(CH_2O)nH(n=8-100)$), Isopropyl-β-D-thiogalactopyranoside ($C_9H_{18}O_5S$), Imidazole ($C_3H_4N_2$), 5- bromo-4-chloro-3-indolyl-β-D-galactopyranoside ($C_{14}H_{15}BrClNO_6$), Nonidet P40 (tergitol), Triton X-100 $C_{14}H_{22}O(C_2H_4O)n$, ethylene glycol-bis (β-aminoethyl ether)-N,N,N′,N′-tetraacetic acid ($C_{14}H_{24}N_2O_{10}$), Glycerol ($C_3H_8O_3$), Xylene cyanol ($C_{25}H_{27}N_2NaO_6S_2$), RNase A, Methanol (CH_3OH), Glacial acetic acid (CH_3COOH), Formalin or formaldehyde (CH_2O ($H{-}CHO$)), Ethanol (C_2H_5OH), Fetal bovine serum (FBS), Dimethyl sulphoxide (C_2H_6OS), 2- mercaptoethanol ($HOCH_2CH_2SH$), Glutamine ($C_5H_{10}N_2O_3$), Pyruvic acid ($C_3H_4O_3$), Penicillin G streptomycin, Phenol (C_6H_5OH), Chloroform ($CHCl_3$), Iso-amyl alcohol ($C_5H_{12}O$), N-lauroylsarcosine ($C_{15}H_{28}NNaO_3$), phenylmethylsulfonylfluoride ($C_7H_7FO_2S$), CSPD substrate, Protease inhibitor cocktail, HEPES buffer ($C_8H_{18}N_2O_4S$). All chemicals were from molecular biology grade and procured from different makes like Sigma Aldrich Chemical Pvt. Ltd., Invitrogen Pvt. Ltd., MP Biomedical USA, HiMedia Pvt. Ltd. India, Alpha Aesar Pvt. Ltd., Sisco Research Lab Pvt. Ltd. India and Otto. Chemie Pvt. Ltd.

2.1.4 Reagents and Kits

Plasmid isolation kit, Gel extraction kit, and PCR purification kit was purchased from Thermo Fisher Scientific, USA and Favorgen Biotech Corporation, Taiwan. T4 DNA ligase, 10X Buffer with Mg++, dNTPs, *Taq* DNA Polymerase, Q5 DNA polymerase, 100bp DNA ladder, 1kb DNA ladder, unstained protein marker, prestained protein marker. TRIzol reagents for RNA isolation, Superscript IV cDNA synthesis kit, Oligo (dT)20, Random hexamers, Dithiothreitol, dNTP mix, Ribonuclease inhibitor, DEPC-treated water, DNA free kit, SYBR green master mix, Protein A/G PLUS-Agarose beads. All antibodies used in the study are listed in Appendix C.

2.2 Methods

2.2.1 Bioinformatics analysis of HomA and HomB

HomA (protein_id AAD06225.1) and HomB (protein_id AAD06437.1) amino acid sequences were used to identify the presence of signal peptides using the tool SignalP-5.0 (http://www.cbs.dtu.dk/services/SignalP/). We selected a Gram-negative signal peptide database for the prediction of a signal peptide in HomA and HomB. Secondary structure predictions for HomA and HomB were performed using NetSurfP-2.0 (http://www.cbs.dtu.dk/services/NetSurfP/). 3D structure predictions were done with AlphaFold2 (https://deepmind.com/research/open-source/alphafold) and I-TASSER (https://zhanglab.ccmb.med.umich.edu/I-TASSER/).

B-cell and T-cell epitopes prediction was done using IEDB tools (https://www.iedb.org/), molecular docking and refinement were done using Patchdock server (https://bioinfo3d.cs.tau.ac.il/PatchDock/php.php). Further, normal mode analysis (NMA) was performed using iMOD server (http://imods.chaconlab.org/). Immune simulation studies were carried out using C-immsim tool (https://www.iac.rm.cnr.it/~filippo/projects/c-immsim-online.html)

2.2.2 Cloning of *homA* and *homB*

Helicobacter pylori J99 (GenBank: AE001439.1) genomic DNA, a kind gift from Prof. Solnick, University of California, Davis, and Dr. Ashish Kumar Mukhopadhyay, NICED, Kolkata, was used as a template for amplifying *homA* (ORF jhp_0649) and *homB* (ORF jhp_0870) genes. The genes for HomA and HomB were PCR amplified from the genomic DNA of *H. pylori* strain J99, using *Pfu* DNA Polymerase with identical primer pair PK610 and PK652 (**Appendix B**) as the N-terminal and C-terminal of these proteins are conserved. Thermal cycles were programmed for 4 minutes as initial

denaturation at 95ºC, followed by 30 cycles of 30 seconds at 92ºC for denaturation, 30 seconds at 55ºC as annealing temperature, 130 seconds at 72ºC for the extension, and a final extension at 72ºC for 10 minutes. Later, the PCR products were cloned into plasmid pBluescript at the *Sma*I site. Based on the restriction pattern, we identified unique clones for *homA* as well as *homB* and later confirmed by DNA sequencing. Subsequently, both the *homA* and *homB* genes were cloned into pET43 at *Nde*I and *Xho*I sites, respectively, to give pHomA and pHomB. The cloning was performed in such a way that the recombinant proteins will express a C-terminal His-tag that will assist in purification. The inserts and vector DNA were ligated, followed by the transformation of ligated samples into DH5α cells. The presence of insert DNA in plasmid constructs was confirmed by colony PCR, further recombinant plasmids were isolated and then confirmed by DNA sequencing.

2.2.3 Expression, purification, and heat modifiability of recombinant HomA and HomB

Recombinant pHomA and pHomB clones were transformed into *E. coli* Rosetta cells. All recombinant strains were grown in a Luria-Bertani medium supplemented with (100 µg/ml) ampicillin. Cells were induced at an optical density at 600 nm of 0.6 by adding isopropyl-b-D-1-thiogalactopyranoside (IPTG) to a final concentration of 0.1 mM at 37°C for 4 hours on an orbital shaker at 220 rpm. Subsequently, the cells were harvested by centrifugation at 6,000*g* for 15 min at 4°C. The pellets were washed and resuspended in a buffer containing 30 ml of 25 mM Tris-Cl pH 7.5, 100 µg of lysozyme, and 500 µM of PMSF added and sonicated at 65-amp, 5 min pulse on and 5 min pulse off for 20 min for 2 cycles. After sonication, the pellet was recovered by centrifugation at 20,000*g* for 30 min at 4°C. Subsequently, the recombinant HomA/HomB protein was purified on Ni-nitrilotriacetic acid affinity chromatography columns at 4°C. Purification of recombinant HomA and HomB protein was confirmed on 8% SDS PAGE gel. Heat modifiability assay was done according to the method

previously reported, briefly, purified HomA and HomB with either detergent {LDAO (1-2mM), CHAPS (6mM), TWEEN20 (0.06-0.08mM)} with respective 4X and 10X CMC concentration and 1 mM lipids (DOPC and DMPC) added samples were boiled at 95°C for 10 min and unboiled protein samples were run on 12% PAGE with 0.5% SDS at 150V in cooling condition.

2.2.4 Trypsin digestion

Recombinant purified proteins (0.5 mg/ml) were treated with 25 µg/ml of trypsin (SRL) for 1 hour at 37°C after which 5 mM phenyl-methylsulfonyl fluoride was added, and the samples were analyzed by SDS-PAGE and semi-native PAGE.

2.2.5 Secondary structure analysis

Circular dichroism (CD) analysis was performed using a Jasco J-815 spectropolarimeter (Jasco, Easton, MD). Far-UV CD spectra were acquired at 25°C in a 1-mm path-length cuvette, with a 1-nm bandwidth, and a scan rate of 20 nm/min. Spectra of each sample were acquired and the baseline was corrected by subtracting the spectral attributes of the buffer. The BeStSel tool (http://bestsel.elte.hu/) was utilized to assess the secondary structure contents of the proteins from their spectra.

2.2.6 Tryptophan fluorescence spectroscopy

Fluorescence spectra were obtained using the FluoroMax-4p spectrofluorometer from Horiba Jobin Yvon (model: FM100) with samples placed in a 1-mm path-length quartz cell at 25°C temperature. The excitation wavelength was 295 nm, and the bandwidth of the excitation monochromator was 2 nm. The folding and denaturing buffers for HomA/HomB were 50 mM Tris-Cl, pH 8.0, 300 mM NaCl, 1- 8 M urea. Tryptophan emission spectra were recorded between 305 and 400 nm. Background spectra without HomA/HomB were subtracted to obtain the final emission curves.

2.2.7 Size exclusion chromatography

For determination of the oligomeric state of HomA and HomB, 1 mg of protein was loaded onto a Superose 12 size exclusion column (GE Healthcare) equilibrated with 50 mM Tris-Cl, pH 8.0, 300 mM NaCl, and lipid and detergent as indicated, at 4°C. Protein was eluted at a flow rate of 0.5 ml/min. The standard molecular weight markers used were 200 kDa (β amylase), 150 kDa (alcohol dehydrogenase), 66 kDa (albumin), 29 kDa (carbonic anhydrase), and 12 kDa (cytochrome C)). The void volume is determined by blue dextran of MW~ 2000 kDa.

2.2.8 ATR-FTIR

Polarized ATR infrared spectra were recorded on a Tensor 27 (Bruker) FTIR spectrometer at a resolution of 2 cm^{-1}, with parallel and perpendicular polarization of the incident beam. 80-100 µg of purified protein was used in a buffer containing 50 mM Tris-Cl, pH 8.0, 300 mM NaCl. Quantitative analysis of the amide I band contour was done using curve fitting, second derivative methods. The spectral range of 1600–1700 cm^{-1} was decomposed using Origin 8.0 software. Buffer spectra without protein were subtracted to obtain the final spectra.

2.2.9 SAXS Data Acquisition, Processing, Analysis and Shape Restoration

SAXS measurements were carried out at the SAXS beamline (BL-18) of the Indus-2 synchrotron (2.5 GeV, 300 mA) source, Indore, India. The X-ray beam of wavelength 0.7749015 Å (16KeV) was used. HomA and HomB protein samples (~2.5 mg/ml) in buffer containing 20mM Tris-Cl pH 8, 200mM NaCl, and 5mM BME were placed inside a “Kapton window cell”, with 4mm path length for SAXS data collection. The data were collected in a q ($4\pi\sin\Theta/\lambda$, where Θ is the scattering angle) range from 0.0096 to 0.361 $Å^{-1}$ for both HomA and HomB using MAR345 imaging plate detector with the sample to

detector distance of 3.24 m. The data were corrected for both solvent and background, and the intensities were radially averaged on a relative scale. For both data-set, the data in the *q*-range 0.095 to 0.154 $Å^{-1}$ for HomA and 0.010 to 0.156 $Å^{-1}$ for HomB were analyzed and modeled mostly by using software tools available in the ATSAS suite (Cantos *et al* 2021). The radius of gyration (*R*g) and absolute intensity *I*(0) (at $q = 0$) values were estimated from pair distance distribution [*P*(*r*)] were calculated by GNOM (Svergun *et al* 1992) of ATSAS suite (Hopkins *et al* 2021). The molecular weight of the HomA and HomB were estimated in a concentration-independent manner from Porod volume (Pilodov *et al* 2019, Hajizadesh *et al* 2018) implemented in RAW software (Mirdita *et al* 2021), as SAXS data were on an arbitrary relative scale. *Ab-initio* bead model for both proteins was generated by the DAMMIN module of the ATSAS package. Simultaneously, the protein structures of HomA and HomB were predicted from AlphaFold 2 online server (Jumper *et al* 2021). The dimeric assembly for both HomA and HomB was manually designed based on the SAXS bead model by using PyMOL. Data have been deposited in the Small Angle Scattering Biological Databank (www.sasbdb.org; ID: HomA; SASDMK7 and HomB; SASDML7). Structural figures were prepared using UCSF Chimera.

2.2.10 Human B-cell culture

Raji human Burkitt's lymphoma cell line was procured from the National Centre for Cell Sciences (NCCS) Pune, India. Cells were cultured in RPMI 1640 medium (Invitrogen) supplement with 10 % FBS (Invitrogen), 50 μM 2-mercaptoethanol (Sigma Aldrich), 2 mM glutamine, 100 μg/ml penicillin G, and 50 μg/mL streptomycin (Invitrogen) at 37°C in 5 % CO_2.

2.2.11 Endotoxin removal of recombinant HomA and HomB

Endotoxins from purified proteins were removed with endotoxin removal columns (Pierce, Thermo Fisher) as per the manufacturer's instructions.

2.2.12 B-cell stimulation with HomA and HomB

Raji B-cells were grown up to 90% confluency. Culture media were changed and grown overnight 5×10^6 cells per plate. The next day purified and endotoxin-free HomA and HomB were re-suspended into PBS and concentrations of proteins were measured with Bradford reagent (HiMedia). Different concentrations of HomA and HomB (10 μg, 50 μg and 100 μg) were added to cells and cells were collected at different time points (1 hour, 4 hours and 8 hours) and for control, PBS was added to cells. Cells were washed three times with PBS and used for RNA isolation or preparation of protein cell extract.

2.2.13 RNA isolation and cDNA synthesis

Total RNA was isolated from 1×10^7 Raji B-cells stimulated with different concentrations and at different times, by using RNAzol reagent as per the manufacturer's protocol (Sigma Aldrich). RNA samples were treated with the DNA free DNA removal kit (Ambion). RNA concentration and purity were quantified using the Nanodrop spectrophotometer (Thermo Scientific). 1 μg of RNA was used to synthesize cDNA by using the prime script 1^{st} strand cDNA synthesis kit (Takara Bio).

2.2.14 Quantitative real-time PCR

The transcription level of GAPDH, AID and its transcriptional regulators NFκB, PAX5, SMAD3, cMYC, STAT6 cMYB, E2F1, T-cell inhibition markers PDL1, IL35, IL10, and TGFβ genes from HomA and HomB stimulated cells were analyzed by using Power SYBR Green PCR Master Mix (Invitrogen) and appropriate primers (**Appendix B**). Similarly, the transcription level of Ig mature transcript

IgV-Cμ, IgV-Cα and IgV-Cγ, V-region, Ig switch germline transcription Iμ-Cμ, Iα-Cα, Iγ-Cγ, switched circular transcript Iγ-Cμ, Iα-Cμ, CSR factors HOXC4, BATF, of HomA and HomB stimulated cells were analyzed by real-time PCR by using 2X kappa SYBR fast qPCR Master Mix (Sigma Aldrich). The qRT-PCR run was performed by using 2X kappa SYBR fast qPCR Master Mix (Sigma Aldrich) on the StepOnePlus (Applied Biosystems) real-time PCR system. PCR conditions used for a run as 92°C for 30 s, 60°C for 45 s and 72°C for 60 s for 40 cycles, in addition to a melt curve. The comparative method threshold cycle was used, and data were normalized with an internal control GAPDH as a constitutively expressed gene. Fold change values for change in gene expression were calculated with respect to the control. At least three independent experiments were performed, and a representative result is shown in the Figure. Error bars represent the standard deviation of technical replicates. Standard deviations of ΔCT and ΔΔCT were calculated as per the manufacturer's guide to performing relative quantitation of gene expression using real-time quantitative PCR, using the formula $SD = (SD1^2 + SD2^2)^{1/2}$, where SD is the standard deviation.

2.2.15 SDS-PAGE and western immunoblotting

1×10^7 stimulated Raji cells were washed 3 times with PBS by centrifuged at 1100 rpm; 4°C for 5 min. Subsequently, cells were lysed in 50 mM Tris-Cl, pH-7.5, 150 mM NaCl, 1 mM EDTA, 1 % Triton-X 100 and Protease inhibitor + DNaseI, 1 μg/ml. 5X sample loading buffer (0.25 M Tris-Cl, pH-6.8, 15% SDS, 50% glycerol, 25% β-mercaptoethanol and 0.01% bromophenol blue) were added to cells and boiled at 95°C. Proteins were separated on a 12% SDS-PAGE gel in a mini protean tetra cell (Bio-Rad). For western blotting, the gel was transferred to the nitrocellulose membrane (Amersham, GE Healthcare). The blots were blocked in Tris-buffer saline, pH-7.5, supplemented with 0.02% Tween 20 (Alfa Aesar) and 5% non-fat dry skimmed milk powder (HiMedia). Western blotting was performed by

using an anti-AID, anti-cMyb and anti-GAPDH (**Appendix C**). Blots were developed by using appropriate chemiluminescence substrate, ECL substrate (Bio-Rad). Finally, chemiluminescence was detected by using the Image quant LAS 4000 Gel Doc system (GE Healthcare).

2.2.16 Immunofluorescence

1×10^7 stimulated Raji cells were washed 3 times with PBS by centrifuged at 1100 rpm; 4°C for 5 min. Cells were fixed in 4% paraformaldehyde (MP Biomedicals) for 20 min and permeabilized with PBS-T (0.1% Triton-X in PBS) for 10 min. Further, the cells were blocked for 30 minutes in PBS-T containing 5% BSA (Sigma Aldrich) and incubated with the primary antibodies anti-AID, anti-cMYB and anti-PDL1 (**Appendix C**), (1:100) overnight at 4°C on a rotating platform. Subsequently, cells were washed with PBS-T three times for 10 min each and were incubated with the secondary antibody, anti-mouse Alexa flour 488 or Alexa flour 594 (**Appendix C**) (1:200) in PBS-T containing 2.5% BSA for 120 min. Later, cells were washed thrice in PBS-T for 10 minutes each. Finally, high-resolution images were taken at 100 X magnifications using a confocal laser scanning microscope (Olympus, FV1200MPE). Mean fluorescent intensities and 3D plots were calculated by Image J software using intden and raw intden values.

2.2.17 Chromatin immunoprecipitation (ChIP) assay

1×10^7 stimulated Raji cells were cross-linked with 36 % formaldehyde (final concentration 1 %) for 10 min at 37°C. The reaction was quenched by adding 125 mM glycine for 5 min at room temperature. Fixed cells were rinsed twice with PBS plus protease inhibitor and resuspended in Cell Lysis Buffer (50 mM Tris-Cl pH-7.5, 150 mM NaCl, 5 mM EDTA, 1% Triton X-100, 0.5 % NP-40 plus protease inhibitor cocktail). The lysate was sonicated for 90 min (30 s on/30 s off) in a probe sonicator (Qsonica sonicator) and centrifuged at 13,200 rpm at 4°C for 10 min. The supernatant was used immediately for ChIP experiments. Supernatants were incubated with an anti-

cMYB antibody, at 1:100 dilution overnight at 4°C on a rota-spin. Afterwards, protein-A agarose beads were washed with cell lysis buffer. Samples were incubated with 20 µl slurry of protein-A on a rota-spin for 2 h at 4°C and pelleted by centrifugation (2000 g, 3 min). Subsequently, pellets were washed three times in 1 ml of ice-cold washing buffer (20 mM Tris-Cl pH-8.0, 5 mM $MgCl_2$, 5 mM $MnCl_2$, 750 mM NaCl and 1.0 % NP-40) with 5 min incubations between spins. Finally, 50 µl of 2 % SDS, 0.1M $NaHCO_3$ was added and incubated for 45 min at 65°C to elute chromatin. Thereafter, chromatin was reverse-cross-linked by adding 6 µl of 5M NaCl and 0.5 µl 30 mg/ml RNase A to ChIP DNA, and 9 µl of 3M NaCl and 0.5 µl 30 mg/ml RNase A to input DNA and incubated at 65°C for 4 h, further DNA was treated with proteinase K (20 mg/ ml) digestion and purified with PCR purification kit (Thermo Scientific). The primers used were PK869 and PK870 (**Appendix B**) for region 2 of the AID gene locus. PCR conditions were 95°C for 30 s, 65°C for 45 s for 40 cycles were used for the amplification of fragments. The data presented are percentage levels of immunoprecipitated DNA to the input DNA. At least three independent experiments were performed, and a representative result is shown in the Figure. Error bars represent the standard deviation of technical replicates.

2.2.18 ELISA Assay

Raji B-cells were grown up to 90% confluency. Culture media were changed and grown overnight 5×10^6 cells per plate. The next day purified and endotoxin-free HomA and HomB were re-suspended into PBS and concentrations of proteins were measured with Bradford reagent (HiMedia). 50 µg concentration of HomA and HomB were added to cells and cells were collected at different time points (1 hour, 4 hours and 8 hours) and for control, PBS was added to cells. Cells were centrifuged at 2000 rpm at 4°C and culture supernatant was collected and stored at 20°C for further use. ELISA for IL35 and IL10

were performed according to the manufacturer's protocol (Krishgen BioSystems).

2.2.19 Cell viability/proliferation assay

25000 stimulated Raji cells were taken out from each time point and 50 µl of MTT (5 mg/ml in PBS) were added and incubated for 3 hours at 37°C. Afterwards, 150 µl DMSO was added to dissolve formazan crystals and incubated for 15 min in dark at room temperature. Absorbance was readout at 590 nm. Each sample was performed with technical triplicates. Error bars represent the standard deviation of technical replicates.

2.2.20 Statistics

Data were analysed using GraphPad PRISM 9.0 (GraphPad Software, San Diego, CA). Results are presented as individual data points and/or mean ± standard deviation (SD). Differences between values were analysed for statistical significance by Student's t-test, the non-parametric Kruskal–Wallis test, one-way or two-way analysis of variance with appropriate multiple comparisons tests. Differences were considered significant at $P < 0.05$.

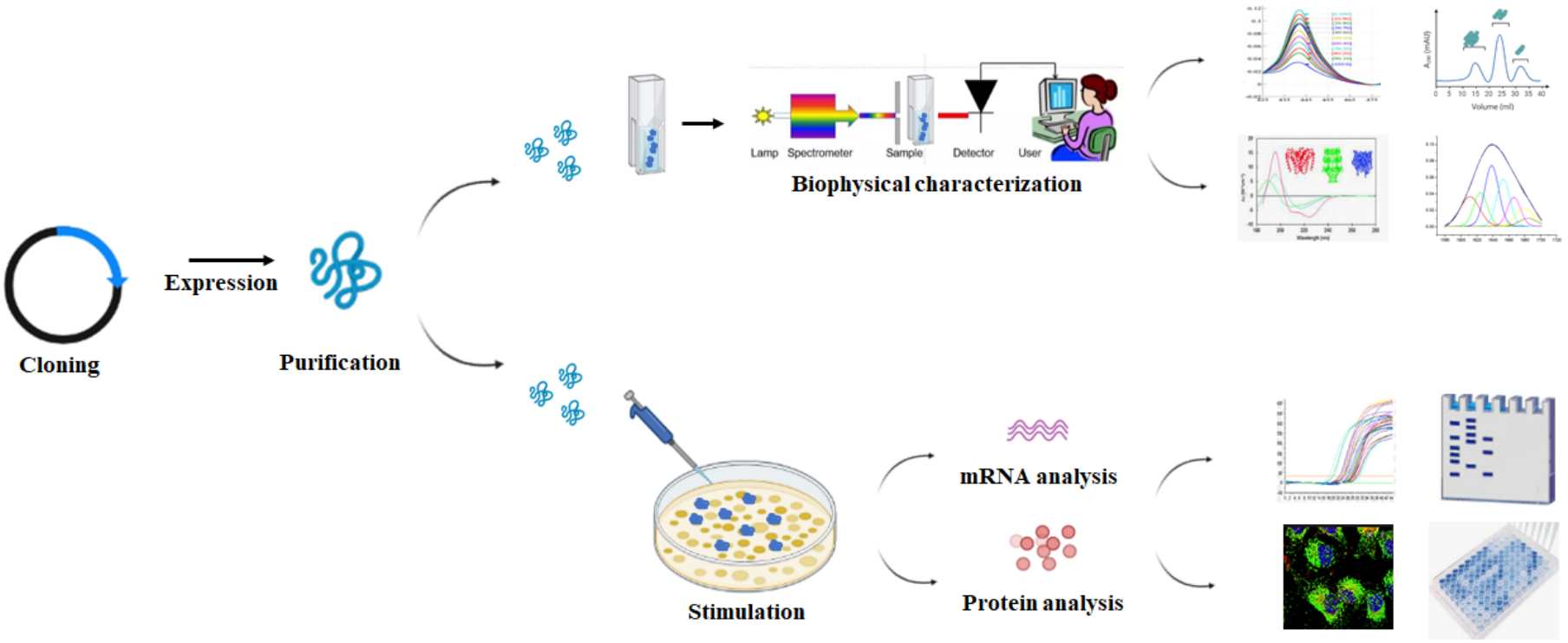

Figure 2.1 Schematic representation of methodology used in the study. In the current study, gene and gene sequence was retrieved and isolated from genomic DNA and genomic DNA sequence from NCBI and proceeded for cloning, protein bacterial expression and purification. Further, the purified protein was used for biophysical structural and functional characterization. Several bioinformatic tools were also used for different structural and functional predictions.

Chapter 3

Chapter 3

Biophysical characterization of the homodimers of HomA and HomB, outer membrane proteins of *Helicobacter pylori*

3.1 Introduction

Gastric cancer is the second most common cause of cancer-associated deaths (Neugut *et al* 1996). Chronic gastritis is the major cause of human gastric cancer caused by the Gram-negative bacterium *Helicobacter pylori*. The International Agency for Research on Cancer (IARC) declared *H. pylori* as a type-1 carcinogen for gastric cancer, which is mediated via chronic gastric inflammation. *H. pylori* is estimated to infect 50% of the world's population (Chiba *et al* 2006, Marshall *et al* 1997). The long-term persistence of *H. pylori* can stimulate a severe immune response that can damage the mucosal lining. Chronic inflammation due to *H. pylori* infection makes it a potentiate agent of acute and chronic gastritis, peptic ulcer disease (PUD), and two forms of cancers, namely, mucosa-associated lymphoid tissue (MALT) lymphoma and gastric adenocarcinoma (Matysiak *et al* 1997, Blaser *et al* 1998, Ernst *et al* 2000, Parsonnet *et al* 1991). Outer membrane proteins (OMPs) of *H. pylori* play a crucial role in the host-pathogen interaction, virulence, and pathogenesis. Upon interaction with the host immune cells, OMPs stimulate the production of pro-inflammatory molecules that may result in an uncontrolled inflammation leading to the transformation of a normal cell to a cancerous cell. Hom (Helicobacter outer membrane) family of OMPs in *H. pylori* consists of four members (HomA, B, C and D). In the *H. pylori* genome jhp0870 open-reading frame (ORF) that codes for HomB outer membrane protein is associated with many stomach diseases and is a novel co-marker for peptic ulcer disease (PUD) (Hussein *et al* 2011, Kang *et al* 2012). homB gene shares 90% sequence similarity with another OMP of the *H. pylori*, which is the

jhp0649 ORF homA, with differences between the 300 bp middle region of these ORFs (Alm *et al* 2000). The Hom OMP family consists of four members, of which homB is the most studied, and evaluated for its prevalence in various peptic diseases. Oleastro *et al*. investigated pathogenesis and immunological response caused by HomB protein in clinical patients and 190 *H. pylori* strain isolated from patients with peptic ulcer disease (PUD) or gastritis were evaluated for the clinical importance of homB. HomB protein contributes to the colonization and persistence of *H. pylori*, and the presence of homB genes affects the number of bacteria adhering to the host cells. Additionally, HomB is also associated with the secretion of the proinflammatory cytokine interleukin-8 (IL-8) (Oleastro *et al* 2008). Outer membrane proteins (OMPs) are distinctive features of Gram-negative bacteria. Most of the OMPs from Gram-negative bacteria form β-barrel, such as OmpA, PhoE, LamB, OmpF, OmpC, FepA, and FhuA from *E. coli*. OMPs are composed of multiple β-sheets arranged in an anti-parallel fashion and thus form a β-barrel. These β-barrel proteins contain the transmembrane domains which interact with the host cell receptors. Additionally, these proteins form a porin-like structure and act as efflux pumps, and are involved in the transport of metabolites, such as BtuB, OprM (Cherezav *et al* 2006, Akama *et al* 2004). Interestingly, these transmembrane β-barrels can exist as monomers or oligomers, for example, OmpF from Salmonella typhimurium forms a trimer of β-barrel (Balasubramaniam *et al* 2012). Interestingly, TolC trimer from *E. coli* forms a single β-barrel (Koronakis *et al* 2004). The β-barrel proteins have the lipid facing hydrophobic and protein facing hydrophilic residues which are arranged alternatively in the transmembrane, enabling the formation of a pore-like structure and extensive inter-strand hydrogen bonding with the non-polar lipid bilayer and the existence of aromatic residues at the water-bilayer interface anchor them in the lipid bilayer and thus result in highly stable transmembrane β-barrels, which do not unfold easily (Wimley *et al* 2003, Bishop *et al* 2001, Ulmschneider *et al* 2001).

Despite the clinical significance of HomA and HomB, their structural characteristics have not been studied in detail. Here, we performed bioinformatics analysis for HomA as well as HomB and observed that these OMPs likely form a small β-barrel, along with a large surface-exposed globular domain. Later, we expressed and purified HomA and HomB, and further used them for their biophysical characterization, using various spectroscopic as well as chromatographic techniques. We also used various detergents and lipids to analyze the structural properties of these OMPs in different conditions. Additionally, SAXS was performed to reveal the three-dimensional shape of these OMPs. These structural characteristics are unique to the *H. pylori* Vf class of autotransporter which are recently reported for Hop family protein (Coppens *et al* 2018) and the least explored for their functional properties.

3.2 Results

3.2.1 *In-silico* analysis of HomA and HomB sequence

Structural aspects of outer membrane protein HomA and HomB from *H. pylori* in bacterial pathogenesis have not been extensively explored. Since HomA and HomB both shares sequence similarity up to 90% and have differences that are confined to the middle region only we did protein sequence alignment using clustal omega (**Fig. 3.1**). Being membrane proteins, HomA and HomB are expected to contain a signal peptide that will enable its insertion in the outer membrane of bacteria. Thus, to identify the presence of a signal peptide for HomA and HomB, we analysed amino acid sequences using the tool SignalP-5.0[25] and observed that both HomA and HomB possess a 16 amino acid N-terminal signal peptide (**Fig. 3.2A**), like other Gram-negative bacteria. Typically, outer membrane proteins from Gram-negative bacteria are synthesized and recognized by the BAM assembly complex via C-terminal consensus sequence X-Z-X-Z-X-Z-Tyr-Z-Phe/Trp (where X is any hydrophobic and Z is any amino acid). To confirm the presence of such a signal at the C-terminal, we performed

Figure 3.1. Protein Sequence alignment between HomA (AAD06225.1) and HomB (AAD06437.1). Sequence alignment was performed by Clustal Omega. Stars are showing identity. The double dot indicates strongly similar properties, and the single dot indicates weakly similar properties. Gaps are showing not identical and not similar in the alignment.

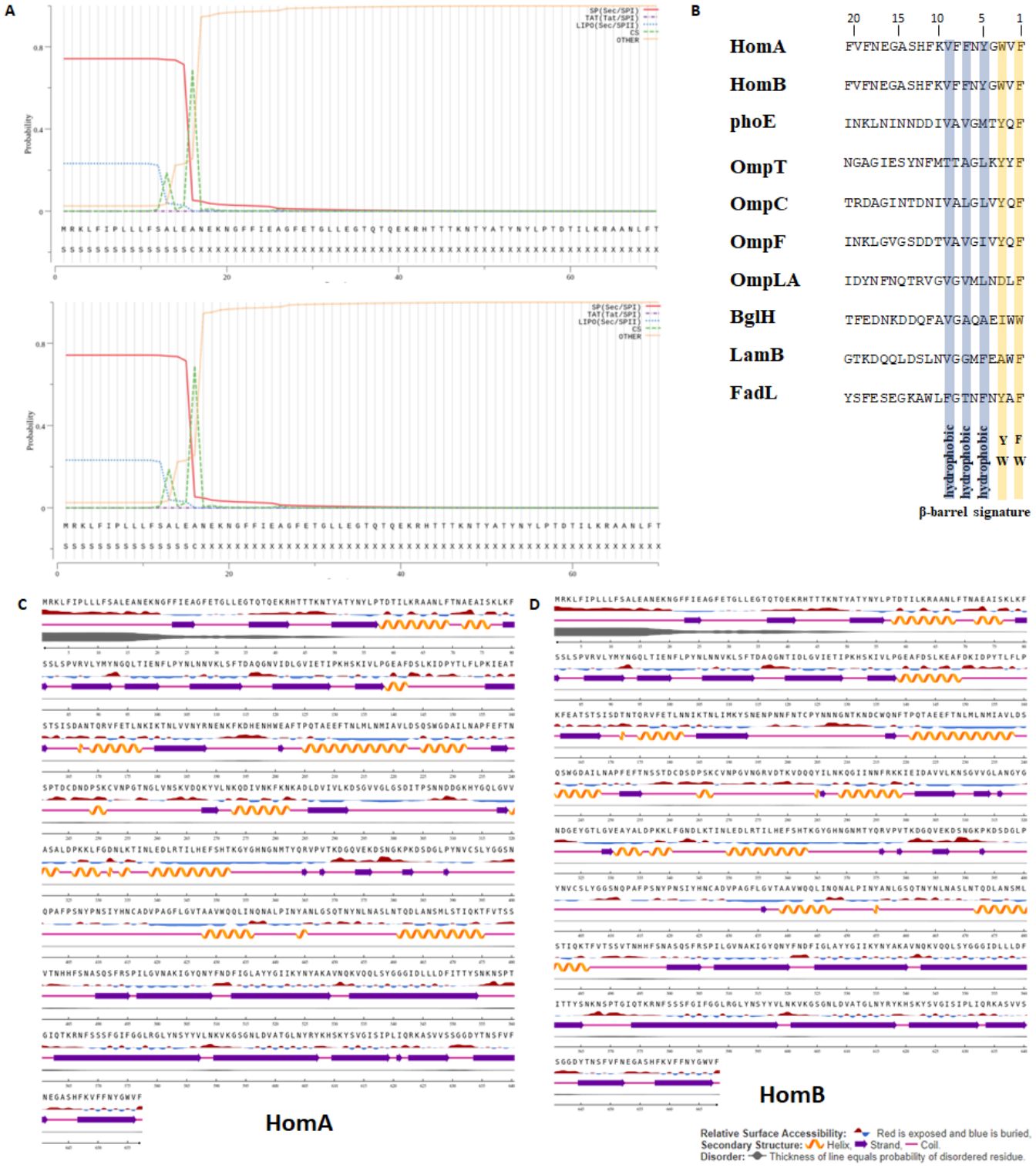

Figure 3.2. ***In silico*** **studies for HomA and HomB. A.** N-terminal outer membrane protein signal sequences prediction of HomA and HomB using SignalP-5.0. **B.** C-terminal β-barrel signature sequence comparison among reported bacterial β-barrel outer membrane proteins with HomA and HomB. **C, D**. Secondary structure contents prediction of HomA and HomB, respectively, using NetSurfP-2.0.

a sequence alignment with most β-barrel proteins from *E. coli* and observed that HomA and HomB also show identical C-terminal consensus signature sequences for β-barrel OMPs (**Fig. 3.2B**). Further, to determine the secondary structure for HomA and HomB, we used the tool NetSurfP-2.0 (Klausen *et al* 2019) and observed that HomA and HomB are likely made up of mixed α helices, β-sheets, and random coils topology, where 22% α-helices, 34% β-sheets and 44% random coils contribute for HomA, and 18.5% α-helices, 38.5% β-sheets and 43% random coils contribute for HomB. Remarkably, N-terminal shows high scale disordered residues, which might be inside or outside the membrane as NetsurfP 2.0 predicts only the secondary structure content and not the location topology (**Fig. 3.2 C, D**). As both HomA and HomB predicted to have a significant number of β-sheets, to know whether these are transmembrane β-strands of outer membrane proteins, we predicted the three-dimensional (3D) structure of HomA and HomB to know the organization of these proteins inside the outer membrane of the bacteria. Here, we employed AlphaFold 2 (Jumper *et al* 2021) (**Fig. 3.3**) and I-TASSER (**Fig. 3.4**) for the prediction of the 3D structure model and observed that both HomA and HomB form β-barrel structures. AlphaFold 2 predicted a small β-barrel domain that is rich in β-sheets, along with a large surface-exposed globular domain which consists of α-helix, β-sheets and random coils (**Fig. 3.3**). Based on the AlphaFold 2 predictions for HomA and HomB, secondary structure contents are 20% α-helix, 43% β-sheets, 37% random coil, and 16% α-helix, 38% β-sheets, 46% random coil, respectively. These predicted models contain 27 β-strands for HomA, and 28 β-strands for HomB, in total. Interestingly, the small barrels for HomA and HomB were made up of 8 β-strands, where N-terminal S1 β-strand is a part of β-barrel which extend to a surface-exposed globular domain and S19 β-strand comes back to be a part of β-barrel. Likely to HomA, N-terminal S1 β-strand of HomB is a part of β-barrel extends to the surface-exposed globular domain and S20 β-strand comes back to be a part of β-barrel (**Fig. 3.5A, B**). We also observed

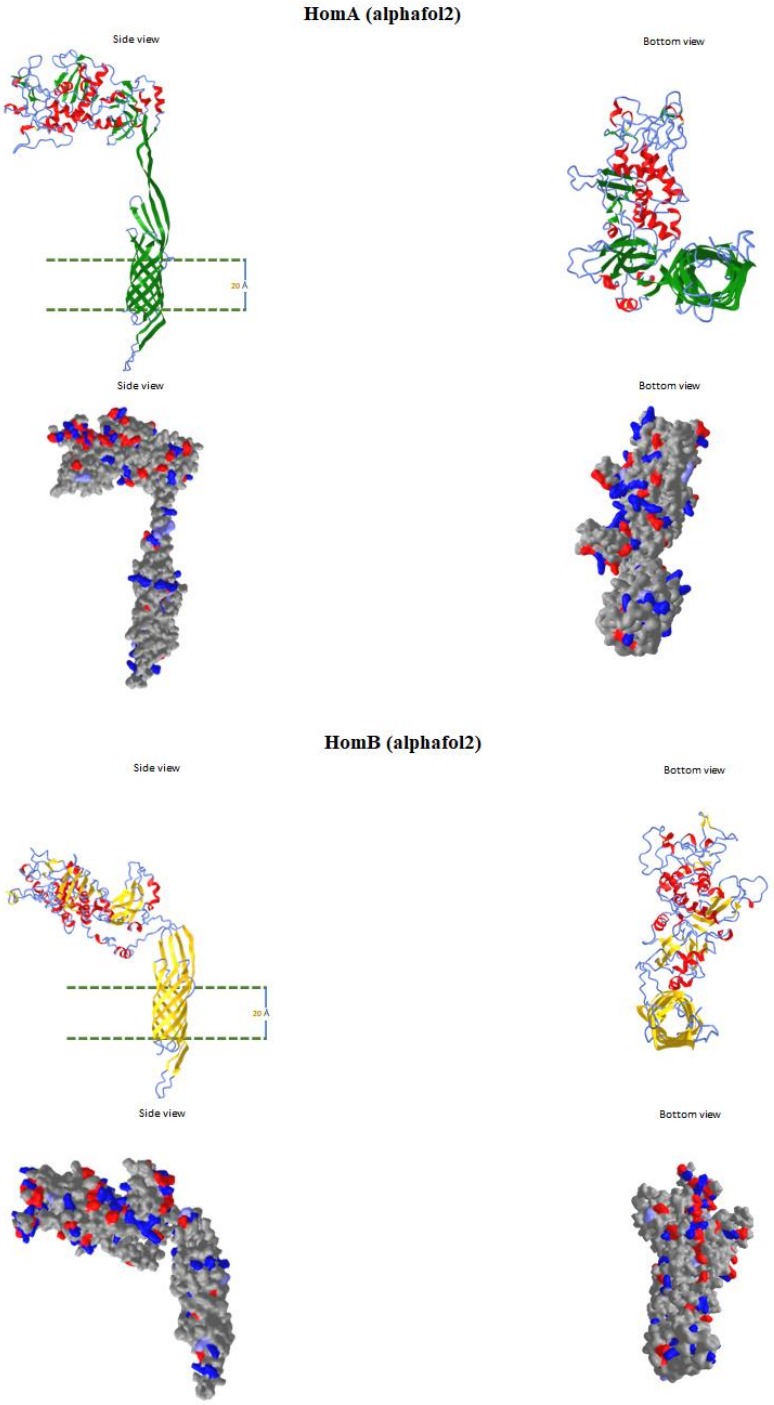

Figure 3.3. Alphafold 2 3D structure prediction of HomA and HomB. A–H. 3D structure predictions of HomA and HomB (without signal peptide) using Alphafold228, side and bottom view for HomA from left to right (**A, B**) β-sheets (green), α-helices (red) and coils (blue); side and bottom view for HomB from left to right (**E, F**) β-sheets (yellow), α-helices (red) and coils (blue). (**C, D**) molecular surface view of charged residues of HomA and (**G, H**) for HomB.

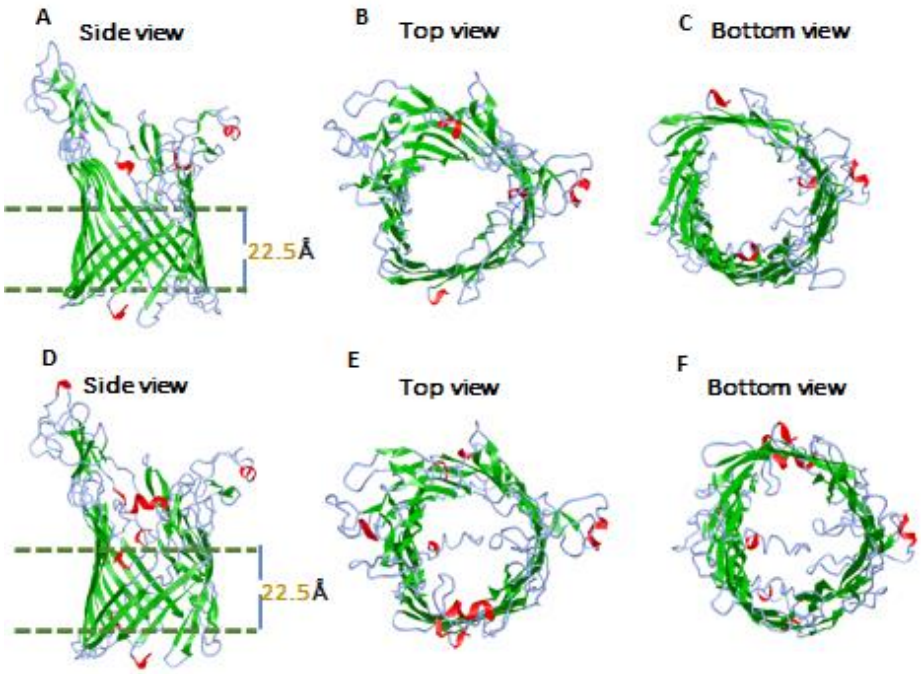

Figure 3.4. I-TASSER 3D structure prediction of HomA and HomB. A-L. 3D structure predictions of HomA and HomB (without signal peptide) using I-TASSER (https://zhanglab.ccmb.med.umich.edu/I-TASSER/), side, top, and bottom view for HomA from left to right (**A-C)**; side, top and bottom view for HomB from left to right (**D-F).**

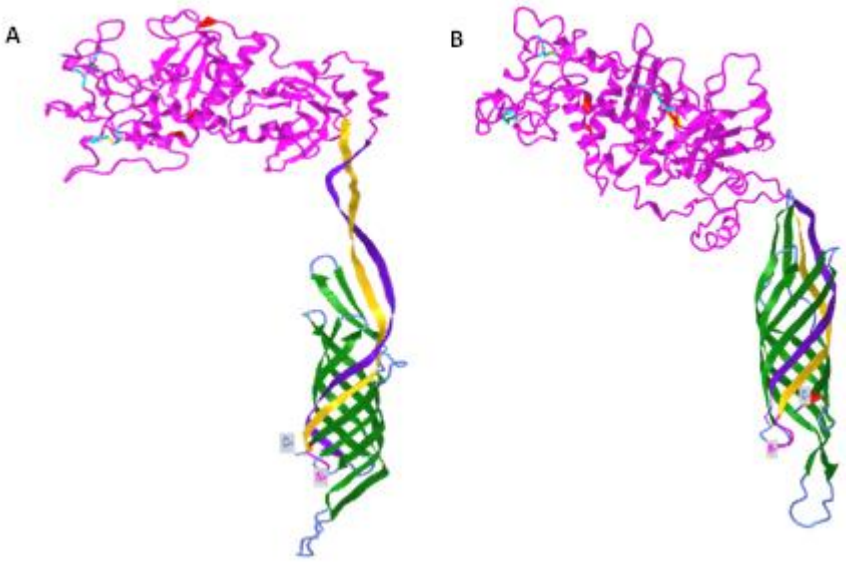

Figure 3.5. Alphafol2 3D structure representation of HomA and HomB. A-B. **A** HomA and **B** HomB, forms small β-barrel, N-terminal S1 β-strand (yellow) is part of β-barrel which extend to form surface-exposed large loop domain and S19 (HomA) and S20(HomB) is β-strand (violet) joined back β-barrel. Cystine residues(cyan) in surface-exposed loop amino acid positions in HomA at 245, 252, 393 and. In HomB at 203, 215, 262, 268, 404 and 427. Tryptophan residues (red) present in the loop as well as β-barrel.

hydrophobic belt around the membrane-embedded portions (20 Å calculated) and predominance of charged residues in both outer as well as the inner portion of the barrel for binding to the lipopolysaccharides molecules, as shown in the molecular surface representation in HomA (**Fig. 3.3C, D**) and HomB (**Fig. 3.3G, H**) models. These in-silico studies suggest that HomA and HomB form a small β-barrel outer membrane protein consisting of 8 β-strands, along with a large surface-exposed globular domain.

3.2.2 Cloning, expression and purification of HomA and HomB

homA and *homB* genes were cloned in *E. coli* to obtain purified HomA and HomB proteins, which were expressed with a C-terminal His-tag. homA and homB genes were PCR amplified from the genomic DNA of *H. pylori* strain J99 with primers (**Appendix B**) and cloned into pBluescript. Based on the restriction pattern, we identified unique clones for HomA and HomB and later confirmed them by DNA sequencing. Subsequently, both the HomA and HomB genes were cloned into pET43 at NdeI and XhoI sites, respectively, to give pHomA and pHomB (**Fig. 3.6A-D**). Cloning of homA/homB in pET43 was confirmed by restriction analysis followed by DNA sequencing. The resultant recombinants were transformed into *E. coli* Rosetta (DE3) cells and induced with 0.1 mM isopropyl-bd-1-thiogalactopyranoside (IPTG). Induced cells were harvested, washed, and resuspended in 500 µl of buffer containing 25 mM Tris-Cl, pH 7.4. Cell lysates were prepared and separated as supernatant and pellet, and supernatant samples were analysed on 8% SDS-PAGE gels to evaluate the amount of protein present in the soluble form. A high level of protein expression of HomA and HomB was observed in the supernatant of induced cells but was absent in the uninduced cells (**Fig. 3.6E, F**). The cloning of homA and homB was performed in such a way that the recombinant protein codes for a C-terminal His-tag for affinity purification. HomA and HomB were purified using a Ni–NTA column using the Akta system (GE healthcare). The input sample was prepared in the equilibration buffer (50 mM Tris-Cl buffer, pH 8.0,

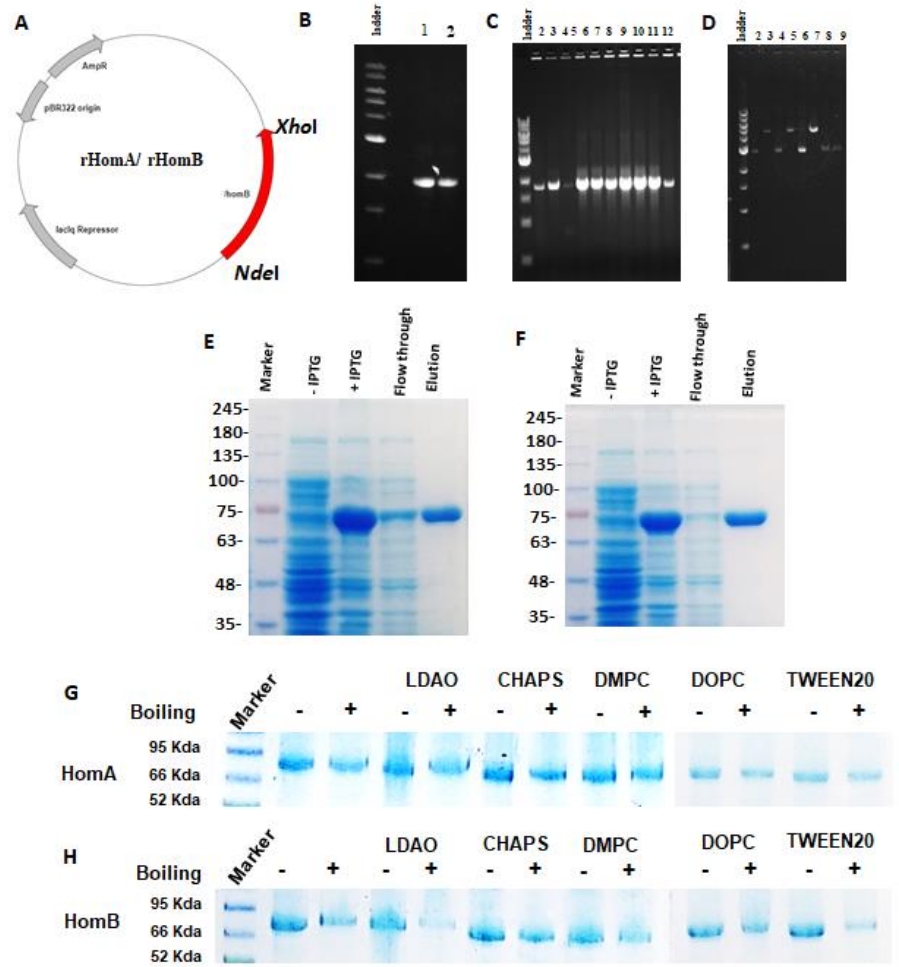

Figure 3.6. Cloning, expression, purification, and heat modifiability of HomA and HomB. A. Cloning strategy of HomA and HomB **B-C**. SDS-PAGE of expression and purification gels of HomA and HomB respectively. For both proteins, SDS-PAGE lane details are: Lane 1, protein marker. Lane 2, uninduced supernatant. Lane 3, induced supernatant. Lane 4, flow-through (purification fraction). Lane 5, elution (purification fraction). **D-E.** Heat modifiability PAGE of HomA (**D**) and HomB (**E**).

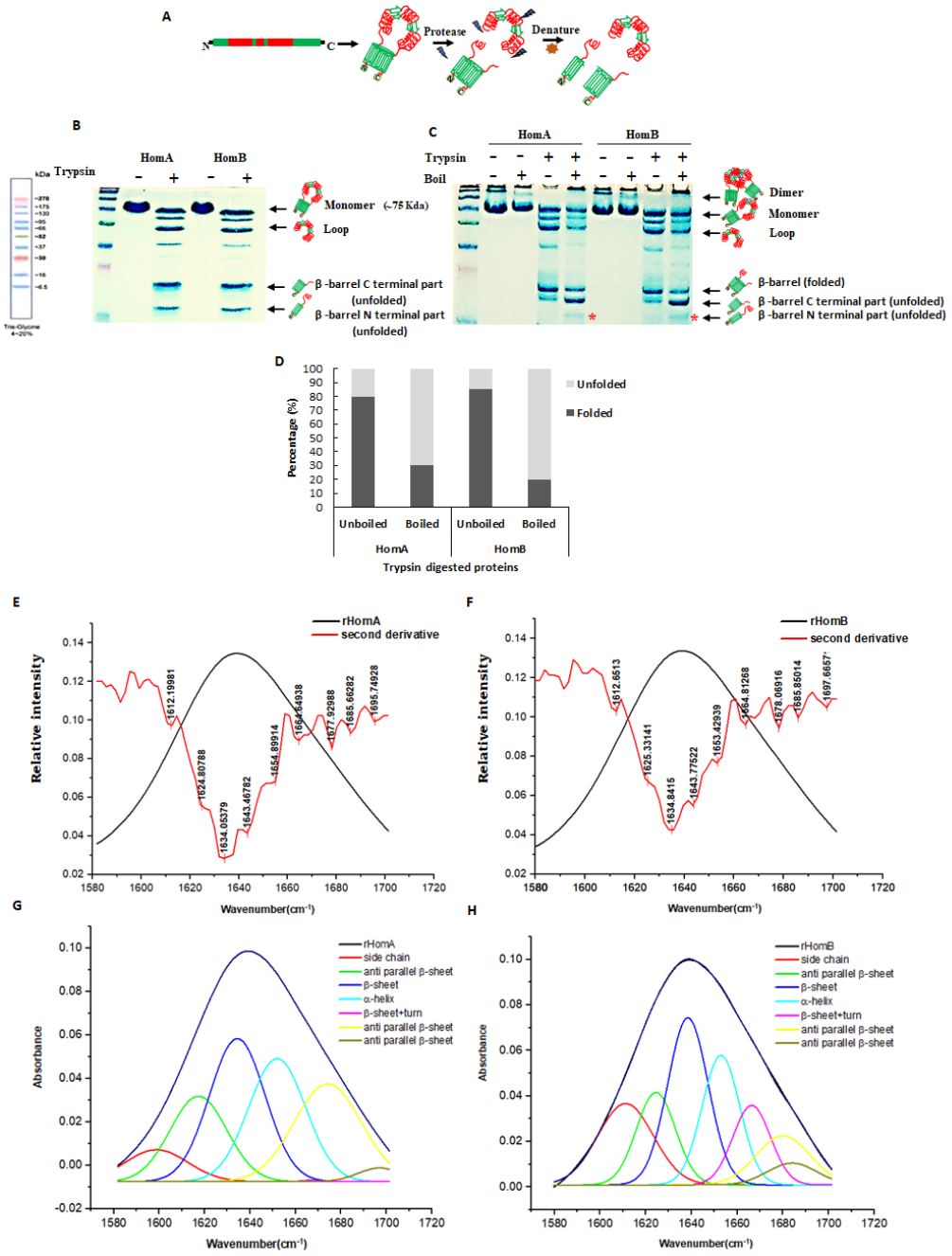

Figure 3.7. Trypsin digestion analysis and ATR-FTIR spectroscopy of HomA and HomB. A. pictorial representation of HomA and HomB protease digestion of scheme. **B.** trypsin digested proteins run onto denaturing SDS-PAGE. **C.** same protein sample run onto the semi-native gel with and without boiling. **D.** percentage of folded and unfolded fractions observed on semi-native PAGE. The red asterisk (*) denotes the N-terminal part that comes out upon unfolding. **E–H.** Secondary structure analysis using curve fitting of the amide I region (1600–1700 cm−1) ATR-FTIR spectroscopy. **E, F.** FTIR absorbance spectra of amide 1 of HomA and HomB, respectively, with their second derivatives. **G, H.** Deconvolution of amide 1 spectra of HomA and HomB, respectively, for secondary structure content analysis. The spectral range of 1600–1700 cm−1 was decomposed using Origin 8.0 software.

300 mM NaCl, and 10 mM imidazole), and loaded on the pre-equilibrated column at a flow rate of 1 ml/min. Subsequently, the column was washed with a wash buffer comprising 50 mM Tris-Cl, pH 8.0, 300 mM NaCl, with 50 mM imidazole. The sample was eluted using an elution buffer comprising 50 mM Tris-Cl, pH 8.0, 300 mM NaCl, with 250 mM imidazole. The samples were collected for analysis by SDS-PAGE. Fig. S1B and C show that the HomA and HomB proteins were able to bind to the Ni–NTA resin, as most of the protein was absent in the flow-through (Fig. S1B and C, lane 4). The size of purified proteins was observed near to 75 kDa on 8% SDS-PAGE for both HomA and HomB. We were able to purify more than 95% pure HomA and HomB proteins (**Fig. 3.6E, F**). Typically, β-barrel proteins show migration differences in boiled and unboiled protein samples during PAGE analysis. Folded β-barrel shows faster migration, whereas unfolded fraction shows slower migration on PAGE. In the case of HomA and HomB, β-barrel is most likely composed of N and C terminal β-strands and upon unfolding that become two separate parts and these migrate as lower size bands. These observations support the *in silico* predicted model of HomA and HomB (**Fig. 3.3**). We also tested the heat modifiability of undigested purified HomA and HomB proteins in the presence of different detergents and lipids. We did not observe a significant migration difference for purified HomA, however, upon incubation with detergents LDAO, TWEEN 20, CHAPS (4X CMC) and lipids DOPC and DMPC (1 mM), a slight migration difference was observed (**Fig. 3.6G**). Similarly, in the case of purified HomB and HomB incubated with detergents LDAO, TWEEN 20 and lipid DOPC show a slight migration difference, whereas DMPC and CHAPS show no heat modifiability (**Fig. 3.6 G**). Since HomA and HomB are likely to contain a small β-barrel with a large globular domain composed of α-helix, β-sheets and random coils and this is possibly the main cause of masking the heat modifiability of these proteins. To investigate the reliability of predicted 3D models of HomA and HomB, purified proteins were treated with protease. Trypsin digestion was carried out

for one hour at 37 °C followed by further analysis via either SDS reducing PAGE or semi-native PAGE (**Fig. 3A–C**). A cartoon representation depicts the possible outcomes of trypsin digestion for HomA and HomB (**Fig. 3.7A**). Incidentally, trypsin has several cleavable sites on HomA and HomB protein sequence, nevertheless, typically β-barrel domains show resistance to protease digestion. As expected from the predicted models (**Fig. 3.3**, the surface-exposed globular domain part corresponds to 40–45 kDa in addition to a 30–35 kDa band of small β-barrel on the gel. Most likely, the N-terminal (16–18 kDa) and C-terminal (22–25 kDa) regions, for HomA and HomB which are rich in β-sheets, come together to form a β-barrel. Interestingly, we observed 3 dominant bands of approximately 45 kDa, 25 kDa and 18 kDa both for HomA and HomB (**Fig. 3.5**. Since β-barrel is likely to be made up of N and C terminals, on a reducing gel two separate bands were observed of the size of around 25 kDa and 18 kDa (**Fig. 3.7 B**). To check whether these two bands are part of β-barrel, the same trypsin digested protein samples were run on a semi-native PAGE. Interestingly, after the denaturation of these samples, we observed two separate bands of the β-barrel domain. The single band in the unboiled samples of HomA and HomB suggests that 80–85% protein is in folded conformation, whereas the boiled samples show only 25–30% fraction in the folded conformation (**Fig. 3C, D**). The additional denatured protein band of the β-barrel domain was observed at around 16–18 kDa (**Fig. 3.7 C,** lane 5 and 9) which is also present in SDS reducing PAGE (**Fig. 3.7 B**), however, this band was not present in the unboiled protein samples on the semi-native gel (**Fig. 3.7 C,** lane 4 and 8).

3.2.3 HomA and HomB are rich in β-sheet and likely form barrel topology

The IR spectra of HomA and HomB proteins were collected to determine and confirm the predicted secondary structures. The secondary structure information of a protein's IR spectrum lies under the Amide I region, which is made up of several overlapping spectra

that are composed of secondary structure elements, such as β-sheet, α-helix, turns, loops and some of them also consist of the side chain absorbance. Here, the Amide I band in the range 1700–1600 cm−1 was plotted with its secondary derivatives. To analyse the secondary structure content of Amide I, we decomposed it to see the individual component spectra position (**Fig. 3.7 E-H**). The second derivative calculation is the easiest and the most common method among a few others, which was employed for data analysis. We observed that HomA and HomB both contain high anti-parallel β-sheet as the peaks were observed at 1634 cm−1, 1685 cm−1, 1695 cm−1, and 1634 cm−1, 1685 cm−1, 1697 cm−1, respectively. However, both proteins also show a peak at 1654 cm−1 for α-helix with a disordered structure peak at 1643 cm−1 (Table 3.1. We performed circular dichroism (CD) experiments to know the secondary structure content of HomA and HomB. Despite sharing more than 92% identity, CD spectra of HomA and HomB are unique. Soluble HomA protein CD spectra show a broad negative peak at around 220 nm and a positive peak at 203 nm, whereas, soluble HomB protein CD spectra show two negative peaks at 214 nm and 221 nm, respectively, and a positive peak at 197 nm (**Fig. 3.8**). Analysis of the CD spectra revealed that the proportion of α-helix (10.5%), β-sheet (39.6%) and Turn (11.5%) for HomA, and α-helix (20%), β-sheet (25.6%), and Turn (14.4%) for HomB. Membrane and detergent environments tend to be amphipathic, and therefore they have different physical properties than aqueous solutions, producing different spectral characteristics for proteins embedded in them. As urea denatured OMPs can refold in micelles of detergents and lipids, we performed CD experiments to study the refolding properties of HomA and HomB. Supplementary Table S3 summarizes deconvoluted data of CD spectra of HomA and HomB in the presence of various lipids and detergents. HomA and HomB show hyperchromic shifts in the presence of LDAO (4× and 10× CMC), DMPC and DOPC (0.25 mM, 0.5 mM, and 1 mM), and TWEEN 20, indicating that incubation of HomA and HomB with these lipids and detergents reduce α-helix content and increases the parallel β-sheet

Table 3.1 Secondary structure content analysis based on selective region (1600-1700 cm^{-1}) FTIR second derivative spectrum of HomA and HomB

S No	Secondary structure content	Peak position (cm^{-1})	
		HomA	HomB
1	Sidechain	1612	1612
2	Anti-parallel β-sheets	1624	1625
3	Parallel β-sheets	1634	1634
4	Disordered	1643	1643
5	α-Helix	1654	1653
6	β-sheets+Turn	1664, 1677	1664, 1678
7	Anti-parallel β-sheets (weak)	1685, 1695	1685, 1697

Table 3.2. Most to least favourable folding conditions for HomA and HomB in detergents and lipids based on the circular dichroism spectra analysis

Folding ranking	Detergent and lipids	
	HomA	HomB
High	LDAO	LDAO; DOPC and DMPC; TWEEN20
Moderate	DOPC and DMPC; TWEEN20	
Low	CHAPS	CHAPS

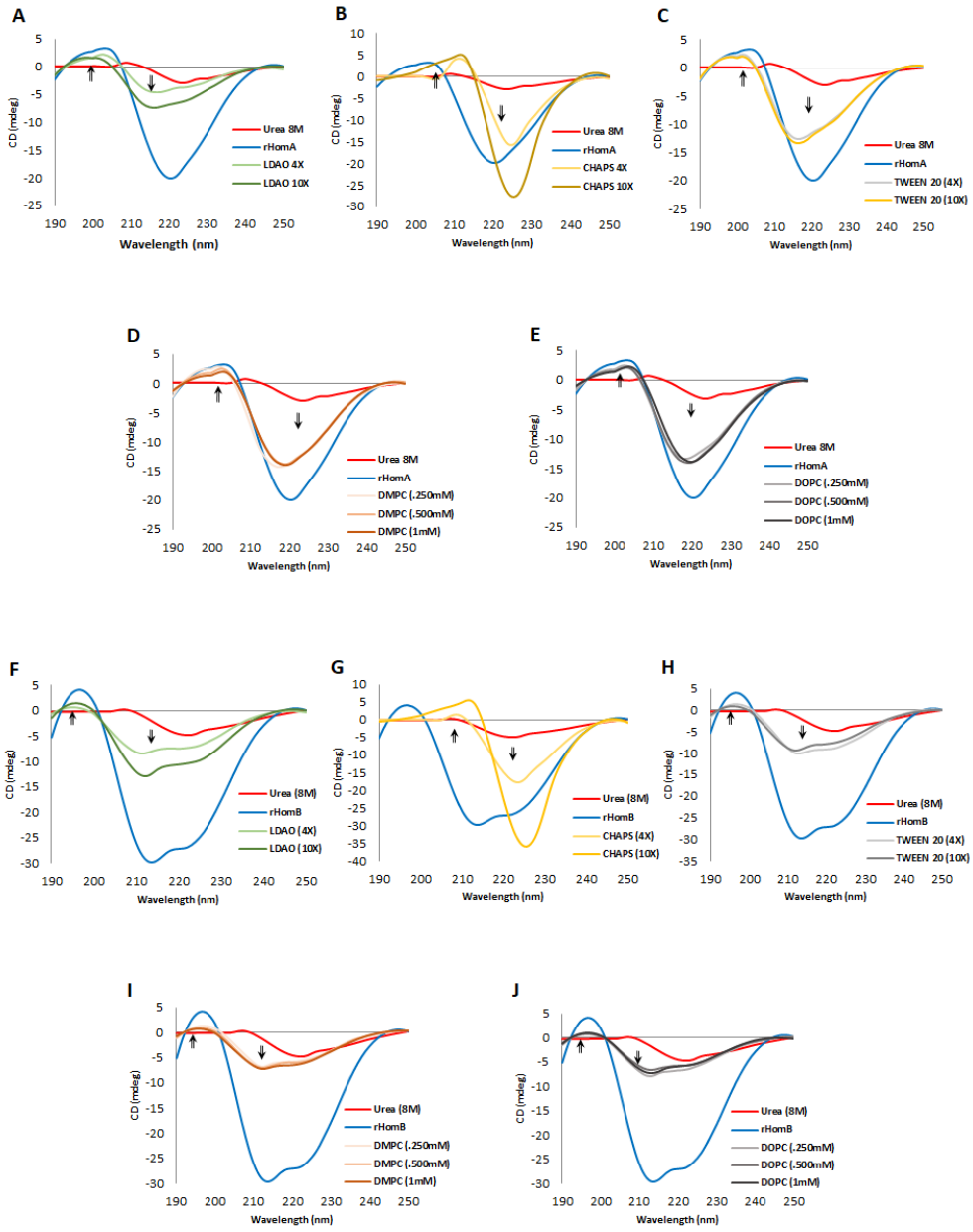

Figure 3.8. Secondary structure Analysis using circular dichroism. **A–C.** CD spectra for HomA, 40-fold dilution to a buffer containing detergent 4x and 10x concentration of CMC, LDAO, CHAPS, and TWEEN 20, respectively. **D, E.** CD spectra for HomA, 40-fold dilution to a buffer containing 0.25 mM, 0.5 mM, and 1 mM DMPC and DOPC lipids, respectively. **F–H.** CD spectra for HomB, 40-fold dilution to a buffer containing detergent 4x and 10x concentration of CMC, LDAO, CHAPS, and TWEEN 20, respectively. **I, J.** CD spectra for HomB, 40-fold dilution to a buffer containing 0.25 mM, 0.5 mM, and 1 mM DMPC and DOPC lipids, respectively.

structure. Contrarily, the addition of CHAPS (4× and 10× CMC) to denatured HomA and HomB proteins did not increase the parallel β-sheet structure (**Table 3.2**). HomA with CHAPS (4× and 10× CMC) reduces α-helix content and increases the turn structures, HomA with TWEEN 20 and LDAO (4× and 10× CMC) reduces α-helix content and increases the parallel β-sheet structure. While, the addition of lipids, such as DMPC and DOPC (0.25 mM, 0.5 mM, and 1 mM) to HomA, demonstrated reduced α-helix content and increased mixed parallel and anti-parallel β-sheet as well as turns in the CD spectra (**Fig. 3.8 A–E**, Appendix D **Table 1**). Likewise, CD spectra analysis of HomB with CHAPS (4× and 10× CMC) demonstrated a reduction in α-helix content and increased turn structures, up to 48%. Similarly, HomB with TWEEN 20 and LDAO (4× and 10× CMC) revealed a reduction in α-helix content and an increase in the parallel and anti-parallel β-sheet structure. Very similar to HomB, the addition of lipids, such as DMPC and DOPC (0.25 mM, 0.5 mM, and 1 mM) to HomA, demonstrated a reduction in α-helix content and an increase in the mixed parallel and anti-parallel β-sheets (**Fig. 3.8 F–J**, Appendix D Table 1).

3.2.4 Effect of pH, detergents, and lipids on the topology of HomA and HomB

Incidentally, HomA and HomB both contain 4 tryptophan amino acid residues (**Fig. 3.5**). The tryptophan residues give fluorescence emission peaks between 300 to 350 nm depending on the polarity of the local environment, and thus can be used to assay predicted topologies. We measured tryptophan fluorescence of recombinant HomA and HomB proteins to study the conformational state of a protein. Folded β-barrel protein gives fluorescence emission maximum near to 330 nm range, called blue-shift, as the tryptophan residues present in the folded β-barrel proteins move from an aqueous environment to the hydrophobic environment (Heuck *et al* 2002). We tested the folding pattern of denatured and purified HomA and HomB proteins in various pH buffers, at different urea concentrations, as well as in the presence of

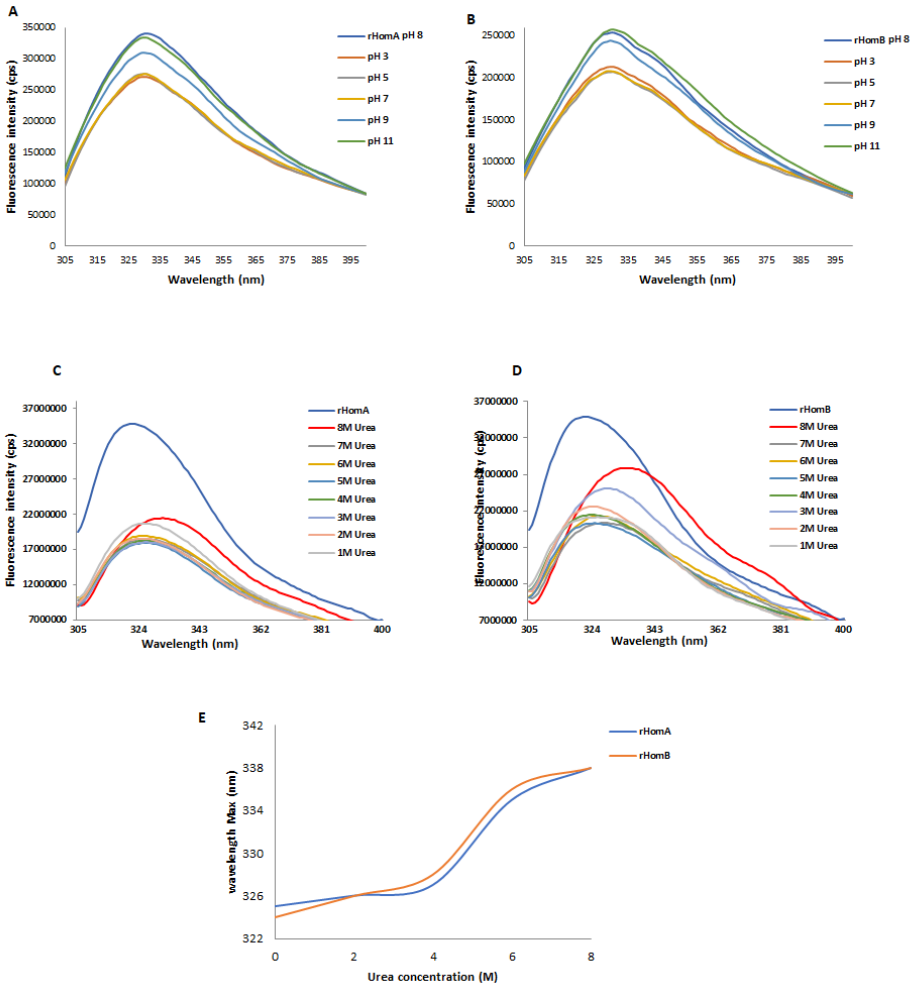

Figure 3.9. Effect of pH and urea on HomA and HomB. A, B. Effect of pH on HomA and HomB Tryptophan fluorescence, respectively. **C, D.** Tryptophan fluorescence spectra of HomA and HomB, respectively, with increasing urea concentration from 1 to 8 M. **E.** Representation of denaturation kinetics for HomA and HomB, respectively, with increasing concentration of urea.

various detergents and lipids. Initially, we checked the effect of pH on HomA and HomB structures, by incubating these proteins in buffers ranging from pH 3.0 to 11.0. We observed that changes in the pH do not affect the structure of these proteins, and it shows fluorescence maxima at 324 nm for HomA and 323 nm for HomB, respectively (**Fig. 3.9 A, B**). Subsequently, we studied the denaturation kinetics of HomA and HomB by employing an increasing concentration of urea from 1 to 8 M. We checked the effect of urea on HomA and HomB structures, by incubating these proteins in buffers containing 1 M to 8 M urea, to understand the denaturation pattern. The addition of urea resulted in the redshift (bathochromic shift) from 324 to 338 nm for HomA, and 323 nm to 340 nm for HomB, respectively (**Fig. 3.9 C–E**). the unfolding of these proteins started at 4 M urea, and a steady decrease in the fluorescence intensity suggests that these proteins are changing their conformations in the presence of increasing concentrations of urea. To understand the refolding pattern from its denatured unfolded states in the presence of urea, we performed a 40-fold dilution of proteins using a buffer containing different concentrations of detergents and lipids, thus diluting urea concentration from 8 M to less than 300 mM. the unfolded HomA protein in 8 M urea has an emission maximum at 338 nm, whereas the folded protein shows an emission maximum at 324–325 nm for CHAPS (4×) and (10×), 327–328 nm for LDAO (4×) and (10×), 325–326 nm for TWEEN 20 (4×) and (10×), 324 nm for DMPC (0.25 mM and 1 mM), 324–325 nm for DOPC (0.25 mM and 1 mM), respectively (**Fig. 3.10 A–E**). Similarly, we observed the unfolded HomB protein in 8 M urea demonstrated emission maximum at 340 nm and the folded proteins show emission maximum 323 nm for CHAPS (4×) and (10×), 324 nm for LDAO (4×) and (10×), 324–325 nm for TWEEN 20 (4×) and (10×), 324–323 nm for DMPC (0.25 mM and 1 mM), 324–323 nm for DOPC (0.25 mM and 1 mM), respectively (**Fig. 3.10 F–J**). The emission spectra for LDAO, TWEEN 20, DMPC, and DOPC show increased fluorescence intensity for the folded proteins, suggesting that HomA and HomB structures are altered with the addition of these

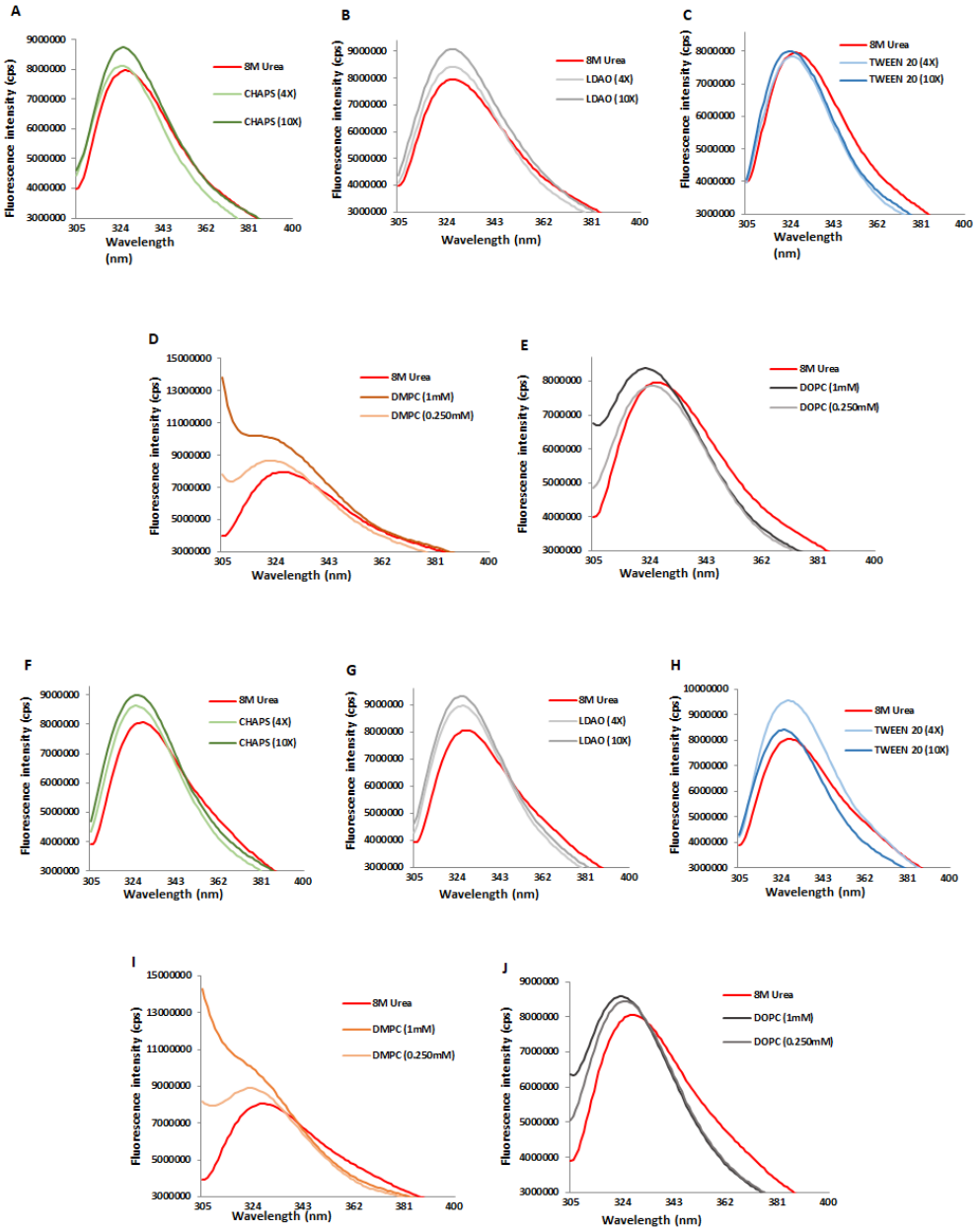

Figure 3.10. Effect of detergents and lipids on HomA and HomB folding. A–C. Tryptophan fluorescence spectra of denatured HomA and 40 folds diluted in buffer containing CHAPS, LDAO, and TWEEN 20 detergents, respectively, 4x and 10x concentration of CMC. **D, E.** Tryptophan fluorescence spectra of denatured HomA and 40 folds diluted in buffer containing DMPC and DOPC (0.25 mM and 1 mM), respectively. **F–H.** Tryptophan fluorescence spectra of denatured HomB and 40 folds diluted in buffer containing CHAPS, LDAO, and TWEEN 20 detergents, respectively, 4x and 10x concentration of CMC. **I, J.** Tryptophan fluorescence spectra of denatured HomB and 40 folds diluted in buffer containing DMPC and DOPC (0.25 mM and 1 mM), respectively.

detergents and lipids. Furthermore, a blue shift (hyperchromic shift) in the emission spectra observed during the refolding, induced by the addition of detergents and lipids, further confirms that both HomA and HomB restores the β-barrel topology in the presence of detergents and lipids.

3.2.5 HomA and HomB exist in monomer and homodimer forms

To assess the oligomeric state of HomA and HomB, we performed size exclusion chromatography experiments. HomA and HomB were incubated with the 10× concentration of CMC of detergents (LDAO, CHAPS, TWEEN 20) or 1 mM of lipids (DMPC, DOPC) in 50 mM Tris-Cl, pH 8.0, and 300 mM NaCl. The size exclusion chromatogram profile shows purified HomA and HomB was eluted in two major fractions which correspond to monomer and dimer forms (**Fig. 3.11 A, B**). In the chromatogram for HomA, the first peak near 7.5 ml is of column void volume, the second hump like peak near 11 ml corresponds to the most likely trimer size of HomA. The third and fourth peaks at 12.5 and 13.5 ml correspond to dimer and monomer of HomA, respectively. The incubation of HomA with LDAO and CHAPS shows a major aggregation peak at column void volume but peaks that correspond to dimer and monomer still exist (**Fig. 3.11 C, D**). Incubation of HomA with TWEEN 20, DOPC and DMPC shows similar chromatograms. Simultaneously, fractions were collected analysed on SDS-PAGE, and approximately 150 kDa and 75 kDa bands were observed which correspond to dimer and monomer size (**Fig. 3.12 B–D**). Likewise, the HomB chromatogram shows prominent peaks for dimer and monomer at 12.5 and 13.5 ml, respectively (**Fig. 3.11. B and 3.12. E**). HomB was predominantly showing peaks for dimer and monomer, whereas the void volume peak was absent for HomB. Incubation of HomB with LDAO shows a peak at void volume, a shoulder peak near 9 ml and dimer, monomer peak at 12.5 and 13.5 ml, respectively (**Fig. 3.11. E**). However, incubation of HomB with CHAPS leads to aggregation, which shows a peak of void volume

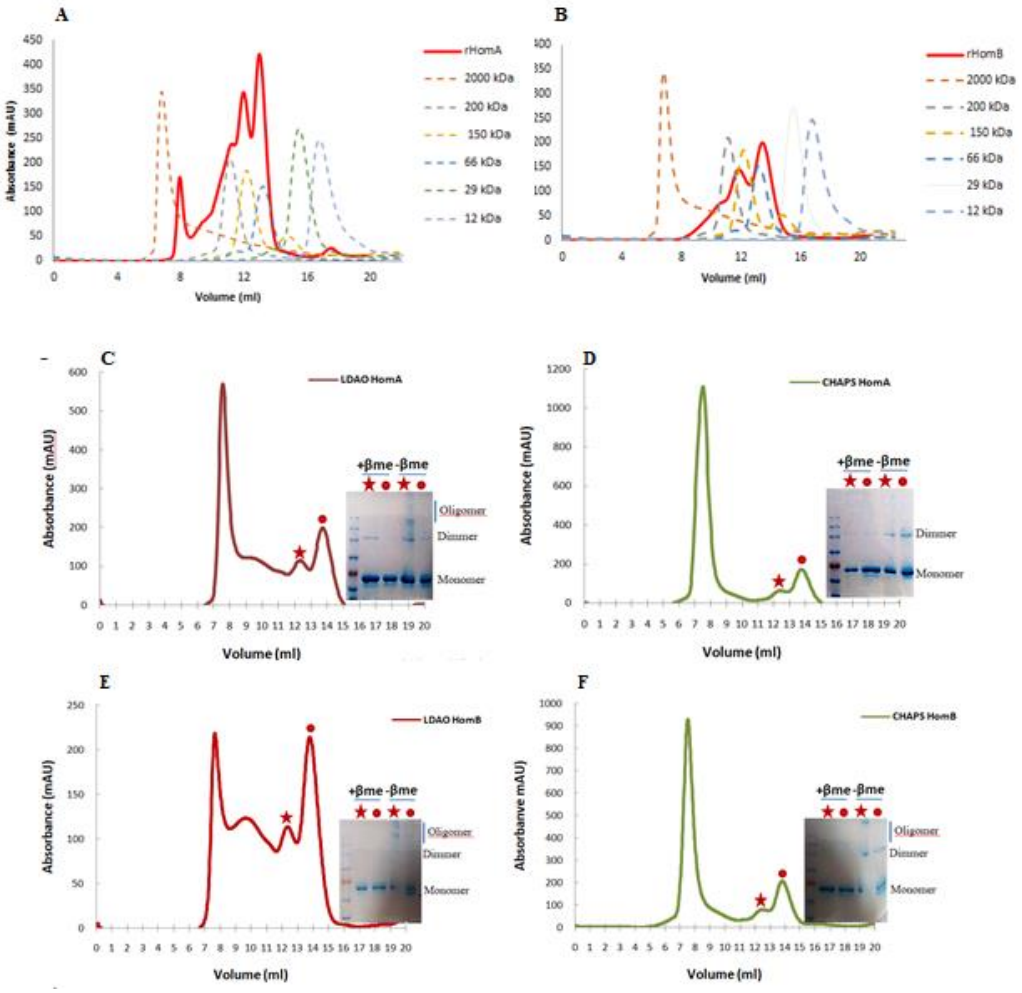

Figure 3.11. A-B. Gel filtration profile of HomA (A) and HomB (B) on Superose 12 column in buffer 50 mM Tris-Cl pH 8.0, 300 mM NaCl. The standard molecular weight markers used were 200 kDa (β amylase), 150 kDa (alcohol dehydrogenase), 66 kDa (albumin), 29 kDa (carbonic anhydrase), and 12 kDa (cytochrome C). The void volume is determined by blue dextran (red colour profile) of MW~ 2000 kDa. Molecular weight for HomA and HomB is estimated to be about 75-70 kDa approx. for monomer peaks respectively and 150 kDa approx. which is equivalent to its dimer. **C, D.** Size-exclusion chromatogram for HomA incubation with 10X of CMC concentration of LDAO, CHAPS, and **E, F.** Size-exclusion chromatogram for HomA incubation with 10X of CMC concentration of LDAO, CHAPS. All the fractions were collected for monomer peak (red ball) and dimer (red star) for both HomA and HomB incubated with either detergent or lipid as mentioned and run onto SDS-PAGE with or without beta-mercaptoethanol (β-me).

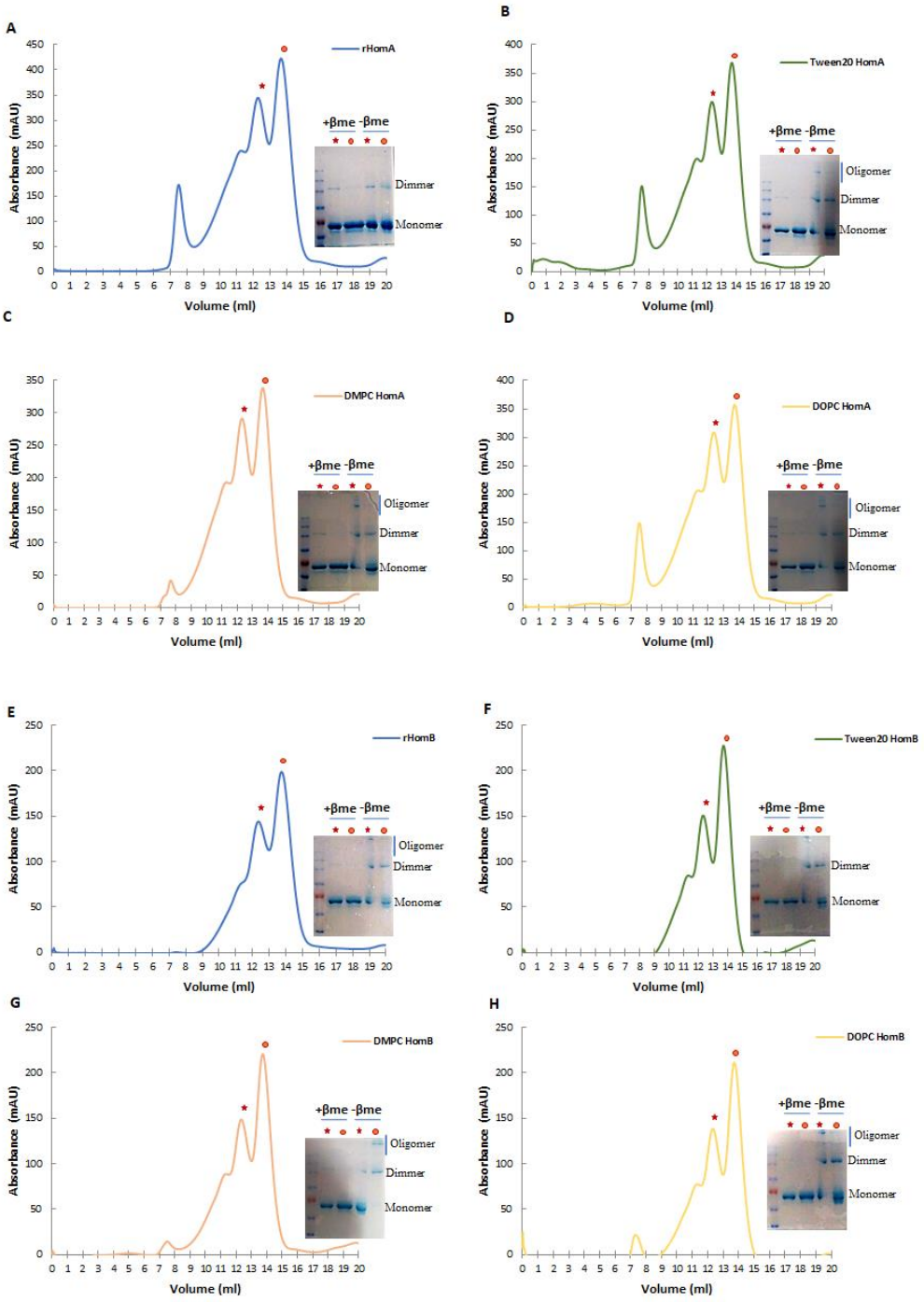

Figure 3.12. HomA and HomB exist in monomer and homodimer forms. A. Chromatogram of size exclusion chromatography of HomA. **B–D.** Size-exclusion chromatogram for HomA incubation with 4x of CMC concentration of TWEEN 20, and 1-mM concentration of DMPC and DOPC lipids, respectively. **E.** Chromatogram of size exclusion chromatography for HomB. **F–H.** Size exclusion chromatogram of HomB incubated with 4x of CMC concentration of TWEEN 20, and 1-mM concentration of DMPC and DOPC lipids, respectively. All the fractions were collected for monomer peak (red ball) and dimer (red star) for both HomA and HomB incubated with either detergent or lipid as mentioned and run onto SDS-PAGE with or without beta-mercaptoethanol (β-me).

at 7.5 ml, although some fraction of dimer and monomer still exist (**Fig. 3.11. F**). DOPC, DMPC, and TWEEN 20 show similar chromatogram peaks with HomB, with little void volume peak in lipids (DOPC, DMPC) incubation (**Fig. 3.12 I, J**). Like HomA, 150 kDa and 75 kDa bands were observed on SDS-PAGE for each collected fraction (**Fig. 3.12 F–H**). Incubation with detergents and lipids of HomA and HomB rearranges the secondary structure of proteins as observed in circular dichroism spectra (**Fig. 3.8 A–J**). Here, incubation with LDAO and CHAPS leads to larger size aggregation of both HomA and HomB proteins, whereas Tween 20 induces aggregation in HomA only. Possibly detergents moieties rearrange the secondary structure of proteins thus leading to the formation of aggregates. However, the addition of lipids favours secondary structures that are similar to the wildtype proteins, and therefore do not show aggregation of proteins. Both proteins show the formation of the homodimer, as confirmed by SDS-PAGE analysis.

3.2.6 Solution structure of HomA and HomB dimers

Small-angle solution scattering data on the aqueous solutions of HomA and HomB were acquired at the BL-18 beamline of the Indus-2 synchrotron source. For Guinier analysis, data with a q-range of 0.00955 to 0.0193 Å−1 for HomA and 0.0106 to 0.0199 Å−1 for HomB was analysed. The Guinnier analysis showed a somewhat similar radius of gyration for HomA and HomB of around~80 Å (**Fig. 3.13**). Indirect Fourier transformation (IFT) of the curves calculated using the GNOM program31 and the experimental curves fitted with SAXS data for HomA and HomB proteins were shown in (**Fig. 3.13**). The pair distance distribution function deduced maximum dimension (Dmax) for HomA and HomB was 280 and 271 Å−1 respectively. Both Guinier and pair distance distribution functions yielded similar Rg values for both proteins, signifying the absence of aggregation or inter-particle interactions in samples. Since the solution scattering data were collected on a relative scale of intensity, the molecular weight of both HomA and HomB from SAXS data was

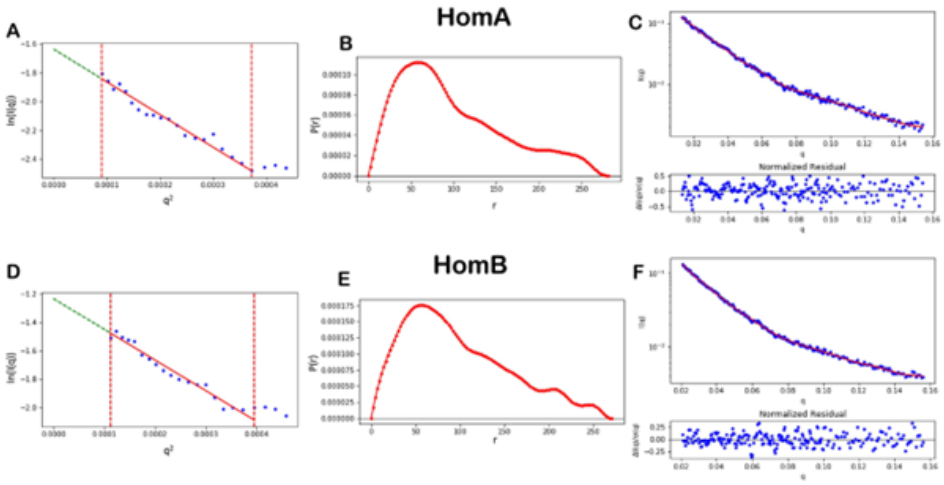

Figure 3.13. Guinier analysis of experimental SAXS data of HomA (A) and HomB (D). Pair distance distribution function [P(r)] for the experimental scattering data of HomA **(B)** and HomB **(E)**. Indirect Fourier transform (IFT) ft of experimental SAXS data of HomA (C; $\chi 2$=0.029) and HomB (D; $\chi 2$=0.0506) in red line and blue dots defines the experimental data.

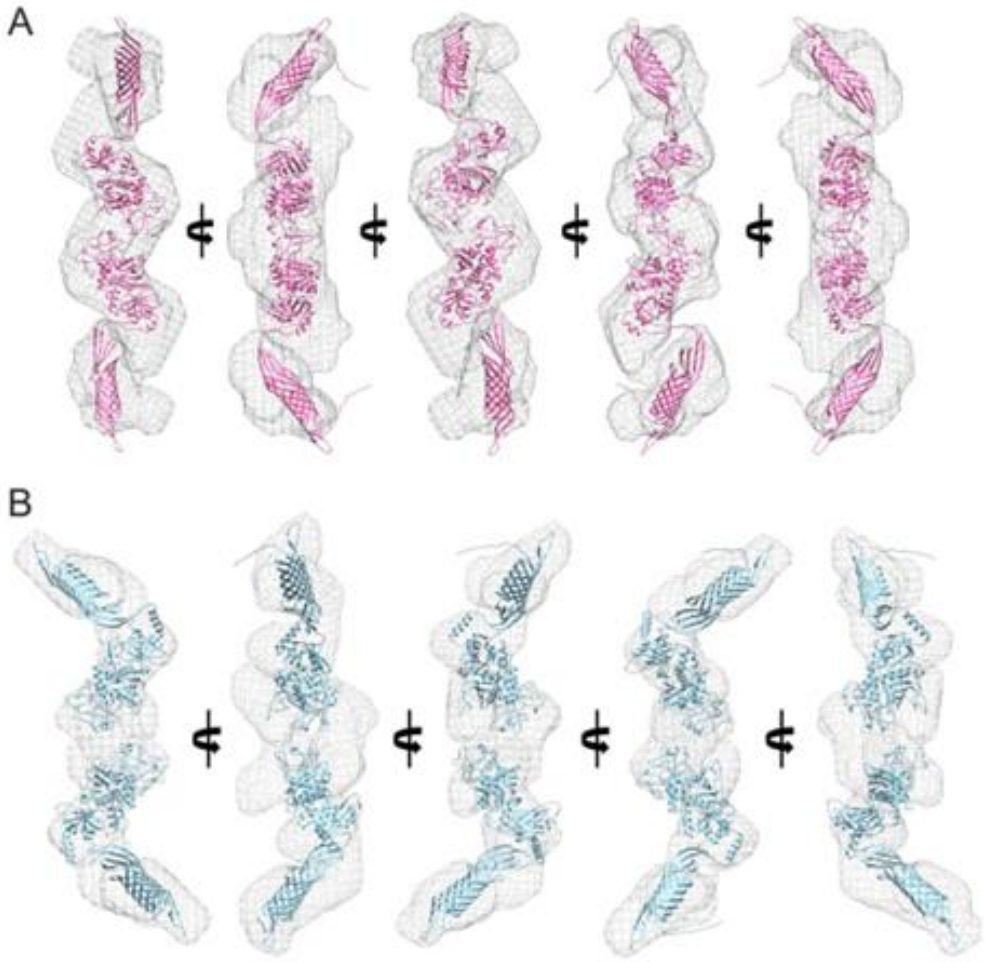

Figure 3.14. Ab initio shape model generated with DAMMIN (grey mesh; envelope at 15 Å resolution) and respective overlaid molecular structure of HomA (A) and HomB (B) in different orientations.

determined by concentration-independent methods (Piladov *et al* 2019, Hajizadeh *et al* 2018). The molecular weight estimated from the experimental SAXS profile indicates that both HomA and HomB are homodimers. Furthermore, AlphaFold 2 deduced the molecular structure of HomA and HomB fits exceptionally well against SAXS ab-initio shape models obtained with the DAMMIN module of ATSAS (**Fig. 3.14**).

3.2.7 Summary

Helicobacter pylori is the major cause of several stomach diseases. It interacts with gut epithelial cells and induces inflammation. Here, we explored the structural aspects of HomA and HomB which are reported for their prevalence in stomach diseases. Interestingly, in-silico studies demonstrated that HomA and HomB possess characteristics of β-barrel OMP, such as a signal peptide at the N-terminal and β-barrel signal at the C-terminal (**Fig. 3.2 A, B**). HomA and HomB both have mixed secondary structure content, nevertheless, β-sheets are predominantly present in both proteins (**Fig. 3.2 C, F**). Additionally, HomA and HomB localize in the outer membrane with 8 transmembrane antiparallel N+C-terminal β-strands connected by the large surface exposed globular domain (**Fig. 3.3 and 3.5**). Furthermore, the secondary structure was confirmed with ATR-FTIR, amid I spectra for HomA and HomB both contain mixed α helices and β-sheets spectra (**Fig. 3.7 E–H**). CD spectra showed HomA and HomB both favours β-barrel structure and the addition of lipids and detergents to the denatured HomA and HomB rearranged proteins favouring antiparallel β-sheets (**Fig. 3.8 A–J**). Interestingly, HomA and HomB were stable at a pH range from 3 to 11 (**Fig. 3.9 A, B**). Additionally, both proteins start unfolding at 2 M of urea, the addition of denatured HomA and HomB to lipids, and detergents refold which was observed in the tryptophan fluorescence spectra (**Fig. 3.10 A–J**). We performed size exclusion chromatography for HomA and HomB and observed peaks that correspond to dimer and monomer. Moreover, incubation of HomA and HomB with detergents shows oligomerization/aggregation

of proteins, however, incubation with lipids shows peaks corresponding to dimer and monomer (**Fig. 3.11 and 3.12**). Furthermore, the solution structure analysis of HomA and HomB using small-angle X-ray scattering (SAXS) experiments confirmed that both HomA and HomB form homodimers (**Fig. 3.13**). OMPs are distinctive features of Gram-negative bacteria and play a crucial role in host-pathogen interaction, virulence, and pathogenesis of bacteria. Our studies will help in a better understanding of *H. pylori* pathogenesis and host-pathogen interactions via OMPs.

Chapter 4

Chapter 4

HomA and HomB, outer membrane proteins of *Helicobacter pylori* down-regulate Activation-induced cytidine deaminase (AID) and Ig switch germline transcription and thereby affect class switch recombination (CSR) of Ig genes in human B-cells

4.1 Introduction

Helicobacter pylori (*H. pylori)* is a Gram-negative bacteria and class one carcinogen for gastric cancer mediated *via* chronic gastric inflammation and associated with stomach disease (Chiba *et al*., 2006). Incidentally, chronic gastritis is a major cause of human gastric cancer. Incidentally, people infected with *H. pylori* are two to ten-fold more prone to develop a risk of peptic ulcer disease and adenocarcinoma than people without *H. pylori* infection or people treated with antibiotics (Hentschel *et al* 1993). Although, most people infected with *H. pylori* do not show symptoms throughout their life, however, eventually all of them develop chronic gastric inflammation (Warren, 2000. In addition, *H. pylori* infection also increase the risk of mucosa-associated lymphoid tissue (MALT) lymphoma about six-fold higher (Nato and Peek 2012, Parsonnet *et al* 1994). MALT lymphoma majorly consisted of small heterogeneous B-cells present near mucosa tissues. *H. pylori* get access to these lymphoid tissues during infection and is closely linked to the development of gastric MALT lymphomas (Kusters *et al* 2006, Zullo *et al* 2010 and Wundisg *et al* 2012).

During infection, B-cells are activated, and germinal center formation takes place in the lymphoid tissue (Tonegawa, 1983). In course of developing adaptive immunity, B-cells fights with pathogens by releasing antibodies. The process involved in producing low-affinity antibodies to high specific affinity antibodies is called affinity maturation. Prolonged B-cell activation leads to affinity maturation which involves somatic hypermutation (SHM) and class switch recombination (CSR). Activation-induced cytidine deaminase (AID) is

a crucial enzyme that takes part in both processes of affinity maturation that results in the diversity of antibodies, and subsequent clonal selection leads to proliferation of high affinity producing B-cells (Meffre and O'Connor, 2019; LeBien and Tedder, 2008; Luman Wang and Chu, 2020). Besides, the positive role of AID in affinity maturation, its off-target activity leads to genomic instabilities and cancer progression. Matsumoto *et al* reported that *in vivo*, AID transgenic mice develop gastric neoplasm which suggested that aberrant AID expression contributes to the development of cancer *via* the accumulation of somatic mutations (Ruprecht and Lanzavecchia, 2006; Pone *et al*., 2010; Rawlings *et al*., 2012; Montes *et al*., 2007, Matsumoto *et al*., 2007).

In addition to antibody-mediated immune response, B-cells also modulates the immune response in antibody independent manner, *via* the release of certain cytokines and presenting antigens to subsets of T-cells (Buendía *et al*., 2002; Moseman *et al*., 2012; Ugrinovic *et al*., 2003). A subset of B-cells, regulatory B-cell (B_{regs}) initially coined by Mizoguchi *et al*, exerts immune-suppressive functions (Mizoguchi *et al*., 2002). Secretion of anti-inflammatory cytokines, such as IL10, IL35 and transforming growth factor-β (TGFβ), results in suppression of T-cells and other cells of innate immune responses (Mizoguchi and Bhan, 2006; Mauri and Bosma, 2012; Fillatreau *et al*., 2002). Interestingly, deficiency of B-cells has been reported with enhanced resistance to pathogenic infections which suggests that B_{regs} cells suppress protective immune responses (Goenka *et al*., 2011; Neves *et al*., 2010; Hilgenberg *et al*., 2014).

H. pylori infection to gastric epithelial cells leads to inflammation, which is majorly associated with a *cagA* gene product, CagA. CagA toxin is directly injected into the host cell *via* a bacterial type IV secretion system (Odenbreit *et al* 2000). Generally, virulent *H. pylori* strains possess numerous well-known outer membrane proteins (OMPs) or adhesions, such as BabA/B, SabA, AlpA/B, OipA and HopZ. There are several families of OMPs have been reported for *H. pylori*. Predominantly five families of OMPs have been studied for

their different roles, family one of Hop (21 members), Hor (12 members), family two of Hof (8 members), family three of Hom (4 members) and family four and five are iron-regulated OMPs (6 members) and efflux pump OMPs (3 members), respectively (Oleastro and Menard 2013).

The *hom* family of OMPs consists of four members, namely *homA, homB, homC and homD*. Out of four members, HomB OMP has been studied for its role in the adhesion and colonization of bacteria in clinical isolates. In addition, the presence of the *homB* gene has been associated with peptic ulcer disease (PUD). In fact, studies suggested that the *homB* gene is related to the adhesion of bacteria and interleukin-8 (IL8) secretion (Oleastro *et al* 2006, 2008). *jhp*0870 open-reading frame (ORF) in *H. pylori* (J99) genome is denoted for gene HomB outer membrane protein. *homB* shares 90% nucleotide similarity with other member *homA*, i.e. ORF *jhp*0649 (Tomb *et al* 1997, Alm *et al* 1999).

Despite the involvement of HomA and HomB OMPs in adherence, the exact role of *H. pylori* in the modulation of B-cells responses to fight pathogens, and how *H. pylori* interact with B-cells during infection, leading to MALT lymphoma development, is not studied in detail. Here, we explored the role of HomA and HomB in modulating B-cell cellular immune response, especially on the aberrant AID expression. Later, we studied their role in the transcriptional regulation of AID expression *via* its activators/repressors levels, and subsequently, we examined class switch recombination of Ig genes. In addition to that, we also investigated the immune-suppressive B-cell responses. Interestingly, we observed that *H. pylori* OMPs, HomA and HomB, demonstrate a dual role. HomA and HomB transiently downregulate Ig switch germline and AID expression and reduce antibody diversity. Additionally, HomA and HomB promote the production of immune-suppressive cytokines and T-cell inhibition markers.

4.2 Results

4.2.1 HomA and HomB down-regulates AID expression

Mature B-cells express AID after stimulation with antigens (Park *et al* 2012). Incidentally, some of the human cancer cell lines, such as (CNE1) nasopharyngeal carcinoma, (A549) lung cancer, (HeLa) cervical cancer and (Raji) B-lymphoma cells, spontaneously express AID (Duan *et al* 2016). To know the effect of HomA and HomB stimulation on the expression of AID in human B-cells, we used Raji cells. We used three concentrations, namely 10 μg, 50 μg and 100 μg, of HomA and HomB for the stimulation experiments, and observed that the addition of HomA and HomB to human Raji B-cells transcriptionally downregulates AID. AID transcription levels were reduced to around 50 % and 60% after 1 hour and 4 hours of exposure, respectively, and restored to back to normal after 8 hours (**Fig. 4.1A-F**), as compared to levels in the untreated cells. Relatively, 50 μg of HomA and HomB shows maximum repression of AID at mRNA level (**Fig. 4.1G**), and therefore we used 50 μg concentration for performing further experiments. The repression of AID transcription following the stimulation with HomA and HomB was also mirrored at the protein level. Immunoblotting of AID was performed with an anti-AID monoclonal antibody, and it showed a clear reduction in AID protein (**Fig. 4.2H-P**). Densitometry of AID immunoblot revealed this to be an approximate 40-50% reduced expression at 1 hour (**Fig. 4.2H-J**) and 50-60% at 4 hours (**Fig. 4.2K-M**), as compared to levels in the untreated cells. Subsequently, AID protein levels were restored to normal at 8 hours (**Fig. 4.2N-P**), indicating that AID mRNA expression and protein levels are reduced after incubation with HomA and HomB, respectively. Overall, the data shows that the addition of HomA and HomB to B-cell significantly downregulate AID expression. In addition to verifying the synergistic effect of both HomA and HomB on AID expression, we co-stimulated B-cells with HomA and HomB (50μg) for 1, 4, and 8 hours and we did not observe drastic differences in AID suppression (**Fig. 4.3A, B and C**) when

compared to HomA and HomB stimulation alone (**Fig. 4.1**). HomA and HomB also do not affect cell proliferation and we did not observe any toxic effect on B-cells and viability due to HomA and HomB stimulation (**Fig. 4.3D**).

4.2.2 HomA and HomB affect AID transcription regulation

Being a dangerous mutator, AID is tightly controlled at transcriptional, post-transcriptional and post-translational levels, and transcription regulation of AID involves transcription factors, enhancers and suppressors. Incidentally, NFκB, PAX, SMAD3, cMYC, STAT6 act as positive regulators of AID expression, while cMYB and E2F act as negative regulators of AID (Zan and Casali 2013). We examine mRNA levels of AID regulators in the B-cells treated with 50 μg concentration of HomA and HomB, respectively, and observed a slight decrease in expression levels of AID activator NFκB at 8 hours in HomA treated cells and at 4 hours in HomB treated cells (**Fig. 4.4A** and **F**) and decreased expression of cMYC at 1 hour in HomA and HomB treated cells (**Fig. 4.4D** and **I**). In contrast, we also observed around 1.5-fold upregulated expression of PAX5 at 1, 4 and 8 hours in HomA treated cells, but no significant change in HomB treated cells (**Fig. 4.4B** and **G**). Similarly, STAT6 shows slight upregulation at 1 hour in HomA treated cells, and 1, 4 and 8 hours in HomB treated cells (**Fig. 4.4E** and **J**), whereas SMAD3 expression was not significantly affected (**Fig. 4.4C** and **H**).

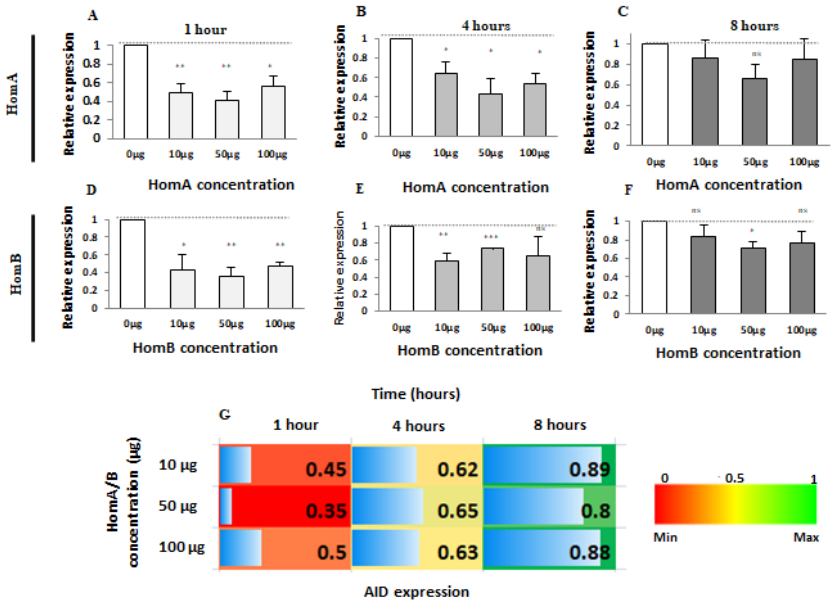

Figure 4.1. AID downregulation in HomA and HomB treated cells. **A-C**, mRNA expression level of AID in HomA treated cells at 1, 4 and 8 hours. **D-F**, mRNA expression level of AID in HomB treated cells at 1, 4 and 8 hours. **G**, Heat map showing the relative expression level of AID in HomA and HomB treated cells.

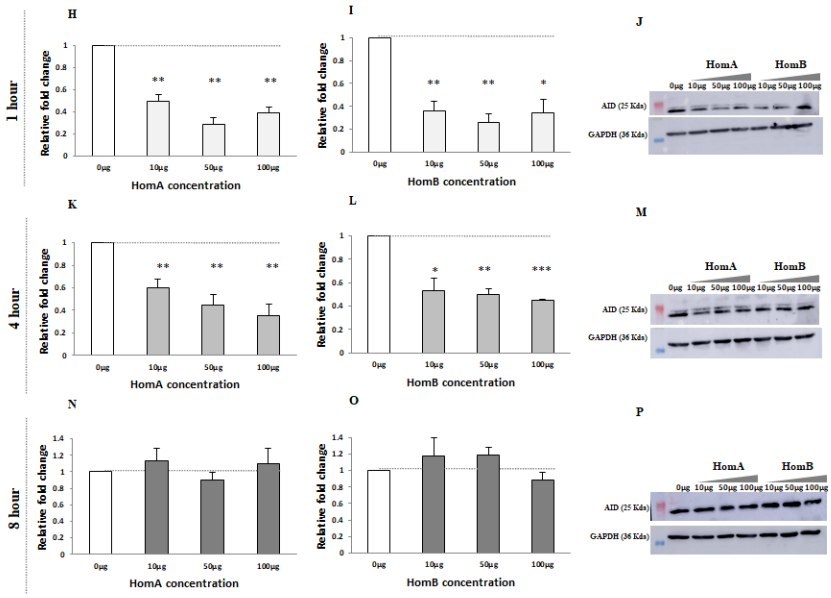

Figure 4.2. AID downregulation in HomA and HomB treated cells. **H-P**, immunoblot of AID in HomA and HomB treated cells at 1 (**H, I and J**), 4 (**K, L and M)** and 8 (**N, O and P**) hours, with densitometry graph representation of immunoblots. Data represented is of two independent experiments as biological duplicates.

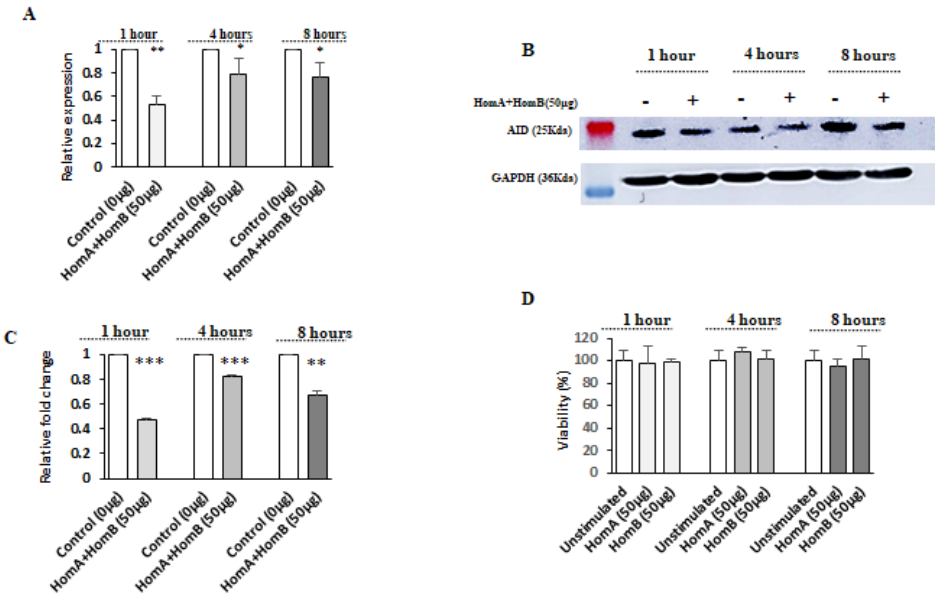

Figure 4.3 HomA+HomB co-stimulation and cell viability assay. A, mRNA expression analysis of AID transcription of HomA and HomB (50µg) co-stimulation of Raji cells at 1, 4 and 8 hours. **B**, immunoblot of AID of HomA+HomB (50 µg) co-stimulation of Raji cells at 1, 4 and 8 hours. **C,** densitometry graph representation of immunoblot of AID. **D,** cell proliferation/viability assay of HomA and HomB (50 µg) stimulation at 1, 4 and 8 hours.

Interestingly, cMYB, a transcriptional repressor of AID, shows significant upregulation, up to 1.5 at 1 hour, in stimulated cells with HomA and HomB, 1.8-fold at 4 hours in HomA stimulated cells and continues up to 8 hours (**Fig. 4.5A** and **D**). To further confirm whether the cMYB transcription is reflected at protein levels, we checked cMYB protein level and we observed 1.6 and 1.5-fold upregulated expression at 1 hour in HomA and HomB treated cells, respectively, and at 4 hours HomA treated cells shows 1.2-fold upregulated expression but not in HomB treated cells (**Fig. 4.5E**, **G** and **H**). At 8 hours cMYB expression was not significantly affected in HomA and HomB treated cells (**Fig. 4.5I**). Since cMYB expression is upregulated, we also investigated cMYB occupancy at region 2 of the AID gene regulatory locus (**Fig. 4.5F**). Interestingly, at 1 hour around 2 and 1.5-fold higher cMYB occupancy was observed in the case of HomA and HomB, respectively, and at 4 hours around 3 and 2.5-fold higher cMYB occupancy was observed in HomA and HomB stimulated cells, respectively. At 8 hours, there was no significant change in cMYB occupancy for both HomA and HomB stimulated cells (**Fig. 4.5J**). Nonetheless, the other repressor of AID, E2F, does not show any significant change in the expression (**Fig. 4.5B** and **D**). Additionally, to further strengthen our observation that there is an inverse relation of AID and cMYB in stimulated cells, we explored the immunofluorescence of cMYB and AID. We observed increased expression of cMYB and decreased expression of AID as well as reduced nuclear localization of AID in HomA and HomB stimulated cells at 1 hour (**Fig. 4.6**), which was restored to normal level at 4 hours and 8 hours (**Fig. 4.7** and **4.8**). These results suggest that overexpression cMYB repressor in HomA and HomB treated cells is likely responsible for the suppression of AID.

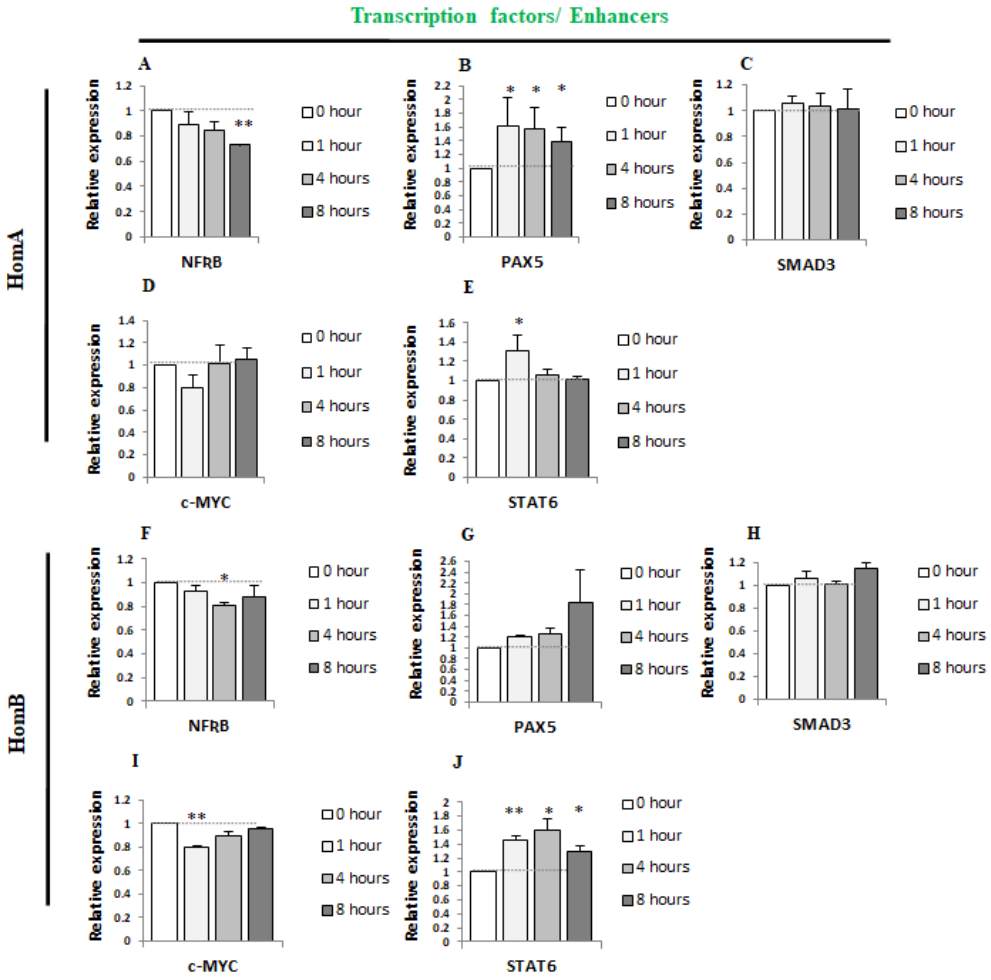

Figure 4.4. AID transcription activator expression analysis. A-E, Transcriptional factors/Enhancer (NFκB, PAX5, SMAD3, c-MYC, and STAT6) mRNA expression analysis of HomA treated cells at 1, 4, and 8 hours. **F-J,** Transcriptional factors/Enhancer (NFκB, PAX5, SMAD3, c-MYC, and STAT6) mRNA expression analysis of HomB treated cells at 1, 4, and 8 hours. Data represented is of two independent experiments as biological duplicates.

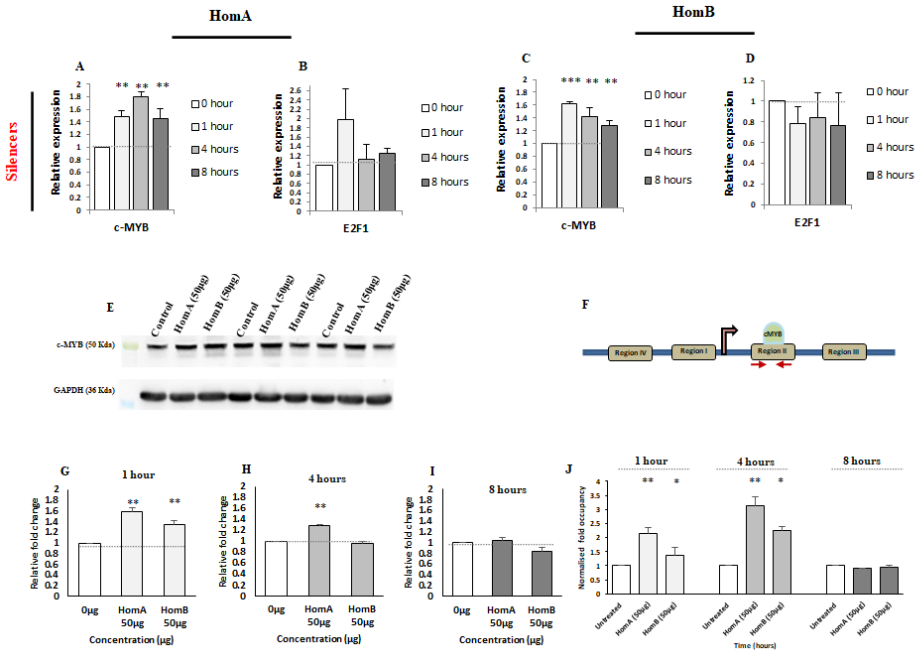

Figure 4.5. AID transcription repressor expression analysis. A-D, m-RNA expression analysis of AID transcription repressor cMYB and E2F1 in HomA and HomB treated cells. **E**, Immunoblot of cMYB of HomA and HomB treated cells. Data represented is of two independent experiments as biological duplicates. **F**, representation of cMYB binding site on the AID *cis*-regulatory region. **G-I,** Densitometry graph representation of immunoblot. **J,** ChIP assay, graph representation of cMYB fold occupancy on AID *cis*-regulatory region. **K,** AID, cMYB expression and AID localization analysis by immunofluorescence. Left to right: bright field visualization of cells, DAPI staining to DNA, FITC staining of AID, 3D plot representation of DAPI and FITC staining, Alexa 594 staining of cMYB, merged image of all staining and brightfield. Data for cMYB ChIP assay qPCR and confocal microscopy are represented as technical duplicates.

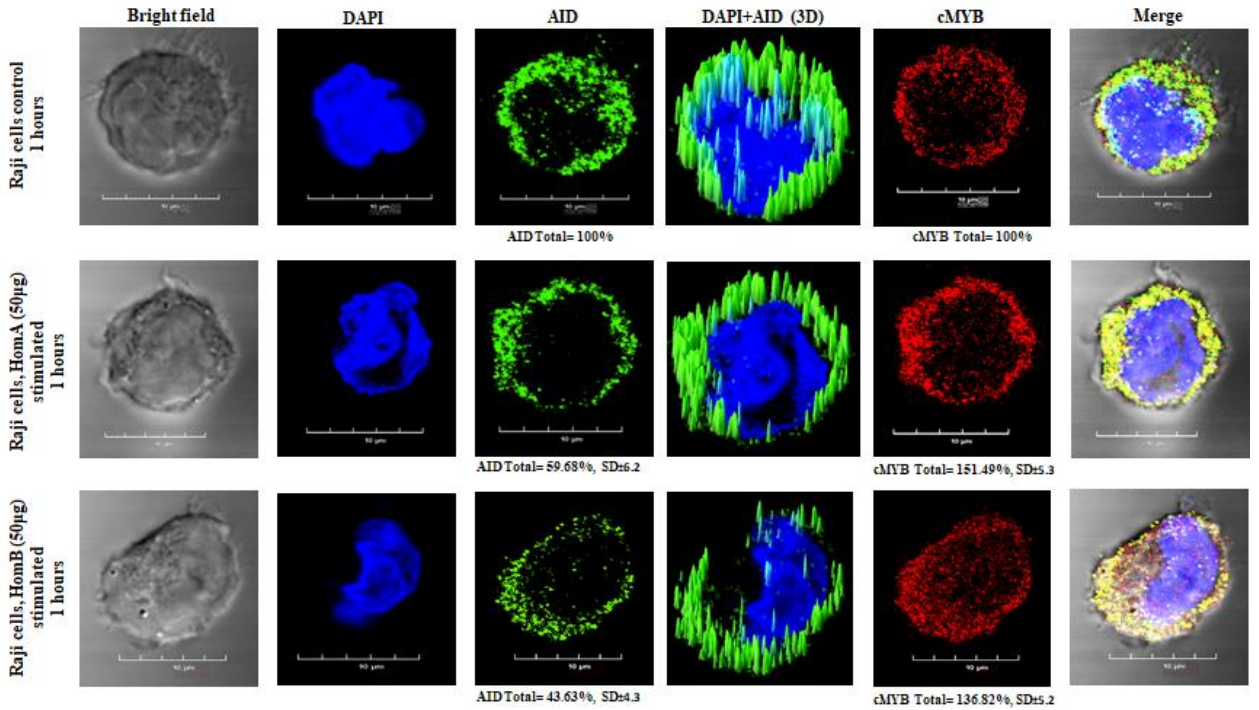

Figure 4.6. AID transcription repressor expression analysis. AID, cMYB expression and AID localization analysis by immunofluorescence. Left to right: bright field visualization of cells, DAPI staining to DNA, FITC staining of AID, 3D plot representation of DAPI and FITC staining, Alexa 594 staining of cMYB, merged image of all staining and brightfield. Data for cMYB ChIP assay qPCR and confocal microscopy are represented as technical duplicates.

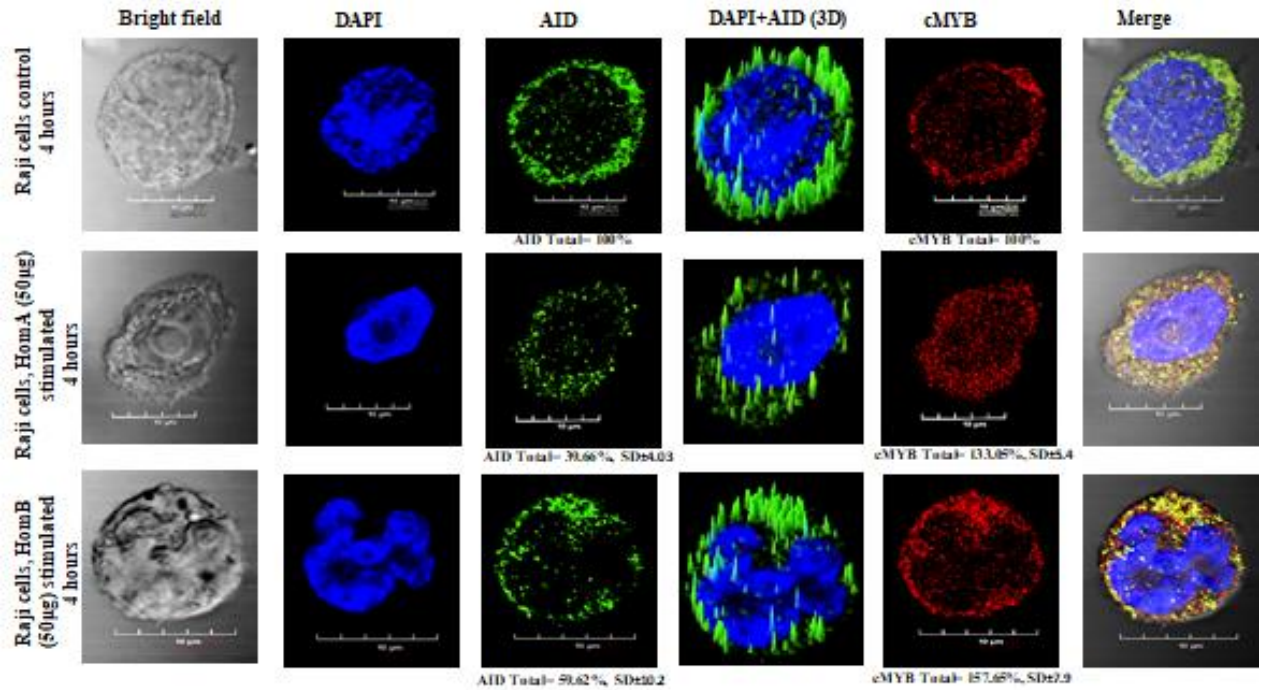

Figure 4.7. AID transcription repressor expression analysis. AID, cMYB expression and AID localization analysis by immunofluorescence. Left to right: bright field visualization of cells, DAPI staining to DNA, FITC staining of AID, 3D plot representation of DAPI and FITC staining, Alexa 594 staining of cMYB, merged image of all staining and brightfield. Data for cMYB ChIP assay qPCR and confocal microscopy are represented as technical duplicates.

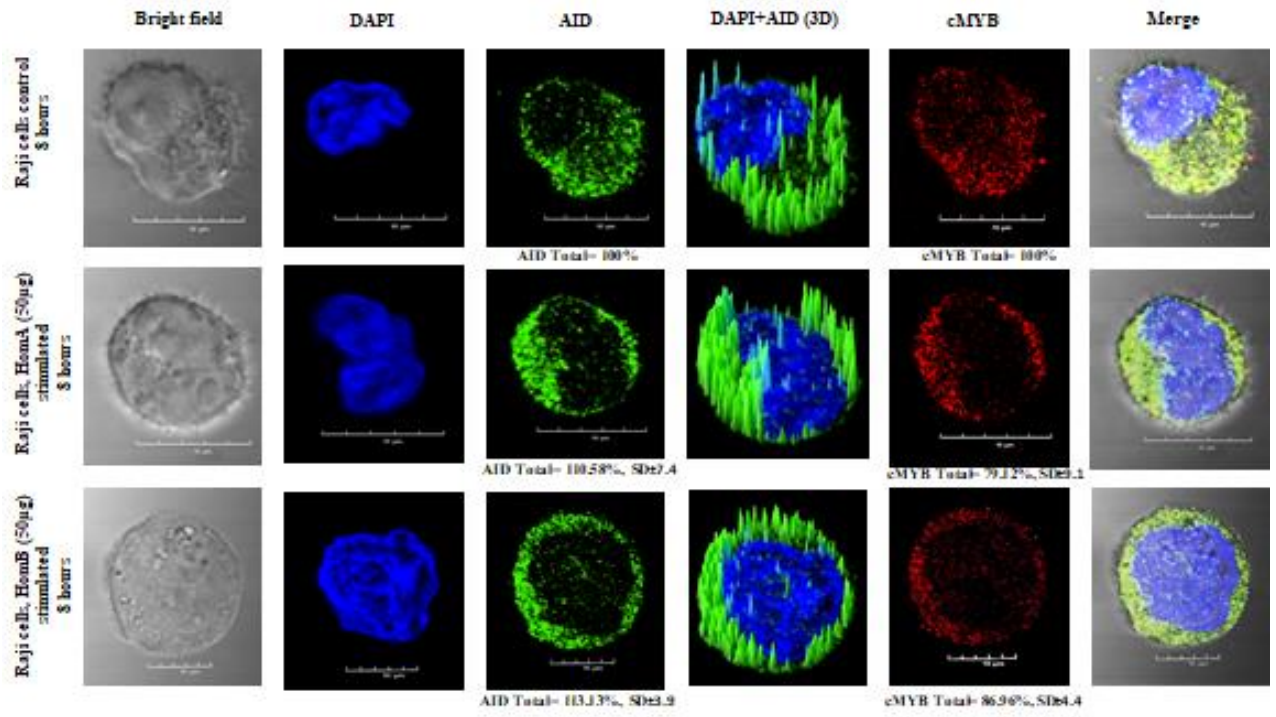

Figure 4.8. AID transcription repressor expression analysis. AID, cMYB expression and AID localization analysis by immunofluorescence. Left to right: bright field visualization of cells, DAPI staining to DNA, FITC staining of AID, 3D plot representation of DAPI and FITC staining, Alexa 594 staining of cMYB, merged image of all staining and brightfield. Data for cMYB ChIP assay qPCR and confocal microscopy are represented as technical duplicates.

4.2.3 HomA and HomB affect CSR of Ig genes

During pathogenic infection or upon encountering any foreign antigens, mature B-cells are activated to generate specific neutralizing antibodies, *via* the process of somatic hypermutation (SHM) and class switch recombination (CSR). Raji cells undergo spontaneous CSR of immunoglobulin gene from IgM to IgA or IgG mature transcript. In this process, the heavy chain constant region of immunoglobulin gets switched from one isotype to another, which determines the final production of immunoglobulin antibody (Duan *et al* 2016). We observed that the HomA and HomB stimulated Raji B-cells show downregulation of AID, a crucial CSR factor (Recaldin *et al* 2018). To investigate whether the incubation of HomA and HomB with Raji cells affects its CSR activity, we examined the mRNA expression level of the mature transcript of the immunoglobulin gene. To identify the outcome of CSR events in the mature Ig transcript, we used combinations of a forward primer at the V-region and different reverse primers for different heavy chain constant regions (**Fig. 4.9A**). First, we checked the expression of IgV-Cμ mature transcript which is usually expressed in mature B-cell before class switching, and we observed that HomA stimulated cells shows 2-to-2.5-fold higher expression in 1, 4 and 8 hours (**Fig. 4.9B)**, whereas HomB stimulated cells demonstrated a 1.5 to 2-fold higher expression of IgM (IgV-Cμ) mature transcript (**Fig. 4.9L**), as compared with the untreated control cells. Similarly, we checked CSR mature transcript product IgV-Cα and IgV-Cγ. In HomA treated cells IgV-Cα expression levels were reduced by 20% at 1 hour, 40% at 4 hours, and restored to normal at 8 hours (**Fig. 4.9C**). Likewise, in HomB stimulated cells, IgV-Cα expression levels were reduced by 50% at 1 hour and by 25% at both 4 and 8 hours (**Fig. 4.9M**). In the same way, we checked for IgV-Cγ expression and observed that in HomA stimulated cells IgV-Cγ expression levels were dramatically reduced by 70% at 1 hour, and 50% at 4 and 8 hours, respectively (**Fig. 4.9D**). HomB stimulated cells also show a similar pattern where at 1-hour IgV-Cγ expression levels

were reduced by 75% and 35% at 4 and 8 hours, respectively (**Fig. 4.9N**).

As we observed higher expression levels of IgV-Cμ as compared to IgV-Cα and IgV-Cγ, to better analyse the effect of HomA and HomB on the CSR process in Raji cells, we checked ratios of IgV-Cμ to IgV-Cα and IgV-Cγ, which were denoted as IgA:IgM and IgG:IgM, respectively. Interestingly in HomA stimulated cells, IgA:IgM and IgG:IgM ratios were around 25-30% (**Fig. 4.9E**) and 20-30% (**Fig. 4.9F**), respectively, at 1 to 8 hours, as compared with the untreated control cells. Alike, in HomB stimulated cells, IgA:IgM and IgG:IgM ratios were around 20-25% (**Fig. 4.9O**) and 20-35% (**Fig. 4.9P**), respectively, at 1 to 8 hours, as compared with the unstimulated control cells. Further, to confirm our observation of reduced CSR, we checked the expression level of Ig switch germline transcription Iμ-Cμ, Iα-Cα, Iγ-Cγ. Increased levels of Iμ-Cμ expression were observed in case of HomA and HomB stimulated cells at 1, 4 and 8 hours (**Fig. 4.9 G and Q**), whereas Iα-Cα, Iγ-Cγ expression levels were decreased at 1 and 4 hours (**Fig. 4.9H-I** and **R-S**). To confirm complete CSR process, we checked the expression of switched circular transcript Iγ-Cμ, Iα-Cμ and interestingly significantly reduced expression of Iγ-Cμ, Iα-Cμ were observed in HomA and HomB stimulated cells (**Fig. 4.9J-K** and **T-U**). These observations indicated a significantly reduced CSR process in HomA and HomB stimulated Raji cells.

Nevertheless, to confirm that the reduced CSR activity is correlated with the decreased AID levels and Ig switch germline transcription in HomA and HomB and not because of diminished transcription of IgV genes, we checked transcription of IgV region in HomA and HomB stimulated cells and compared with the un-stimulated control cells. We observed that transcription of the IgV gene was not altered in HomA and HomB stimulated cells at all the time points (1, 4 and 8 hours) as compared with the control cells (**Fig. 4.8V** and **W**). In addition to AID, other factors such as BATF, HOXC4

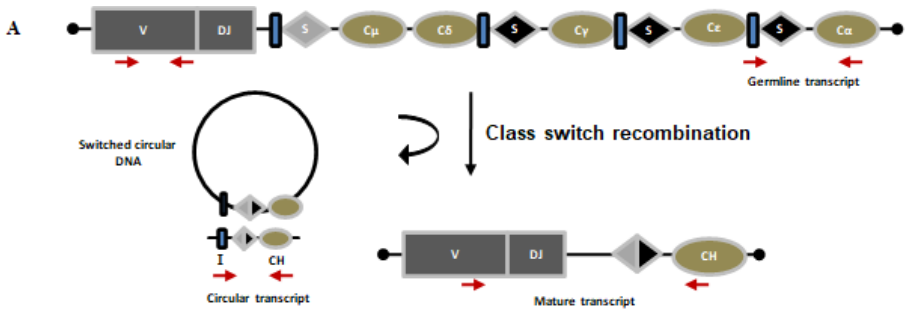

Figure 4.9. HomA and HomB reduce the induction of class switching to IgA and IgG. A, Schematic representation of VDJ and constant region immunoglobin gene and primer location (red arrow).

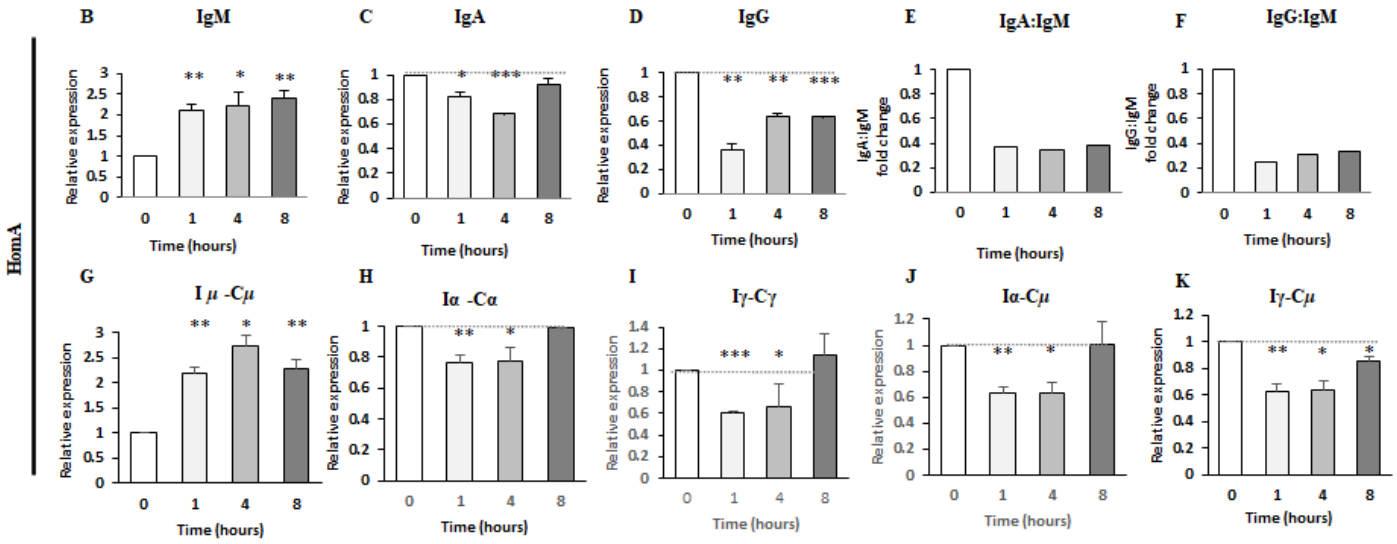

Figure 4.9. HomA and HomB reduce the induction of class switching to IgA and IgG. B-D, mRNA expression analysis of IgM, IgA and IgG mature transcript of HomA treated cells. **E-F**, IgA to IgM and IgG to IgM ratio analysis in HomA treated cells. **G-I**, mRNA expression analysis of Ig switch germline transcript of HomA treated cells. **J-K**, switched circle transcript mRNA analysis of HomA treated cells. **L-N**, mRNA expression analysis of IgM, IgA and IgG mature transcript of HomB treated cells. **O-P**, IgA to IgM and IgG to IgM ratio analysis in HomB treated cells. **Q-S**, mRNA expression analysis of Ig switch germline transcript of HomA treated cells. **T-U**, switched circle transcript mRNA analysis of HomA treated cells IgA to IgM and IgG to IgM ratio analysis in HomB treated cells. **V-W**, IgV region mRNA expression analysis of immunoglobulin gene at 1, 4 and 8 hours in HomA and HomB treated cells. Data represented is of two independent experiments as biological duplicates.

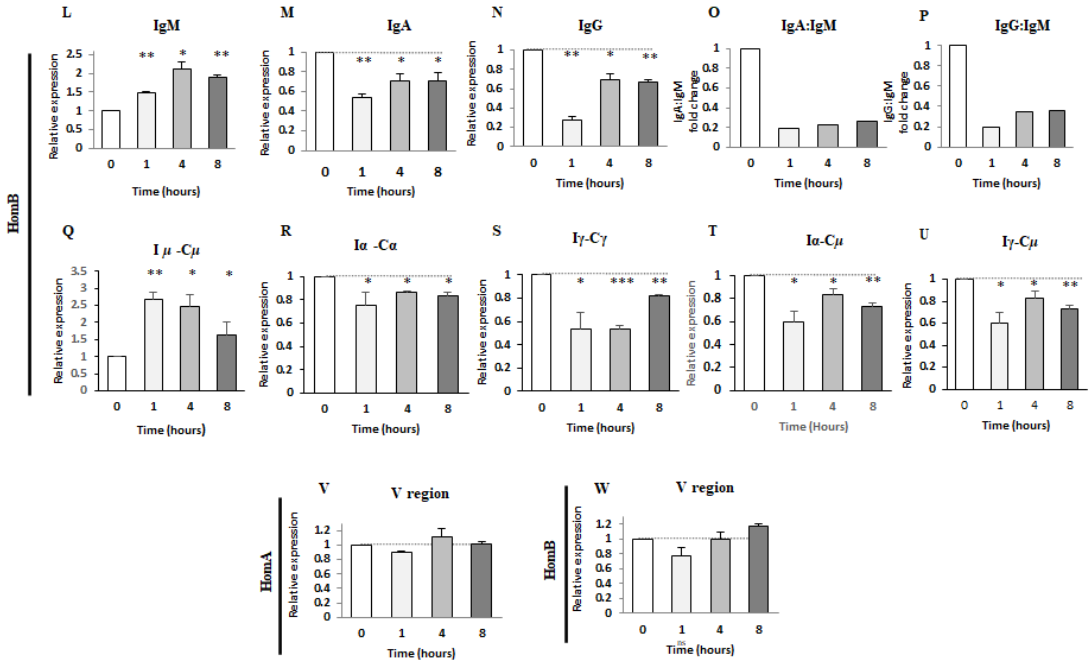

Figure 4.9. HomA and HomB reduce the induction of class switching to IgA and IgG. L-N, mRNA expression analysis of IgM, IgA and IgG mature transcript of HomB treated cells. **O-P**, IgA to IgM and IgG to IgM ratio analysis in HomB treated cells. **Q-S**, mRNA expression analysis of Ig switch germline transcript of HomA treated cells. **T-U**, switched circle transcript mRNA analysis of HomA treated cells IgA to IgM and IgG to IgM ratio analysis in HomB treated cells. **V-W**, IgV region mRNA expression analysis of immunoglobulin gene at 1, 4 and 8 hours in HomA and HomB treated cells. Data represented is of two independent experiments as biological duplicates.

affect the CSR process (Park 2012). In line with the AID repressed data (**Fig. 4.1** and **4.2**), we also checked the expression levels of BATF and HOXC4 (CSR factors) in cells stimulated with HomA and HomB and compared them with the levels in the unstimulated control cells. Incidentally, there was no significant change in the expression of HOXC4 (**Fig. 4.10A** and **C**) and BATF (**Fig. 4.10B** and **D**) in HomA and HomB stimulated Raji cells as compared to that in control cells. These results suggest that the reduced AID levels, along with reduced Ig switch germline transcription, in HomA and HomB stimulated B-cells eventually affect the CSR process, leading to significantly lower switching of antibody from IgM to IgA, IgG (**Fig. 4.9E, F** and **J, K**).

4.2.4 HomA and HomB upregulate T-cell inhibition markers

In addition to producing highly specific antibodies, B-cells modulate the immune response, *via* the release of certain cytokines and presenting antigens to subsets of T-cells. Thus, to gain better insights into the immune suppressive role of B-cells, upon HomA and HomB stimulation, we analysed mRNA expression of T-cell inhibition markers, such as PDL1, IL35, IL10 and TGFβ. Interestingly, PDL1 expression levels were around 1.5 to 1.8-fold higher in HomA stimulated cells as compared to the unstimulated control cells (**Fig. 4.11A**). Similarly, we observed 1.4-fold, 1.5-fold and 1.8-fold higher expression levels of PDL1 at 1, 4 and 8 hours, respectively, in HomB stimulated cells as compared to the unstimulated control cells (**Fig. 4.11E)**. A similar observation of higher surface expression of PDL1 was confirmed by confocal microscopy of HomA and HomB stimulated cells at 1, 4 and 8 hours (**Fig. 4.12**, **4.13** and **4.14**).

IL-35 is another inhibitory cytokine involved in the T-cell function that is composed of the IL-12 α chain p35 and the IL-27 β chain Ebi3 (Epstein-Barr virus-induced gene 3) (Su *et al* 2013). We analysed the mRNA expression levels of Ebi3 and observed around 2-fold increased expression at 1 hour, 1.2-fold at 4 hours and 8 hours in HomA stimulated cells as compared to the unstimulated control cells

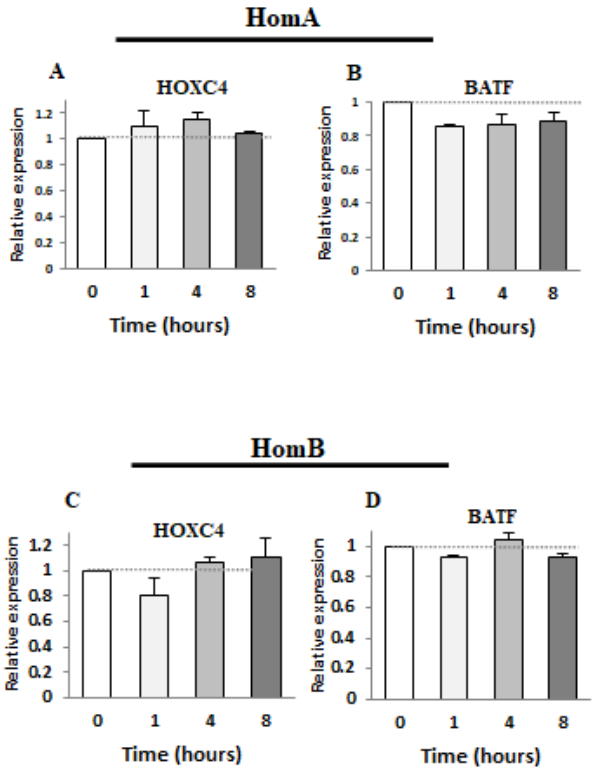

Figure 4.10. Effect of HomA and HomB on CSR factors. **A-B,** CSR factors (HOXC4 and BATF) expression analysis in HomA treated cells at 1, 4 and 8 hours. **C-D,** CSR factors (HOXC4 and BATF) expression analysis in HomB treated cells at 1, 4 and 8 hours. Data represented is of two independent experiments as biological duplicates.

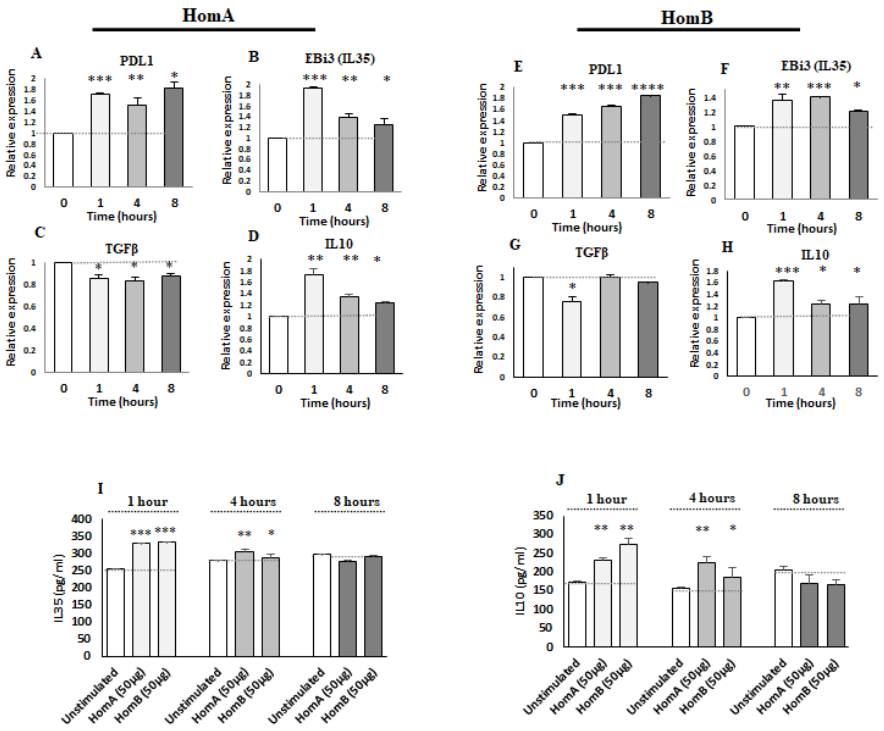

Figure 4.11. HomA and HomB upregulate T-cell inhibition markers. A-D, T-cell inhibition markers (PDL1, IL35, TGFβ) mRNA expression analysis in HomA treated cells at 1, 4 and 8 hours. **E-H,** T-cell inhibition markers (PDL1, IL35, TGFβ) mRNA expression analysis in HomA treated cells at 1, 4 and 8 hours. **I**, ELISA analysis of secretory IL35 at 1, 4 and 8 hours of HomA and HomB treated cells. **J**, ELISA analysis of secretory IL35 at 1, 4 and 8 hours of HomA and HomB treated cells. Data represented are of two independent experiments as biological duplicates.

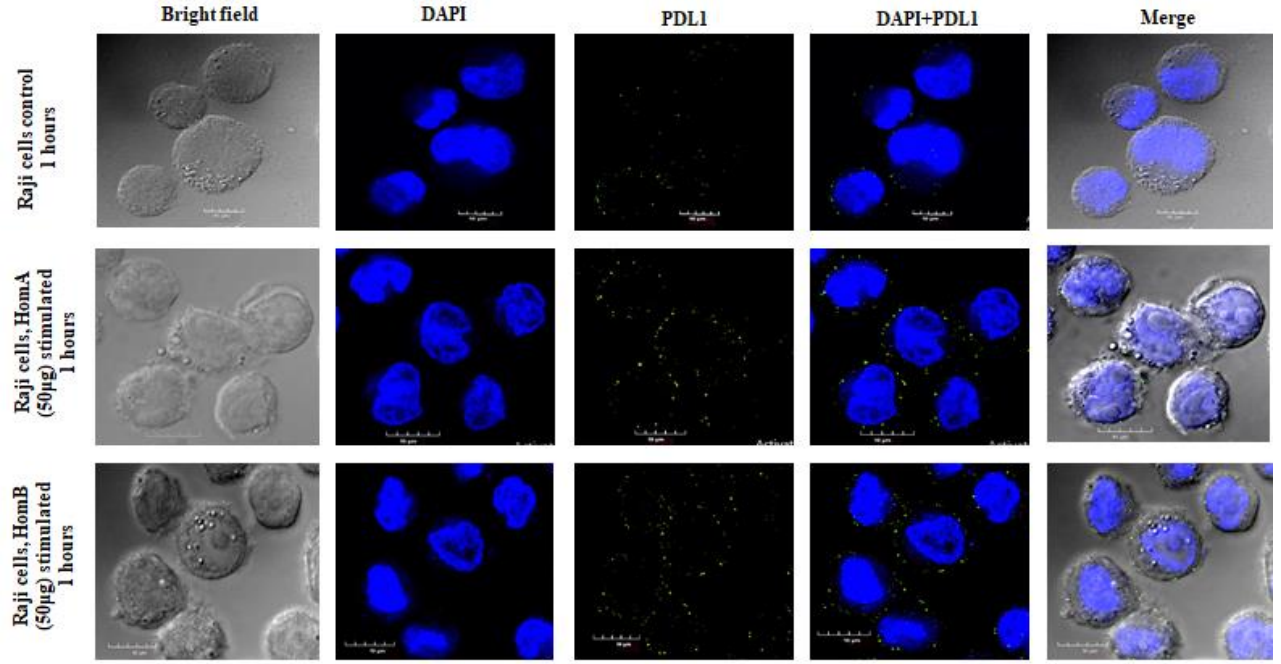

Figure 4.12. HomA and HomB upregulate T-cell inhibition markers. PDL1 surface expression and localization analysis by immunofluorescence, 1-hour stimulation of Raji cells with HomA and HomB (50 µg), **Left** to right: bright field visualization of cells, DAPI staining to DNA, FITC staining of PDL1, merged of DNA (DAPI) and PDL1 (FITC) staining and merged image of all staining and brightfield. Data for PDL1 confocal microscopy are represented as technical duplicates.

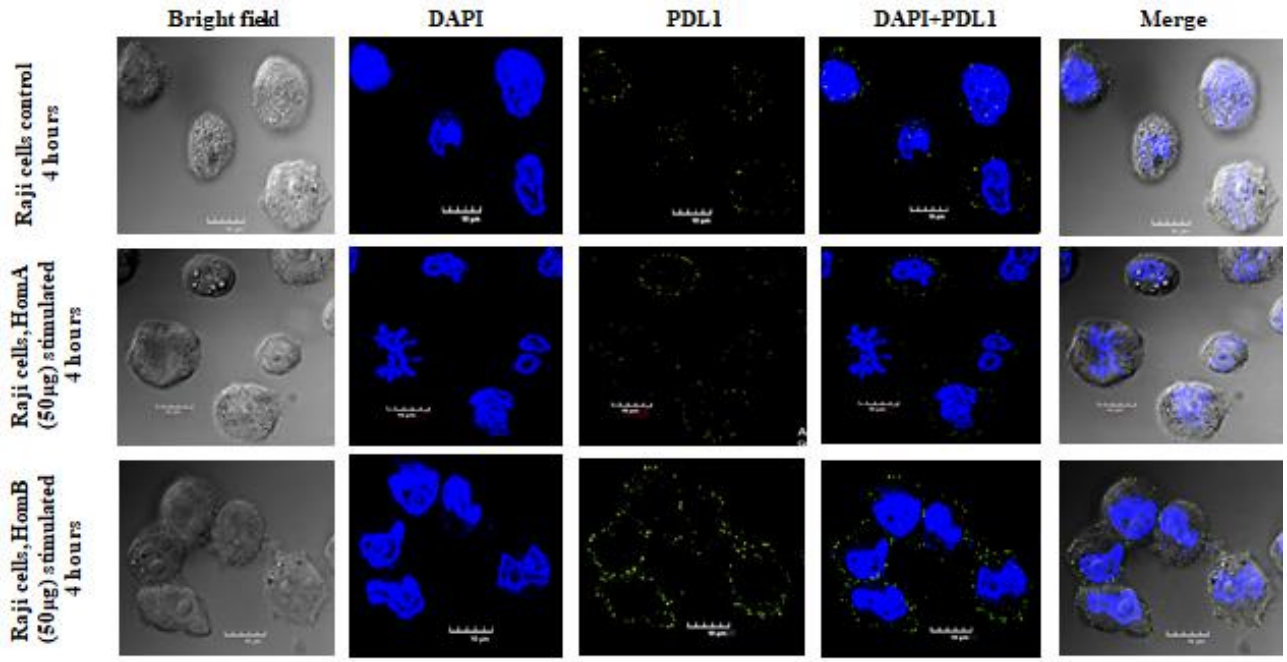

Figure 4.13. HomA and HomB upregulate T-cell inhibition markers. PDL1 surface expression and localization analysis by immunofluorescence, 4-hour stimulation of Raji cells with HomA and HomB (50 µg), **Left** to right: bright field visualization of cells, DAPI staining to DNA, FITC staining of PDL1, merged of DNA (DAPI) and PDL1 (FITC) staining and merged image of all staining and brightfield. Data for PDL1 confocal microscopy are represented as technical duplicates.

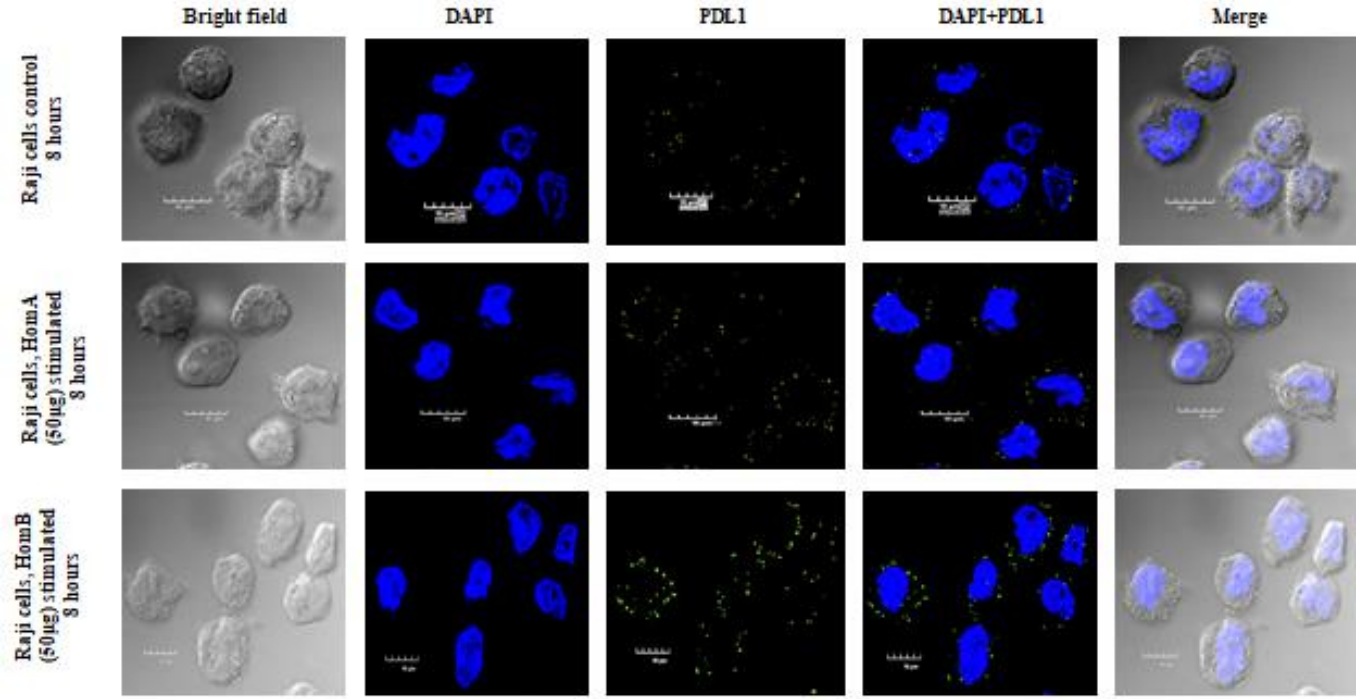

Figure 4.14. HomA and HomB upregulate T-cell inhibition markers. PDL1 surface expression and localization analysis by immunofluorescence, 8-hour stimulation of Raji cells with HomA and HomB (50 µg), **Left** to right: bright field visualization of cells, DAPI staining to DNA, FITC staining of PDL1, merged of DNA (DAPI) and PDL1 (FITC) staining and merged image of all staining and brightfield. Data for PDL1 confocal microscopy are represented as technical duplicates.

(**Fig. 4.11B**). Likewise, we observed that the Ebi3 expression was 1.5-fold at 1 hour and 4 hours which got restored to normal levels at 8 hours (**Fig. 4.11F**). Similar to PDL1 and IL35, we checked TGFβ expression in HomA and HomB stimulated cells and observed that the TGFβ expression was reduced by 15-20% at 1, 4 and 8 hours, as compared with the unstimulated control cells (**Fig. 4.11C** and **G**). Furthermore, we verified secreted IL35 levels using an ELISA assay in HomA and HomB treated cells and observed that the IL35 levels were significantly higher at 1 hour in HomA and HomB treated cells as compared to untreated control cells (**Fig. 4.11I**). Similarly, we estimated the secreted IL10 levels using an ELISA assay and observed that IL10 levels were significantly higher at 1 hour in HomA (33%) and HomB (58%) treated cells as compared to untreated cells (**Fig. 4.11J**). Likewise, IL10 levels were 45% and 20% higher at 4 hours in HomA and HomB treated cells, and subsequently restored to the normal at 8 hours (**Fig. 4.11J**), Nevertheless, IL35 levels were unchanged at 4 and 8 hours in HomA and HomB treated cells as compared to the unstimulated control cells (**Fig. 4.11I**).

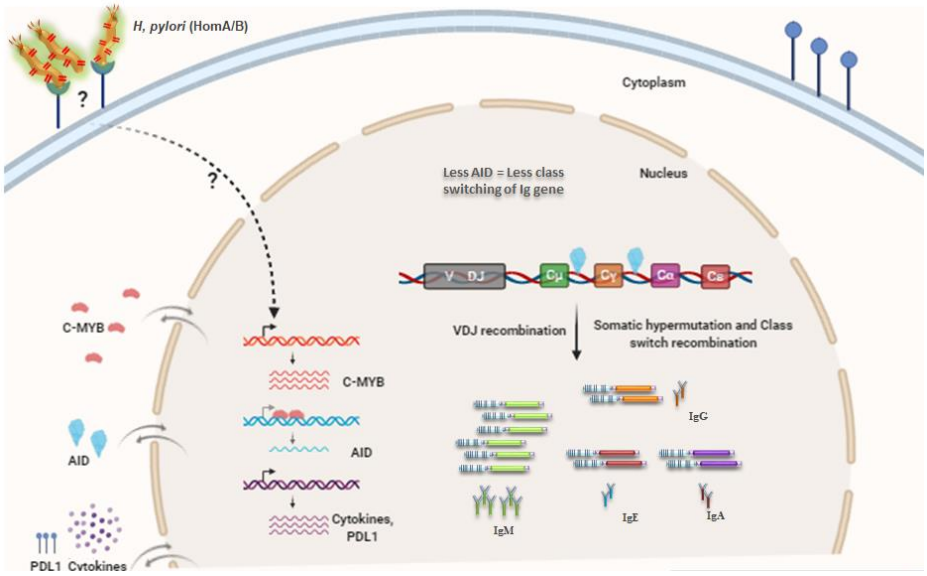

Figure 4.15. Proposed molecular mechanism of B-cell response with HomA and HomB. A graphical representation of the molecular mechanism of downregulation of AID and CSR, as well as upregulated expression of T-cell inhibition markers in B-cells, stimulated with HomA and HomB.

4.3 Summary

In summary, HomA and HomB OMPs of *H. pylori*, which are present on the outer surface of bacteria can interact with host cell surface receptors and subsequently modulate host cellular signalling. We identified a new role and a possible molecular mechanism of *H. pylori* OMPs, HomA and HomB, in modulating B-cell response and subsequent interference in CSR events, leading to reduced antibody diversity (**Fig. 4.15**). Our study indicates a dual role of HomA and HomB, by suppressing B-cell antibody diversity as well as *via* B_{regs} cells polarisation to suppress the adaptive immune system by interfering with T-cell-B-cell communication. These results suggest that HomA and HomB can act as a two-edged sword and can contribute as one of the mechanisms for escaping the immune responses and having a persistent infection of *H. pylori*. This report gives a better understanding of the *H. pylori* pathogenesis leading to gastric diseases as well as MALT lymphoma.

Chapter 5

Chapter 5

Immunoinformatic characterization of globular domains of HomA and HomB, for potential sub-unit vaccine candidate against *Helicobacter pylori*

5.1 Introduction

Gastric cancer, almost 700,000 cost lives of people worldwide (Testerman and Morris 2014). *H. pylori* is the most associated factor with gastric diseases, out of which maximum cases remain asymptomatic and 10% of those infections develops gastric adenocarcinoma, mucosa-associated lymphoid tissue (MALT) lymphoma and peptic ulcer (Cover and Blaser 2009; Salama *et al*. 2013; Yamaoka 2018). The virulent outer membrane proteins of pathogens play important role in host-pathogen interaction (Viala *et al*. 2004). *H. pylori* pathogenesis involves motility, adherence, and virulence toxins which together facilitates chronic infection. Outer membrane proteins help *H. pylori* in adhesion and such as BabA, SabA, HpA, Omp18 and HomB (Lundström *et al*. 2001; Voland *et al*. 2003, Mónica *et al* 2013). In addition to it, flagellar proteins such as FlaA and FlaB assist add bacterial motility and help in moving and colonizing *H.* pylor*i* (Allan *et al*. 2000; Josenhans *et al*. 1995).

Toll-like receptors (TLRs) plays important role in recognizing pathogen-associated molecular patterns (PAMPs) and stimulating the immune system. Epitopes present on the interacting surface of pathogens get identified and further downstream signals are activated by TLRs (Bhattacharya *et al*. 2020b; Netea *et al*. 2004). Being on the outer surface, the outer membrane proteins become crucial as well as prominent vaccine candidates. Till now there is no effective and specific antibiotics or drug available to target or to eradicate *H. pylori* (Meza *et al*. 2017; Testerman and Morris 2014). Researchers are

finding the best strategy to develop vaccines to combat *H. pylori* infection and antibiotics resistant strains. Conventional and classical strategies to develop vaccine has some limitations such as long duration time, whole pathogen (live attenuated) which are generally nonspecific and carry a risk of reverting virulence. Therefore, scientists are exploring immunoinformatic approaches to develop subunit vaccine candidates (Bhattacharya *et al*. 2020a; Dhal *et al*. 2019; Pandey *et al*. 2018).

HomA and HomB, virulent marker proteins help *H. pylori* adherence and biofilm formation. We have previously reported that HomA and HomB are likely to form a small β-barrel with a surface-exposed globular domain (Tamrakar *et al* 2021), In addition to that both the proteins also interfere with the antibody diversity process in human B-cells (Tamrakar *et al* 2022). We hypothesis that surface-exposed globular domains of HomA and HomB are likely to play important role in host-pathogen interaction and can be potential protein domains to exposed to host immune cells. In the current study, we have used immunoinformatic approaches to explore B and T-cell epitopes in globular domains of HomA and HomB for the potential subunit vaccine candidates.

5.2 Results

5.2.1 Secondary and 3D structure of the globular domain of HomA and HomB

HomA and HomB are likely to form small β-barrel with surface-exposed globular domains. Interestingly, small β-barrel of HomA and HomB is identical in sequence and made up of discounted N and C terminal. 57 N terminal and 186 amino acid residues contribute to forming β-sheet structures which is a part of a small β-barrel. However, the middle region of both the protein forms globular domains which appear to be hydrophilic in nature thus most likely to form a surface exposed globular loop (Tamrakar *et al* 2021).

We have predicted the middle region structure with alphafold2 and secondary structure content with NetsurfP2.0. As previously reported middle region of HomA and HomB residues ranging from 57-470 and 57-480 amino acids respectively, forms topology like globular domains containing the mixed secondary structure of α-helices, β-sheets, and coils (**Fig. 5.1**).

5.2.2 Prediction of B and T-cell epitopes

B cell and T-cell epitope were predicted using an online IEDB server. Bepiperd and IEDB showed that the globular domain of HomA and HomB contains B-cell epitopes across the region especially towards the middle and C terminus (**Fig. 5.2 A** and **C**, respectively) with β-turns, flexibility and observed to be highly antigenic in nature (**Fig. 5.2 B, E F and D, G, H** respectively). These globular domains were also assessed for surface accessibility and hydrophilicity potential, it was observed both the globular domains show high surface accessibility and hydrophilicity predominantly at the middle region (**Fig. 5.2 I, J, and K, L** respectively). We observed positive value for epitopes and their characteristics predicted when compared to threshold value st by the software itself. We also used Alphafold2 predicted PDB to explore linear and conformational B-cell epitopes on the basis of the structure via the ellipro IEDB tool. We have selected the Top 10 models for linear epitopes based on score (**Fig. 5.3 A-J, HomA** and **Fig. 4 A-J HomB**). Various length of B-cell linear epitopes was predicted which are mentioned in **Table 5.1**. Both the sequence of globular domains shows high flexibility index, which provides chances to distantly located different amino acids to come together and form conformational epitopes. Ellipro stool also predicted conformational epitopes based on the PDB structure for HomA (**Fig. 5.3 K-M)** and HomB (**Fig. 5.4 K-O**) the amino acids residues which take part in the formation of conformational epitopes are mentioned in **Table 5.2**.

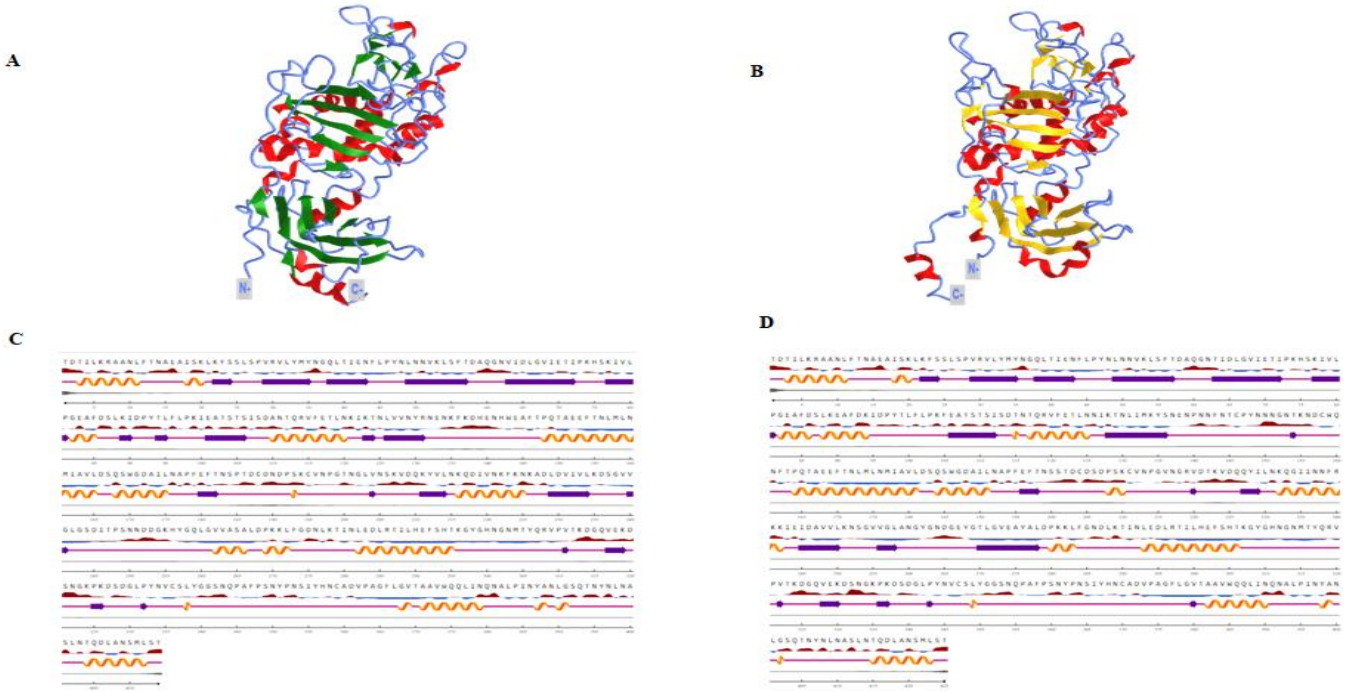

Figure 5.1 Secondary and tertiary structure prediction. (**A-B)** Alphafold2 3D structure of the globular domain of HomA and HomB respectively, (**C-D**) NetsurfP2.0 secondary structure content prediction of the globular domain of HomA and HomB, respectively.

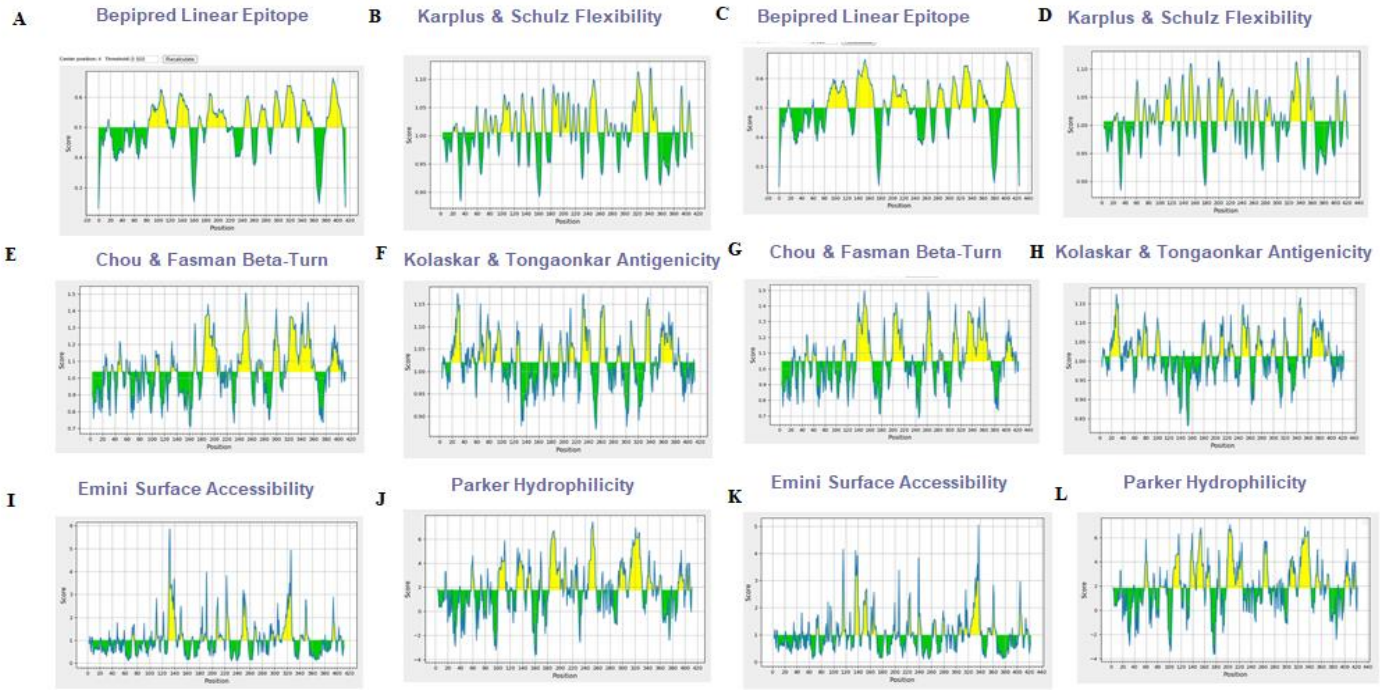

Figure 5.2. **IEDB predicts β-turn, hydrophilicity, flexibility, and surface accessibility of B cell epitopes of HomA and HomB globular domain**. (**A, C**) Linear B-cell epitopes, (**B-D**) Karplus & Schulz Flexibility Prediction. (**E-G**) Chou & Fasman Beta-Turn Prediction. (**F-H**) Kolaskar & Tongaonkar antigenicity. (**I, K**). Emini Surface Accessibility Prediction. (**J, K**). Parker Hydrophilicity Prediction Results.

T-cell epitopes were also predicted on globular domains of HomA and HomB. Predicted results in units of IC50nM for combinatorial library and SMM_align. Therefore, a lower number indicates higher affinity. This high affinity is necessary for potential T cell epitopes. CD4+ T cell epitopes binding to MHC class II molecules and CD8 + T cell epitopes binding to MHC class I are mentioned in **Table 5.2, 5.3** for HomA and **5.5, 5.6** for HomB.

5.2.3 Immune simulation by the globular domain of HomA and HomB

The immune simulation study was determined by C-immsim for globular domains of HomA and HomB to explore the generation of adaptive immunity and the immune interactions. After every injection dose, the primary immune response was increased significantly and as gradual elevation or decrease rates of the different immunoglobulins were observed. Moreover, the secondary immune response was also increased (**Fig. 5.5** and **5.6 A** HomA and HomB respectively). Active B-cells, (**Fig 5.5** and **5.6 B, C**), plasma B-cell (**Fig 5.5** and **5.6 D**), helper T-cells (**Fig. 5.5** and **5.6 K, E, F**), and regulatory and cytotoxic T cells (**Fig. 5.5** and **5.6 G−H**) responses were higher and stable showing minimal decay for over 350 days. Moreover, these results indicate that after every injection, and booster dose strong secondary immune response, increasing clearance of antigens, and strong immune memory generation occur. In addition to that, good antigen presentation was also observed by these antigen-presenting cells from active epithelial cells, NK cells, dendritic cells, and macrophage cells concentrations (**Fig. 5.5** and **5.6 L-O**). interestingly, the administration of antigen was also capable of forming a good number of different kinds of cytokines (**Fig. 5.5** and **5.6 I**).

Table 5.1. HomA, B-cell liner epitopes

No.	Chain	Start	End	Peptide	Number of residues	Score
1	A	309	327	VPVTKDGQVEKDSNGKPKD	19	0.779
2	A	79	99	VLPGEAFDSLKIDPYTLFLPK	21	0.771
3	A	333	362	YNVCSLYGGSNQPAFPSNYPNSIYHNCADV	30	0.751
4	A	388	414	ANLGSQTNYNLNASLNTQDLANSMLST	27	0.746
5	A	56	71	FTDAQGNVIDLGVIET	16	0.726
6	A	131	147	RNENKFKDHENHWEAFT	17	0.708
7	A	33	38	YMYNGQ	6	0.692
8	A	234	240	LKDSGVV	7	0.689
9	A	246	255	ITPSNNDDGK	10	0.689
10	A	105	110	TSISDA	6	0.679
11	A	183	217	NSPTDCDNDPSKCVNPGTNGLVNSKVDQKYVLNKQ	35	0.656
12	A	1	21	TDTILKRAANLFTNAEAISKL	21	0.603
13	A	274	279	GDNLKT	6	0.589

Table 5.2. HomA, B-cell conformational epitopes

No.	Residues	Number of residues	Score
1	A:N176, A:A177, A:P178, A:F179, A:E180, A:T182, A:N183, A:S184, A:P185, A:T186, A:D187, A:C188, A:D189, A:N190, A:D191, A:P192, A:S193, A:K194, A:C195, A:V196, A:N197, A:P198, A:G199, A:T200, A:N201, A:G202, A:L203, A:V204, A:N205, A:S206, A:K207, A:V208, A:D209, A:Q210, A:K211, A:Y212, A:V213, A:L214, A:N215, A:Q217, A:N301, A:G302, A:V309, A:P310, A:V311, A:T312, A:K313, A:D314, A:G315, A:Q316, A:V317, A:E318, A:K319, A:D320, A:S321, A:N322, A:G323, A:K324, A:P325, A:K326, A:P332, A:Y333, A:N334, A:V335, A:C336, A:S337, A:L338, A:Y339, A:G340, A:G341, A:S342, A:N343, A:Q344, A:P345, A:A346, A:F347, A:P348, A:S349, A:N350, A:Y351, A:P352, A:N353, A:S354, A:I355, A:Y356, A:H357, A:N358, A:C359, A:A360, A:D361, A:V362	91	0.696
2	A:T1, A:D2, A:T3, A:I4, A:L5, A:R7, A:A8, A:A9, A:N10, A:L11, A:T13, A:N14, A:A15, A:E16, A:A17, A:S19, A:K20, A:L21, A:Y33, A:M34, A:Y35, A:N36, A:G37, A:Q38, A:N48, A:N50, A:N51, A:K53, A:F56, A:T57, A:D58, A:A59, A:Q60, A:G61, A:N62, A:V63, A:I64, A:D65, A:L66, A:G67, A:V68, A:E70, A:T71, A:P73, A:V79, A:L80, A:P81, A:G82, A:E83, A:A84, A:F85, A:D86, A:S87, A:L88, A:I90, A:D91, A:P92, A:Y93, A:T94, A:L95, A:F96, A:L97, A:P98, A:I100, A:T105, A:S106, A:I107, A:S108, A:D109, A:A110, A:Q113, A:R131, A:N132, A:E133, A:N134, A:K135, A:F136, A:K137, A:D138, A:H139, A:E140, A:N141, A:H142, A:W143, A:E144, A:A145, A:F146, A:L234, A:K235, A:D236, A:S237, A:G238, A:V239, A:V240, A:D268, A:K270, A:G274, A:D275, A:N276, A:L277, A:K278, A:T279, A:N386, A:A388, A:N389, A:G391, A:S392, A:Q393, A:T394, A:N395, A:Y396, A:N397, A:L398, A:N399, A:A400, A:S401, A:L402, A:N403, A:T404, A:Q405, A:D406, A:L407, A:A408, A:N409, A:S410, A:M411, A:L412, A:S413, A:T414	129	0.696
3	A:K226, A:I246, A:T247, A:P248, A:S249, A:N250, A:N251, A:D252, A:D253, A:G254, A:K255	11	0.65

Table 5.3. HomA, T-cell MHCI epitopes

Allele	Start	End	Length	Peptide	Core	Icore	Score
HLA-A*02:01	271	280	10	KLFGDNLKTI	KLFGDNLTI	KLFGDNLKTI	0.646597
HLA-A*01:01	24	33	10	SSLSPVRVLY	SSSPVRVLY	SSLSPVRVLY	0.630021
HLA-B*27:02	113	122	10	QRVFETLNKI	QRFETLNKI	QRVFETLNKI	0.551582
HLA-A*01:01	347	356	10	FPSNYPNSIY	FSNYPNSIY	FPSNYPNSIY	0.549115
HLA-A*01:01	387	396	10	YANLGSQTNY	YANLGSQTY	YANLGSQTNY	0.51508
HLA-A*02:01	233	242	10	VLKDSGVVGL	VLDSGVVGL	VLKDSGVVGL	0.476862
HLA-A*02:01	20	29	10	KLKFSSLSPV	KLFSSLSPV	KLKFSSLSPV	0.281863
HLA-A*01:01	107	116	10	ISDANTQRVF	ISDANTQRF	ISDANTQRVF	0.281521
HLA-A*01:01	203	212	10	LVNSKVDQKY	LVNSVDQKY	LVNSKVDQKY	0.270123
HLA-A*02:01	337	346	10	SLYGGSNQPA	SLYGGSNQA	SLYGGSNQPA	0.265166
HLA-A*02:01	25	34	10	SLSPVRVLYM	SLSPVVLYM	SLSPVRVLYM	0.212954
HLA-A*01:01	38	47	10	QLTIENFLPY	QTIENFLPY	QLTIENFLPY	0.196094
HLA-A*02:01	93	102	10	YTLFLPKIEA	YLFLPKIEA	YTLFLPKIEA	0.189009
HLA-B*27:02	87	96	10	SLKIDPYTLF	SKIDPYTLF	SLKIDPYTLF	0.169619

Table 5.4. HomA, T-cell MHCII epitopes

Allele	Start	End	Length	Peptide	Percentile_Rank
HLA-DRB1*01:01	20	34	15	KLKFSSLSPVRVLYM	0.01
HLA-DRB1*01:01	19	33	15	SKLKFSSLSPVRVLY	0.01
HLA-DRB1*01:01	21	35	15	LKFSSLSPVRVLYMY	0.03
HLA-DRB1*01:01	18	32	15	ISKLKFSSLSPVRVL	0.07
HLA-DRB1*01:01	17	31	15	AISKLKFSSLSPVRV	0.1
HLA-DRB1*01:01	22	36	15	KFSSLSPVRVLYMYN	0.11
HLA-DRB1*01:01	23	37	15	FSSLSPVRVLYMYNG	0.67
HLA-DRB1*04:01	20	34	15	KLKFSSLSPVRVLYM	2.5
HLA-DRB1*04:01	19	33	15	SKLKFSSLSPVRVLY	2.6
HLA-DRB1*04:01	42	56	15	ENFLPYNLNNVKLSF	2.7
HLA-DRB1*01:01	116	130	15	FETLNKIKTNLVVNY	2.7
HLA-DRB1*04:01	18	32	15	ISKLKFSSLSPVRVL	3
HLA-DRB1*04:01	21	35	15	LKFSSLSPVRVLYMY	3.2
HLA-DRB1*04:01	43	57	15	NFLPYNLNNVKLSFT	3.4

Table 5.5. HomB, B-cell liner epitopes

No.	Chain	Start	End	Peptide	Number of residues	Score
1	A	402	425	GSQTNYNLNASLNTQDLANSMLST	24	0.818
2	A	79	104	VLPGEAFDSLKEAFDKIDPYTLFLPK	26	0.808
3	A	320	338	VPVTKDGQVEKDSNGKPKD	19	0.763
4	A	344	373	YNVCSLYGGSNQPAFPSNYPNSIYHNCADV	30	0.749
5	A	136	162	SNENPNNFNTCPYNNNGNTKNDCWQNF	27	0.737
6	A	50	70	NNVKLSFTDAQGNTIDLGVIE	21	0.697
7	A	33	38	YMYNGQ	6	0.693
8	A	1	7	TDTILKR	7	0.686
9	A	109	115	STSISDT	7	0.669
10	A	251	255	KNSGV	5	0.649
11	A	199	233	NSSTDCDSDPSKCVNPGVNGRVDTKVDQQYILNKQ	35	0.645
12	A	285	290	GNDLKT	6	0.532
13	A	263	266	GNDG	4	0.518

Table 5.6. HomB, B-cells conformational epitopes

No.	Residues	Number of residues	Score
1	A:D96, A:P97, A:Y98, A:T99, A:L100, A:F101	6	0.91
2	A:N408, A:L409, A:N410, A:A411, A:S412, A:L413, A:N414, A:T415, A:Q416, A:D417, A:L418, A:A419, A:N420, A:S421, A:M422, A:L423, A:S424, A:T425	18	0.897
3	A:T1, A:D2, A:T3, A:I4, A:L5, A:K6, A:R7, A:Y33, A:M34, A:Y35, A:N36, A:G37, A:Q38, A:N50, A:N51, A:K53, A:S55, A:F56, A:T57, A:D58, A:A59, A:Q60, A:G61, A:N62, A:T63, A:I64, A:D65, A:L66, A:G67, A:V68, A:P73, A:V79, A:L80, A:P81, A:G82, A:E83, A:A84, A:F85, A:D86, A:S87, A:L88, A:K89, A:E90, A:A91, A:F92, A:D93, A:K94, A:I95, A:L102, A:P103, A:K104, A:S109, A:T110, A:S111, A:I112, A:S113, A:D114, A:T115, A:Q118, A:G402, A:S403, A:Q404, A:T405, A:N406, A:Y407	65	0.711
4	A:T13, A:N14, A:A15, A:E16, A:S136, A:N137, A:E138, A:N139, A:P140, A:N141, A:N142, A:F143, A:N144, A:T145, A:C146, A:P147, A:Y148, A:N149, A:N150, A:N151, A:G152, A:N153, A:T154, A:K155, A:N156, A:D157, A:C158, A:W159, A:Q160, A:N161, A:F162, A:K251, A:N252, A:S253, A:G254, A:V255	36	0.705
5	A:L191, A:N192, A:A193, A:P194, A:F195, A:E196, A:T198, A:N199, A:S200, A:S201, A:T202, A:D203, A:C204, A:D205, A:S206, A:D207, A:P208, A:S209, A:K210, A:C211, A:V212, A:N213, A:P214, A:G215, A:V216, A:N217, A:G218, A:R219, A:V220, A:D221, A:T222, A:K223, A:V224, A:D225, A:Q226, A:Q227, A:Y228, A:I229, A:L230, A:N231, A:Q233, A:N312, A:G313, A:V320, A:P321, A:V322, A:T323, A:K324, A:D325, A:G326, A:Q327, A:V328, A:E329, A:K330, A:D331, A:S332, A:N333, A:G334, A:K335, A:P336, A:K337, A:P343, A:Y344, A:N345, A:V346, A:C347, A:S348, A:L349, A:Y350, A:G351, A:G352, A:S353, A:N354, A:Q355, A:P356, A:A357, A:F358, A:P359, A:S360, A:N361, A:Y362, A:P363, A:N364, A:S365, A:I366, A:Y367, A:H368, A:N369, A:C370, A:A371, A:D372, A:V373	92	0.687
6	A:G263, A:N264, A:D265, A:G266, A:E267	5	0.503

Table 5.7. HomB, T-cell MHCI epitopes

Allele	Seq_Num	Start	End	Peptide	Core	Icore	Score
HLA-A*01:01	1	219	228	RVDTKVDQQY	RVDTVDQQY	RVDTKVDQQY	0.888972
HLA-A*01:01	1	24	33	SSLSPVRVLY	SSSPVRVLY	SSLSPVRVLY	0.630021
HLA-A*01:01	1	358	367	FPSNYPNSIY	FSNYPNSIY	FPSNYPNSIY	0.549115
HLA-A*01:01	1	398	407	YANLGSQTNY	YANLGSQTY	YANLGSQTNY	0.51508
HLA-A*02:01	1	282	291	KLFGNDLKTI	KLFGDLKTI	KLFGNDLKTI	0.48301
HLA-B*27:02	1	118	127	QRVFETLNNI	QRFETLNNI	QRVFETLNNI	0.431395
HLA-A*01:01	1	112	121	ISDTNTQRVF	ISDTNTQRF	ISDTNTQRVF	0.327095
HLA-A*02:01	1	20	29	KLKFSSLSPV	KLFSSLSPV	KLKFSSLSPV	0.281863
HLA-A*02:01	1	348	357	SLYGGSNQPA	SLYGGSNQA	SLYGGSNQPA	0.265166
HLA-A*02:01	1	249	258	VLKNSGVVGL	VLNSGVVGL	VLKNSGVVGL	0.261371
HLA-A*02:01	1	25	34	SLSPVRVLYM	SLSPVVLYM	SLSPVRVLYM	0.212954
HLA-A*01:01	1	38	47	QLTIENFLPY	QTIENFLPY	QLTIENFLPY	0.196094
HLA-A*01:01	1	335	344	KPKDSDGLPY	KPDSDGLPY	KPKDSDGLPY	0.161594
HLA-A*01:01	1	165	174	QTAEEFTNLM	QTEEFTNLM	QTAEEFTNLM	0.151

Table 5.8. HomB, T-cell MHCII epitopes

Allele	Start	End	Peptide	Percentile_Rank
HLA-DRB1*01:01	20	34	KLKFSSLSPVRVLYM	0.01
HLA-DRB1*01:01	19	33	SKLKFSSLSPVRVLY	0.01
HLA-DRB1*01:01	21	35	LKFSSLSPVRVLYMY	0.03
HLA-DRB1*01:01	18	32	ISKLKFSSLSPVRVL	0.07
HLA-DRB1*01:01	17	31	AISKLKFSSLSPVRV	0.1
HLA-DRB1*01:01	22	36	KFSSLSPVRVLYMYN	0.11
HLA-DRB1*01:01	23	37	FSSLSPVRVLYMYNG	0.67
HLA-DRB1*04:01	118	132	QRVFETLNNIKTNLI	1.5
HLA-DRB1*04:01	119	133	RVFETLNNIKTNLIM	1.5
HLA-DRB1*03:01	239	253	FRKKIEIDAVVLKNS	1.8
HLA-DRB1*03:01	242	256	KIEIDAVVLKNSGVV	1.8
HLA-DRB1*03:01	241	255	KKIEIDAVVLKNSGV	1.8
HLA-DRB1*03:01	238	252	NFRKKIEIDAVVLKN	1.8
HLA-DRB1*03:01	237	251	NNFRKKIEIDAVVLK	1.8

5.2.4 Molecular docking with TLR4 and Normal mode analysis

Molecular docking between vaccine candidate toll-like receptors is an important fundamental and promising process to characterize the interaction and binding affinity between the vaccine constructs and the human Toll-like receptors (here TLR4). The crystal structure of human TLR4, downloaded from the RCSB protein data bank (PDB ID: 4G8a) was used for molecular docking. Molecular docking between TLR4 and predicted globular domain PDB was carried out with a patchdock web server. Docked results were further submitted for refinement to the fire dock. The topmost high interface score docking models are shown in **Fig. 5.7.** Flexibility in biological macromolecules is an important characteristic of protein-protein interactions. Therefore, we have chosen TLR4-HomA globular domain docking model (**Fig. 5.7 C**) for normal mode analysis. Interestingly, in the docking model, 47 amino acid residues interact with TLR4 which contains B-cell and T-Cell both the epitopes and are common for both HomA and HomB (**Table 5.1 and 5.5,** T-cell containing B-cell epitopes is highlighted in cyan colour). The complex deformability mainly depends on the individual distortion of each residue (Cα atom), presented through coloured hinges in the chain (**Fig. 5.6 A**). We used the iMODs server for calculation, the average RMS represented as B-factor, the B-factor plot represents the stable structure docked molecules shown in **Fig. 5.8 B**. The server calculated the eigenvalue as 7.365205e−05, as represented in **Fig. 5.8 C**. Moreover, the eigenvalue and the variance are inversely related associated with each normal mode (**Fig. 5.8 D**). The covariance matrix represents correlated,

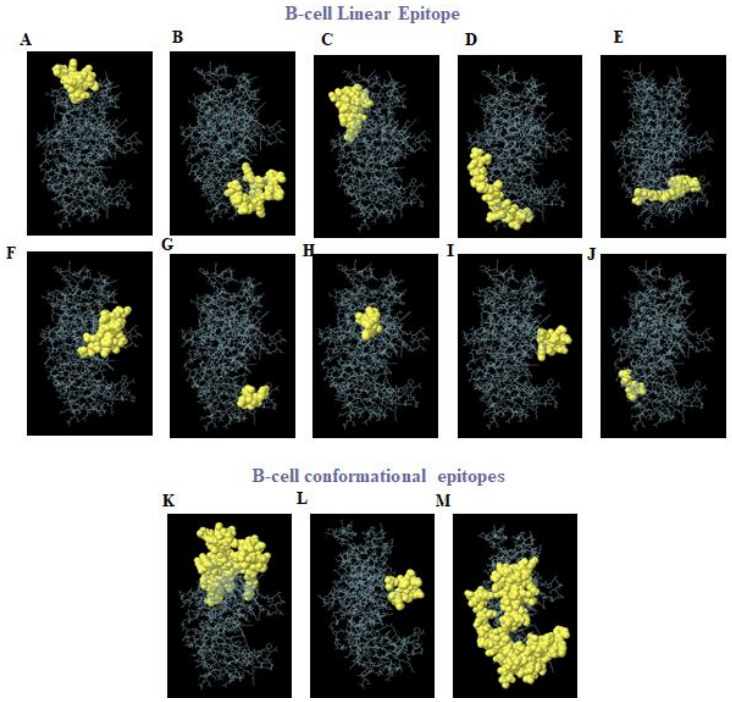

Figure 5.3 3D representation of linear and discontinuous B-cell epitopes of HomA globular domain. (**A-J**) Ellipro B-cell linear epitopes of HomA, (**K-M**) Ellipro B-cell conformational epitopes.

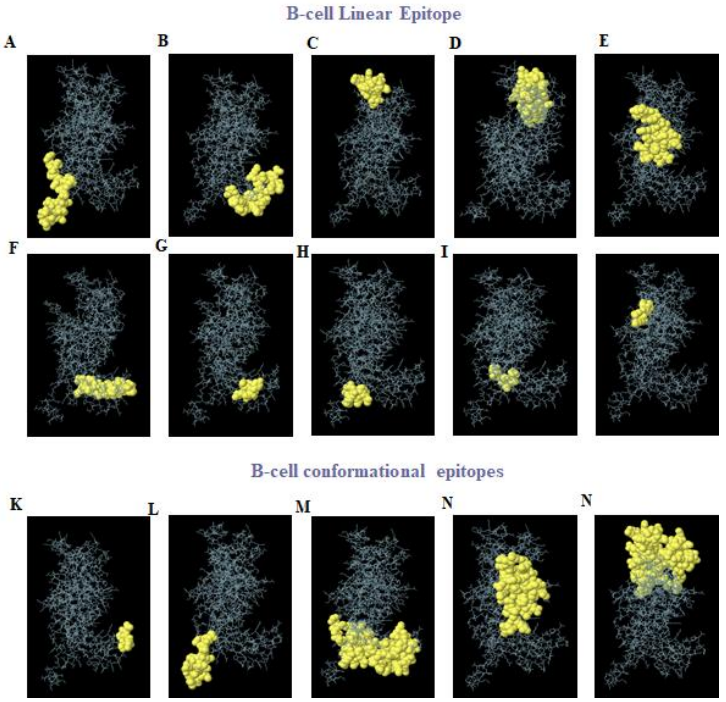

Figure 5.4 3D representation of linear and discontinuous B-cell epitopes of HomB globular domain. (**A-J**) Ellipro B-cell linear epitopes of HomA, (**K-M**) Ellipro B-cell conformational epitopes.

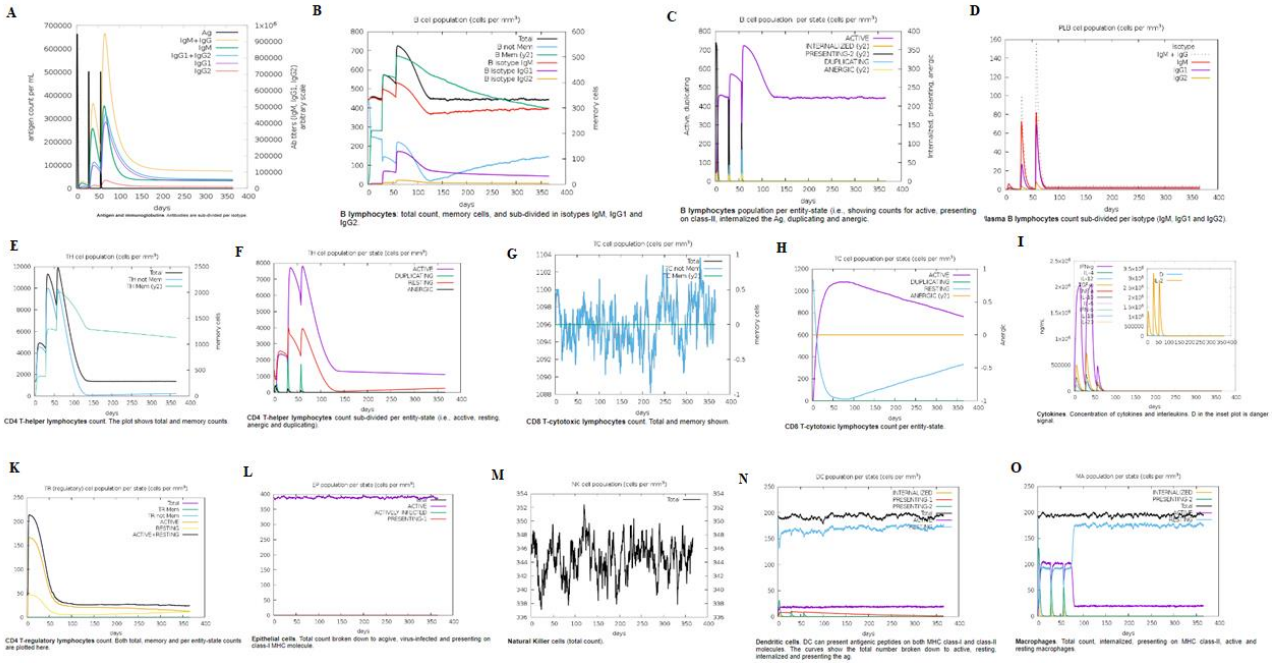

Figure 5.5. **Immune simulation of the HomA globular domain**; (A) immunoglobulin and immunocomplex response to the antigen, (B) B lymphocyte total count, (C) B lymphocyte population per entity state, (D) plasma B lymphocyte count, (E) CD4 T-helper lymphocyte count, (F) CD4 T-helper lymphocyte count subdivided per entity state, (G) CD8 T-cytotoxic lymphocyte count, (H) CD8 T-cytotoxic lymphocyte count per entity state, (I) concentration of cytokines, natural killer cell population, (K) CD4 T-regulatory lymphocyte count, (L) Epithelial cells count, (M) NK cell count, (N) dendritic cell per state.

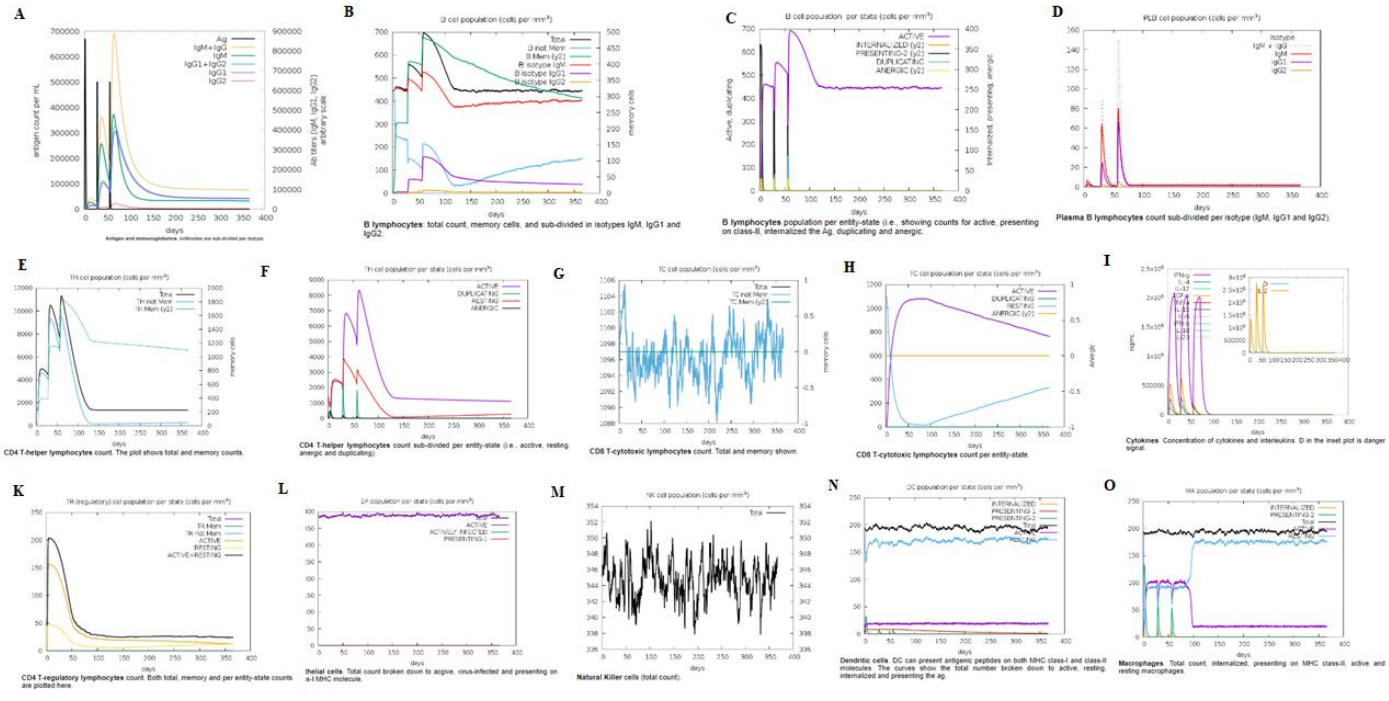

Figure 5.6. **Immune simulation of the HomB globular domain**; (A) immunoglobulin and immunocomplex response to the antigen, (B) B lymphocyte total count, (C) B lymphocyte population per entity state, (D) plasma B lymphocyte count, (E) CD4 T-helper lymphocyte count, (F) CD4 T-helper lymphocyte count subdivided per entity state, (G) CD8 T-cytotoxic lymphocyte count, (H) CD8 T-cytotoxic lymphocyte count per entity state, (I) concentration of cytokines, natural killer cell population, (K) CD4 T-regulatory lymphocyte count, (L) Epithelial cells count, (M) NK cell count, (N) dendritic cell per state.

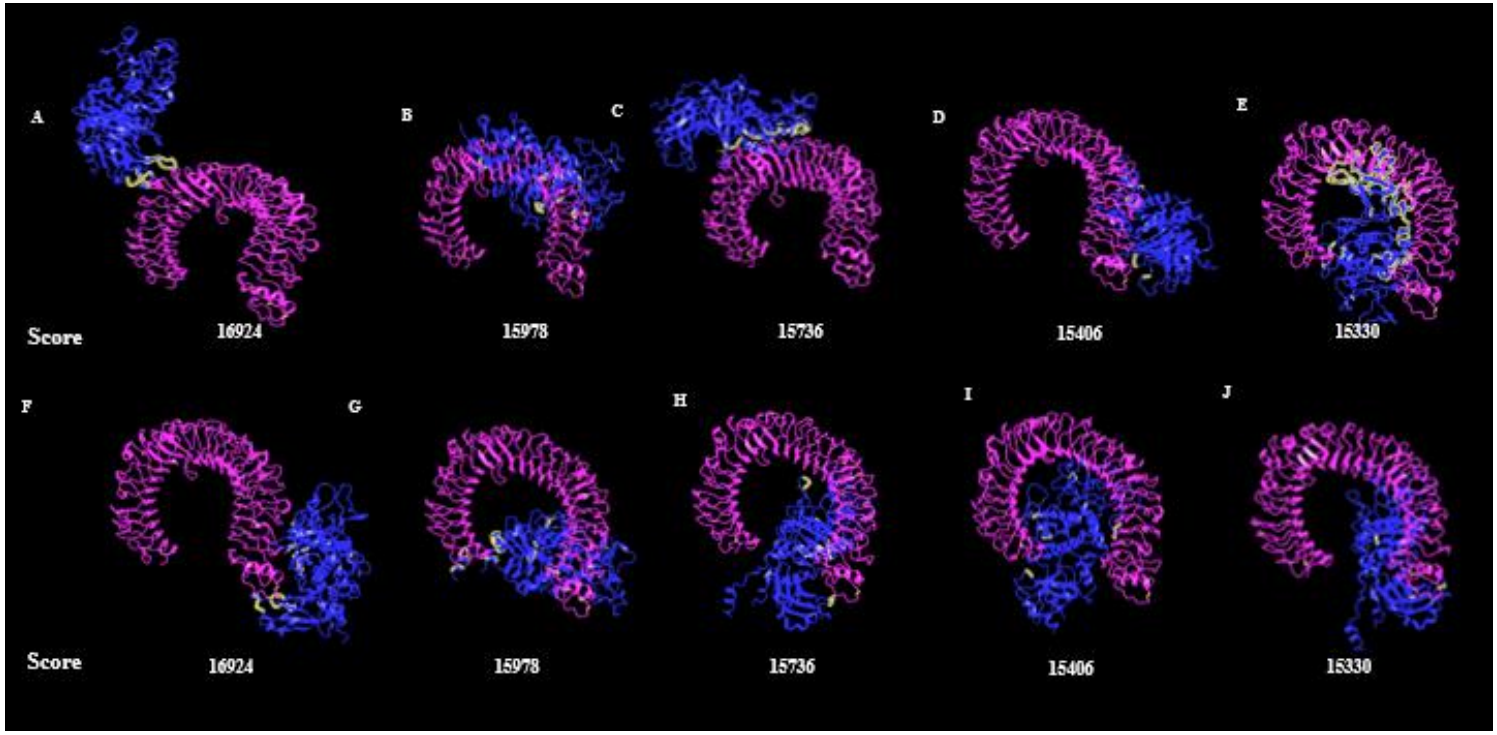

Fig. 5.7 Molecular docking between TLR4 and globular domain of HomA and HomB. (A-E) top 5 high interface score docking complex of TLR4- globular domain of HomA. (**F-J**) top 5 high interface score docking complex of TLR4- globular domain of HomB.

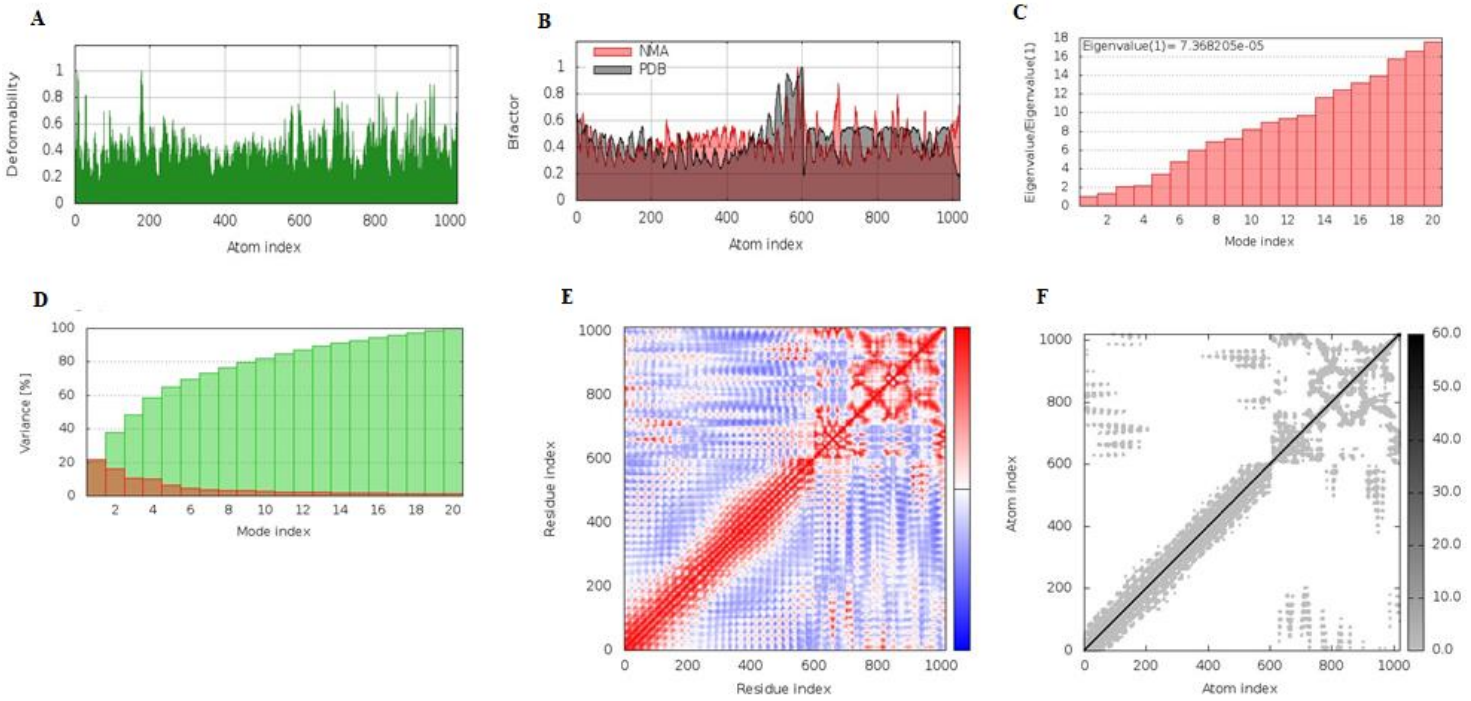

Figure. 5.8 Results of iMODS A. deformability plot; **B.** B-factor; **C.** Eigenvalue; **D**. variance plot; **E.** covariance matrix analysis; **F**. elastic network model.

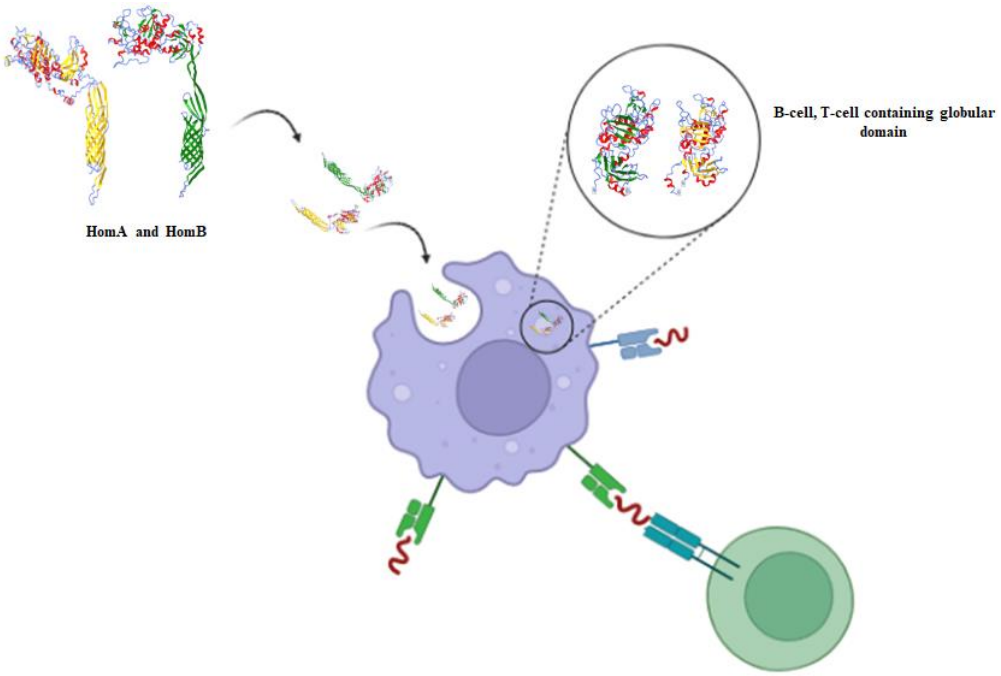

Figure 5.9. Cartoon representation epitopes processing and presentation of B-cell and T-cell containing globular domain of HomA and HomB.

uncorrelated, or anti-correlated motions with respect to interacting residues, the with colours graph where correlated, uncorrelated, or anti-correlated motions are represented by red, white, and blue colours, respectively (**Fig. 5.8E**). In addition to that, an elastic network model shows docked protein molecule (Cα) atoms are interconnected with "springs" of certain strengths (the darker greys representation of the stiffer springs).

5.3 Summary

We have used the reverse vaccinology approach to explore the globular domain or HomA and HomB for the development of potential vaccine candidates. The predicted secondary and tertiary structure shows mixed content and globular topology (**Fig. 5.1**). Both the domains predict to form B-cell linear and conformational and T-cell (MHCI and MHCII) epitopes, which shows good antigenicity (**Fig. 5.2** and **5.3**). Interestingly, the immune simulation shows both the protein elicited simultaneous strong cellular and humoral immune responses in humans (**Fig. 5.4** and **5.5**). 3D structures of globular domains show their binding affinity with human TLR4 receptors and elicit cellular responses (**Fig. 5.6** and **5.7**). Though we found immunogenic response in our study through *in silico* approaches there is a strong requirement of *in-vitro* and *in-vivo* studies to validate the effectiveness, immunogenicity and most vital host safety to vaccine structure before human trials.

Chapter 6

Chapter 6
Conclusion and scope of future work

6.1 Introduction

The outer membrane acts as the first line of defence for Gram-negative bacteria against bactericidal and toxic compounds. This membrane works as a barrier that is impermeable to large, charged molecules and also participates in bacterial pathogenicity. Porins are water-filled pore-like structures that span the outer membrane and control the transport of hydrophilic molecules. Achouak *et al*, studied multiple facets of bacterial porins (Yang *et al* 2016). Bacterial porins interact and adhere to the host tissues for evasion of host-defence mechanisms and can elicit innate and acquired immune responses. Di Donato *et al*, reported that *S. typhimurium* porins inhibit phagocytic activity by activating the adenylate cyclase system (Donato *et al* 1986). *S. typhimurium* porins can induce the activation of the complement system by acting both on the classic pathway as well as on the alternative pathway (Galdiero *et al* 1984). Severe infections caused by Gram-negative bacteria remain a major cause of morbidity and mortality in the site of the ongoing development of new antimicrobial agents (Lazaron *et al* 1984). The mechanism that pathogenic Gram-negative bacteria use to infect host cells has been extensively studied. The outer membrane component of Gram-negative bacteria, such as LPS and OMPs, are involved in pathogenesis and virulence. The β-barrel structure of OMP forms a pore-like assembly and aids in biologically functional activities, such as nutrient transport. Additionally, it provides an osmotically compatible environment, which is essential for the survival of bacteria. Porins are highly immunogenic and act as epitopes on the bacterial surface. Moreover, they are also involved in the emergence of multi-drug resistant bacterial strains. In general, they are conserved in a bacterial species or even in a bacterial family and have high homology with primary amino

acid sequence and secondary structure which are antigenically related with each other (Roy *et al* 1994, Snijder *et al* 1999). Although cell signalling stimulation by OMPs of Gram-negative bacteria is extensively studied, the interacting receptors of the host cell with porins are not well characterized. The surface-exposed loops present in the β-barrel structure can be used to make synthetic peptides for vaccination that can mimic antigenic epitopes present on OMPs (Galdiero *et al* 2003, Hughes *et al* 1992). Monoclonal antibodies against purified OMPs give specificity to the diagnostic tests and overcome the problem of cross-reactivity by selecting unique antigenic sites. In fact, commercial monoclonal antibodies are available for mitochondrial Outer membrane β-barrels (OMBBs) VDAC1 and Sam50, but not for other typical OMPs of different microorganisms.

6.2 Biophysical characterization of homodimers of HomA and HomB, outer membrane proteins from *Helicobacter pylori*

OMPs play a crucial role in several important physiological functions like ionic regulation, cell adhesion, host-pathogen interaction as well as pathogenesis, and structural information of these OMPs is vital for understanding their function and regulation. The present study provides several structural insights for OMPs of the Hom (Helicobacter outer membrane) family members of *H. pylori*, HomA and HomB. HomB is reported to be expressed at the *H. pylori* outer membrane and participates in bacterial adherence and inflammation. Furthermore, the dismissal of HomB causes significantly low production of IL-8. Moreover, it is also recognized by antibodies present in the human serum, which indicates that the surface-exposed regions of HomB likely interact with the host cell receptors (Oleastro *et al* 2008). We performed bioinformatics analysis to predict the presence of a signal peptide (**Fig. 3.2**), which ensures that these proteins are likely membrane proteins. Furthermore, we confirmed the presence of the C-terminal signature β-barrel sequence (**Fig. 3.2**). Typically, β-barrel OMPs from Gram-negative bacteria, such as *E. coli* as well as others possess a C-terminal signature sequence, which

makes these unique from other topological OMPs. This sequence helps OMPs to fold in a barrel shape, via the BAM complex (Vogt *et al* 1999). Nevertheless, more recent works also reported another consensus having − 6 (glycine), − 3 (aromatic), − 2 (basic or large polar) and − 1 (aromatic) amino acids positions at C-terminal (Doyle *et al* 2019). This consensus may slightly vary from Gram-negative species to species (Struyve *et al* 1991). The homB and homA share 90% similarity, with only difference in the 300 bp central region. This difference does not make significant changes in the secondary structure and topology of both proteins. Our in-silico analysis shows (**Fig. 3.2**) the membrane location of the C-terminal conserved β-barrel domain for HomA and HomB where N-terminal β-strand is also a part of β-barrel (**Fig. 3.3** and **3.5**). I-TASSER also predicted a high C-score, a large size β-barrel model homologue with 22 β-strand bacterial plant-ferredoxin receptors FusA, for both HomA and HomB with slight variations (**Fig. 3.4**). However, trypsin digestion experiments suggest that the real structures for HomA and HomB are closer to the predicted models using AlphaFold 2 (**Fig. 3.3 A–D**). Generally, bacteria display a great variety of outer membrane proteins that participates in nutrient transport, host signaling manipulation, adhesion, and virulence. Meuskens *et al*. reviewed different types of secretion systems of Gram-negative bacteria where these auto-transporters (ATs) have been categorized in 5 classes (Va-Ve), based on their structure and function characteristics. Additionally, they also describe another unique class of secretion system Vf. The Vf class of ATs contain a surface-exposed loop/globular domain inserted between the N and C-terminal regions (Meuskens *et al* 2019). These characteristics are unique structural features to the *H. pylori* Hop family outer membrane protein. For example, BabA protein shows a surface-exposed domain between the first and second β-strand of an 8-stranded β-barrel and contains no additional passenger at either terminus of the protein. Thus, the proposed passenger is an extended loop of the β-barrel domain and the β-barrel is smaller than that of any other Ats (Coppens *et al* 2018). Similarly, Hom family members, HomA and HomB also likely to form

disconnected small β-barrel where N-terminal β-strand (S1) is extended to a surface-exposed globular domain and connected back to C-terminal β-barrel with β-strand S19 in case of HomA and S20 in HomB (**Fig. 3.3 A, B**). Although Vf class proteins are proposed to be a part of AT family, their structural topology is very different from the other types of ATs. Therefore, it is a subject of investigation whether these proteins do possess secretion mechanisms like other ATs or they possess some other unique feature for bacterial survival and pathogenesis. Heat modifiability is one of the peculiar features of β-barrel proteins where proteins show migration differences between boiled and unboiled samples applied to PAGE analysis (Noinaj *et al* 2015). We observed heat modifiability of HomA and HomB to some extent (**Fig. 3.6**), however, this was not as striking as some of the reports for other OMPs due to small β-barrel and large exposed loop. Normally, OMPs forming β-barrel structures are mostly rich in β-sheets. Many of the OMPs β-sheet structures are extensively studied with IR spectroscopy, which gives spectra containing a sum of peaks of the secondary structure content such, as β-sheet (parallel and antiparallel), α-helix, as well as coils/turns and this information lies under Amid I band of the spectra. HomA and HomB show a high β-sheet secondary structure content with parallel and anti-parallel β-sheets (**Fig. 3.7 E–H**), which supports the in-silico secondary structure contents of being a β-barrel protein. Moreover, CD data strongly suggest that both HomA and HomB are rich in β-sheets that enables the formation of a β-barrel structure. Renaturation of urea denatured HomA and HomB into a buffer containing detergents or lipids leads to changes in the secondary structure content of both proteins (Appendix D). We observed that the addition of detergents (LDAO and TWEEN 20) and lipids (DMPC and DOPC) favours either parallel or antiparallel β-sheets secondary structure (**Fig. 3.8A–J**) and possibly assists in folding or restoring these proteins to a native β-barrel structure. Conversely, we did not observe the restoration of the structure of HomA and HomB in the presence of CHAPS (**Fig. 3.8 B,G**). In short, detergents (LDAO and TWEEN 20) and lipids (DMPC

and DOPC) restore and favour the folded protein spectra, as CD experiments suggest that these lipids and detergents provide the most favourable environment for the refolding of urea denatured HomA, and CHAPS provides a least favoured environment for refolding of HomA and HomB proteins. **Table 3.2** summarises the folding ranking of the most to least favourable folding conditions for HomA and HomB in a few detergents and lipids, based on the circular dichroism spectra analysis. Interestingly, HomA and HomB both are stable between pH range from 3 to 11 and remain in folded confirmations, as analysed using Trp fluorescence experiments (**Fig. 3.9 A, B**). A wide range of pH stability provides plasticity to proteins. Porin from Yersinia pseudotuberculosis was studied for its wide pH range (2.0 to 8.0) for its plasticity and structural rearrangement (Novikova *et al* 2007, Kim *et al* 2007). β-barrel proteins show a blue-shift and a few folds less intensity in Trp fluorescence spectra upon unfolding (Kim *et al* 2007). Trp spectra for HomA and HomB proteins show both 15 nm red-shifted fluorescence emission profiles along with a twofold loss in intensity upon unfolding in the presence of urea (**Fig. 3.9 C–E**), similar to a typical characteristic of a transmembrane beta-barrel protein. Moreover, the addition of unfolded proteins in buffers containing detergents and lipids promotes the folding of the proteins (**Fig. 3.10 A–J**). Incubation of unfolded HomA to buffer containing TWEEN 20 detergent shows blue shift but the intensity of spectra does not increase significantly which suggest it might not be the most favourable folding condition (**Fig. 3.10C**). OMPs form β-barrel and can exist in multimeric forms. Arvind *et al*. characterized TrpC/D, a pore-forming OMP from Treponema pallidum, CD suggest that it forms β-barrel and exists in monomer and trimer forms (Anand *et al* 2012). Interestingly, we also observed that HomA and HomB proteins exist in two dominant forms, i.e. a monomer as well as a dimer. Earlier reports for OmpF from E. coli reassembled as a trimer are resistant to the denaturing action of sodium dodecyl sulphate (SDS) at room temperature (Anand *et al* 2012, Rosenbush *et al* 1974). The denatured monomer migrates faster than the dimer and trimer in a gel during

SDS-PAGE. HomA and HomB also show resistance to denaturation by SDS when it was run on SDS-PAGE, and we observed both monomer and dimer bands. The addition of detergents leads to oligomerization of proteins, but dimer and monomer still exist, as evident from the SDS-PAGE analysis of fractions of size exclusion chromatography experiments performed with or without β-mercaptoethanol (**Fig. 3.11 and 3.12**). The *ab-initio* structure of both HomA and HomB predicted from AlphaFold 2 has almost similar structural organization. Both proteins consist of two domains, the surface-exposed globular domain and a β-barrel domain with a hydrophobic patch suggesting its transmembrane nature (**Fig. 3.3**). Both domains were connected with a flexible neck, primarily consisting of loops. We believe this flexible neck provides the necessary degree of freedom for the surface-exposed globular domain against the membrane-anchored β-barrel domain to explore the best possible orientation for optimal ligand interaction. The size exclusion chromatography of both HomA and HomB shows the presence of dimer in the solution. The analysis of experimental SAXS data of both HomA and HomB showed the molecular weight of the scattering species very close to dimer supporting the presence of dimer species in solution. SDS-PAGE analysis of the dimeric fraction of HomA and HomB suggests the involvement of covalent interaction in dimerization (**Fig. 3.11 and 3.12**). Based on the SAXS data, the prepared dimer model of both proteins has their dimer interface in the loop region of the surface-exposed globular domain (**Fig. 3.3**). Interestingly, the four cysteine residues of HomA (245, 252, 393, 416) and all six cysteine residues (203, 215, 261, 268, 404, 427) of HomB are located in the loops of the globular domain (**Fig. 3.5**). In such a surface-exposed oxidizing environment, these cysteine residues between homo (HomA2, HomB2) or hetero (HomA–HomB) globular domain could form disulphide bond/s to stabilize the oligomeric assembly. We believe that the oligomerization of HomA and HomB protein enables them to form stronger receptor-ligand interaction by harnessing the avidity of combined interaction between multiple receptors and ligands. Similar oligomeric association of receptor could

be seen in Receptor tyrosine kinase signalling pathways like JAK-STAT signalling, insulin-GLUT4 signaling (Hubbard *et al* 2007), etc. OMPs greatly help in the colonization of bacteria and persistent infection. For example, OMPs such as BabA, SabA, and HopC interact with Globo H, hexaglycosylceramide, Sialyl-Lewis, Collagen IV, Laminin, respectively (Oleastro 2013). Additionally, various β-barrel forming OMPs from *H. pylori*, HopE, and OMPLA help in the regulation and adaptation to the surrounding environment (Bina *et al* 2017, Vollan *et al* 2017). Thus, HomA and HomB dimers also play a crucial role in the biology of these proteins. Future experiments will aid in delineating how dimeric association is pivotal to the functions of these proteins in *H. pylori* pathogenesis. Since these loop regions in β-barrel or the surface-exposed globular domain of OMP plays important role in oligomerization states (Lopes *et al* 2019), and here also the surface-exposed globular domain likely contributes to dimer formation. Some of the hypothetical proteins (K74_10375, K747_09130, and K747_06625) and outer membrane protein is associated with biofilm formation, HomD, a member of Hom OMP family is associated with moderate biofilm former (58.3%) to hyper biofilm former (66.7%) *H. pylori* strains (Wong *et al* 2016). Recently, Stephanie *et al.* reported that homB expression is related to biofilm formation and regulated with pH and ArsRS dependent manner, and HomB helps *H. pylori* in hyper biofilm formation (Servetasc *et al* 2018). HomA and HomB both are stable at a wide range of pH from acidic to basic pH (**Fig. 3.9**), it might be one of the reasons for biofilm formation and *H. pylori* survival in environmental pH stress conditions. The data presented herein gives structural insights that cysteine residues present on the surface-exposed domains (**Fig. 3.3**) are expected to be involved in the homodimer formation of HomA and HomB. Such dimerization assisted by HomA and HomB likely play an important role in cell-cell interactions, and thus might assist in biofilm formation. Biofilm formation is not only a crucial survival strategy but also aids in persistent and successful infection. Biofilm also protects bacteria from antibiotics and helps in evading immune response and homB is also

associated with antibiotic resistance of *H pylori* (Haddadi *et al* 2020). C-terminal β-barrel of HomA and HomB forms pore-like structure topology (**Fig. 3.3**) and indicates porin channel-like properties, which might play an important role in the transport of biomolecules, including antibiotics. Investigation of HomA and HomB, especially their porin like functions, will not only provide a clue on their possible role in antibiotic resistance but also offer these proteins as potential therapeutic candidates. The further structural characterization will provide new insights into the molecular mechanism of *H. pylori* pathogenesis.

6.3 HomA and HomB, outer membrane proteins of Helicobacter pylori down-regulate activation-induced cytidine deaminase (AID) and Ig switch germline transcription and thereby affect class switch recombination (CSR) of Ig genes in human B-cells

H. pylori is classified as a class I carcinogen by the world health organization (WHO). *H. pylori* is not only interacting with gastric epithelial cells but also host immune cells and modulates the functioning to escape the immune response. Molinari *et al.* showed that VacA, a toxin secreted by *H. pylori* altered the antigen presentation by B-cells which possibly result in impaired adaptive responses via interrupting T-cell B-cell communication (Molinari *et al*., 1998). In addition to the enigma of *H. pylori* and immune cell interaction, an interesting study by Matthijs *et al.* in the 90s reported a decreased level of antibodies against *H. pylori* in arthritis patients (Janssen *et al*., 1992). Similarly, Birkholz and Marianne *et al.* also reported reduced IgA antibodies in gastric adenocarcinoma patients (Birkholz *et al*., 1998; Quiding-J¨ arbrink *et al*., 2009). Based on the finding of these studies we were interested to know how *H. pylori* interplays with the immune system and here we focused on B-cells. OMPs are the foremost bacterial factors that interact with the host cells and the molecular mechanism of interaction between the OMPs and immune cells is not well understood. It is proposed that OMPs may be activating the host cells similar to that of the LPS but via an

independent mechanism. OMPs help bacteria to adhere to the host cells, and subsequently provoke the release of inflammatory cytokines and thus modulate intracellular signalling (Safaralizadeh *et al*., 2017). Oleastro *et al*. reported HomB OMP significantly contributes to the pathogenicity of *H. pylori* and can be considered as a virulence factor (Oleastro *et al*., 2008). Similarly, Reza *et al*. reported a significant prevalence of HomA and HomB with different gastric malignancies, such as gastritis, peptic ulcer and gastric cancer (Ise *et al*., 2011). AID is the key player of antibody diversity and also an important factor of CSR. Here, we have used Raji cells (Burkitt lymphoma) as a model to investigate the effect of HomA and HomB, OMPs of *H. pylori*, on the AID expression and CSR process. Although Raji cells demonstrate aberrant expression profiles and genome alteration of different genes, it has been widely used to study B-cells characteristics, such as immune complex, immune modulation, BCR signalling and aberrant expression of immunoglobulin gene (Duan *et al*., 2016; Caeser *et al*., 2019; Van Belle *et al*., 2016; Gururajan *et al*., 2006; Niu *et al*., 2012; Dussault *et al*., 2008; Singer and Williamson, 1980). Nevertheless, further validation of these observations on clinical samples, such as PBMC from gastric patients or animal models will help develop therapeutics against *H. pylori* infection and explore HomA and HomB as potential virulence factors. We expressed and purified HomA and HomB, and stimulated human B-cells. We observed a reduced AID expression at mRNA as well as protein level up to 60 % initially at 1 h and 50 % at 4 h, which was restored to normal levels at 8 h (**Fig. 4.1 and 4.2**). AID is regulated by several transcription activators and repressors (Zan and Casali, 2013). We investigated the mRNA expression of NFκB, SMAD3, cMYC, and STAT6 and these were not significantly affected in both HomA and HomB stimulated cells. In contrast, increased mRNA expression PAX5 was observed in HomA stimulated cells but not observed in HomB stimulated cells (**Fig. 4.4A-J**). Further, we analysed the mRNA expression of transcriptional repressors of AID, and interestingly, cMYB shows significantly higher expression around 1.5 to 2-folds at 1, 4 and 8 h, in cells stimulated with HomA and

HomB. cMYB act as a repressor of AID and binds to region 2 (positions +121 to +2221) of the AID gene. In fact, in our ChIP experiments, we observed significantly higher cMYB occupancy at region 2 of the AID gene in HomA and HomB stimulated cells as compared to the unstimulated control cells. Tran *et al*. reported that siRNA mediated knockdown of cMYB increases the AID expression, which is tested via luciferase activity, suggesting that any change in cMYB expression is directly related to its suppressive consequences to its target genes such as AID. Additionally, these studies revealed that enhancers/transcription factor, such as Pax5 activity, was not adequate to balance or counter the suppressive effect of cMYB, suggesting that cMYB works independently as a negative regulator to counteract the positive regulators. The higher expression of negative regulators works as a feedback response to balance over the expression of AID (Tran *et al*., 2010). We have observed increased expression of cMYB in HomA and HomB treated cells and decreased expression and nuclear localization of AID simultaneously (**Fig. 4.5 and 4.6**). Besides cMYB, another transcriptional repressor, E2F did not show significantly increased expression (**Fig. 4.5A–D**). In agreement with the data, we believe cMYB most likely contributes towards reduced expression AID in cells stimulated with HomA and HomB. Class switch recombination and AID activity are greatly dependent on the transcription of Ig genes. Transcription provides single-stranded DNA for AID deamination reaction and consequently creates double-strand breaks which further results in isotype switching of the constant region from Cμ to Cγ, Cα, and Cε. Reduced AID expression is strongly related to fewer CSR events. Timothy *et al*. studied miR-29 role in AID suppression via directly targeting the AID gene and showed reduced CSR which is in relation to AID expression level (Recaldin *et al*., 2018). Similarly, Zhi *et al*. reported, changes in AID levels directly affect the CSR of Ig genes in cancer cells including the Raji B-cells (Duan *et al*., 2016). In agreement with the studies published, we also investigated the correlation of AID expression level with CSR of Ig genes. We employed qRT-PCR and checked the expression level of Ig

mature transcript for IgM, IgA, and IgG which are spontaneously expressed in Raji B-cells. Interestingly we observed around 2-fold increased expression of IgV-Cμ in both HomA and HomB stimulated cells. IgV-Cα expression was repressed up to 20–40 % at 1 and 4 h in HomA stimulated cells and 50− 40% were repressed at 1, 4 and 8 h, in HomB treated cells. IgV-Cγ expression was also repressed in HomA and HomB stimulated cells nearly 70 % at 1 h and 40 % at 4 and 8 h. Since IgV-Cμ expression level was 2-fold increased, we analysed it with respect to ratios as IgA:IgM and IgG:IgM, which was reduced to 20–25 % and 20–35 %, respectively. As our studies revealed a significantly reduced CSR process in HomA and HomB stimulated Raji cells, to rule out the possibility of changes in the transcription of IgV genes, we checked the transcription of the IgV region and observed that transcription of IgV genes did not show any significant change upon stimulation of HomA and HomB. In addition to AID, we also checked the mRNA expression of two important CSR factors, BATF and HOXC4. BATF acts as a global regulator for both AID transcription and Ig germline transcription (Mai *et al*., 2010). Similarly, HOXC4 also regulates AID transcription and CSR (D'Elios *et al*., 1997). Expression levels of both of them were not significantly affected by HomA and HomB, which strongly indicate that the reduced CSR of Ig genes was primarily due to a reduction in AID expression. *H. pylori* upregulates PDL1 and contributes to the apoptosis of effector T-cells by occupying PD-1 on their surface (Ise *et al*., 2011). Earlier studies reported that *H. pylori*-infected children show fewer antibodies production; the possible cause considered T-cell polarization towards Tregs cells and less activation of TH cells which in turn induce B-cell responses (Soares *et al*., 2005). Although many studies have been performed to study T-cell response against *H. pylori*, B-cell response, as well as their regulation in reaction to *H. pylori* infection is not well understood yet. Similar to T_{reg}s cells, B-cells are also differentiated to Bregs cells as a subset of the population that can act as an immune negative regulator (Mizoguchi *et al*., 2002). Here, we tested whether the OMPs from *H. pylori*, HomA and HomB, can induce B_{reg}s cell

response. Strikingly, we observed increased expression PDL1, IL35 and IL10. IL35 and IL10 are the cytokines that inhibit T-cell activation (Freeman *et al*., 2012) and PDL1 is known to induce T-cell apoptosis (Chiu *et al*., 2018). This upregulation of PDL1, IL35 and IL10 can possibly contribute to the suppression of the immune response to *H. pylori*-associated MALT lymphoma. Most likely, *H. pylori* has coevolved with the human host and adopted novel strategies to evade the sturdy innate and adaptive immune response.

6.4 Immunoinformatic characterization of globular domains of HomA and HomB, for potential sub-unit vaccine candidate against *Helicobacter pylori*

H. pylori has been a successful pathogen due to its survival and immune evasion strategies. Chronic infection is increasing day by day in developed as well as developing countries. Several studies indicate chronic infection possibility leads to gastric carcinoma (Correa 1995; Leung *et al*. 2004; Nomura *et al*. 1991). Further, persistent infection with *H. pylori* leads to chronic gastritis, multifocal atrophic gastritis, rarely intestinal metaplasia (Correa 1995). Many treatments have been used to treat *H. pylori*, but till now, no effective vaccine candidate is available for the prevention of *H. pylori* infection. In the current study, we have used globular domains of HomA and HomB, virulence outer membrane protein marker to explore the possibility of the development of subunit vaccine candidates. We have predicted B-cell and T-cell epitopes with IEDB online server. High score antigenicity with surface accessibility of potential linear as well as conformational epitopes was observed (**Fig. 5.2, 5.3** and **5.4**). The main advantage of the epitope-based vaccine is that it can generate specific and strong immune responses against epitopes and enhance binding affinity with the target receptor (Bhattacharya *et al*. 2020, Moise *et al*. 2015, Terry *et al*. 2015). For the development of both humoral and cytotoxic immune responses, T-cell epitopes derived from B-cell epitopes were identified. HomA and HomB globular domains were used for immune simulation. Administration of globular domains with continuous two booster doses

predicted to elicit strong humoral as well as cellular immune responses. Further innate immune cytokines were high, and NK and macrophages counts were also high and active during vaccine administration. In addition to that antigen presentation cells such as epithelial and dendritic cells count were also active (**Fig. 5.5** and **5.6**). Meza *et al*. reported multi epitope-based peptide (MEBP) vaccine candidates against *H. pylori* using the reverse vaccinology approach (Meza *et al*. 2017). They predicted both B and T-cell epitopes of four virulent proteins (FliD, Urease B, VacA and CagA) for designing a MEBP vaccine candidate against *H. pylori*. Lately, Khan *et al*. did the same and predicted B-cell and T-cell epitopes from different virulent proteins (CagA, OipA, GroEL and VacA) and planned a MEBP vaccine against *H. pylori* (Khan *et al*. 2019). Generally, selected common epitopes to elicit the immune response with the target molecules for the next step of cellular cascades (Zhou *et al*. 2009). Now, in this work, we found common B and T-cell epitopes mentioned in **Tables 5.1** and **5.5**. Subsequently, we have performed a molecular docking study between TLR4 and globular domains of HomA and HomB. Patchdock server demonstrated the binding interaction of complex, we have selected the top 5 high interface scoring complex (**Fig. 5.7**). Out of which we have selected globular domain of HomA-TLR4 complex for NMA study to analyse the molecular mobility, comparative deformability. The eigenvalue was noted as 7.3682e−05 which indicates the better flexibility of the docking complex (**Fig. 5.8**).

6.5 Conclusion and Future directions

Outer membrane proteins (OMPs) are gaining more attention as alternative combating strategies to fight against pathogens. OMPs plays multi-dimensional role such as host-pathogen interaction, host environment adaptation, and host-immune system evasion. HomA and HomB have been reported for increased *H. pylori* adhesion and hyper biofilm formation. Due to clinical significance, these two OMPs become important research targets. Since there were no structural and functional insights are known to date, we investigated the biophysical aspect of structural studies, the functional role of HomA and HomB to human B-cells and the potential of HomA and HomB to be utilized as sub-unit vaccine candidates. A cartoon representation of the present thesis work is presented in **Fig. 6.1**.

We have performed biophysical characterization of HomA and HomB. Interestingly, both the proteins are likely to form small β-barrel with a surface-exposed globular domain. These unique topologies also have been reported for special class (Vf) of autotransporter for *H. pylori*. A well-designed experimental study is needed to confirm the fundamental porin or auto-transporter role of HomA and HomB. Crystallization of HomA and HomB will also provide crucial and accurate structural information.

However, we have explored the functional role of HomA and HomB with human B-cells, where we found that these proteins transiently stall the antibody diversity process via downregulation of AID. This finding was probably the cause of low antibody diversity and production in patients with *H. pylori*-associated gastric disease. In addition to that, we have also observed polarization of B-cells to act as B_{reg} cells, which generally plays a negative role by suppressing the immune system by inhibiting T-cell activation. Additionally, we have also explored the potential of HomA and HomB as sub-unit vaccine candidates. We used bioinformatics tools to predict B and T-cell epitopes present in the surface-exposed globular domain of HomA and

HomB. Further, we also used these protein domains for immune simulation to check whether they elicit a human humoral and cellular immune response. Interestingly immune simulation shows a strong immune response. Nevertheless, for making successful subunit vaccine candidates, these *in silico* observations need to be validated by *in-vitro* and *in-vivo* studies.

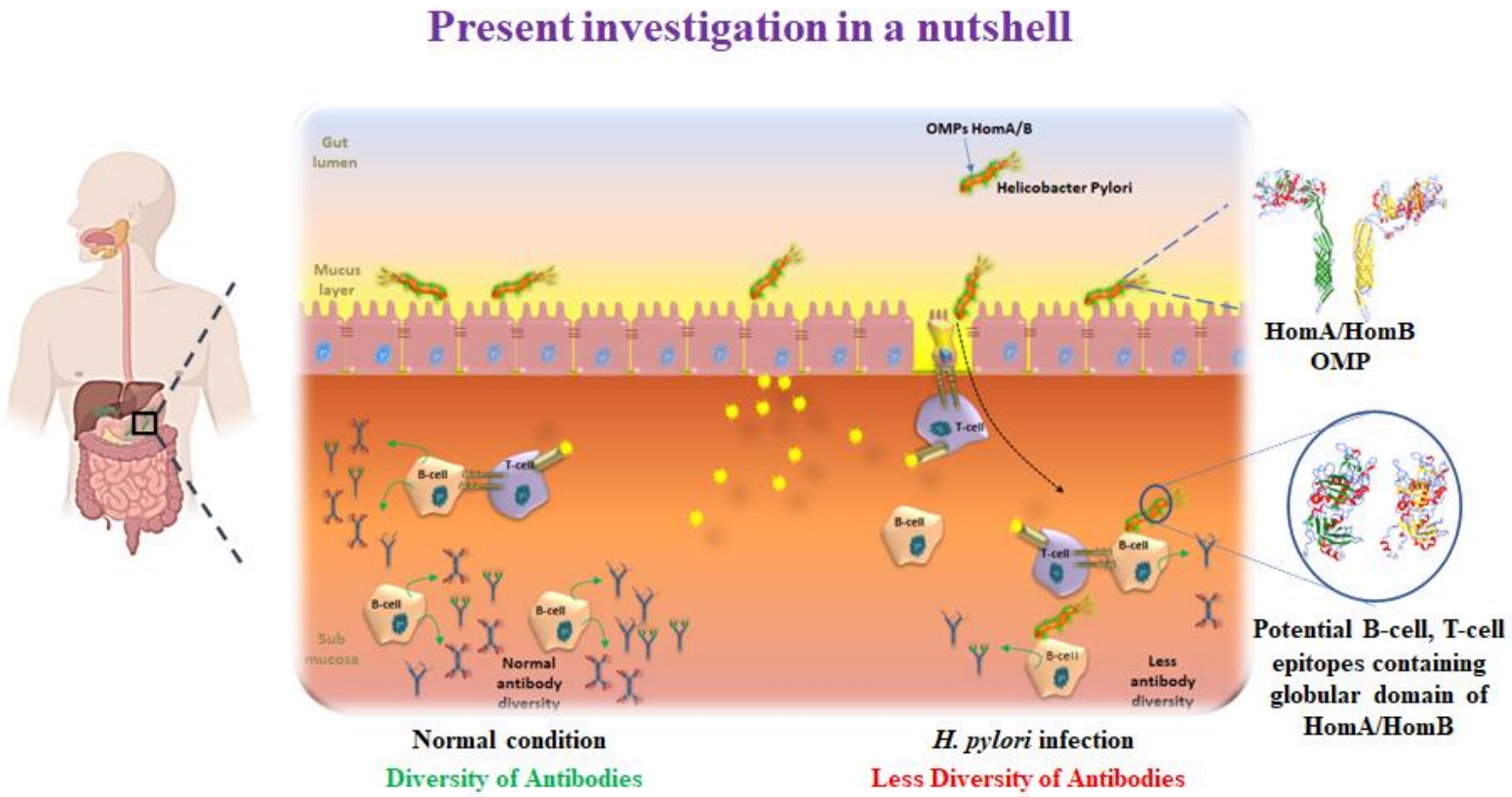

Figure 6.1. Cartoon representation of summary of chapters 3, 4 and 5 work, presented in the thesis.

Appendix-A

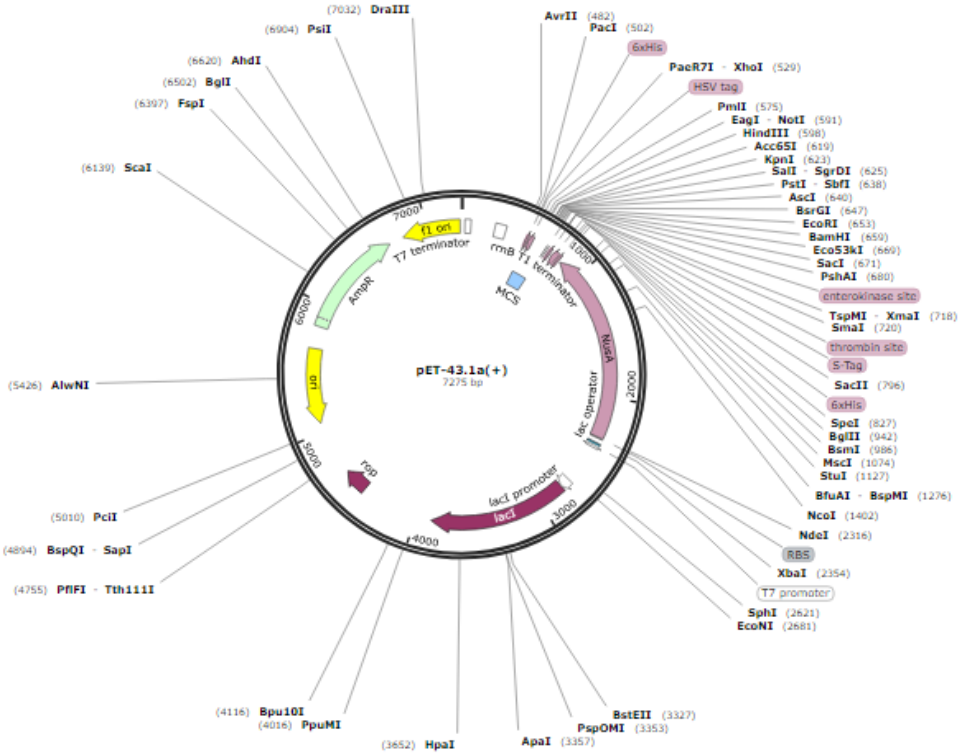

1. **pET43a**

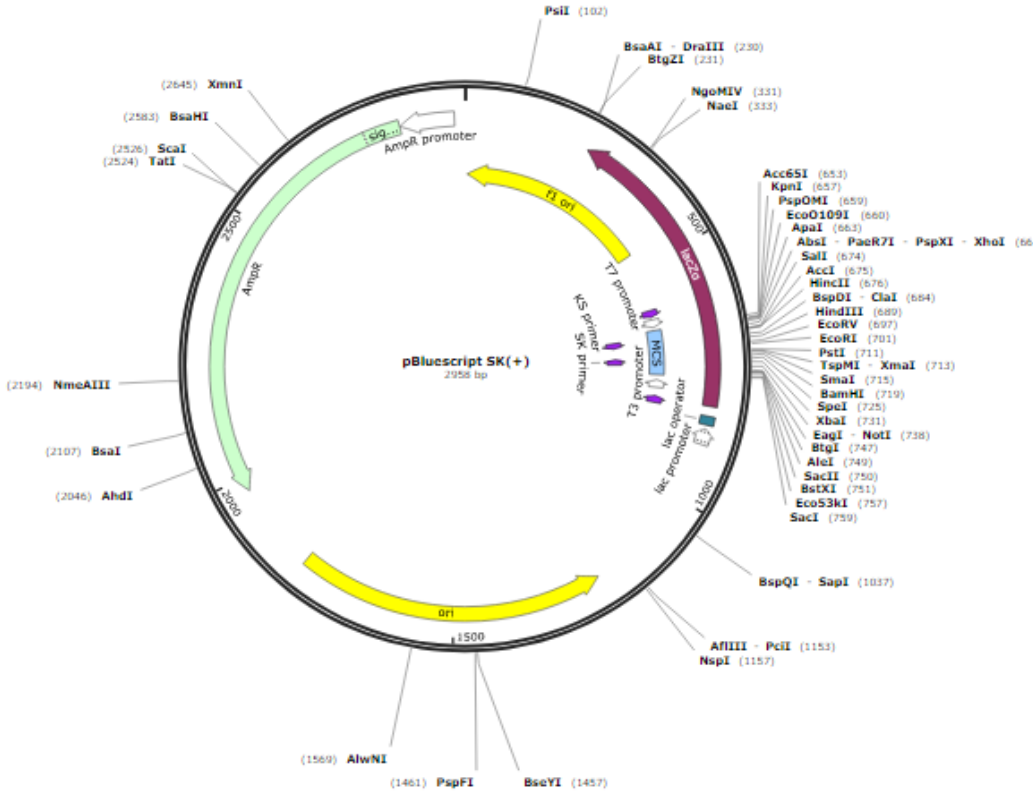

1. **pBluescript (pBSK)**

Appendix-B

Primers used in the study

SN	Primer name	Gene	Primer sequence (5′-3′)
1	PK632	AID Sense	AAATGTCCGCTGGGCTAAG
2	PK633	AID Antisense	GAGGAAGAGCAATTCCACGT
3	PK646	GAPDH Sense	GAGTCAACGGATTTGGTCGT
4	PK647	GAPDH Antisense	GAGGTCAATGAAGGGGTCAT
5	PK728	cMYB Sense	TACAATGCGTCGGAAGGTCG
6	PK729	cMYB Antisense	GCGGAGCCTGAGCAAAACC
7	PK730	E2F1 Sense	GTGTAGGACGGTGAGAGCAC
8	PK731	E2F1 Antisense	TCAAGGGTAGAGGGAGTTGG
9	PK732	NFκB p65 Sense	GACCTGAATGCTGTGCGGC
10	PK733	NFκB p65 Antisense	GAGCGGGTGTGTGACAATGA
11	PK734	PAX5 Sense	GACCTGAATGCTGTGCGGC
12	PK735	PAX5 Antisense	GCACCGGAGACTCCTGAATAC
13	PK738	cMYC Sense	AAAGGCCCCCAAGGTAGTTA
14	PK739	cMYC Antisense	GCACAAGAGTTCCGTAGCTG
15	PK746	STAT6 Sense	AGTGCAGCGGCTCTATGTCGAC
16	PK747	STAT6 Antisense	CACCGAGGCCTGAAGGTGC
17	PK748	SMAD3 Sense	ATGTCAACAGGAATGCAGCAGTGG
18	PK749	SMAD3 Antisense	ATAGCGCTGGTTACAGTTGGGAGA
19	PK781	V_HDJ_H (FR3) sense	GACACGGCTGTGTATTACTGTGCG
20	PK782	Cμ Antisense	CCGAATTCAGACGAGGGGGAAAAGGGTT

21	PK784	Cα Antisense	GGGTGGCGGTTAGCGGGGTCTTGG
22	PK786	PD-L1 sense	GGCATTTGCTGAACGCAT
23	PK787	PD-L1 Antisense	CAATTAGTGCAGCCAGGT
24	PK812	Cγ Antisense	GTGGGCACTCGACACAACATTTGCG
25	PK813	IL10 Sense	5TCTCCGAGATGCCTTCAGCAGA
26	PK814	IL10 Antisense	TCAGACAAGGCTTGGCAACCCA
27	PK815	EBI3 Sense	AGCACATCATCAAGCCCGAC
28	PK816	EBI3 Antisense	GCTCCCTGCGCTTGTAACG
29	PK 821	HoxC4 Sense	CTACCTGACCCGAAGGAGAA
30	PK 822	HoxC4 Antisense	TGACCTCACTTTGGTGTTGG
31	PK 827	V_HDJ_H (FR3) Antisense	CAGTAATACACGGCCGTGTC
32	PK 802	TGFβ Sense	TCGCCAGAGTGGTTATCTT
33	PK 803	TGFβ Antisense	TAGTGAACCCGTTGATGTCC
34	PK 798	BATF Sense	AGCGAAGACCTGGAGAAACA
35	PK 799	BATF Antisense	TTCAGCACCGACGTGAAGTA
36	PK861	Iμ Sense	GTGATTAAGGAGAAACACTTTGAT
37	PK862	Iγ1/2 Sense	GGGCTTCCAAGCCAACAGGGCAGGACA
38	PK863	Iα1/2 Sense	CAGCAGCCCTCTTGGCAGGCAGCCAG
39	PK864	Cμ(CT) Antisense	GTTGCCGTTGGGGTGCTGGAC
40	PK869	cMYB (chip) Sense	GTTCTTCAGAAAATTTTCTTGAGGTCAGACAATG
41	PK870	cMYB (chip) Sense	CTGCTGATTTTACCTTTGCTTTCCATTTTACTTTG
42	PK610F	HomA/B forward	GGC**CATatg**agaaaactattcatcccacttttatta

43	PK652R	HomA/B Reverse	ATGC**CTCGAG**aaacacccacccgtaattg

Appendix-C

Antibodies used in the study

SN	Protein	Antibody details
1	AID	Anti-AID Monoclonal antibody (ZA001) Invitrogen
2	cMYB	c-Myb Polyclonal antibody **(**A304-138A) Bethyl Laboratories, Thermo Fisher
3	GAPDH	anti GAPDH (0411, sc-47724) Santacruz
4	PDL1	CD274 (PDL1, B7-H1) Monoclonal Antibody (14-5983-82), Invitrogen
5	Rabbit IgG (H+L)	Alexa fluor 594, A21207, Invitrogen
6	Mouse IgG (H+L)	Alexa fluor 488, A11001, Invitrogen

Appendix-D

Table 1. Secondary structure analysis using circular dichroism spectra

SNo	Sample	α-Helix %		Anti-parallel β-sheets %			Parallel β-sheets %	Turn %	Other %	NRMSD
		Regular	Distorted	Left twisted	Relaxed	Right twisted				
1	HomA	10.5	0	22.1	0	3.5	13.5	11..5	38.4	0.09
2	HomA CHAPS (4X)	8	0	12.7	0	0	0	52.9	26.4	0.11
3	HomA CHAPS (10X)	11.0	0	17.7	0	0	0	50	21.3	0.14
4	HomA TWEEN 20 (4X)	12.0	0	6.4	0	13.2	38.7	0	29.7	0.11
5	HomA TWEEN 20 (10X)	11.0	0	4.1	0	15.4	39.3	0	30.2	0.10
6	HomA LDAO (4X)	0	0	1.1	0	7.4	33.9	12.5	45.1	0.03
7	HomA LDAO (10X)	0	3.3	0	0	10.7	41.7	1.8	42.6	0.04
8	HomA DMPC (0.250mM)	14.1	0	10.4	0	9.6	38.2	0	27.7	0.10
9	HomA DMPC (0.500mM)	14.7	0	15.1	0	7.4	28.4	4.5	29.9	0.09
10	HomA DMPC (1mM)	16.2	0	14.9	0	7.9	25.2	4.7	31.2	0.10
11	rHomA DOPC (0.250mM)	11.6	0	13.9	0	7.7	32.3	3.2	31.3	0.09
12	rHomA DOPC (0.500mM)	15.8	0	15.5	0	6.7	27.3	4.9	29.8	0.10
13	HomA DOPC (1mM)	16.0	0	22.7	0	3.1	17.3	10.6	30.2	0.10
14	HomB	12.0	8.0	0	1.6	10.0	14.4	14.4	39.9	0.02
15	HomB CHAPS (4X)	0	2.7	11.8	3.3	13.2	3.8	23.2	41.9	0.05
16	HomB CHAPS (10X)	9.1	0	15.9	0	0	0	47.7	27.3	0.12
17	HomB TWEEN 20 (4X)	9.7	7.3	0	5.5	11.3	13.9	13.4	38.9	0.02
18	HomB TWEEN 20 (10X)	9.7	7.3	0	5.5	11.3	13.9	0	38.9	0.02

19	HomB LDAO (4X)	8.2	9.0	0	7.1	14.8	6.2	14.6	40.1	0.02
20	HomB LDAO (10X)	13.8	10.0	0	2.2	11.5	9.3	14.1	39.1	0.02
21	HomB DMPC (0.250mM)	5.5	7.4	0.9	10.8	17.6	4.1	13.7	39.9	0.02
22	HomB DMPC (0.500mM)	15.4	10.6	0	0	9.5	10.3	13.4	40.8	0.02
23	HomB DMPC (1mM)	5.8	6.9	0.8	10.4	17.5	5.2	13.4	40.0	0.02
24	HomB DOPC (0.250mM)	6.8	6.8	0	9.2	15.6	8.5	13.5	39.6	0.02
25	HomB DOPC (0.500mM)	5.1	7.0	1.1	11.1	16.6	6.0	13.7	39.5	0.02
26	HomB DOPC (1mM)	6.0	6.6	0	10.9	16.6	7.5	13.4	39.0	0.02

References

Achouak, W., Heulin, T. and Pagès, J.M., 2001. Multiple facets of bacterial porins. *FEMS microbiology letters*, *199*(1), pp.1-7.

Akama, H., Kanemaki, M., Yoshimura, M., Tsukihara, T., Kashiwagi, T., Yoneyama, H., Narita, S.I., Nakagawa, A. and Nakae, T., 2004. Crystal structure of the drug discharge outer membrane protein, OprM, of Pseudomonas aeruginosa: dual modes of membrane anchoring and occluded cavity end. *Journal of Biological Chemistry*, *279*(51), pp.52816-52819.

Akdis, M., Aab, A., Altunbulakli, C., Azkur, K., Costa, R.A., Crameri, R., Duan, S., Eiwegger, T., Eljaszewicz, A., Ferstl, R. and Frei, R., 2016. Interleukins (from IL-1 to IL-38), interferons, transforming growth factor β, and TNF-α: Receptors, functions, and roles in diseases. *Journal of Allergy and Clinical Immunology*, *138*(4), pp.984-1010.

Akira, S., Uematsu, S. and Takeuchi, O., 2006. Pathogen recognition and innate immunity. *Cell*, *124*(4), pp.783-801.

Allan, E., Dorrell, N., Foynes, S., Anyim, M. and Wren, B.W., 2000. Mutational analysis of genes encoding the early flagellar components of Helicobacter pylori: evidence for transcriptional regulation of flagellin A biosynthesis. *Journal of bacteriology*, *182*(18), pp.5274-5277.

Alm, R.A., Bina, J., Andrews, B.M., Doig, P., Hancock, R.E. and Trust, T.J., 2000. Comparative genomics of Helicobacter pylori: analysis of the outer membrane protein families. *Infection and immunity*, *68*(7), pp.4155-4168.

Alm, R.A., Ling, L.S.L., Moir, D.T., King, B.L., Brown, E.D., Doig, P.C., Smith, D.R., Noonan, B., Guild, B.C., Dejonge, B.L. and Carmel, G., 1999. Genomic-sequence comparison of two unrelated isolates of the human gastric pathogen Helicobacter pylori. *Nature*, *397*(6715), pp.176-180.

Anand, A., Luthra, A., Dunham-Ems, S., Caimano, M.J., Karanian, C., LeDoyt, M., Cruz, A.R., Salazar, J.C. and Radolf, J.D., 2012. TprC/D (Tp0117/131), a trimeric, pore-forming rare outer membrane protein of Treponema pallidum, has a bipartite domain structure. *Journal of bacteriology*, *194*(9), pp.2321-2333.

Armenteros, J.A., Tsirigos, K.D., Sønderby, C.K., Petersen, T.N., Winther, O., Brunak, S., von Heijne, G. and Nielsen, H., 2019. SignalP 5.0 improves signal peptide predictions using deep neural networks. *Nat Biotechnol*, *37*(4), pp.420-423.

Arnold, T., Poynor, M., Nussberger, S., Lupas, A.N. and Linke, D., 2007. Gene duplication of the eight-stranded β-barrel OmpX produces a functional pore: a scenario for the evolution of transmembrane β-barrels. *Journal of molecular biology*, *366*(4), pp.1174-1184.

Avilés-Jiménez, F., Reyes-Leon, A., Nieto-Patlán, E., Hansen, L.M., Burgueño, J., Ramos, I.P., Camorlinga-Ponce, M., Bermúdez, H., Blancas, J.M., Cabrera, L. and Ribas-Aparicio, R.M., 2012. In vivo expression of Helicobacter pylori virulence genes in patients with gastritis, ulcer, and gastric cancer. *Infection and immunity*, *80*(2), pp.594-601.

Bäckhed, F., Rokbi, B., Torstensson, E., Zhao, Y., Nilsson, C., Seguin, D., Normark, S., Buchan, A.M.J. and Richter-Dahlfors, A., 2003. Gastric mucosal recognition of Helicobacter pylori is independent of Toll-like receptor 4. *The Journal of infectious diseases*, *187*(5), pp.829-836.

Balasubramaniam, D., Arockiasamy, A., Kumar, P.D., Sharma, A. and Krishnaswamy, S., 2012. Asymmetric pore occupancy in crystal structure of OmpF porin from Salmonella typhi. *Journal of structural biology*, *178*(3), pp.233-244.

Baldermann, C., Lupas, A., Lubieniecki, J. and Engelhardt, H., 1998. The regulated outer membrane protein Omp21 from

Comamonas acidovorans is identified as a member of a new family of eight-stranded β-sheet proteins by its sequence and properties. *Journal of bacteriology*, *180*(15), pp.3741-3749.

Balkwill, F. and Mantovani, A., 2001. Inflammation and cancer: back to Virchow?. *The lancet*, *357*(9255), pp.539-545.

Banerjee, P., Biswas, A. and Biswas, T., 2008. Porin-incorporated liposome induces Toll-like receptors 2-and 6-dependent maturation and type 1 response of dendritic cell. *International immunology*, *20*(12), pp.1551-1563.

Baslé, A., Rummel, G., Storici, P., Rosenbusch, J.P. and Schirmer, T., 2006. Crystal structure of osmoporin OmpC from E. coli at 2.0 Å. *Journal of molecular biology*, *362*(5), pp.933-942.

Baumann, U., Mansouri, E. and Von Specht, B.U., 2004. Recombinant OprF–OprI as a vaccine against Pseudomonas aeruginosa infections. *Vaccine*, *22*(7), pp.840-847.

Berstad, A.E., Høgåsen, K., Bukholm, G., Moran, A.P. and Brandtzaeg, P., 2001. Complement activation directly induced by Helicobacter pylori. *Gastroenterology*, *120*(5), pp.1108-1116.

Bhattacharya, M., Malick, R.C., Mondal, N., Patra, P., Pal, B.B., Patra, B.C. and Das, B.K., 2019. Computational characterization of epitopic region within the outer membrane protein candidate in Flavobacterium columnare for vaccine development. *Journal of Biomolecular Structure and Dynamics*.

Bhattacharya, M., Sharma, A.R., Mallick, B., Sharma, G., Lee, S.S. and Chakraborty, C., 2020. Immunoinformatics approach to understand molecular interaction between multi-epitopic regions of SARS-CoV-2 spike-protein with TLR4/MD-2 complex. *Infection, Genetics and Evolution*, *85*, p.104587.

Bhattacharya, M., Sharma, A.R., Sharma, G., Patra, P., Mondal, N., Patra, B.C., Lee, S.S. and Chakraborty, C., 2020. Computer

aided novel antigenic epitopes selection from the outer membrane protein sequences of Aeromonas hydrophila and its analyses. *Infection, Genetics and Evolution*, *82*, p.104320.

Bina, J., Bains, M. and Hancock, R.E., 2000. Functional expression in Escherichia coli and membrane topology of porin HopE, a member of a large family of conserved proteins in Helicobacter pylori. *Journal of bacteriology*, *182*(9), pp.2370-2375.

Birkholz, S., Schneider, T., Knipp, U., Stallmach, A. and Zeitz, M., 1998. Decreased Helicobacter pylori-specific gastric secretory IgA antibodies in infected patients. *Digestion*, *59*(6), pp.638-645.

Bishop, C.M., Walkenhorst, W.F. and Wimley, W.C., 2001. Folding of β-sheets in membranes: specificity and promiscuity in peptide model systems. *Journal of molecular biology*, *309*(4), pp.975-988.

Blaser, M.J., 1998. Helicobacter pylori and gastric diseases. *Bmj*, *316*(7143), pp.1507-1510.

Boncristiano, M., Paccani, S.R., Barone, S., Ulivieri, C., Patrussi, L., Ilver, D., Amedei, A., D'Elios, M.M., Telford, J.L. and Baldari, C.T., 2003. The Helicobacter pylori vacuolating toxin inhibits T cell activation by two independent mechanisms. *The Journal of experimental medicine*, *198*(12), pp.1887-1897.

Boquet, P. and Ricci, V., 2012. Intoxication strategy of Helicobacter pylori VacA toxin. *Trends in microbiology*, *20*(4), pp.165-174.

Braun, G. and Cole, S.T., 1984. DNA sequence analysis of the Serratia marcescens ompA gene: implications for the organisation of an enterobacterial outer membrane protein. *Molecular and General Genetics MGG*, *195*(1), pp.321-328.

Brok, R.G., Brinkman, E., Van Boxtel, R., Bekkers, A.C., Verheij, H.M. and Tommassen, J., 1994. Molecular characterization of enterobacterial pldA genes encoding outer membrane phospholipase A. *Journal of bacteriology*, *176*(3), pp.861-870.

Brok, R.G.P.M., Boots, A.P., Dekker, N., Verheij, H.M. and Tommassen, J., 1998. Sequence comparison of outer membrane phospholipases A: implications for structure and for the catalytic mechanism. *Research in microbiology*, *149*(10), pp.703-710.

Buendía, A.J., Del Río, L., Ortega, N., Sánchez, J., Gallego, M.C., Caro, M.R., Navarro, J.A., Cuello, F. and Salinas, J., 2002. B-cell-deficient mice show an exacerbated inflammatory response in a model of Chlamydophila abortus infection. *Infection and immunity*, *70*(12), pp.6911-6918.

Buti, L., Spooner, E., Van der Veen, A.G., Rappuoli, R., Covacci, A. and Ploegh, H.L., 2011. Helicobacter pylori cytotoxin-associated gene A (CagA) subverts the apoptosis-stimulating protein of p53 (ASPP2) tumor suppressor pathway of the host. *Proceedings of the National Academy of Sciences*, *108*(22), pp.9238-9243.

Butz, H., Rácz, K., Hunyady, L. and Patócs, A., 2012. Crosstalk between TGF-β signaling and the microRNA machinery. *Trends in pharmacological sciences*, *33*(7), pp.382-393.

C. Liu, T. Hashizume, T. K. Ochiai, K. Fujihashi and M. Yamamoto. Oral immunization with *Porphyromonas gingivalis* outer membrane protein and CpG oligodeoxynucleotides elicits T helper 1 and 2 cytokines for enhanced protective immunity. *Mol. Oral. Microbiol.*, 2010, 25, 178-189.

Caeser, R., Di Re, M., Krupka, J.A., Gao, J., Lara-Chica, M., Dias, J.M., Cooke, S.L., Fenner, R., Usheva, Z., Runge, H.F. and

Beer, P.A., 2019. Genetic modification of primary human B cells to model high-grade lymphoma. *Nature communications*, *10*(1), pp.1-16.

Cai, Y., Kurita-Ochiai, T., Kobayashi, R., Hashizume, T. and Yamamoto, M., 2013. Nasal immunization with the 40-kDa outer membrane protein of Porphyromonas gingivalis plus cholera toxin induces protective immunity in aged mice. *Journal of Oral Science*, *55*(2), pp.107-114.

Cerqueira, C., Manfroi, B. and Fillatreau, S., 2019, August. IL-10-producing regulatory B cells and plasmocytes: molecular mechanisms and disease relevance. In *Seminars in Immunology* (Vol. 44, p. 101323). Academic Press.

Chatterjee, A., Chatterjee, S. and Bandyopadhyay, S.K., 2012. H. pylori-induced gastric ulcer: pathophysiology and herbal remedy. *Int J Biol Med Res*, *3*(1), pp.1461-1465.

Chen, X., Xu, Z., Li, L., Chen, H. and Zhou, R., 2012. Identification of conserved surface proteins as novel antigenic vaccine candidates of Actinobacillus pleuropneumoniae. *Journal of microbiology*, *50*(6), pp.978-986.

Cheng, H.H., Tseng, G.Y., Yang, H.B., Wang, H.J., Lin, H.J. and Wang, W.C., 2012. Increased numbers of Foxp3-positive regulatory T cells in gastritis, peptic ulcer and gastric adenocarcinoma. *World journal of gastroenterology: WJG*, *18*(1), p.34.

Cherezov, V., Yamashita, E., Liu, W., Zhalnina, M., Cramer, W.A. and Caffrey, M., 2006. In meso structure of the cobalamin transporter, BtuB, at 1.95 Å resolution. *Journal of molecular biology*, *364*(4), pp.716-734.

Chiba, T., Seno, H., Marusawa, H., Wakatsuki, Y. and Okazaki, K., 2006. Host factors are important in determining

clinical outcomes of Helicobacter pylori infection. *Journal of gastroenterology*, *41*(1), pp.1-9.

Chiu, Y.M., Tsai, C.L., Kao, J.T., Hsieh, C.T., Shieh, D.C., Lee, Y.J., Tsay, G.J., Cheng, K.S. and Wu, Y.Y., 2018. PD-1 and PD-L1 up-regulation promotes T-cell apoptosis in gastric adenocarcinoma. *Anticancer research*, *38*(4), pp.2069-2078.

Coppens, F., Castaldo, G., Debraekeleer, A., Subedi, S., Moonens, K., Lo, A. and Remaut, H., 2018. Hop-family *Helicobacter* outer membrane adhesins form a novel class of Type 5-like secretion proteins with an interrupted β-barrel domain. *Molecular Microbiology*, *110*(1), pp.33-46.

Cover, T.L. and Blaser, M.J., 2009. *Helicobacter pylori* in health and disease. *Gastroenterology*, *136*(6), pp.1863-1873.

Cover, T.L., 1996. The vacuolating cytotoxin of Helicobacter pylori. *Molecular microbiology*, *20*(2), pp.241-246.

Cowan, S.W., Schirmer, T., Rummel, G., Steiert, M., Ghosh, R., Pauptit, R.A., Jansonius, J.N. and Rosenbusch, J.P., 1992. Crystal structures explain functional properties of two E. coli porins. *Nature*, *358*(6389), pp.727-733.

Crabtree, J.E., Wyatt, J.I., Sobala, G.M., Miller, G., Tompkins, D.S., Primrose, J.N. and Morgan, A.G., 1993. Systemic and mucosal humoral responses to *Helicobacter pylori* in gastric cancer. *Gut*, *34*(10), pp.1339-1343.

Dang, V. D., Hilgenberg, E., Ries, S., Shen, P. and Fillatreau, S., 2014. From the regulatory functions of B cells to the identification of cytokine-producing plasma cell subsets. *Current opinion in immunology*, *28*, pp.77-83.

Das, A., Ellis, G., Pallant, C., Lopes, A.R., Khanna, P., Peppa, D., Chen, A., Blair, P., Dusheiko, G., Gill, U. and Kennedy, P.T., 2012. IL-10–producing regulatory B cells in the pathogenesis of

chronic hepatitis B virus infection. *The Journal of Immunology*, *189*(8), pp.3925-3935.

Davis, R.J., 2000. Signal transduction by the JNK group of MAP kinases. *Inflammatory Processes:*, pp.13-21.

De Mot, R. and Vanderleyden, J., 1994. The C-terminal sequence conservation between OmpA-related outer membrane proteins and MotB suggests a common function in both gram-positive and gram-negative bacteria, possibly in the interaction of these domains with peptidoglycan. *Molecular microbiology*, *12*(2), pp.333-336.

Dekker, N., 2000. Outer-membrane phospholipase A: known structure, unknown biological function: MicroReview. *Molecular microbiology*, *35*(4), pp.711-717.

Dekker, N., Tommassen, J., Lustig, A., Rosenbusch, J.P. and Verheij, H.M., 1997. Dimerization regulates the enzymatic activity of Escherichia coli outer membrane phospholipase A. *Journal of Biological Chemistry*, *272*(6), pp.3179-3184.

D'Elios, M.M., Manghetti, M., De Carli, M., Costa, F., Baldari, C.T., Burroni, D., Telford, J.L., Romagnani, S. and Del Prete, G., 1997. T helper 1 effector cells specific for Helicobacter pylori in the gastric antrum of patients with peptic ulcer disease. *The Journal of Immunology*, *158*(2), pp.962-967.

Dhal, A.K., Pani, A., Mahapatra, R.K. and Yun, S.I., 2019. An immunoinformatics approach for design and validation of multi-subunit vaccine against Cryptosporidium parvum. *Immunobiology*, *224*(6), pp.747-757.

Di Donato, A., Draetta, G.F., Illiano, G., Tufano, M.A., Sommese, L. and Galdiero, F., 1986. Do porins inhibit the macrophage phagocyting activity by stimulating the adenylate

cyclase?. *Journal of cyclic nucleotide and protein phosphorylation research*, *11*(2), pp.87-97.

Doig, P., Exner, M.M., Hancock, R.E. and Trust, T.J., 1995. Isolation and characterization of a conserved porin protein from Helicobacter pylori. *Journal of Bacteriology*, *177*(19), pp.5447-5452.

Doyle, M.T. and Bernstein, H.D., 2019. Bacterial outer membrane proteins assemble via asymmetric interactions with the BamA β-barrel. *Nature communications*, *10*(1), pp.1-13.

Duan, Z., Zheng, H., Liu, H., Li, M., Tang, M., Weng, X., Yi, W., Bode, A.M. and Cao, Y., 2016. AID expression increased by TNF-α is associated with class switch recombination of Igα gene in cancers. *Cellular & molecular immunology*, *13*(4), pp.484-491.

Ducken, D.R., Brown, W.C., Alperin, D.C., Brayton, K.A., Reif, K.E., Turse, J.E., Palmer, G.H. and Noh, S.M., 2015. Subdominant outer membrane antigens in Anaplasma marginale: conservation, antigenicity, and protective capacity using recombinant protein. *PloS one*, *10*(6), p.e0129309.

Dussault, N., Ducas, E., Racine, C., Jacques, A., Paré, I., Côté, S. and Néron, S., 2008. Immunomodulation of human B cells following treatment with intravenous immunoglobulins involves increased phosphorylation of extracellular signal-regulated kinases 1 and 2. *International immunology*, *20*(11), pp.1369-1379.

Dutzler, R., Rummel, G., Albertí, S., Hernández-Allés, S., Phale, P.S., Rosenbusch, J.P., Benedi, V.J. and Schirmer, T., 1999. Crystal structure and functional characterization of OmpK36, the osmoporin of Klebsiella pneumoniae. *Structure*, *7*(4), pp.425-434.

Ernst, P.B. and Gold, B.D., 2000. The disease spectrum of Helicobacter pylori: the immunopathogenesis of gastroduodenal

ulcer and gastric cancer. *Annual Reviews in Microbiology*, *54*(1), pp.615-640.

Evans, D.J., Frank, D.W., Finck-Barbançon, V., Wu, C. and Fleiszig, S.M., 1998. Pseudomonas aeruginosa invasion and cytotoxicity are independent events, both of which involve protein tyrosine kinase activity. *Infection and immunity*, *66*(4), pp.1453-1459.

Exner, M.M., Doig, P., Trust, T.J. and Hancock, R.E., 1995. Isolation and characterization of a family of porin proteins from Helicobacter pylori. *Infection and Immunity*, *63*(4), pp.1567-1572.

Faller, M., Niederweis, M. and Schulz, G.E., 2004. The structure of a mycobacterial outer-membrane channel. *Science*, *303*(5661), pp.1189-1192.

Fillatreau, S., Sweenie, C.H., McGeachy, M.J., Gray, D. and Anderton, S.M., 2002. B cells regulate autoimmunity by provision of IL-10. *Nature immunology*, *3*(10), pp.944-950.

Finamore, E., Vitiello, M., D'Isanto, M., Galdiero, E., Falanga, A., Kampanaraki, A., Raieta, K. and Galdiero, M., 2009. Evidence for IL-6 promoter nuclear activation in U937 cells stimulated with Salmonella enterica serovar Typhimurium porins. *European Cytokine Network*, *20*(3), pp.140-147.

Forman, D., De Backer, G., Elder, J., Moller, H., Damotta, L.C., Roy, P., Abid, L., Tjonneland, A., Boeing, H., Haubrich, T. and Wahrendorf, J., 1993. Epidemiology of, and risk-factors for, *Helicobacter-pylori* infection among 3194 asymptomatic subjects in 17 populations. *Gut*, *34*(12), pp.1672-1676.

Freeman, B.E., Hammarlund, E., Raué, H.P. and Slifka, M.K., 2012. Regulation of innate CD8+ T-cell activation mediated by cytokines. *Proceedings of the National Academy of Sciences*, *109*(25), pp.9971-9976.

G.L. Hold, K.S. Lee, A. Kalantzis, C.B. Jackson, L. O'Connor, N. Murata-Kamiya, M. Hatakeyama, L.M. Judd, A.S. Giraud, T.R. Menheniott, *Helicobacter pylori* CagA triggers expression of the bactericidal lectin REG3c via gastric STAT3 activation, PLoS One 7 (2012) e30786.

G.T. Van Nhieu Jiménez-Soto, L.F., Kutter, S., Sewald, X., Ertl, C., Weiss, E., Kapp, U., Rohde, M., Pirch, T., Jung, K., Retta, S.F. and Terradot, L., 2009. Helicobacter pylori type IV secretion apparatus exploits β1 integrin in a novel RGD-independent manner. *PLoS pathogens*, *5*(12), p.e1000684.

Galdiero, F., Tufano, M.A., Sommese, L., Folgore, A. and Tedesco, F., 1984. Activation of complement system by porins extracted from Salmonella typhimurium. *Infection and Immunity*, *46*(2), pp.559-563.

Galdiero, M., Galdiero, M., Finamore, E., Rossano, F., Gambuzza, M., Catania, M.R., Teti, G., Midiri, A. and Mancuso, G., 2004. Haemophilus influenzae porin induces Toll-like receptor 2-mediated cytokine production in human monocytes and mouse macrophages. *Infection and immunity*, *72*(2), pp.1204-1209.

Galdiero, M., Vitiello, M. and Galdiero, S., 2003. Eukaryotic cell signaling and transcriptional activation induced by bacterial porins. *FEMS microbiology letters*, *226*(1), pp.57-64.

Galdiero, M., Vitiello, M., Sanzari, E., D'Isanto, M., Tortora, A., Longanella, A. and Galdiero, S., 2002. Porins from Salmonella enterica serovar Typhimurium activate the transcription factors activating protein 1 and NF-κB through the Raf-1-mitogen-activated protein kinase cascade. *Infection and immunity*, *70*(2), pp.558-568.

Galdiero, S. and Gouaux, E., 2004. High resolution crystallographic studies of α-hemolysin–phospholipid complexes define heptamer–lipid head group interactions: Implication for

understanding protein–lipid interactions. *Protein Science*, *13*(6), pp.1503-1511.

Galdiero, S., Capasso, D., Vitiello, M., D'Isanto, M., Pedone, C. and Galdiero, M., 2003. Role of surface-exposed loops of Haemophilus influenzae protein P2 in the mitogen-activated protein kinase cascade. *Infection and immunity*, *71*(5), pp.2798-2809.

Galdiero, S., Falanga, A., Cantisani, M., Tarallo, R., Elena Della Pepa, M., D'Oriano, V. and Galdiero, M., 2012. Microbe-host interactions: structure and role of Gram-negative bacterial porins. *Current Protein and Peptide Science*, *13*(8), pp.843-854.

Galdiero, S., Vitiello, M., Amodeo, P., D'Isanto, M., Cantisani, M., Pedone, C. and Galdiero, M., 2006. Structural requirements for proinflammatory activity of porin P2 Loop 7 from Haemophilus influenzae. *Biochemistry*, *45*(14), pp.4491-4501.

Gebert, B., Fischer, W., Weiss, E., Hoffmann, R. and Haas, R., 2003. Helicobacter pylori vacuolating cytotoxin inhibits T lymphocyte activation. *Science*, *301*(5636), pp.1099-1102.

Ghosh, S., Chakraborty, K., Nagaraja, T., Basak, S., Koley, H., Dutta, S., Mitra, U. and Das, S., 2011. An adhesion protein of Salmonella enterica serovar Typhi is required for pathogenesis and potential target for vaccine development. *Proceedings of the National Academy of Sciences*, *108*(8), pp.3348-3353.

Giacomini, E., Rizzo, F., Etna, M.P., Cruciani, M., Mechelli, R., Buscarinu, M.C., Pica, F., D'Agostini, C., Salvetti, M., Coccia, E.M. and Severa, M., 2018. Thymosin-α1 expands deficient IL-10-producing regulatory B cell subsets in relapsing–remitting multiple sclerosis patients. *Multiple Sclerosis Journal*, *24*(2), pp.127-139.

Givskov, M., Olsen, L. and Molin, S., 1988. Cloning and expression in Escherichia coli of the gene for extracellular phospholipase A1 from Serratia liquefaciens. *Journal of bacteriology*, *170*(12), pp.5855-5862.

Gobert, A.P., McGee, D.J., Akhtar, M., Mendz, G.L., Newton, J.C., Cheng, Y., Mobley, H.L. and Wilson, K.T., 2001. Helicobacter pylori arginase inhibits nitric oxide production by eukaryotic cells: a strategy for bacterial survival. *Proceedings of the National Academy of Sciences*, *98*(24), pp.13844-13849.

Goenka, R., Parent, M.A., Elzer, P.H. and Baldwin, C.L., 2011. B cell–deficient mice display markedly enhanced resistance to the intracellular bacterium Brucella abortus. *Journal of Infectious Diseases*, *203*(8), pp.1136-1146.

Gupta, S., Kumar, D., Vohra, H. and Kumar, N., 1999. Involvement of signal transduction pathways in Salmonella typhimurium porin activated gut macrophages. *Molecular and cellular biochemistry*, *194*(1), pp.235-243.

Gururajan, M., Jennings, C.D. and Bondada, S., 2006. Cutting edge: constitutive B cell receptor signaling is critical for basal growth of B lymphoma. *The Journal of Immunology*, *176*(10), pp.5715-5719.

Haddadi, M.H., Negahdari, B., Asadolahi, R. and Bazargani, A., 2020. Helicobacter pylori antibiotic resistance and correlation with cagA motifs and homB gene. *Postgraduate medicine*, *132*(6), pp.512-520.

Hajizadeh, N.R., Franke, D., Jeffries, C.M. and Svergun, D.I., 2018. Consensus Bayesian a ssessment of protein molecular mass from solution X-ray scattering data. *Scientific reports*, *8*(1), pp.1-13.

Heffernan, E.J., Wu, L., Louie, J., Okamoto, S., Fierer, J. and Guiney, D.G., 1994. Specificity of the complement resistance and cell association phenotypes encoded by the outer membrane protein genes rck from Salmonella typhimurium and ail from Yersinia enterocolitica. *Infection and immunity*, *62*(11), pp.5183-5186.

Hentschel E, Brandstatter G, Dragoisics B, Hirschl AM, Nemec H, Schütze K, *et al.* Effect of ranitidine and amoxicillin plus metronidazole on the eradication of Helicobacter pylori and the recurrence of duodenal ulcer. *N Engl J Med* 1993;328:308-12

Heuck, A.P. and Johnson, A.E., 2002. Pore-forming protein structure analysis in membranes using multiple independent fluorescence techniques. *Cell biochemistry and biophysics*, *36*(1), pp.89-101.

Hubbard, S.R. and Miller, W.T., 2007. Receptor tyrosine kinases: mechanisms of activation and signaling. *Current opinion in cell biology*, *19*(2), pp.117-123.

Hughes, E.E., Gilleland, L.B. and Gilleland Jr, H.E., 1992. Synthetic peptides representing epitopes of outer membrane protein F of Pseudomonas aeruginosa that elicit antibodies reactive with whole cells of heterologous immunotype strains of P. aeruginosa. *Infection and immunity*, *60*(9), pp.3497-3503.

Hussein, N.R., 2011. A study of Helicobacter pylori outer-membrane proteins (hom) A and B in Iraq and Turkey. *Journal of Infection and Public Health*, *4*(3), pp.135-139.

Hwang, P.M., Choy, W.Y., Lo, E.I., Chen, L., Forman-Kay, J.D., Raetz, C.R., Privé, G.G., Bishop, R.E. and Kay, L.E., 2002. Solution structure and dynamics of the outer membrane enzyme PagP by NMR. *Proceedings of the National Academy of Sciences*, *99*(21), pp.13560-13565.

Ihan, A., Pinchuk, I.V. and Beswick, E.J., 2012. Inflammation, Immunity, and Vaccines for H elicobacter pylori Infection. *Helicobacter*, *17*, pp.16-21.

Ilver, D., Arnqvist, A., Ogren, J., Frick, I.M., Kersulyte, D., Incecik, E.T., Berg, D.E., Covacci, A., Engstrand, L. and Borén, T., 1998. Helicobacter pylori adhesin binding fucosylated histo-blood

group antigens revealed by retagging. *Science*, *279*(5349), pp.373-377.

Ise, W., Kohyama, M., Schraml, B.U., Zhang, T., Schwer, B., Basu, U., Alt, F.W., Tang, J., Oltz, E.M., Murphy, T.L. and Murphy, K.M., 2011. The transcription factor BATF controls the global regulators of class-switch recombination in both B cells and T cells. *Nature immunology*, *12*(6), pp.536-543.

J. T. Poolman, J. Bacterial outer membrane protein vaccines. In Novel Strategies in Design and Production of Vaccines, S. Cohen, and A. Shafferman, eds. Plenum, New York, 1996, 73–77.

Jain, P., Luo, Z.Q. and Blanke, S.R., 2011. Helicobacter pylori vacuolating cytotoxin A (VacA) engages the mitochondrial fission machinery to induce host cell death. *Proceedings of the National Academy of Sciences*, *108*(38), pp.16032-16037.

Janssen, M., Dijkmans, B.A., Vandenbroucke, J.P., Van Duijn, W., Pena, A.S. and Lamers, C.B., 1992. Decreased level of antibodies against Helicobacter pylori in patients with rheumatoid arthritis receiving intramuscular gold. *Annals of the rheumatic diseases*, *51*(9), pp.1036-1038.

Jeannin, P., Bottazzi, B., Sironi, M., Doni, A., Rusnati, M., Presta, M., Maina, V., Magistrelli, G., Haeuw, J.F., Hoeffel, G. and Thieblemont, N., 2005. Complexity and complementarity of outer membrane protein A recognition by cellular and humoral innate immunity receptors. *Immunity*, *22*(5), pp.551-560.

Jeannin, P., Renno, T., Goetsch, L., Miconnet, I., Aubry, J.P., Delneste, Y., Herbault, N., Baussant, T., Magistrelli, G., Soulas, C. and Romero, P., 2000. OmpA targets dendritic cells, induces their maturation and delivers antigen into the MHC class I presentation pathway. *Nature immunology*, *1*(6), pp.502-509.

Jeanteur, D., Lakey, J.H. and Pattus, F., 1991. The bacterial porin superfamily: sequence alignment and structure prediction. *Molecular microbiology*, *5*(9), pp.2153-2164.

Josenhans, C., Labigne, A. and Suerbaum, S., 1995. Comparative ultrastructural and functional studies of Helicobacter pylori and Helicobacter mustelae flagellin mutants: both flagellin subunits, FlaA and FlaB, are necessary for full motility in Helicobacter species. *Journal of bacteriology*, *177*(11), pp.3010-3020.

Jumper, J., Evans, R., Pritzel, A., Green, T., Figurnov, M., Ronneberger, O., Tunyasuvunakool, K., Bates, R., Žídek, A., Potapenko, A. and Bridgland, A., 2021. Highly accurate protein structure prediction with AlphaFold. *Nature*, *596*(7873), pp.583-589.

Jung, S.W., Sugimoto, M., Graham, D.Y. and Yamaoka, Y., 2009. homB status of Helicobacter pylori as a novel marker to distinguish gastric cancer from duodenal ulcer. *Journal of clinical microbiology*, *47*(10), pp.3241-3245.

Kalampokis, I., Venturi, G.M., Poe, J.C., Dvergsten, J.A., Sleasman, J.W. and Tedder, T.F., 2017. The regulatory B cell compartment expands transiently during childhood and is contracted in children with autoimmunity. *Arthritis & Rheumatology*, *69*(1), pp.225-238.

Kang, J., Jones, K.R., Jang, S., Olsen, C.H., Yoo, Y.J., Merrell, D.S. and Cha, J.H., 2012. The geographic origin of Helicobacter pylori influences the association of the homB gene with gastric cancer. *Journal of clinical microbiology*, *50*(3), pp.1082-1085.

Kao, J.Y., Zhang, M., Miller, M.J., Mills, J.C., Wang, B., Liu, M., Eaton, K.A., Zou, W., Berndt, B.E., Cole, T.S. and Takeuchi, T., 2010. Helicobacter pylori immune escape is mediated by

dendritic cell–induced Treg skewing and Th17 suppression in mice. *Gastroenterology*, *138*(3), pp.1046-1054.

Kaplan-Türköz, B., Jiménez-Soto, L.F., Dian, C., Ertl, C., Remaut, H., Louche, A., Tosi, T., Haas, R. and Terradot, L., 2012. Structural insights into Helicobacter pylori oncoprotein CagA interaction with β1 integrin. *Proceedings of the National Academy of Sciences*, *109*(36), pp.14640-14645.

Karin, M., Liu, Z.G. and Zandi, E., 1997. AP-1 function and regulation. *Current opinion in cell biology*, *9*(2), pp.240-246.

Katz, S.I., Parker, D. and Turk, J.L., 1974. B-cell suppression of delayed hypersensitivity reactions. *Nature*, *251*(5475), pp.550-551.

Khoder, A., Sarvaria, A., Alsuliman, A., Chew, C., Sekine, T., Cooper, N., Mielke, S., De Lavallade, H., Muftuoglu, M., Fernandez Curbelo, I. and Liu, E., 2014. Regulatory B cells are enriched within the IgM memory and transitional subsets in healthy donors but are deficient in chronic GVHD. *Blood, The Journal of the American Society of Hematology*, *124*(13), pp.2034-2045.

Killmann, H., Herrmann, C., Wolff, H. and Braun, V., 1998. Identification of a new site for ferrichrome transport by comparison of the FhuA proteins of Escherichia coli, Salmonella paratyphi B, Salmonella typhimurium, and Pantoea agglomerans. *Journal of bacteriology*, *180*(15), pp.3845-3852.

Kim, H.S., Lee, M.B., Lee, D., Min, K.Y., Koo, J., Kim, H.W., Park, Y.H., Kim, S.J., Ikutani, M., Takaki, S. and Kim, Y.M., 2019. The regulatory B cell–mediated peripheral tolerance maintained by mast cell IL-5 suppresses oxazolone-induced contact hypersensitivity. *Science advances*, *5*(7), p.eaav8152.

Klausen, M.S., Jespersen, M.C., Nielsen, H., Jensen, K.K., Jurtz, V.I., Soenderby, C.K., Sommer, M.O.A., Winther, O.,

Nielsen, M., Petersen, B. and Marcatili, P., 2019. NetSurfP-2.0: Improved prediction of protein structural features by integrated deep learning. *Proteins: Structure, Function, and Bioinformatics*, *87*(6), pp.520-527.

Koebnik, R. and Krämer, L., 1995. Membrane Assembly of Circularly Permuted Variants of theE. coliOuter Membrane Protein OmpA. *Journal of molecular biology*, *250*(5), pp.617-626.

Koebnik, R., Locher, K.P. and Van Gelder, P., 2000. Structure and function of bacterial outer membrane proteins: barrels in a nutshell. *Molecular microbiology*, *37*(2), pp.239-253.

Kohlhaas, S., Garden, O.A., Scudamore, C., Turner, M., Okkenhaug, K. and Vigorito, E., 2009. Cutting edge: the Foxp3 target miR-155 contributes to the development of regulatory T cells. *The Journal of Immunology*, *182*(5), pp.2578-2582.

Korniotis, S., Gras, C., Letscher, H., Montandon, R., Mégret, J., Siegert, S., Ezine, S., Fallon, P.G., Luther, S.A., Fillatreau, S. and Zavala, F., 2016. Treatment of ongoing autoimmune encephalomyelitis with activated B-cell progenitors maturing into regulatory B cells. *Nature communications*, *7*(1), pp.1-13.

Koronakis, V., Eswaran, J. and Hughes, C., 2004. Structure and function of TolC: the bacterial exit duct for proteins and drugs. *Annual review of biochemistry*, *73*(1), pp.467-489.

Kusters, J.G., Van Vliet, A.H. and Kuipers, E.J., 2006. Pathogenesis of Helicobacter pylori infection. *Clinical microbiology reviews*, *19*(3), pp.449-490.

Lagunes-Servin, H., Torres, J., Maldonado-Bernal, C., Pérez-Rodríguez, M., Huerta-Yépez, S., Madrazo de la Garza, A., Muñoz-Pérez, L., Flores-Luna, L., Ramón-García, G. and Camorlinga-Ponce, M., 2013. Toll-Like Receptors and Cytokines

are Upregulated during H elicobacter pylori Infection in Children. *Helicobacter*, *18*(6), pp.423-432.

Lamb, A. and Chen, L.F., 2013. Role of the Helicobacter pylori-induced inflammatory response in the development of gastric cancer. *Journal of cellular biochemistry*, *114*(3), pp.491-497.

Lamb, A., Yang, X.D., Tsang, Y.H.N., Li, J.D., Higashi, H., Hatakeyama, M., Peek, R.M., Blanke, S.R. and Chen, L.F., 2009. Helicobacter pylori CagA activates NF-κB by targeting TAK1 for TRAF6-mediated Lys 63 ubiquitination. *EMBO reports*, *10*(11), pp.1242-1249.

Lazaron, V. and Barke, R.A., 1999. Gram-negative bacterial sepsis and the sepsis syndrome. *Urologic Clinics of North America*, *26*(4), pp.687-699.

LeBien, T.W. and Tedder, T.F., 2008. B lymphocytes: how they develop and function. *Blood, The Journal of the American Society of Hematology*, *112*(5), pp.1570-1580.

Li, G., Wulan, H., Song, Z., Paik, P.A., Tsao, M.L., Goodman, G.M., MacEachern, P.T., Downey, R.S., Jankowska, A.J., Rabinowitz, Y.M. and Learch, T.B., 2015. Regulatory B cell function is suppressed by smoking and obesity in H. pylori-infected subjects and is correlated with elevated risk of gastric cancer. *PLoS One*, *10*(7), p.e0134591.

Li, H., Ye, M.Z., Peng, B., Wu, H.K., Xu, C.X., Xiong, X.P., Wang, C., Wang, S.Y. and Peng, X.X., 2010. Immunoproteomic identification of polyvalent vaccine candidates from Vibrio parahaemolyticus outer membrane proteins. *Journal of Proteome Research*, *9*(5), pp.2573-2583.

Lopes-Rodrigues, M., Zanuy, D., Alemán, C., Michaux, C. and Perpète, E.A., 2018. 3D structure of a Brucella melitensis porin:

molecular modelling in lipid membranes. *Journal of Biomolecular Structure and Dynamics*.

Lü, L., Cao, H.D., Zeng, H.Q., Wang, P.L., Wang, L.J., Liu, S.N. and Xiang, T.X., 2009. Recombinant mycobacterium smegmatis mc2155 vaccine expressing outer membrane protein 26 kDa antigen affords therapeutic protection against Helicobacter pylori infection. *Vaccine*, *27*(7), pp.972-978.

Lu, Y.S., Gerrity, L.W., Afendis, S.J., Watkins, L. and Pakes, S.P., 1988. Distribution of a monoclonal antibody-recognized protective protein immunogen on the outer membranes of Pasteurella multocida rabbit isolates. *Journal of clinical microbiology*, *26*(7), pp.1326-1330.

Lu, Y.S., Lai, W.C., Pakes, S.P. and Nie, L.C., 1991. A monoclonal antibody against a Pasteurella multocida outer membrane protein protects rabbits and mice against pasteurellosis. *Infection and immunity*, *59*(1), pp.172-180.

Luman Wang YF, Chu Y. "Regulatory B Cells". In: J Wang, editor. B cells in immunity and tolerance Advances in Experimental Medicine and Biology. Singapore: Springer (2020). p. 87–103.

Lundgren, A., Suri-Payer, E., Enarsson, K., Svennerholm, A.M. and Lundin, B.S., 2003. Helicobacter pylori-specific CD4+ CD25high regulatory T cells suppress memory T-cell responses to H. pylori in infected individuals. *Infection and immunity*, *71*(4), pp.1755-1762.

Lundström, A.M., Blom, K., Sundaeus, V. and Bölin, I., 2001. HpaA shows variable surface localization but the gene expression is similar in different Helicobacter pylori strains. *Microbial pathogenesis*, *31*(5), pp.243-253.

M. Galdiero, M. D'Amico, F. Gorga, C. Di Filippo, M. D'Isanto, M. Vitiello, A. Longanella, A. Tortora. *Haemophilus*

influenzae porin contributes to signaling of the inflammatory cascade in rat brain. *Infect. Immun.*, 2001, 69, 221-227.

Macnab, R.M., 1999. The bacterial flagellum: reversible rotary propellor and type III export apparatus. *Journal of bacteriology*, *181*(23), pp.7149-7153.

Mahdavi, J., Sondén, B., Hurtig, M., Olfat, F.O., Forsberg, L., Roche, N., Ångström, J., Larsson, T., Teneberg, S., Karlsson, K.A. and Altraja, S., 2002. Helicobacter pylori SabA adhesin in persistent infection and chronic inflammation. *Science*, *297*(5581), pp.573-578.

Mahdavi, J., Sondén, B., Hurtig, M., Olfat, F.O., Forsberg, L., Roche, N., Ångström, J., Larsson, T., Teneberg, S., Karlsson, K.A. and Altraja, S., 2002. Helicobacter pylori SabA adhesin in persistent infection and chronic inflammation. *Science*, *297*(5581), pp.573-578.

Maiti, B., Shetty, M., Shekar, M., Karunasagar, I. and Karunasagar, I., 2011. Recombinant outer membrane protein A (OmpA) of Edwardsiella tarda, a potential vaccine candidate for fish, common carp. *Microbiological Research*, *167*(1), pp.1-7.

Manalastas-Cantos, K., Konarev, P.V., Hajizadeh, N.R., Kikhney, A.G., Petoukhov, M.V., Molodenskiy, D.S., Panjkovich, A., Mertens, H.D., Gruzinov, A., Borges, C. and Jeffries, C.M., 2021. ATSAS 3.0: expanded functionality and new tools for small-angle scattering data analysis. *Journal of Applied Crystallography*, *54*(1), pp.343-355.

Manalastas-Cantos, K., Konarev, P.V., Hajizadeh, N.R., Kikhney, A.G., Petoukhov, M.V., Molodenskiy, D.S., Panjkovich, A., Mertens, H.D., Gruzinov, A., Borges, C. and Jeffries, C.M., 2021. ATSAS 3.0: expanded functionality and new tools for small-angle scattering data analysis. *Journal of Applied Crystallography*, *54*(1), pp.343-355.

Mangel, W.F., Toledo, D.L., Brown, M.T., Worzalla, K., Lee, M. and Dunn, J.J., 1994. [27] Omptin: An Escherichia coli outer membrane proteinase that activates plasminogen. In *Methods in Enzymology* (Vol. 244, pp. 384-399). Academic Press.

Marshall, B. and Warren, J.R., 1984. Unidentified curved bacilli in the stomach of patients with gastritis and peptic ulceration. *The lancet*, *323*(8390), pp.1311-1315.

Marshall, B.J., McGechie, D.B., Rogers, P.A. and Clancy, R.J., 1985. Pyloric Campylobacter infection and gastroduodenal disease. *Medical Journal of Australia*, *142*(8), pp.439-444.

Massari, P., Henneke, P., Ho, Y., Latz, E., Golenbock, D.T. and Wetzler, L.M., 2002. Cutting edge: Immune stimulation by neisserial porins is toll-like receptor 2 and MyD88 dependent. *The Journal of Immunology*, *168*(4), pp.1533-1537.

Massari, P., Ram, S., Macleod, H. and Wetzler, L.M., 2003. The role of porins in neisserial pathogenesis and immunity. *Trends in microbiology*, *11*(2), pp.87-93.

Massari, P., Visintin, A., Gunawardana, J., Halmen, K.A., King, C.A., Golenbock, D.T. and Wetzler, L.M., 2006. Meningococcal porin PorB binds to TLR2 and requires TLR1 for signaling. *The Journal of Immunology*, *176*(4), pp.2373-2380.

Matsumoto, Y., Marusawa, H., Kinoshita, K., Endo, Y., Kou, T., Morisawa, T., Azuma, T., Okazaki, I.M., Honjo, T. and Chiba, T., 2007. Helicobacter pylori infection triggers aberrant expression of activation-induced cytidine deaminase in gastric epithelium. *Nature medicine*, *13*(4), pp.470-476.

Mattsson, A., Quiding-Jarbrink, M., Lonroth, H., Hamlet, A., Ahlstedt, I. and Svennerholm, A.M., 1998. Antibody-secreting cells in the stomachs of symptomatic and asymptomatic Helicobacter pylori-infected subjects. *Infection and immunity*, *66*(6), pp.2705-2712.

Matysiak-Budnik, T. and Megraud, F., 1997. Epidemiology of Helicobacter pylori infection with special reference to professional risk. *Journal of physiology and pharmacology: an official journal of the Polish Physiological Society*, *48*, pp.3-17.

Mauri, C. and Bosma, A., 2012. Immune regulatory function of B cells. *Annual review of immunology*, *30*, pp.221-241.

Meffre, E. and O'Connor, K.C., 2019. Impaired B-cell tolerance checkpoints promote the development of autoimmune diseases and pathogenic autoantibodies. *Immunological Reviews*, *292*(1), pp.90-101.

Melo, R., Richer, L., Johnson, D.L. and Gomes-Solecki, M., 2016. Oral immunization with OspC does not prevent tick-borne Borrelia burgdorferi infection. *PLoS One*, *11*(3), p.e0151850.

Meuskens, I., Saragliadis, A., Leo, J.C. and Linke, D., 2019. Type V secretion systems: an overview of passenger domain functions. *Frontiers in Microbiology*, *10*, p.1163.

Meza, B., Ascencio, F., Sierra-Beltrán, A.P., Torres, J. and Angulo, C., 2017. A novel design of a multi-antigenic, multistage and multi-epitope vaccine against Helicobacter pylori: an in silico approach. *Infection, Genetics and Evolution*, *49*, pp.309-317.

Micsonai, A., Wien, F., Bulyáki, É., Kun, J., Moussong, É., Lee, Y.H., Goto, Y., Réfrégiers, M. and Kardos, J., 2018. BeStSel: a web server for accurate protein secondary structure prediction and fold recognition from the circular dichroism spectra. *Nucleic acids research*, *46*(W1), pp.W315-W322.

Milot Mirdita, Sergey Ovchinnikov, Martin Steinegger. ColabFold - Making protein folding accessible to all. bioRxiv 2021.08.15.456425; doi: https://doi.org/10.1101/2021.08.15.456425

Mimuro, H., Suzuki, T., Tanaka, J., Asahi, M., Haas, R. and Sasakawa, C., 2002. Grb2 is a key mediator of Helicobacter pylori CagA protein activities. *Molecular cell*, *10*(4), pp.745-755.

Mittal, R., Krishnan, S., Gonzalez-Gomez, I. and Prasadarao, N.V., 2011. Deciphering the roles of outer membrane protein A extracellular loops in the pathogenesis of Escherichia coli K1 meningitis. *Journal of Biological Chemistry*, *286*(3), pp.2183-2193.

Mizoguchi, A. and Bhan, A.K., 2006. A case for regulatory B cells. *The Journal of Immunology*, *176*(2), pp.705-710.

Mizoguchi, A., Mizoguchi, E., Takedatsu, H., Blumberg, R.S. and Bhan, A.K., 2002. Chronic intestinal inflammatory condition generates IL-10-producing regulatory B cell subset characterized by CD1d upregulation. *Immunity*, *16*(2), pp.219-230.

Moise, L., Gutierrez, A., Kibria, F., Martin, R., Tassone, R., Liu, R., Terry, F., Martin, B. and De Groot, A.S., 2015. iVAX: An integrated toolkit for the selection and optimization of antigens and the design of epitope-driven vaccines. *Human vaccines & immunotherapeutics*, *11*(9), pp.2312-2321.

Molinari, M., Salio, M., Galli, C., Norais, N., Rappuoli, R., Lanzavecchia, A. and Montecucco, C., 1998. Selective inhibition of Ii-dependent antigen presentation by Helicobacter pylori toxin VacA. *The Journal of experimental medicine*, *187*(1), pp.135-140.

Montes, C.L., Acosta-Rodríguez, E.V., Merino, M.C., Bermejo, D.A. and Gruppi, A., 2007. Polyclonal B cell activation in infections: infectious agents' devilry or defense mechanism of the host?. *Journal of leukocyte biology*, *82*(5), pp.1027-1032.

Moraes, T.F., Bains, M., Hancock, R.E. and Strynadka, N.C., 2007. An arginine ladder in OprP mediates phosphate-specific

transfer across the outer membrane. *Nature structural & molecular biology*, *14*(1), pp.85-87.

Moseman, E.A., Iannacone, M., Bosurgi, L., Tonti, E., Chevrier, N., Tumanov, A., Fu, Y.X., Hacohen, N. and von Andrian, U.H., 2012. B cell maintenance of subcapsular sinus macrophages protects against a fatal viral infection independent of adaptive immunity. *Immunity*, *36*(3), pp.415-426.

Mueller, D., Tegtmeyer, N., Brandt, S., Yamaoka, Y., De Poire, E., Sgouras, D., Wessler, S., Torres, J., Smolka, A. and Backert, S., 2012. c-Src and c-Abl kinases control hierarchic phosphorylation and function of the CagA effector protein in Western and East Asian *Helicobacter pylori* strains. *The Journal of clinical investigation*, *122*(4), pp.1553-1566.

Müller, A., 2012. Multistep activation of the Helicobacter pylori effector CagA. *The Journal of clinical investigation*, *122*(4), pp.1192-1195.

Murata-Kamiya, N., Kurashima, Y., Teishikata, Y., Yamahashi, Y., Saito, Y., Higashi, H., Aburatani, H., Akiyama, T., Peek, R.M., Azuma, T. and Hatakeyama, M., 2007. Helicobacter pylori CagA interacts with E-cadherin and deregulates the β-catenin signal that promotes intestinal transdifferentiation in gastric epithelial cells. *Oncogene*, *26*(32), pp.4617-4626.

Murphy KM, Travers P, Walport M. Janeway's immunobiology. 7th ed. New York: Garland Science; 2007.

Nakamura, K. and Mizushima, S., 1976. Effects of heating in dodecyl sulfate solution on the conformation and electrophoretic mobility of isolated major outer membrane proteins from Escherichia coli K-12. *The Journal of Biochemistry*, *80*(6), pp.1411-1422.

Nessa, J., Chart, H., Owen, R.J. and Drasar, B., 2001. Human serum antibody response to Helicobacter pylori whole cell antigen

in an institutionalized Bangladeshi population. *Journal of applied microbiology*, *90*(1), pp.68-72.

Neta, R. and Salvin, S.B., 1974. Specific suppression of delayed hypersensitivity: the possible presence of a suppressor B cell in the regulation of delayed hypersensitivity. *The Journal of Immunology*, *113*(6), pp.1716-1725.

Netea, M.G., Van der Graaf, C., Van der Meer, J.W. and Kullberg, B.J., 2004. Toll-like receptors and the host defense against microbial pathogens: bringing specificity to the innate-immune system. *Journal of leukocyte biology*, *75*(5), pp.749-755.

Neugut, A.I., Hayek, M. and Howe, G., 1996, June. Epidemiology of gastric cancer. In *Seminars in oncology* (Vol. 23, No. 3, pp. 281-291).

Neves, P., Lampropoulou, V., Calderon-Gomez, E., Roch, T., Stervbo, U., Shen, P., Kühl, A.A., Loddenkemper, C., Haury, M., Nedospasov, S.A. and Kaufmann, S.H., 2010. Signaling via the MyD88 adaptor protein in B cells suppresses protective immunity during Salmonella typhimurium infection. *Immunity*, *33*(5), pp.777-790.

Niu, N., Zhang, J., Huang, T., Sun, Y., Chen, Z., Yi, W., Korteweg, C., Wang, J. and Gu, J., 2012. IgG expression in human colorectal cancer and its relationship to cancer cell behaviors. *PloS one*, *7*(11), p.e47362.

Noinaj, N., Kuszak, A.J. and Buchanan, S.K., 2015. Heat modifiability of outer membrane proteins from Gram-negative bacteria. In *The BAM Complex* (pp. 51-56). Humana Press, New York, NY.

Noto, J.M. and Peek, R.M., 2012. Helicobacter pylori: an overview. *Helicobacter Species*, pp.7-10.

Novikova, O.D., Kim, N.Y., Luk'yanov, P.A., Likhatskaya, G.N., Emel'yanenko, V.I. and Solov'eva, T.F., 2007. Effects of pH on structural and functional properties of porin from the outer membrane of Yersinia pseudotuberculosis. II. Characterization of pH-induced conformational intermediates of yersinin. *Biochemistry (Moscow) Supplement Series A: Membrane and Cell Biology*, *1*(2), pp.154-162.

Novikova, O.D., Kim, N.Y., Luk'yanov, P.A., Likhatskaya, G.N., Emel'yanenko, V.I. and Solov'eva, T.F., 2007. Effects of pH on structural and functional properties of porin from the outer membrane of Yersinia pseudotuberculosis. II. Characterization of pH-induced conformational intermediates of yersinin. *Biochemistry (Moscow) Supplement Series A: Membrane and Cell Biology*, *1*(2), pp.154-162.

Odenbreit, S., Puls, J., Sedlmaier, B., Gerland, E., Fischer, W. and Haas, R., 2000. Translocation of Helicobacter pylori CagA into gastric epithelial cells by type IV secretion. *Science*, *287*(5457), pp.1497-1500.

Oettinger, M.A., Schatz, D.G., Gorka, C. and Baltimore, D., 1990. RAG-1 and RAG-2, adjacent genes that synergistically activate V (D) J recombination. *Science*, *248*(4962), pp.1517-1523.

Oleastro, M. and Ménard, A., 2013. The role of Helicobacter pylori outer membrane proteins in adherence and pathogenesis. *Biology*, *2*(3), pp.1110-1134.

Oleastro, M. and Ménard, A., 2013. The role of Helicobacter pylori outer membrane proteins in adherence and pathogenesis. *Biology*, *2*(3), pp.1110-1134.

Oleastro, M., Cordeiro, R., Ferrand, J., Nunes, B., Lehours, P., Carvalho-Oliveira, I., Mendes, A.I., Penque, D., Monteiro, L., Mégraud, F. and Ménard, A., 2008. Evaluation of the clinical significance of homb a novel candidate marker of helicobacter

pylori strains associated with peptic ulcer disease. *Journal of Infectious Diseases*, *198*(9), pp.1379-1387.

Oleastro, M., Cordeiro, R., Ferrand, J., Nunes, B., Lehours, P., Carvalho-Oliveira, I., Mendes, A.I., Penque, D., Monteiro, L., Mégraud, F. and Ménard, A., 2008. Evaluation of the clinical significance of homb a novel candidate marker of helicobacter pylori strains associated with peptic ulcer disease. *Journal of Infectious Diseases*, *198*(9), pp.1379-1387.

Oleastro, M., Cordeiro, R., Ménard, A. and Gomes, J.P., 2010. Allelic diversity among Helicobacter pylori outer membrane protein genes homB and homA generated by recombination. *Journal of bacteriology*, *192*(15), pp.3961-3968.

Oleastro, M., Cordeiro, R., Ménard, A., Yamaoka, Y., Queiroz, D., Mégraud, F. and Monteiro, L., 2009. Allelic diversity and phylogeny of homB, a novel co-virulence marker of Helicobacter pylori. *BMC microbiology*, *9*(1), pp.1-12.

Oleastro, M., Cordeiro, R., Yamaoka, Y., Queiroz, D., Mégraud, F., Monteiro, L. and Ménard, A., 2009. Disease association with two Helicobacter pylori duplicate outer membrane protein genes, homB and homA. *Gut Pathogens*, *1*(1), pp.1-7.

Oleastro, M., Monteiro, L., Lehours, P., Mégraud, F. and Ménard, A., 2006. Identification of markers for Helicobacter pylori strains isolated from children with peptic ulcer disease by suppressive subtractive hybridization. *Infection and immunity*, *74*(7), pp.4064-4074.

Oleastro, M., Monteiro, L., Lehours, P., Mégraud, F. and Ménard, A., 2006. Identification of markers for Helicobacter pylori strains isolated from children with peptic ulcer disease by suppressive subtractive hybridization. *Infection and immunity*, *74*(7), pp.4064-4074.

Ostberg, K.L., Russell, M.W. and Murphy, T.F., 2009. Mucosal immunization of mice with recombinant OMP P2 induces antibodies that bind to surface epitopes of multiple strains of nontypeable Haemophilus influenzae. *Mucosal immunology*, *2*(1), pp.63-73.

Palframan, S.L., Kwok, T. and Gabriel, K., 2012. Vacuolating cytotoxin A (VacA), a key toxin for Helicobacter pylori pathogenesis. *Frontiers in cellular and infection microbiology*, *2*, p.92.

Pandey, R.K., Bhatt, T.K. and Prajapati, V.K., 2018. Novel immunoinformatics approaches to design multi-epitope subunit vaccine for malaria by investigating anopheles salivary protein. *Scientific reports*, *8*(1), pp.1-11.

Park, S.R., 2012. Activation-induced cytidine deaminase in B cell immunity and cancers. *Immune Network*, *12*(6), pp.230-239.

Park, S.R., Zan, H., Pal, Z., Zhang, J., Al-Qahtani, A., Pone, E.J., Xu, Z., Mai, T. and Casali, P., HoxC4 binds to the AICDA/Aicda promoter to induce AID expression, class switch DNA recombination and somatic hypermutation.

Parsonnet, J., Friedman, G.D., Vandersteen, D.P., Chang, Y., Vogelman, J.H., Orentreich, N. and Sibley, R.K., 1991. Helicobacter pylori infection and the risk of gastric carcinoma. *New England Journal of Medicine*, *325*(16), pp.1127-1131.

Parsonnet, J., Hansen, S., Rodriguez, L., Gelb, A.B., Warnke, R.A., Jellum, E., Orentreich, N., Vogelman, J.H. and Friedman, G.D., 1994. Helicobacter pylori infection and gastric lymphoma. *New England Journal of Medicine*, *330*(18), pp.1267-1271.

Piiadov, V., Ares de Araújo, E., Oliveira Neto, M., Craievich, A.F. and Polikarpov, I., 2019. SAXSMoW 2.0: online calculator of

the molecular weight of proteins in dilute solution from experimental SAXS data measured on a relative scale. *Protein Science*, *28*(2), pp.454-463.

Pimentel-Nunes, P., Goncalves, N., Boal-Carvalho, I., Afonso, L., Lopes, P., Roncon-Albuquerque Jr, R., Henrique, R., Moreira-Dias, L., Leite-Moreira, A.F. and Dinis-Ribeiro, M., 2013. Helicobacter pylori induces increased expression of Toll-like receptors and decreased Toll-interacting protein in gastric mucosa that persists throughout gastric carcinogenesis. *Helicobacter*, *18*(1), pp.22-32.

Pone, E.J., Zan, H., Zhang, J., Al-Qahtani, A., Xu, Z. and Casali, P., 2010. Toll-like receptors and B-cell receptors synergize to induce immunoglobulin class-switch DNA recombination: relevance to microbial antibody responses. *Critical Reviews™ in Immunology*, *30*(1).

Pore, D., Mahata, N. and Chakrabarti, M.K., 2012. Outer membrane protein A (OmpA) of Shigella flexneri 2a links innate and adaptive immunity in a TLR2-dependent manner and involvement of IL-12 and nitric oxide. *Journal of Biological Chemistry*, *287*(15), pp.12589-12601.

Portal-Celhay, C. and Perez-Perez, G.I., 2006. Immune responses to Helicobacter pylori colonization: mechanisms and clinical outcomes. *Clinical science*, *110*(3), pp.305-314.

Qiao, S., Luo, Q., Zhao, Y., Zhang, X.C. and Huang, Y., 2014. Structural basis for lipopolysaccharide insertion in the bacterial outer membrane. *Nature*, *511*(7507), pp.108-111.

Quiding-Järbrink, M., Sundström, P., Lundgren, A., Hansson, M., Bäckström, M., Johansson, C., Enarsson, K., Hermansson, M., Johnsson, E. and Svennerholm, A.M., 2009. Decreased IgA antibody production in the stomach of gastric adenocarcinoma patients. *Clinical immunology*, *131*(3), pp.463-471.

R. Morona, M. Klose, U. Henning. *Escherichia coli* K-12 outer membrane protein (OmpA) as a bacteriophage receptor: analysis of mutant genes expressing altered proteins. *J. Bacteriol.*, 1984, 159, 570-578

Raju, D., Hussey, S., Ang, M., Terebiznik, M.R., Sibony, M., Galindo–Mata, E., Gupta, V., Blanke, S.R., Delgado, A., Romero–Gallo, J. and Ramjeet, M.S., 2012. Vacuolating cytotoxin and variants in Atg16L1 that disrupt autophagy promote Helicobacter pylori infection in humans. *Gastroenterology*, *142*(5), pp.1160-1171.

Rassow, J. and Meinecke, M., 2012. Helicobacter pylori VacA: a new perspective on an invasive chloride channel. *Microbes and infection*, *14*(12), pp.1026-1033.

Rawlings, D.J., Schwartz, M.A., Jackson, S.W. and Meyer-Bahlburg, A., 2012. Integration of B cell responses through Toll-like receptors and antigen receptors. *Nature Reviews Immunology*, *12*(4), pp.282-294.

Ray, A., Chatterjee, N.S., Bhattacharya, S.K. and Biswas, T., 2003. Porin of Shigella dysenteriae enhances mRNA levels for Toll-like receptor 2 and MyD88, up-regulates CD80 of murine macrophage, and induces the release of interleukin-12. *FEMS Immunology & Medical Microbiology*, *39*(3), pp.213-219.

Recaldin, T., Hobson, P.S., Mann, E.H., Ramadani, F., Cousins, D.J., Lavender, P. and Fear, D.J., 2018. miR-29b directly targets activation-induced cytidine deaminase in human B cells and can limit its inappropriate expression in naive B cells. *Molecular immunology*, *101*, pp.419-428.

Rosenbusch, J.P., 1974. Characterization of the major envelope protein from Escherichia coli: regular arrangement on the peptidoglycan and unusual dodecyl sulfate binding. *Journal of Biological Chemistry*, *249*(24), pp.8019-8029.

Rosenshine, I., Donnenberg, M.S., Kaper, J.B. and Finlay, B.B., 1992. Signal transduction between enteropathogenic

Escherichia coli (EPEC) and epithelial cells: EPEC induces tyrosine phosphorylation of host cell proteins to initiate cytoskeletal rearrangement and bacterial uptake. *The EMBO journal*, *11*(10), pp.3551-3560.

Roy, S., Das, A.B., Ghosh, A.N. and Biswas, T., 1994. Purification, pore-forming ability, and antigenic relatedness of the major outer membrane protein of Shigella dysenteriae type 1. *Infection and immunity*, *62*(10), pp.4333-4338.

Ruprecht, C.R. and Lanzavecchia, A., 2006. Toll-like receptor stimulation as a third signal required for activation of human naive B cells. *European journal of immunology*, *36*(4), pp.810-816.

Safaralizadeh, R., Dastmalchi, N., Hosseinpourfeizi, M. and Latifi-Navid, S., 2017. Helicobacter pylori virulence factors in relation to gastrointestinal diseases in Iran. *Microbial pathogenesis*, *105*, pp.211-217.

Schmees, C., Prinz, C., Treptau, T., Rad, R., Hengst, L., Voland, P., Bauer, S., Brenner, L., Schmid, R.M. and Gerhard, M., 2007. Inhibition of T-cell proliferation by Helicobacter pylori γ-glutamyl transpeptidase. *Gastroenterology*, *132*(5), pp.1820-1833.

Schmiel, D.H., Wagar, E., Karamanou, L., Weeks, D. and Miller, V.L., 1998. Phospholipase A of Yersinia enterocolitica contributes to pathogenesis in a mouse model. *Infection and Immunity*, *66*(8), pp.3941-3951.

Schulz, G.E., 2002. The structure of bacterial outer membrane proteins. *Biochimica et Biophysica Acta (BBA)-Biomembranes*, *1565*(2), pp.308-317.

Servetas, S.L., Doster, R.S., Kim, A., Windham, I.H., Cha, J.H., Gaddy, J.A. and Merrell, D.S., 2018. ArsRS-dependent regulation of homB contributes to Helicobacter pylori biofilm formation. *Frontiers in microbiology*, *9*, p.1497.

Shang, J., Zha, H. and Sun, Y., 2020. Phenotypes, functions, and clinical relevance of regulatory B cells in cancer. *Frontiers in Immunology*, p.2757.

Shimamura, T., Habu, S., Hashimoto, K. and Sasaki, S., 1984. Feedback suppression of the immune response in vivo: III. Lyt-1+ B cells are suppressor-inducer cells. *Cellular immunology*, *83*(1), pp.221-224.

Singer, P.A. and Williamson, A.R., 1980. Cell surface immunoglobulin μ and γ chains of human lymphoid cells are of higher apparent molecular weight than their secreted counterparts. *European Journal of Immunology*, *10*(3), pp.180-186.

Snijder, H.J., Kingma, R.L., Kalk, K.H., Dekker, N., Egmond, M.R. and Dijkstra, B.W., 2001. Structural investigations of calcium binding and its role in activity and activation of outer membrane phospholipase A from Escherichia coli. *Journal of molecular biology*, *309*(2), pp.477-489.

Snijder, H.J., Ubarretxena-Belandia, I., Blaauw, M., Kalk, K.H., Verheij, H.M., Egmond, M.R., Dekker, N. and Dijkstra, B.W., 1999. Structural evidence for dimerization-regulated activation of an integral membrane phospholipase. *Nature*, *401*(6754), pp.717-721.

Soares, T.D.F., Rocha, G.A., Rocha, A.M.C., Corrêa-Oliveira, R., Martins-Filho, O.A., Carvalho, A.S.T., Bittencourt, P., Oliveira, C.A., Faria, A.M.C. and Queiroz, D.M.M., 2005. Phenotypic study of peripheral blood lymphocytes and humoral immune response in Helicobacter pylori infection according to age. *Scandinavian journal of immunology*, *62*(1), pp.63-70.

Song, L., Hobaugh, M.R., Shustak, C., Cheley, S., Bayley, H. and Gouaux, J.E., 1996. Structure of staphylococcal α-hemolysin, a heptameric transmembrane pore. *Science*, *274*(5294), pp.1859-1865.

Soto, G.E. and Hultgren, S.J., 1999. Bacterial adhesins: common themes and variations in architecture and assembly. *Journal of bacteriology*, *181*(4), pp.1059-1071.

Stoorvogel, J., Van Bussel, M.J., Tommassen, J. and Van De Klundert, J.A., 1991. Molecular characterization of an Enterobacter cloacae outer membrane protein (OmpX). *Journal of bacteriology*, *173*(1), pp.156-160.

Struyvé, M., Moons, M. and Tommassen, J., 1991. Carboxy-terminal phenylalanine is essential for the correct assembly of a bacterial outer membrane protein. *Journal of molecular biology*, *218*(1), pp.141-148.

Su, L.C., Liu, X.Y., Huang, A.F. and Xu, W.D., 2018. Emerging role of IL-35 in inflammatory autoimmune diseases. *Autoimmunity Reviews*, *17*(7), pp.665-673.

Suzuki, J., Ohnsihi, H., Shibata, H., Wada, A., Hirayama, T., Iiri, T., Ueda, N., Kanamaru, C., Tsuchida, T., Mashima, H. and Yasuda, H., 2001. Dynamin is involved in human epithelial cell vacuolation caused by the Helicobacter pylori–produced cytotoxin VacA. *The Journal of clinical investigation*, *107*(3), pp.363-370.

Svergun, D.I., 1992. Determination of the regularization parameter in indirect-transform methods using perceptual criteria. *Journal of applied crystallography*, *25*(4), pp.495-503.

Takenaka, R., Yokota, K., Ayada, K., Mizuno, M., Zhao, Y., Fujinami, Y., Lin, S.N., Toyokawa, T., Okada, H., Shiratori, Y. and Oguma, K., 2004. Helicobacter pylori heat-shock protein 60 induces inflammatory responses through the Toll-like receptor-triggered pathway in cultured human gastric epithelial cells. *Microbiology*, *150*(12), pp.3913-3922.

Talebi Bezmin Abadi, A., Rafiei, A., Ajami, A., Hosseini, V., Taghvaei, T., Jones, K.R. and Merrell, D.S., 2011. Helicobacter pylori homB, but not cagA, is associated with gastric cancer in Iran. *Journal of clinical microbiology*, *49*(9), pp.3191-3197.

Tamrakar, A. and Kodgire, P., 2022. HomA and HomB, outer membrane proteins of Helicobacter pylori down-regulate activation-induced cytidine deaminase (AID) and Ig switch germline transcription and thereby affect class switch recombination (CSR) of Ig genes in human B-cells. *Molecular immunology*, *142*, pp.37-49.

Tamrakar, A., Singh, A., Chodhrary, M. and Kodgire, P., 2017. Fighting with Gram-negative enemy: Can outer membrane proteins aid in the rescue. *Chem. Biol. Lett*, *4*(1), pp.9-19.

Tamrakar, A., Singh, R., Kumar, A., Makde, R.D. and Kodgire, P., 2021. Biophysical characterization of the homodimers of HomA and HomB, outer membrane proteins of Helicobacter pylori. *Scientific reports*, *11*(1), pp.1-19.

Testerman, T.L. and Morris, J., 2014. Beyond the stomach: an updated view of Helicobacter pylori pathogenesis, diagnosis, and treatment. *World journal of gastroenterology: WJG*, *20*(36), p.12781.

Thai, T.H., Calado, D.P., Casola, S., Ansel, K.M., Xiao, C., Xue, Y., Murphy, A., Frendewey, D., Valenzuela, D., Kutok, J.L. and Schmidt-Supprian, M., 2007. Regulation of the germinal center response by microRNA-155. *Science*, *316*(5824), pp.604-608.

Thanassi, D.G., Saulino, E.T., Lombardo, M.J., Roth, R., Heuser, J. and Hultgren, S.J., 1998. The PapC usher forms an oligomeric channel: implications for pilus biogenesis across the outer membrane. *Proceedings of the National Academy of Sciences*, *95*(6), pp.3146-3151.

Tian, H., Fu, F., Li, X., Chen, X., Wang, W., Lang, Y., Cong, F., Liu, C., Tong, G. and Li, X., 2011. Identification of the immunogenic outer membrane protein A antigen of Haemophilus parasuis by a proteomics approach and passive immunization with monoclonal antibodies in mice. *Clinical and Vaccine Immunology*, *18*(10), pp.1695-1701.

Tomb, J.F., White, O., Kerlavage, A.R., Clayton, R.A., Sutton, G.G., Fleischmann, R.D., Ketchum, K.A., Klenk, H.P., Gill, S., Dougherty, B.A. and Nelson, K., 1997. The complete genome sequence of the gastric pathogen Helicobacter pylori. *Nature*, *388*(6642), pp.539-547.

Tonegawa, S., 1983. Somatic generation of antibody diversity. *Nature*, *302*(5909), pp.575-581.

Tosi, M.F. and Czinn, S.J., 1990. Opsonic activity of specific human IgG against Helicobacter pylori. *Journal of Infectious Diseases*, *162*(1), pp.156-162.

Tran, T.H., Nakata, M., Suzuki, K., Begum, N.A., Shinkura, R., Fagarasan, S., Honjo, T. and Nagaoka, H., 2010. B cell–specific and stimulation-responsive enhancers derepress Aicda by overcoming the effects of silencers. *Nature immunology*, *11*(2), pp.148-154.

Tsai, H.F. and Hsu, P.N., 2010. Interplay between Helicobacter pylori and immune cells in immune pathogenesis of gastric inflammation and mucosal pathology. *Cellular & molecular immunology*, *7*(4), pp.255-259.

Tsang, Y.H., Lamb, A., Romero-Gallo, J., Huang, B., Ito, K., Peek, R.M., Ito, Y. and Chen, L.F., 2010. Helicobacter pylori CagA targets gastric tumor suppressor RUNX3 for proteasome-mediated degradation. *Oncogene*, *29*(41), pp.5643-5650.

Tummala, S., Keates, S. and Kelly, C.P., 2004. Update on the immunologic basis of Helicobacter pylori gastritis. *Current opinion in gastroenterology*, *20*(6), pp.592-597.

Turvey, S.E. and Broide, D.H., 2010. Innate immunity. *Journal of Allergy and Clinical Immunology*, *125*(2), pp.S24-S32.

Ugrinovic, S., Ménager, N., Goh, N. and Mastroeni, P., 2003. Characterization and Development of T-Cell Immune Responses in B-Cell-Deficient (Igh-6−/−) Mice with Salmonella enterica Serovar TyphimuriumInfection. *Infection and immunity*, *71*(12), pp.6808-6819.

Ulmschneider, M.B. and Sansom, M.S., 2001. Amino acid distributions in integral membrane protein structures. *Biochimica et Biophysica Acta (BBA)-Biomembranes*, *1512*(1), pp.1-14.

Van Belle, K., Herman, J., Boon, L., Waer, M., Sprangers, B. and Louat, T., 2016. Comparative in vitro immune stimulation analysis of primary human B cells and B cell lines. *Journal of immunology research*, *2016*.

Van Gelder, P., Saint, N., Van Boxtel, R., Rosenbusch, J.P. and Tommassen, J., 1997. Pore functioning of outer membrane protein PhoE of Escherichia coli: mutagenesis of the constriction loop L3. *Protein engineering*, *10*(6), pp.699-706.

Viala, J., Chaput, C., Boneca, I.G., Cardona, A., Girardin, S.E., Moran, A.P., Athman, R., Mémet, S., Huerre, M.R., Coyle, A.J. and DiStefano, P.S., 2004. Nod1 responds to peptidoglycan delivered by the Helicobacter pylori cag pathogenicity island. *Nature immunology*, *5*(11), pp.1166-1174.

Vigorito, E., Perks, K.L., Abreu-Goodger, C., Bunting, S., Xiang, Z., Kohlhaas, S., Das, P.P., Miska, E.A., Rodriguez, A., Bradley, A. and Smith, K.G., 2007. microRNA-155 regulates the generation of immunoglobulin class-switched plasma cells. *Immunity*, *27*(6), pp.847-859.

Vogel, H. and Jähnig, F., 1986. Models for the structure of outer-membrane proteins of Escherichia coli derived from raman spectroscopy and prediction methods. *Journal of molecular biology*, *190*(2), pp.191-199.

Vogt, J. and Schulz, G.E., 1999. The structure of the outer membrane protein OmpX from Escherichia coli reveals possible mechanisms of virulence. *Structure*, *7*(10), pp.1301-1309.

Vollan, H.S., Tannæs, T., Caugant, D.A., Vriend, G. and Bukholm, G., 2017. Outer membrane phospholipase A's roles in Helicobacter pylori acid adaptation. *Gut pathogens*, *9*(1), pp.1-13.

Wang, J., Brooks, E.G., Bamford, K.B., Denning, T.L., Pappo, J. and Ernst, P.B., 2001. Negative selection of T cells by Helicobacter pylori as a model for bacterial strain selection by immune evasion. *The Journal of Immunology*, *167*(2), pp.926-934.

Warren, J.R., 2000. Gastric pathology associated with Helicobacter pylori. *Gastroenterology Clinics of North America*, *29*(3), pp.705-751.

Warrington, R., Watson, W., Kim, H.L. and Antonetti, F.R., 2011. An introduction to immunology and immunopathology. *Allergy, Asthma & Clinical Immunology*, *7*(1), pp.1-8.

Watanabe, Y., 2002. Effect of various mild surfactants on the reassembly of an oligomeric integral membrane protein OmpF porin. *Journal of protein chemistry*, *21*(3), pp.169-175.

Wen, Z., Boddicker, M.A., Kaufhold, R.M., Khandelwal, P., Durr, E., Qiu, P., Lucas, B.J., Nahas, D.D., Cook, J.C., Touch, S. and Skinner, J.M., 2016. Recombinant expression of Chlamydia trachomatis major outer membrane protein in E. Coli outer membrane as a substrate for vaccine research. *BMC microbiology*, *16*(1), pp.1-13.

West, A.P., Koblansky, A.A. and Ghosh, S., 2006. Recognition and signaling by toll-like receptors. *Annu. Rev. Cell Dev. Biol.*, *22*, pp.409-437.

Wimley, W.C., 2003. The versatile β-barrel membrane protein. *Current opinion in structural biology*, *13*(4), pp.404-411.

Wong, E.H.J., Ng, C.G., Chua, E.G., Tay, A.C.Y., Peters, F., Marshall, B.J., Ho, B., Goh, K.L., Vadivelu, J. and Loke, M.F., 2016. Comparative genomics revealed multiple Helicobacter pylori genes associated with biofilm formation in vitro. *PLoS One*, *11*(11), p.e0166835.

Wroblewski, L.E., Peek Jr, R.M. and Wilson, K.T., 2010. Helicobacter pylori and gastric cancer: factors that modulate disease risk. *Clinical microbiology reviews*, *23*(4), pp.713-739.

Wu, H., Su, Z. and Barnie, P.A., 2020. The role of B regulatory (B10) cells in inflammatory disorders and their potential as therapeutic targets. *International Immunopharmacology*, *78*, p.106111.

Wündisch, T., Dieckhoff, P., Greene, B., Thiede, C., Wilhelm, C., Stolte, M. and Neubauer, A., 2012. Second cancers and residual disease in patients treated for gastric mucosa-associated lymphoid tissue lymphoma by Helicobacter pylori eradication and followed for 10 years. *Gastroenterology*, *143*(4), pp.936-942.

Xu, X., Liu, Z., Fang, M., Yu, H., Liang, X., Li, X., Liu, X., Chen, C. and Jia, J., 2012. Helicobacter pylori CagA induces ornithine decarboxylase upregulation via Src/MEK/ERK/c-Myc pathway: implication for progression of gastric diseases. *Experimental Biology and Medicine*, *237*(4), pp.435-441.

Yahiro, K., Akazawa, Y., Nakano, M., Suzuki, H., Hisatune, J., Isomoto, H., Sap, J., Noda, M., Moss, J. and Hirayama, T., 2015. Helicobacter pylori VacA induces apoptosis by accumulation of connexin 43 in autophagic vesicles via a Rac1/ERK-dependent pathway. *Cell death discovery*, *1*(1), pp.1-15.

Yang, J., Yan, R., Roy, A., Xu, D., Poisson, J. and Zhang, Y., 2015. The I-TASSER Suite: protein structure and function prediction. *Nature methods*, *12*(1), pp.7-8.

Yang, Q., Pan, Y.L., Wang, K.Y., Wang, J., He, Y., Wang, E.L., Liu, T., Geng, Y., Chen, D.F. and Huang, X.L., 2016. OmpN, outer membrane proteins of Edwardsiella ictaluri are potential vaccine candidates for channel catfish (Ictalurus punctatus). *Molecular Immunology*, *78*, pp.1-8.

Yuan, J., Li, P., Tao, J., Shi, X., Hu, B., Chen, H. and Guo, X., 2009. H. pylori escape host immunoreaction through inhibiting

ILK expression by VacA. *Cellular & molecular immunology*, *6*(3), pp.191-197.

Zan, H. and Casali, P., 2013. Regulation of Aicda expression and AID activity. *Autoimmunity*, *46*(2), pp.83-101.

Zhao, Y., Yokota, K., Ayada, K., Yamamoto, Y., Okada, T., Shen, L. and Oguma, K., 2007. Helicobacter pylori heat-shock protein 60 induces interleukin-8 via a Toll-like receptor (TLR) 2 and mitogen-activated protein (MAP) kinase pathway in human monocytes. *Journal of medical microbiology*, *56*(2), pp.154-164.

Zullo, A., Hassan, C., Cristofari, F., Andriani, A., De Francesco, V., Ierardi, E., Tomao, S., Stolte, M., Morini, S. and Vaira, D., 2010. Effects of Helicobacter pylori eradication